**School of Civil and Mechanical Engineering**

# Polyvinyl Alcohol / Starch/ Glycerol/ Halloysite Nanotube Bionanocomposites for Biodegradable Packaging Applications

**Zainab Waheed Abdullah**

**This thesis is presented for the Degree of**
**Doctor of Philosophy**
**of**

**Curtin University**

**July 2019**

# DECLARATION

To the best of my knowledge and belief this thesis contains no material previously published by any other.

This thesis contains no material which has been accepted for the award of any other degree or diploma in any University.

Signature:

Date: 12/07/2019

# ABSTRACT

Environmental pollution due to solid plastic wastes has drawn great attention over decades in academia and industries. Using petroleum-based (non-biodegradable) polymers in several daily applications particularly for food packaging applications have an even more severe impact on the environment. A small portion of these solid plastic wastes are recycled, and the rest is accumulated in the environment. As such, it is essential to replace petroleum-based polymers with other biodegradable polymers. Most these biodegradable polymers have limited mechanical, thermal and barrier properties leading to their limited applications as neat polymers alone. Consequently, it is motivated by the material development of new biopolymer blends and bionanocomposites to meet stringent requirements of food packaging.

In this work, novel bionanocomposite films were developed as sustainable food-packaging materials. Polyvinyl alcohol (PVA)/ starch (ST)/ glycerol (GL)/ halloysite nanotube (HNT) bionanocomposite films at HNT contents of 0.25, 0.5, 1, 3 and 5 wt% were successfully manufactured using the solution casting method and, further characterised for their particular applications as food packaging materials. The effects of material composition and HNT content on mechanical, thermal and optical properties, water resistance and biodegradability were holistically investigated along with the identified morphological structures. Migration rates of material constituents particularly HNTs when contacting with food simulants were evaluated in terms of overall material migration and nanofiller migration rates accordingly. Modelling approaches for water vapour and gas permeabilities have been also successfully implemented based on Nielsen model and Cussler model in good agreement with experimental results. Additionally, prepared bionanocomposite films were confirmed

to be effective food-packaging materials for lipidic and acidic fruits in comparison with the controlled samples and different PVA blend films.

In term of morphological structures, there was no phase separation observed for PVA/ST/GL blends with smooth surfaces. Bionanocomposite films showed good dispersion of HNTs up to 1 wt%, then small HNT agglomeration was observed at 3 and 5 wt% HNTs.

Blending PVA with ST and GL highly improved biodegradation rate and elongation at break of PVA/ST/GL blends, respectively, despite the reductions in tensile strength and Young' modulus when compared with those of neat PVA. An opposite trend was detected for bionanocomposite films in term of biodegradation rate and elongation at break as opposed to PVA/ST/GL blends in spite of being still better than neat PVA in addition to the improvements in tensile strength and Young's modulus up to 1 wt% HNTs. The remarkable reductions in tensile strength and Young's modulus of bionanocomposite films were found when HNT content exceeded 1 wt% due to HNT agglomeration.

Thermal stability of PVA/ST/GL blends in term of melting temperature ($T_m$) and decomposition temperature diminished though good miscibility between constituents was evidently shown as a result of single glass transition temperature ($T_g$) of PVA/ST/GL blends. On the other hand, $T_g$ and $T_m$ of bionanocomposites increased with the inclusion of HNTs at different rates as well as a linear increase in decomposition temperature was indicative of enhancing the thermal stability of such bionanocomposite films relative to those of PVA/ST/GL blends.

The transparency (*T%*) of PVA/ST/GL blends was slightly reduced as opposed to that of neat PVA. However, such a reduction appeared to be more pronounced for

bionanocomposite films along with increasing their surface roughness when increasing the HNT content from 0.25 to 5 wt%.

Water resistance including water absorption capacity ($W_a$) and water solubility ($W_s$) of PVA/ST/GL blends were found to slightly decline along with a very minor improvement in water contact angle in contrast to those of neat PVA. On the other hand, bionanocomposite films possessed much higher water contact angles when compared with those of PVA blends resulting in a significant reduction in $W_a$ and $W_s$ of bionanocomposite films.

Whereas, water vapour transmission rate (*WVTR*) and water vapour permeability (*WVP*) of such PVA blends were observed to be increased as opposed to those of neat PVA. A further increase was also reported when the temperature level was increased from 25 to 55ºC and the relative humidity (RH) gradient was increased from 10 to 70%. The incorporation of HNTs within bionanocomposite films significantly decreased the *WVTR* and *WVP* at all temperature levels in a good fitting relationship with Arrhenius equation. Moreover, the presence of HNTs diminished the sensitivity of bionanocomposite films with the variation of RH gradient. A similar trend was also observed for both oxygen and air permeabilities at ambient conditions.

The experimental data associated with *WVP* and gas permeability of bionanocomposite films up to 1 wt% HNTs showed good agreement with Nielsen model based on regular HNT dispersion as well as random HNT dispersion of bionanocomposite films when reinforced with 3 and 5 wt% HNTs with the application of a typical aspect ratio of as-received HNTs. On the other hand, by using accurately measured aspect ratios of HNTs embedded in bionanocomposite films, it was clearly demonstrated that the HNT contents in range of 0.25-5 wt% in such bionanocomposites yielded better agreement between experimental data and Nielsen

model based on regular HNT dispersion with variable aspect ratios. Whereas, Cussler model for both regular and random HNT dispersion indicated a good correlation with experimental data of bionanocomposite films up to 1 wt% HNTs in both cases of typical aspect ratio of HNT and accurately measured counterparts.

The overall migration rates of PAV/ST/GL blends and corresponding bionanocomposite films exceeded the overall migration limits (OML) in hydrophilic foodstuffs as opposed to being within the OML in lipidic and acidic foodstuffs. The migration rates of HNTs in hydrophilic, lipidic and acidic foodstuffs increased linearly with increasing the HNT content in bionanocomposite films.

Finally, bionanocomposite films reinforced with 1 wt% HNTs were successfully used to package fresh cut avocados and peaches with much lower weight loss rate and fungi-growth free characteristic as compared with those controlled fruits and packaged with neat PVA and PVA/ST/GL blends.

# ACKNOWLEDGEMENTS

Without a doubt, the first and foremost sincere acknowledgment I wish to express for the completion of this PhD dissertation is to God who gave me this opportunity and the ability to complete such a difficult journey with success.

Next, I am indebted to my supervisor Dr. Yu Dong for his continued contribution, dedication, wisdom and enormous supports. His kind understanding and unconditional supports not only helped me to successfully complete this PhD dissertation, but also inspired me to think of opportunities and challenges encountered in real life from different perspectives. Such a strong working relationship developed with him is anticipated to continue in the near future. I would also like to extend my sincere gratitude to my co-supervisor A/Prof. Ian Davis for his kind assistance. I would thank Prof. Ian Howard for his continued support as a chairperson in my PhD supervisory committee.

The PhD journey requires different types and levels of supports and I owe too much to the technical staff at the Department of Mechanical Engineering, particularly Mr. Graeme Watson, Mr. David Collier, and Mr. Andy Viereckl. I would also like to extend my sincere appreciation to Ms. Elaine Millers at Microscopy and Microanalysis Facility, the John deLaeter Centre, Dr. Thomas Becker at School of Molecular and Life Sciences (MLS) and Mr. Andrew Chan at WA School of Mines: Minerals, Energy and Chemical Engineering all at Curtin University.

Special thanks to my parents as well as my sisters and brothers (Intisar, Fatima, Hussein, and Hayder). They, at different critical points, have been considered as

spiritual supports. I extend my sincere gratitude to my husband (Ali) for being such a wonderful husband. This long journey would not have been possible without him.

Last, but not least, I want to acknowledge the Higher Committee for Education Development (HCED) in Iraq to support my PhD scholarship at Curtin University as well as Curtin University for providing me this opportunity to complete my research goal in the proactive learning environment.

# BIOGRAPHY AND PUBLICATIONS

## Biography

Zainab Waheed Abdullah received her B.Sc. degree in September 2005 and M.Sc. degree in January 2011 in Material Engineering at Engineering College-Baghdad, Middle Technical University, Iraq. She had worked at the same University since November 2005. She has gained good research experience in material preparation as well as destructive and non-destructive material testing. She was previously a manager of the metallurgy laboratory from November 2005 to October 2008, then was appointed to be an assistant lecturer in Material Engineering Department in March 2011. She has been a member of the Iraqi Engineers Association since 2006. She commenced her PhD studies at the School of Civil and Mechanical Engineering, Curtin University in December 2015.

## Publications

1. Abdullah, Zainab Waheed, Yu Dong, Polyvinyl Alcohol/Halloysite Nanotube Bionanocomposites as Biodegradable Packaging Materials, 6 chapters, Springer Nature, Singapore, in press.
2. Abdullah, Zainab Waheed, Y. Dong. 2020 “Sustainable food packaging materials using bionanocomposite films”, *JEC Composites Magazine*, 134:116-119.
3. Abdullah, Zainab Waheed, Yu Dong, Ning Han, Shaomin Liu. 2019. “Water and gas barrier properties of poly(vinyl) alcohol (PVA)/starch (ST)/glycerol (GL)/halloysite nanotube (HNT) bionanocomposite films: Experimental

characterisation and modelling approach.” *Composites Part B* 174: 107033. doi.org/10.1016/j.compositesb.2019.107033. (Impact Factor: 6.864)

4. Abdullah, Zainab Waheed, and Yu Dong. 2019. "Biodegradable and Water Resistant Poly(vinyl) Alcohol (PVA)/ Starch (ST)/ Glycerol (GL)/ Halloysite Nanotube (HNT) Nanocomposite Films for Sustainable Food Packaging. "*Frontiers in Materials* 6: 58. doi:10.3389/fmats.2019.00058. (Impact Factor: 2.689)
5. Abdullah, Zainab Waheed, and Yu Dong. 2018. "Recent Advances and Perspectives on Starch Nanocomposites for Packaging Applications.” *Journal of Materials Science* 53, no. 22: 15319-5339. doi:10.1007/s10853-018-2613-9. (Impact Factor:3.442)
6. Abdullah, Zainab Waheed, and Yu Dong. 2017. "Preparation and Characterisation of Poly(vinyl) Alcohol (PVA)/ starch (ST)/ halloysite Nanotube (HNT) Nanocomposite Films as Renewable Materials. "*Journal of Materials Science* 53, no. 5: 3455-469. doi:10.1007/s10853-017-1812-0. (Impact Factor: 3.442)
7. Abdullah, Zainab Waheed, Yu Dong, Ian Jeffery Davies, and Salim Barbhuiya. 2017. "PVA, PVA Blends, and Their Nanocomposites for Biodegradable Packaging Application." *Polymer-Plastics Technology and Engineering* 56, no. 12: 1307-344. doi:10.1080/03602559.2016.1275684. (Impact Factor: 1.705)

# TABLE OF CONTENTS

# LIST OF FIGURES

# LIST OF TABLES

# Chapter 1: Introduction

## 1.1 Background

Petroleum-based polymers replaced other materials like metals, ceramics, and wood in a wide variety of applications such as appliances, constructions and material packaging about half a century ago (Shah et al. 2008; Arora and Padua 2010). These polymers such as polyethylene (PE), polystyrene (PS), polyamide (PA), polyvinyl chloride (PVC) and polypropylene (PP) become indispensable in most industrial sectors due to their reasonable mechanical, thermal and barrier properties as well as low cost, relatively lightweight feature and excellent processability (Siracusa et al. 2008; Souza and Fernando 2016). According to the global market for polymeric consumption, about 322 million tons of polymers were consumed in 2015, which was increased by 3.5% as compared with that in 2014 (Mangaraj et al. 2018). Material packaging applications are on the top place at 42% of this consumption, particularly for food packaging in form of sheets, films, cups, trays, and bottles due to the shift from reusable to single-use products (Silvestre, Duraccio and Cimmino 2011; Ramos et al. 2018). Moreover, 79% of this annual consumption is accumulated in the natural environment as plastic wastes since only 9% of this consumption is recycled while 12% is burned leading to the significant increase in global warming (Geyer, Jambeck and Law 2017). Together, the lack of petroleum-based resources and their high cost of extraction, as well as, their shortage in the next 60 years motivated the researchers in both academia and industrial sectors to find alternative and eco-friendly polymeric resources (Silvestre, Duraccio and Cimmino 2011; Mishra et al. 2018).

Biopolymers , also known as biodegradable, biocompatible, environmentally friendly, sustainable, renewable and green polymers have been developed rapidly in material

packaging sectors in the last decade (Rhim and Ng 2007). The global market of biopolymers reached 103 thousand tonnes in 2016 with a further expansion expected to reach 884 thousand tons by 2020 (Mangaraj et al. 2018; Ramos et al. 2018). Biopolymers are produced from alternative resources such as the direct extraction from biomass and chemical synthesis from biomass as well as the production from microbial resources (Rhim, Park and Ha 2013; Mensitieri et al. 2011). Although these biopolymers are widely available, relatively cheap, non-toxic, and possess high reactivity, biocompatible and biodegradable along with acceptable strength, they still have limited applications due to weak thermal stability and poor barrier properties (Sorrentino, Gorrasi and Vittoria 2007; Rhim, Park and Ha 2013; Teodorescu, Bercea and Morariu 2018). Food packaging requires a combination of science, technology, and art to provide physical protection of products in order to keep their quality and shelf life by minimising the water and gas permeabilities at the least price (Rhim and Ng 2007; Rhim, Park and Ha 2013; Mangaraj et al. 2018). The most popular scenario to overcome these limitations are developing polymer nanocomposite systems for packaging applications because nanocomposite systems meet most requirements for food packaging materials (Arora and Padua 2010; Souza and Fernando 2016). Nanotechnology has drawn great attention in packaging applications due to the creation of new material systems with unique properties resulting from using nanoscaled materials with large surface-area-to-volume ratio leading to the improvement of chemical and thermal stabilities, better mechanical and barrier properties as well as lower density compared with micro-and macroscaled materials (Cerqueira, Vicente and Pastrana 2018). According to Duncan (2011) and Youssef and El-Sayed (2018), the association of nanotechnology in food packaging applications was worth US$ 4.13 billion in 2008, and increased to US$ 7.3 billion in 2014 with an

annual increase up to 12% as well as nanotechnology is expected to reach US$ 3 trillion in 2020 across the global economy. For instance, Noshirvani et al. (2016) prepared polyvinyl alcohol (PVA)/ starch (ST)/ montmorillonite nanoclay (MMT) nanocomposites with an increase in tensile strength by 17.38% and a reduction in water vapour permeability (*WVP)* by 16.46% as compared with those of PVA/ST blends, which could be efficiently used for food packaging applications. Furthermore, improving the mechanical and barrier properties of PVA/graphene oxide nanocomposite films helped to improve the shelf life of banana fruits that were packaged with such films as opposed to control fruits (Loryuenyong et al. 2015).

PVA is a synthetic water-soluble biopolymer. It has good mechanical and thermal properties as well as relatively high cost and limited biodegradability in some environments like soil (Sapalidis, Katsaros and Kanellopoulos 2011). As a typical water-soluble polymer, PVA has many hydroxyl groups leading to decrease in water resistance such as *WVP* (Chiellini et al. 2003). On the other hand, it has low gas permeability and good biocompatibility as well as nontoxicity for increasing its applications in medical sectors such as contact lens, eye drops and tissue-adhesion barriers and packaging sectors like food packaging (Baker et al. 2012; Gaaz et al. 2015; Teodorescu, Bercea and Morariu 2018). PVA is blended successfully with other biopolymers such as ST to improve its biodegradability (Tânase et al. 2016), chitosan for better antimicrobial properties (He and Xiong 2012), poly(lactic) acid (PLA) to improve mechanical and thermal properties (Li, Chen and Wang 2014). On the other hand, barrier properties of PVA can be promoted significantly with the incorporation of nanofillers (Huang et al. 2012).

ST is a completely biodegradable and biocompatible biopolymer. It belongs to the polysaccharide family with alternative resources like wheat, potato, rice, corn,

cassava, etc. (García et al. 2015). ST has high brittleness and limited processability as a neat polymer due to strong hydrogen bonds between its macromolecules. As such, neat ST is replaced with thermoplastic starch (TPS) by the gelatinisation in the presence of plasticisers in order to improve the flexibility (Shi et al. 2007). In most cases, ST is blended with other polymers to improve their biodegradability because it has high biodegradability in different environments like soil, compost and enzymes (Tânase et al. 2016). PVA/ST blends have been widely investigated for food packaging applications since 1980 despite poor water resistance owing to their high hydrophilicity (Liu, Fing and Yi 1999).

Halloysite nanotubes (HNTs) are natural deposits of aluminosilicate clays similar to the chemical structure of kaolinite with hollow-tubular morphology (Joussein et al. 2005). They have moderate hydrophobicity due to the lower number of hydroxyl groups as well as the presence of shared $AlO_6$ and $SiO_4$ groups to improve their dispersion within polymers matrices (Gaaz et al. 2015; Nakagaito et al. 2019). Moreover, HNTs have inherently high thermal stability and mechanical strength as well as nontoxicity and flame retardant nature (Tully, Fakhrullin and Lvov 2015). Consequently, HNTs are used as nanofillers in nanocomposites targeting several biomedical applications such as drug delivery systems, wound dressing and so on (Zhang et al. 2016). HNTs are the superior nanofiller candidate for many nanocomposite systems due to their high aspect ratio and unique properties (Zhang et al. 2016) such as PVA/HNT nanocomposites (Zhou et al. 2010), ST/HNT nanocomposites (Schmitt et al. 2015), PLA/HNT nanocomposites (Dong et al. 2015b) , etc.

## 1.2 Research objectives

To eliminate environmental plastic wastes, new ecofriendly material systems should be explored and developed to focus on commercial applications particularly in food packaging. In general, food-packaging materials are required to possess good mechanical, thermal, optical and barrier properties in order to keep food quality in handling and storage processes as well as biodegrade over a relatively short period of time to reduce the plastic waste issue (Rhim, Park and Ha 2013; Rhim and Ng 2007), as illustrated in Figure 1-1. In the meantime, these materials should make a good balance between the aspects of material performance, cost, environment and human health through the selection of available raw materials, processing methods and interaction with food products as well as human beings (Silvestre, Duraccio and Cimmino 2011; Ray et al. 2006). The general material performance of PVA/ST blends has been developed over a few decades in material-packaging applications with the inclusion of nanofillers such as montmorillonite (MMT) (Tian et al. 2017b), metal oxide like nano-silicon dioxide ($SiO_2$) (Tang et al. 2008) and nano-zinc oxide (ZnO) (Akhavan, Khoylou and Ataeivarjovi 2017), bamboo nanofibrils (Guimarães Jr. et al. 2015) and hybrid nanofillers of cellulose nanocrystals (CNCs) and MMTs (Noshirvani et al. 2016). To our best knowledge, there was no work carried out to use HNTs with PVA/ST blends particularly in terms of food packaging applications.

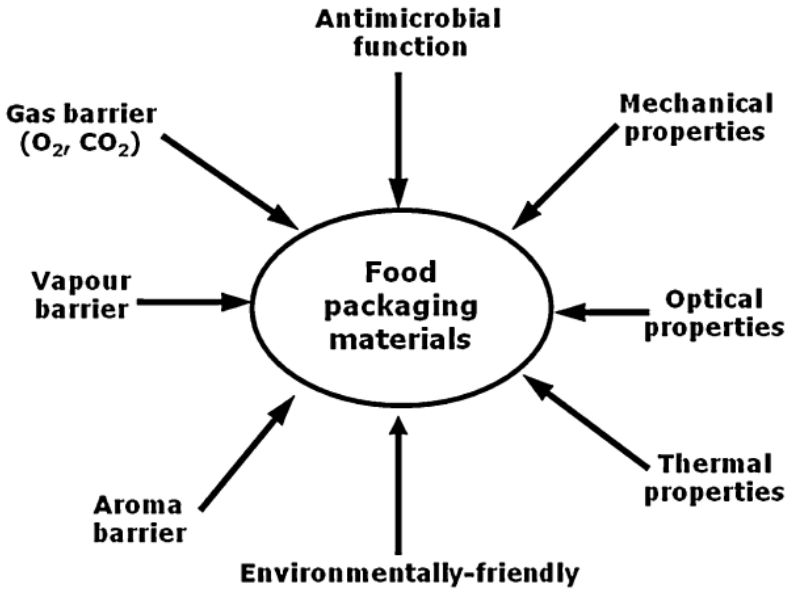


Figure 1-1. General requirements for food-packaging materials (Rhim, Park and Ha 2013)

In this study, PVA/ST/GL/HNT bionanocomposite films were manufactured using a solution casting process with remarkable improvements in mechanical, thermal and barrier properties when compared with those of PVA/ST/GL blends alone. Such bionanocomposites films were also successfully applied as biodegradable food packaging materials for lipidic and acidic fruits with better shelf life according to the following steps:

1. Manufacturing PVA/ST/GL/HNT bionanocomposite films at different HNT contents of 0.25, 0.5, 1, 3 and 5 wt% using a solution casting method.
2. Studying mechanical, thermal and optical properties of PVA/ST/GL/HNT bionanocomposite films in relation to the HNT contents and morphological structures.
3. Investigating the biodegradation behaviour and water resistance of bionanocomposite films associated with the content of each components in bionanocomposites.

4. Evaluating the effects of different temperatures and relative humidity gradients on the *WVTR* and *WVP* of bionanocomposite films.
5. Applying two different theoretical models, namely Nielsen model and Cussler model to predict the *WVP* and gas permeability of bionanocomposite films in comparison with experimental data to evaluate the effect of nanofiller dispersion and aspect ratio of HNTs.
6. Using PVA/ST/GL blends and bionanocomposite films as packaging materials to evaluate the migration rates of films and HNTs when in contact with food simulants and shelf life of foodstuffs.

## 1.3 Thesis outline

This thesis consists of eight chapters as illustrated below, see Figure 1-2:

- Chapter 1 presents the background about petroleum-based polymers, their accumulated problem and replacement with biopolymers particularly for material packaging applications. Moreover, brief information about PVA, ST and HNTs as well as their applications and properties are also mentioned.
- Chapter 2 reviews with details the previous literatures related to biopolymers particularly neat PVA, PVA blends and corresponding bionanocomposite systems. Manufacturing methods with their properties such as morphological, mechanical, thermal and barrier properties are also covered. Theoretical models that have been developed to predict *WVP* and gas permeability are explicitly reviewed.

- Chapter 3 explains the main characteristics of selected materials including PVA, ST, HNTs and other reagents. The detailed material preparation method is described along with the use of all relevant characterisation techniques.
- Chapter 4 presents the morphological structures of PVA/ST/GL/HNT bionanocomposite films using a microscopic analysis and HNT intercalation is discussed via X-ray diffraction (XRD) and Fourier transformation infrared (FTIR) analyses. Mechanical, thermal and optical properties are correlated with their morphological structures in order to understand their processing-structure-property relationship.
- Chapter 5 covers water absorption capacity, water solubility and water contact angel of PVA/ST/GL/HNT bionanocomposite films in terms of water resistance. The biodegradation of bionanocomposites using soil burial tests is elaborated with respect to morphological structures.
- Chapter 6 details the effect of temperature and relative humidity gradient on the *WVTR* and *WVP* of bionanocomposite films as well as air and oxygen permeabilities at ambient conditions. The experimental data of *WVP* and gas permeability are compared with Nielsen model and Cussler model for both well-aligned and randomly dispersed HNTs in bionanocomposite films.
- Chapter 7 discusses about the overall migration rate and HNT migration rate of bionanocomposite films when in contact with different food simulants. Moreover, real applications of these films as food packaging materials are also studied particularly targeting lipidic and acidic foodstuffs.
- Chapter 8 summarises the main findings and provide the recommendations for future work.

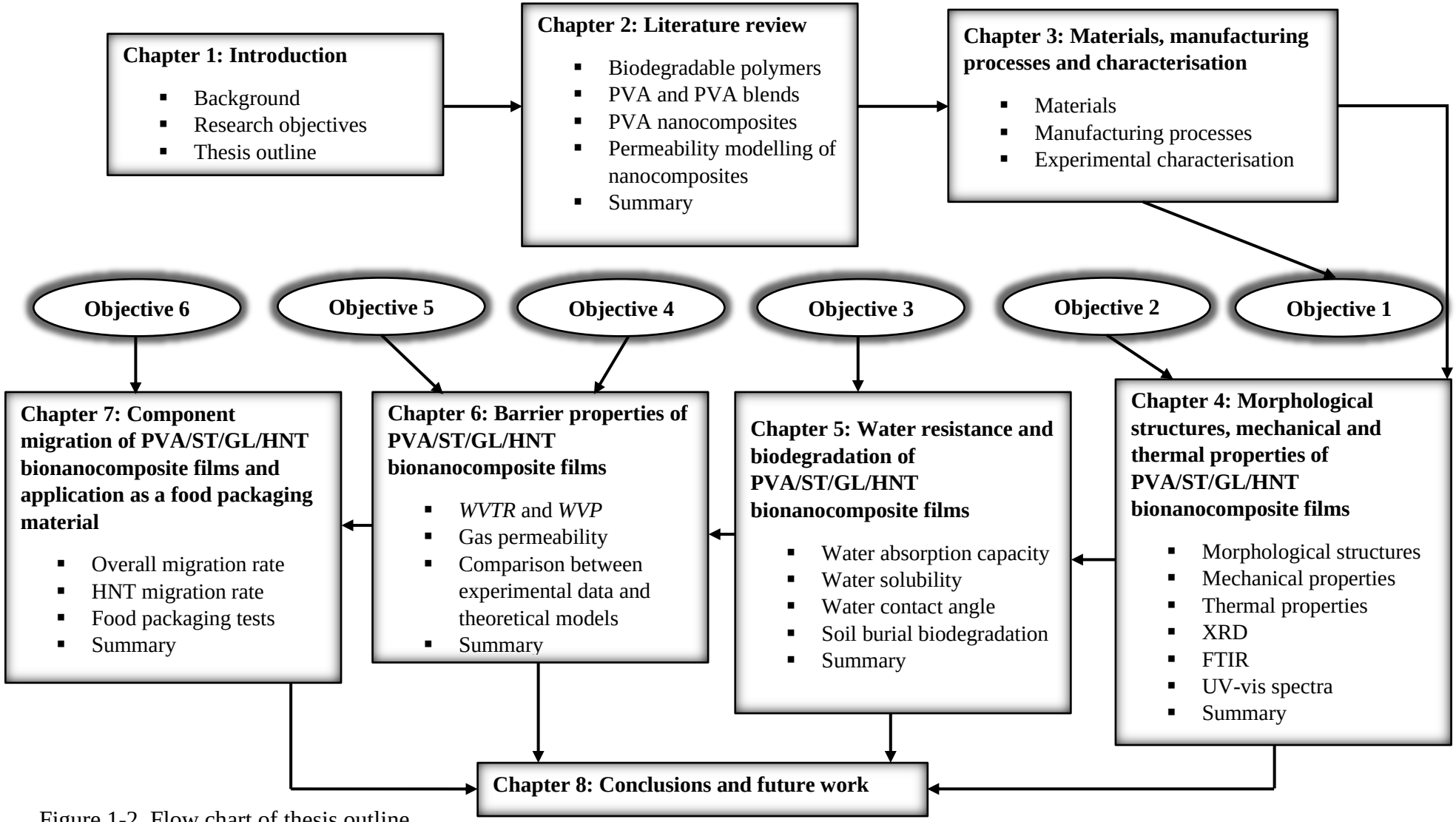


Figure 1-2. Flow chart of thesis outline

# Chapter 2: Literature Review

## 2.1 Biodegradable polymers

### 2.1.1 Concept of biodegradability

Biodegradation can be defined as a natural decomposition process of organic materials, which breaks down to simple components by an enzymatic action of microorganisms such as bacteria and fungi in appropriate environmental conditions (Shah et al. 2008; Avérous and Pollet 2012; Chandra and Rustgi 1998). This process is mostly associated with the loss of mechanical properties and change of chemical characteristics (Souza and Fernando 2016). New simple biomass, water and $CO_2$ are the end products of this process in the presence of oxygen (aerobic conditions) or methane without oxygen (anaerobic conditions) (Lucas et al. 2008; Avérous and Pollet 2012). Furthermore, biodegradable materials like biodegradable polymers can be validated according to ASTM-D20-96, EN-13432-2000, ISO-472 and DIN-103.2 standards as such materials can suffer from bonding scission in the backbone leading to significant changes in their chemical and morphological structures under particular environmental conditions and by the action of microorganisms (Avérous and Pollet 2012; Chandra and Rustgi 1998). These environmental conditions include temperature, relative humidity, type and number of available microorganisms. In the other words, biodegradation is much faster at the temperature range of 50-70ºC when compared with that at room temperature. It is also the case for relative humidity because biodegradation becomes faster in humid soil than normal counterpart (Siracusa et al. 2008; Rhim, Park and Ha 2013). In addition to environmental conditions, biodegradation can also be controlled by other material-related factors like molecular weight, length of polymeric chains, crystallinity

degree, treatment history, functional groups and additives like plasticisers (Shah et al. 2008; Souza and Fernando 2016).

Biodegradation process involves multi-steps as follows (Lucas et al. 2008; Shah et al. 2008):

- Biodeterioration: Biodegradable polymers are fragmented into very small fractions by the action of microorganisms.
- Depolymerisation: Small fractions of polymers are cleaved by microorganisms with a significant reduction in molecular weight to produce monomers, oligomers and dimers.
- Some of the molecules are produced in the step of depolymerisation, which are consumed by microorganism cells and go across the plasmic membranes. Whereas, the rest of molecules may stay in the extracellular surroundings subjected to different modifications.
- Assimilation: Consumed molecules are integrated into the metabolism of microorganisms to produce energy, storage vesicles and new biomass.
- Mineralisation: $CO_2$, $N_2$, $CH_4$, $H_2O$ and different salts are finally released from intracellular metabolites to the environment after complete oxidisation (Shah et al. 2008; Lucas et al. 2008).

The biodegradation of polymers can be determined using several standard testing methods (Shah et al. 2008; Lucas et al. 2008):

- Visual changes: Biodegradable polymers show visible changes like increased surface roughness, colour changes, fragmentation, crack and hole formation. These changes can be indicative of biodegradation but cannot be used as an evaluation method. Scanning electron microscopy (SEM) and/or atomic force

microscopy (AFM) are generally employed to obtain more informative details relating to biodegradation mechanism and steps.

- Measurements of weight loss: Biodegradable polymers have their mass loss as the degradation is in progress. Therefore, weight loss or residual polymer weight was employed to evaluate the biodegradation rate. Thorough cleaning of polymeric samples is a crucial point during this process particularly with the soil and composting biodegradation.
- Variations of material properties: When polymer samples show weight loss, their rheological properties are also altered accordingly. Mechanical properties, particularly tensile strength, is highly sensitive to weight change causing a reduction in material thickness as well as thermal properties like glass transition temperature ($T_g$) and degree of crystallinity ($X_c$) that are significantly changed as an indicator of material degradation.
- Product formation: $CO_2$ is the end product in a biodegradation process under aerobic conditions by the consumption of $O_2$ to obtain oxidised carbon in polymeric samples. Hence the evaluation of $O_2$ consumption and $CO_2$ production is another signal of biodegradation as well as the generation of other end-products like glucose and acids (Shah et al. 2008; Lucas et al. 2008).

### 2.1.2 Classification of biopolymers

Biopolymers can be classified according to their resources and synthesis processes as follows (Rhim, Park and Ha 2013; Avérous and Pollet 2012; Mensitieri et al. 2011; Averous and Boquillon 2004):

- Biopolymers are extracted directly from biomass resources including plant carbohydrate (e.g. starch, cellulose, agar, etc.), plant and animal protein (e.g.

soy protein, collagen, gelatin, etc.), plant and animal lipids (e.g. wax and fatty acids).

- Biopolymers are chemically synthesised from biomass resources (e.g. polylactic acid (PLA)) and from petrochemical resources (e.g. PVA, poly(glycolic acid) (PGA), poly(ε-caprolactone) (PCL), etc.).
- Biopolymers are produced by microbial fermentation such as microbial polyesters (e.g. poly(hydroxyalkanoates) (PHAs), poly(β-hydroxybutyrate) (PHB), etc.) and microbial polysaccharides (e.g. curdlan and pullulan) (Avérous and Pollet 2012; Averous and Boquillon 2004; Rhim, Park and Ha 2013; Mensitieri et al. 2011), as shown in Figure 2-1.

Most of these neat biopolymers have limited applications because of their poor thermal and barrier properties as well as limited processability despite their good biodegradability, biocompatibility, nontoxicity and viability. Consequently, blending biopolymers with other petroleum-based polymers as well as reinforcing them with nanofillers are a feasible solution to diminishing these limitations (Rhim, Park and Ha 2013; Hu and Wang 2016).

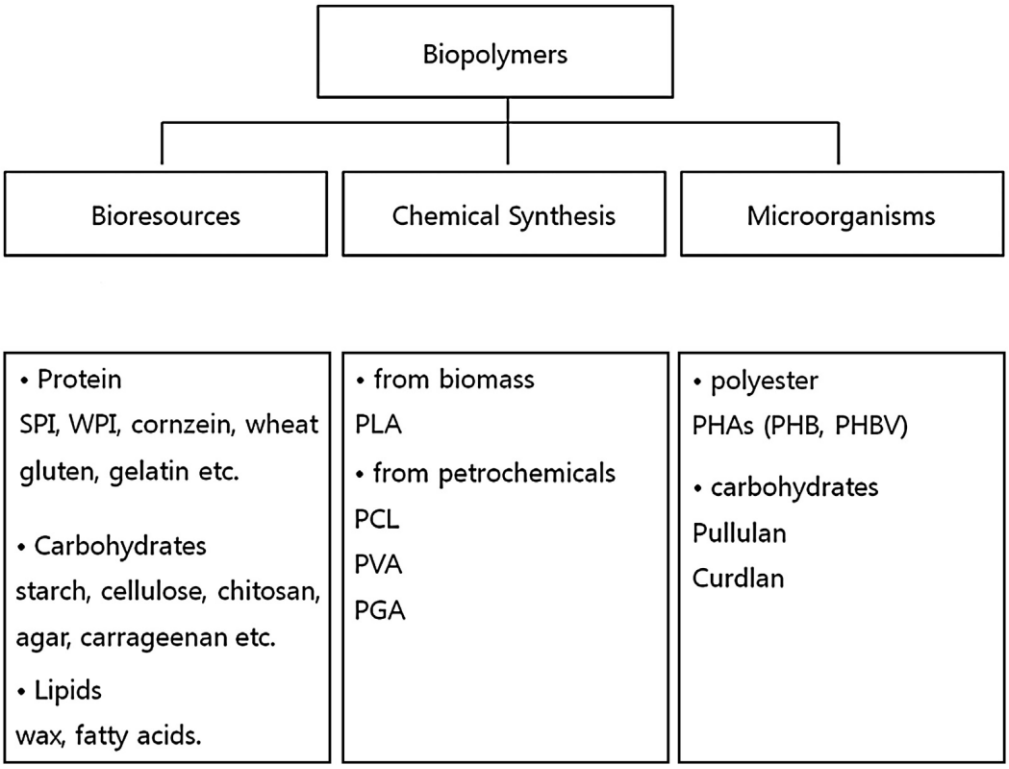


Figure 2-1. Classification of biopolymers (Rhim, Park and Ha 2013)

## 2.2 PVA and PVA blends

PVA is a water-soluble polymer with hydrocarbon backbone (Chiellini et al. 2003; Gaaz et al. 2015). It was synthesised first in 1924 by Herrmann and Haehnel by means of the hydrolysis of polyvinyl acetate (PVAc) with potassium hydroxide in ethanol (Sapalidis, Katsaros and Kanellopoulos 2011; Saxena 2004). PVA is not produced from the direct polymerisation of corresponding monomers. It is manufactured today from the parent homopolymer PVAc (Sapalidis, Katsaros and Kanellopoulos 2011; Chiellini et al. 2003; Ray and Bousmina 2005). Vinyl acetate is polymerised in the presence of alcohol solution like methanol or ethanol via a free-radical mechanism to produce PVAc, and PVA is synthesised by hydrolysing PVAc in one-pot reactor (Chiellini et al. 2003; Mohsin, Hossin and Haik 2011b). Depending on the hydrolysis degree (HD) of PVAc, different grades of PVA can be produced in a wide range of molecular weight from $20\times10^3$ to $400\times10^3$ g/mol and HD levels of 70-99%. PVA is a

semicrystalline polymer consisting of 1,3-diol or 1,2-diol units relative to HD of PVAc with many hydroxyl groups on the surfaces (Gaaz et al. 2015; Mousa, Dong and Davies 2016), as shown in Figure 2-2.

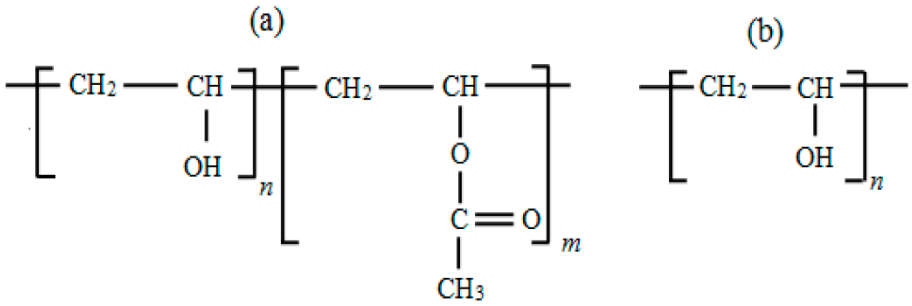


Figure 2-2. Schematic diagram of PVA chemical structures: (a) partial-hydrolysis PVA and (b) full-hydrolysis PVA (Gaaz et al. 2015)

Molecular weight and HD determine most PVA properties, as stated in Figure 2-3. For example, tensile strength, adhesion strength, water and solvent resistance of PVA increase with increasing molecular weight and HD while the solubility, water sensitivity and flexibility decrease (Gaaz et al. 2015; Baker et al. 2012; Tang and Alavi 2011).

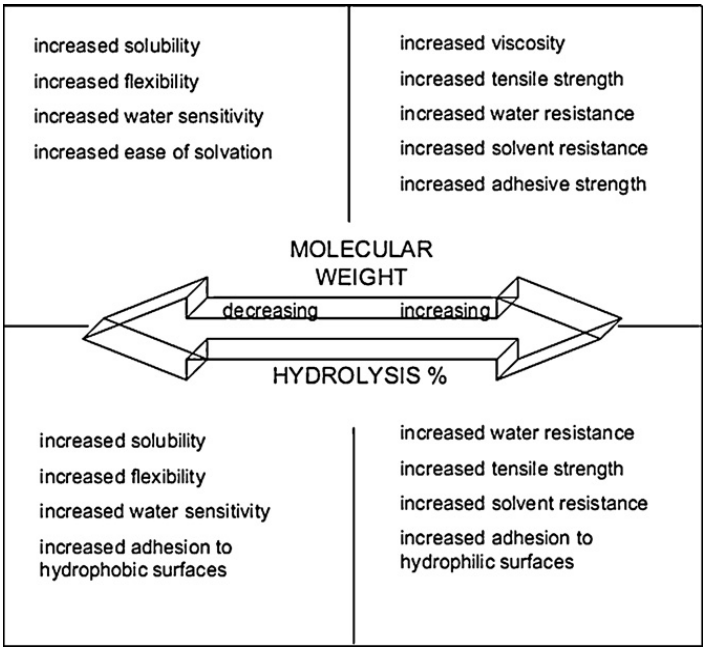


Figure 2-3. Effects of molecular weight and HD on PVA properties (Tang and Alavi 2011)

Full-hydrolysis PVA has limited ductility, and its melting temperature ($T_m$) is very close to the decomposition counterpart. As a result, it is not considered as a thermoplastic material without plasticisers (Jang and Lee 2003; Li, Chen and Wang 2014; Mohsin, Hossin and Haik 2011b). Plasticisers can be defined as a low molecular weight, non-volatile organic compound in possession of a high boiling temperature without the separation from the blends with the reduction of the $T_m$ and $T_g$ for polymers to improve their material processability and flexibility (Sreedhar et al. 2006; Zhang and Han 2006). Consequently, the addition of plasticisers is essential to diminish these limitations particularly during a thermal process like blow moulding and screw extrusion that are widely employed for material packaging applications (Li, Chen and Wang 2014). PVA starts the thermal decomposition around 150ºC, during which many water molecules would release from polymeric molecules to be recovered with the addition of water and/or organic plasticisers (Chiellini et al. 2003). Furthermore, the presence of plasticisers improves the flexibility and reduces the shrinkage during the processing, handling and storage steps (Li, Chen and Wang 2014). On the other hand, partial-hydrolysis PVA is a copolymer of vinyl acetate and vinyl alcohol due to the presence of some residual acetate groups (Roohani et al. 2005). These groups diminish the formation of hydrogen bonding with adjacent hydroxyl groups in PVA blends leading to the decrease in water resistance of blends owing to many free hydroxyl groups. Consequently, partial-hydrolysis PVA is not a suitable option for applications requiring high water resistance like material packaging (Mishra and Rao 1999; Gohil, Bhattacharya and Ray 2006). PVA has good mixed features of properties like good transparency, nontoxicity, odorlessness, compatibility, relatively high biodegradability in some environments and high mechanical properties despite its poor barrier properties, limited thermal stability and relatively high cost compared with

petroleum-based polymers. In order to overcome these limitations by blending PVA with other polymers and/or incorporating nanofillers, PVA is an ideal base material for many different applications particularly in biomedical devices and food packaging (Baker et al. 2012; Gaaz et al. 2015; Sapalidis, Katsaros and Kanellopoulos 2011), so plasticised full-hydrolysis PVA has been used as the main material for our bionanocomposites in this study. Consequently, in the following sections, the most popular PVA blends and nanocomposite systems are discussed.

### 2.2.1 PVA/ST blends

ST is a completely biodegradable, biocompatible and renewable polymer belonging to polysaccharide family. It is a naturally available polymer with relatively good transparency, non-toxicity, odorlessness, tastelessness and cost-effectiveness (García et al. 2015). ST has a chemical formula $C_6H_{10}O_5$ consisting of two different biomacromolecules that are known as amylose and amylopectin as well as minor contents of protein, phosphor and lipids (Corre, Bras and Dufresne 2010; Whistler and Daniel 2000). Amylose has linear biomacromolecules in which $_D$-glucose units are linked by α(1-4) linkage with the molecular weight of $10^5$-$10^6$ g/mol. Whereas, amylopectin has multi-branched biomacromolecules where $_D$-glucose units are linked by α(1-4) at the backbone and α(1-6) at the branches with a relatively high molecular weight of $10^7$-$10^9$ g/mol when compared with amylose counterpart (Visakh 2015; García et al. 2015; Corre, Brase and Dufresne 2010), as illustrated in Figure 2-4.

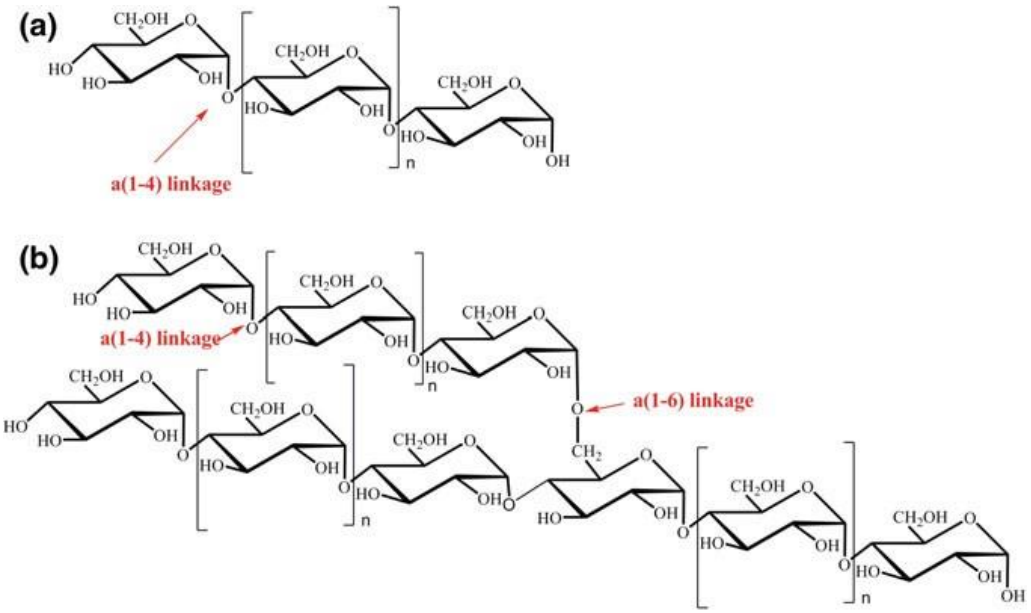


Figure 2-4. Chemical structures of starch : (a) amylose and (b) amylopectin (García et al. 2015)

ST is a semicrystalline polymer with its crystallinity degree ranging from 15 to 45% depending on amylose and amylopectin contents (Shi et al. 2007). The approximate contents of these two macromolecular polymer components are in range of 15-30% for amylose and 70-80% for amylopectin depending on ST resources (García et al. 2015; Avérous and Halley 2009), as summarised in Table 2-1.

Table 2-1. Amylose and amylopectin contents of starch corresponding to their resources

| Starch | Amylose (%) | Amylopectin (%) | References |
|---|---|---|---|
| Maize | 26-28 | 71-73 | (Avérous and Halley 2009) |
| | 25 | 75 | (Robyt 2008) |
| Waxy maize | <1 | >99 | (García et al. 2015; Avérous and Halley 2009) |
| | 0 | 100 | (Robyt 2008) |
| Amylomaize | 48-77 | 23-52 | (García et al. 2015) |

| | | | |
|---|---|---|---|
| | 50-80 | 20-50 | (Avérous and Halley 2009) |
| Amylomaize-5 | 53 | 47 | (Robyt 2008) |
| Corn | 17-25 | 75-83 | (García et al. 2015) |
| High-amylose corn | 55-70 | 30-45 | (García et al. 2015) |
| Amylomaize-7 | 70 | 30 | (Robyt 2008) |
| Potato | 17-24 | 76-83 | (García et al. 2015) |
| | 20-25 | 74-79 | (Avérous and Halley 2009) |
| | 22 | 78 | (Robyt 2008) |
| Wheat | 20-25 | 75-80 | (García et al. 2015) |
| | 26-27 | 72-73 | (Avérous and Halley 2009) |
| | 23 | 77 | (Robyt 2008) |
| Rice | 15-35 | 65-85 | (García et al. 2015) |
| | 19 | 81 | (Robyt 2008) |
| Chickpeas | 30-40 | 60-70 | (García et al. 2015) |
| Tapioca (cassava) | 19-22 | 28-81 | (García et al. 2015) |
| | 17 | 83 | (Robyt 2008) |
| Banana | 17-24 | 76-83 | (García et al. 2015) |
| | 20 | 80 | (Robyt 2008) |
| Cush-cush Yam | 9-15 | 85-91 | (García et al. 2015) |
| Shoti | 30 | 70 | (Robyt 2008) |

ST with many hydrogen bonds between molecules can restrict the mobility of polymeric chains, reduce the flexibility and increase the brittleness (Shi et al. 2007). Furthermore, the $T_m$ of ST at 220-224ºC is close to its decomposition temperature at 220ºC, which makes it hard for material processability as a neat polymer. Consequently, TPS generated in a gelatinisation process is used widely instead of neat ST (Shi et al. 2007). Gelatinisation process is defined as the process to destroy highly

organised crystalline phase of ST and convert it to the amorphous phase in order to produce a plasticised ST paste in the presence of heat, water and/or plasticisers. In this process, hydrogen bonds between ST molecules are replaced with other bonds between the molecules of ST and plasticisers, leading to the improvement of flexibility and reduction in $T_m$ (Avérous and Halley 2009; Majdzadeh-Ardakani, Navarchian and Sadeghi 2010b). TPS still has limitations such as high water sensitivity, poor mechanical strength, limited dimensional and thermal stability (Chiou et al. 2005; Jose et al. 2015). Consequently, blending PVA with ST enhances mechanical and barrier properties of ST as well as improves PVA biodegradability with the cost reduction (Rahmat et al. 2009; Jose et al. 2015). Tănase et al. (2016) found that soil biodegradation of PVA/ST blends could be improved by 32.45% with increasing the ST content from 0 to 20 wt% when compared with that of neat PVA. PVA/ST blends have been widely studied since 1980s for the film production via casting and calendaring methods in order to replace polystyrene in material packaging (Liu, Fing and Yi 1999). These blends have high compatibility in the presence of plasticisers corresponding to chemical interactions between their hydroxyl groups to produce strong hydrogen bonds (Tang and Alavi 2011; Luo, Li and Lin 2012; Tănase et al. 2015; Wang et al. 2015), as illustrated in Figure 2-5. Sin et al. (2010b) confirmed via differential scanning calorimetry (DSC) the compatibility of PVA/ST blends to a certain degree and the addition of 25-35 wt% ST to PVA yielded strong bonding interactions between PVA and ST similar to those between neat PVA molecules.

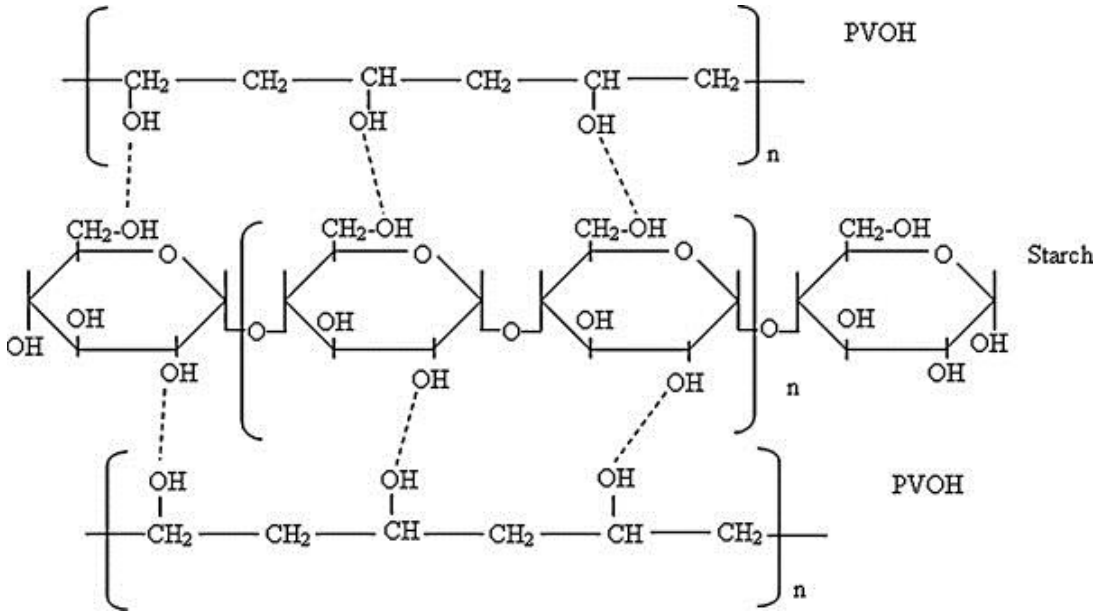


Figure 2-5. Hydrogen bonds between PVA and ST (marked with dashed lines) (Tang and Alavi 2011). Note that PVOH is PVA

Glycerol (GL) is the best material candidate as a plasticiser for PVA/ST blends due to their close solubility parameters, namely 21.10, 22.50 and 23.40 $MPa^{1/2}$ for PVA, ST and GL, respectively (Rahman et al. 2010). Zanela et al. (2015) prepared PVA/ST/GL blends with different blend ratios of 50:20:30, 30:40:30, 40:20:40:, 45:20:35, 30:30:40, and 32.5:32.5:35 by weight, and investigated the effect of each component on their properties. All blend ratios reflected good processability with homogeneous morphological structures. Moreover, their results showed that a high content of PVA improved mechanical and barrier properties, whereas a higher GL content reduced the mechanical strength and improved elongation at break due to its plasticisation effect. Furthermore, much higher ST content improved biodegradability and reduce water resistance. Overall, the blend ratio is a crucial factor to determine the resulting properties.

### 2.2.2 PVA/PLA blends

PLA is a biodegradable aliphatic polyester that is synthesised from biomass resources like potato, corn and cane sugar (Castro-Aguirre et al. 2016) with a chemical structure, as illustrated in Figure 2-6. Lactic acid monomers (L- and D-lactic acid) are obtained chemically or biologically from the fermentation of carbohydrates by lactic bacteria like *Lactobacillus* genius. Then PLA with low molecular weight can be produced from these monomers by the polycondensation reaction (Avérous and Pollet 2012; Ray and Bousmina 2005). Whereas, high-molecular-weight PLA is obtained by means of open ring polymerisation (ORP) of lactide monomer (Avérous 2004; Avérous and Pollet 2012). Different kinds of PLA are commercially available depending on L/D-lactic acid ratio such as PLLA (100% L-lactic acid) and PDLLA (copolymer of D, L-lactic acid) (Avérous and Pollet 2012).

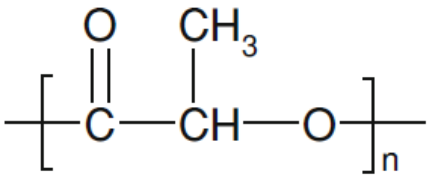


Figure 2-6. Chemical structure of PLA (Avérous and Pollet 2012)

Although PLA has good mechanical, thermal and barrier properties as well as biodegradability (Ray and Bousmina 2005), it has limited applications due to low flexibility and high hydrophobic nature leading to poor water uptake and slow hydrolytic degradation rates (Zhang, Xu and Jiang 2012). These limitations can be overcome by blending PLA with other biopolymers and petroleum-based polymers (Mousa, Dong and Davies 2016). PVA is one of these polymers that can blend widely with PLA to improve mechanical and thermal properties as well as water resistance of PVA (Huang et al. 2018). According to Shuai et al. (2000), PVA/PLA blends had good

miscibility due to the existence of single peaks for $T_g$ and $T_m$ in DSC curves. Similarly, Restrepo et al. (2018) and Yeh et al. (2008) found that the single $T_g$ was good evidence of the formation of a compatible binary system for PVA/PLA blends because of the interaction between hydroxyl groups of PVA with carbonyl groups of PLA. Moreover, PVA/PLA blends have better mechanical properties compared with neat polymers (Li, Chen and Wang 2014). In addition, Hu, Wang and Tang (2013) prepared composite films by mixing PVA with ST/lactic acid graft (ST-g-PLA) copolymers. Their results showed the tensile strength and elongation at break for ST-g-PLA/PVA films were increased by 69.15 and 84.39%, respectively, as well as the water absorption was decreased by 50.39% when compared with those of ST/PVA films.

### 2.2.3 PVA/chitin blends

Chitin is a biodegradable and biocompatible polymer extracted from the shells of insects, crabs, shrimps and lobsters through the decalcification (i.e. acidic treatment), deproteination (i.e. alkaline treatment) and finally decolourisation for industrial-scaled production (Van den Broek et al. 2015). Chitin consists of β-(1→4)-2-acetamido-2-deoxy-$_D$-glucopyranose units with small amounts of β-(1→4)-2-amino-2-deoxy-d-glucopyranose residues (Van den Broek et al. 2015; Chandra and Rustgi 1998; Avérous and Pollet 2012), as shown in Figure 2-7. It is a highly acetylated biopolymer and widely available in nature as the secondary to cellulose (Avérous and Pollet 2012). When the acetylation degree of chitin is less than 50%, it would be known as chitosan (Van den Broek et al. 2015). This polymer has antimicrobial activities and is insoluble in water, but it also has the ability of water retention and moistening properties. As such, it is mainly applicable for packaging and cosmetic sectors (Chandra and Rustgi 1998).

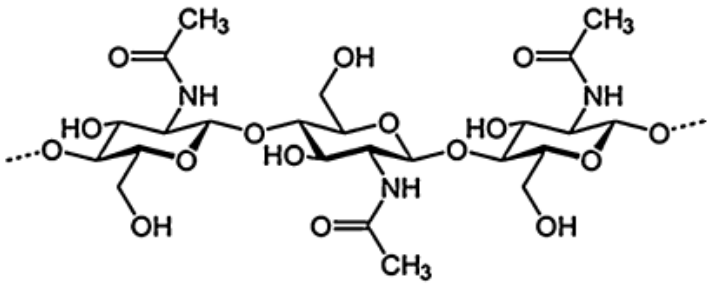

Figure 2-7. Chemical structure of Chitin (Van den Broek et al. 2015)

Chitin has a highly ordered crystalline structure with a number of intra- and intermolecular hydrogen bonds (Avérous and Pollet 2012). According to Aoi, Takasu and Okada (1995), this rigid crystalline structure is the main reason for poor water solubility and high intractability. Consequently, blending chitin with other biocompatible polymers like PVA could diminish these limitations (Aoi, Takasu and Okada 1995). Their DSC results showed that PVA/chitin blends had a single $T_g$ due to high miscibility between components and this $T_g$ decreased with increasing the chitin content from 0 to 70 wt%. Furthermore, the biodegradability of PVA blends is relatively high in the presence of chitin because chitin is a completely biodegradable polymer (Takasu et al. 1998).

### 2.2.4 PVA/chitosan blends

Chitosan is a linear aliphatic polyamide copolymer obtained mainly from the deacetylation of chitin, which is available in seafood crusts with a molecular structure of β(1,4)-2-amino-2-deoxy-$_D$-glucose (Ray and Bousmina 2005; Van den Broek et al. 2015; Mujtaba et al. 2019), as shown in Figure 2-8. The cationic amino groups distribute around the chitosan's backbone resulting in antimicrobial properties against fungi, yeast and bacteria (Van den Broek et al. 2015). Chitosan is a semicrystalline polymer and the degree of crystallinity and many other properties like viscosity and solubility are controlled by the deacetylation degree and molecular weight (Avérous

and Pollet 2012; Kasai 2018). The molecular weight and deacetylation degree range from $5\times10^3$ to $1\times10^6$ g/mol and 2 to 60%, respectively, depending on the source of chitosan (Avérous and Pollet 2012).

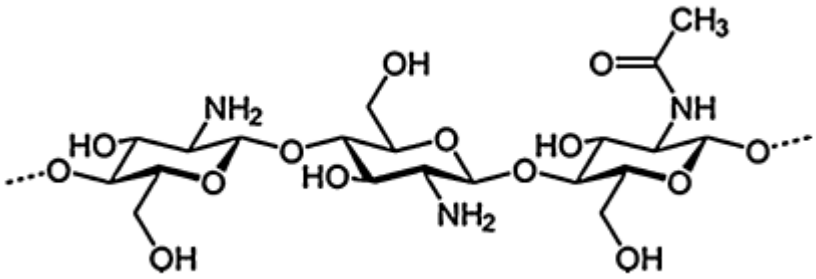


Figure 2-8. Chemical structure of chitosan (Van den Broek et al. 2015)

Chitosan is a biodegradable polymer belonging to polysaccharide family with nontoxicity, wide availability, cost effectiveness, insolubility in water and most organic solvents, but it can be dissolved in acidic solutions with a pH value being lower than 6.3 (Van den Broek et al. 2015; Hu and Wang 2016). Furthermore, it has excellent processability and good barrier properties against gas and aroma despite limited mechanical strength (Giannakas et al. 2016; Tripathi, Mehrotra and Dutta 2009). Consequently, blending hydrophilic PVA with biological active chitosan could produce beneficial antimicrobial films with acceptable mechanical and barrier properties for many applications like food packaging by improving their shelf life (He and Xiong 2012; Tripathi, Mehrotra and Dutta 2009). Liu, Wang and Lan (2018) reported that PVA/chitosan blends at a weight blend ratio of 70:30 demonstrated smooth and homogenous surfaces on SEM morphology without typical defects such as phase separation, pores, bubbles and cracks, which was considered as an evidence of good compatibility between components. Nevertheless, increasing the chitosan content up to 35 wt% in PVA/chitosan blends showed high surface roughness. Similarly, He and Xiong (2012) found PVA/chitosan blends had homogenous

morphological structures with the aid of SEM due to the good compatibility between components. Furthermore, the swelling degree of PVA/chitosan blends at a blend ratio of 2:3 in distilled water could be reduced by 60% when compared with that of neat PVA counterparts due to an overall balance between hydroxyl groups of PVA and amino groups of chitosan. This led to a built-up rigid structure with the minimum number of free hydroxyl groups interacting with water molecules. Moreover, Tripathi, Mehrotra and Dutta (2009) used PVA/chitosan blends as a coating solution for fresh tomatoes, and their results showed a clear decline of fungi growth rate as opposed to uncoated counterparts, as well as an increase in the shelf life.

### 2.2.5 PVA/gelatin blends

Gelatin is a completely biodegradable, biocompatible and water-soluble polymer (Chandra and Rustgi 1998). It is prepared mainly from collagen extracted from fibrous tissues of skins, bones, blood vessels and intervertebral disc (Avérous and Pollet 2012; Djagny, Wang and Xu 2001). Depending on different pre-treatment methods of collagen, two types of gelatin are produced. Type A gelatin is derived by using acidic treatment and type B gelatine is obtained from alkaline treatment (Ray and Bousmina 2005; Djagny, Wang and Xu 2001). Both types consist of approximately 19-amino acid groups that are joined by peptide linkages with a typical structure of –Ala–Gly–Pro–Arg–Gly–Glu–4Hyp–Gly–Pro– (Ray and Bousmina 2005; Chandra and Rustgi 1998), illustrated in Figure 2-9. Gelatin is widely used for food industry due to its transparency, clarity, purity, nontoxicity and non-irritation as well as for pharmaceutical and medical applications (Chandra and Rusrgi 1998; Djagny, Wang and Xu 2001).

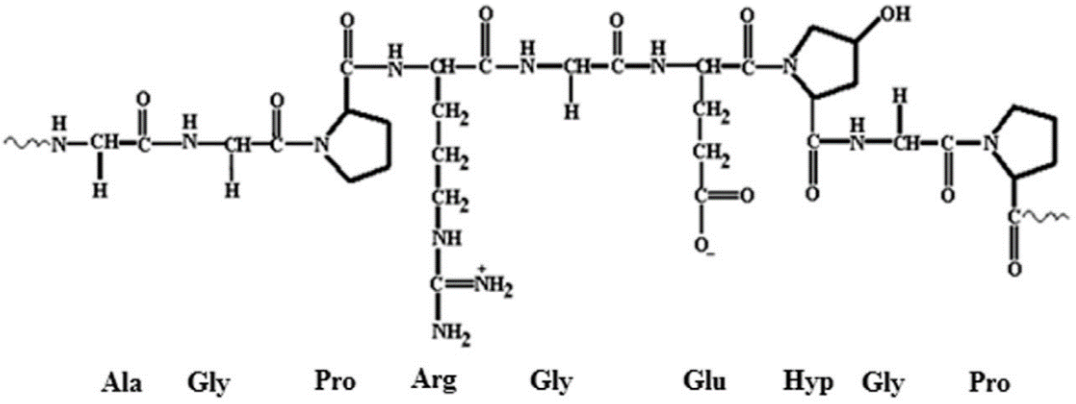


Figure 2-9. Chemical structure of gelatin (Devi et al. 2017)

The presence of triple helix in the gelatin structure is the main reason for high strength and poor water swelling. Consequently, blending gelatin with hydrophilic polymers like PVA could improve the swelling properties (Pawde and Deshmukh 2008A; Pal 2007). On the other hand, PVA/gelatin blends possess high ability to form films and hydrogels, which makes such blends a good material candidate for many biomedical applications (Liu et al. 2010; Pal 2007; Ino 2013). Furthermore, Pawde and Deshmukh (2008a) also reported that the poor electrical conductivity of PVA could be overcome when blended with gelatin. Blending PVA with gelatin changed the PVA structure by decreasing both of chain space and free-volume dipoles leading to the change of blend polarisation behaviour at different frequencies along with the enhancement of electrical properties.

### 2.2.6 Manufacturing processes

Solution casting, extrusion and melt blending are the most popular manufacturing processes used to prepare neat PVA and PVA blend films according to

Table 2-2. In solution casting process, PVA and/or other polymers are dissolved in a suitable solvent like water and acidic solution at specific temperature levels depending on polymer properties by continuous mixing to minimise bubbles within the solution.

Then the completely clear solution is cast in the mould and dried in an oven or under the ambient condition (Gohil, Bhattacharya and Ray 2006; Sin et al. 2010b; Jayasekara et al. 2004; Zhou et al. 2009). The same procedure was followed by Mohsin, Hossin and Haik (2011b, 2011a) to prepare plasticised PVA films with glycerol and sorbitol by dissolving 5 wt% PVA in 10 ml distilled water at 90ºC using magnetic stirring. Different plasticiser contents were added to the completely dissolved PVA by continuous stirring for 6 h in order to produce a homogenous solution, which was then cast on PTFE plates and dried at 80ºC in a vacuum oven. Solution casting has been deemed as the best processing method for PVA/ST blends since 1980s because PVA can easily degrade in melt processing (Tang and Alavi 2011). From an economic viewpoint, solution casting is an unacceptable manufacturing process as a result of limited efficiency and relatively high cost when compared with thermoplastic processing using extrusion or melt blending (Tang and Alavi 2011; Zou, Qu and Zou 2008, 2007).

Table 2-2. PVA blends prepared in different manufacturing processes

| **Polymer blend** | **Manufacturing process** | **Reference** |
|---|---|---|
| Plasticised PVA | Solution casting | (Mohsin, Hossin and Haik 2011a, 2011b; Lim and Wan 2008) |
| Plasticised PVA | Extrusion | (Kopcilova et al. 2012) |
| Cross-linked PVA | Solution casting | (Lim et al. 2015; Gohil, Bhattacharya and Ray 2006) |

| | | |
|---|---|---|
| PVA/ST | Solution casting | (Zhou et al. 2009; Jayasekara et al. 2004; Ismail and Zaaba 2011; Aydın and Ilberg 2016; Shi et al. 2008; Tudorachi 2000; Das et al. 2010; Ramaraj 2007b, 2007a; Sin et al. 2010b; Yoon, Cough and Park 2006, 2007; Yin 2005) |
| PVA/ST | Extrusion | (Wang et al. 2015; Mao et al. 2002; Zou, Qu and Zou 2007, 2008; Sin et al. 2010a; Zanela et al. 2015, 2018) |
| PVA/ST | Melt blending | (Tănase et al. 2015; Chai et al. 2009; Tian et al. 2017a) |
| PVA/PLA | Extrusion | (Li, Chen and Wang 2014; Gajria and 1996) |
| PVA/PLA | Melt blending | (Restrepo et al. 2018; Yeh et al. 2008) |
| Chitosan/PVA/PLA | Solution casting | (Zhang, Xu and Jiang 2012; Grande and Carvalho 2011) |
| PVA/chitin | Solution casting | (Aoi, Takasu and Okada 1995; Takasu et al. 1998; Aoi, Takasu and Okada 1997) |

| | | |
|---|---|---|
| PVA/chitosan | Solution casting | (He 2012; Tripathi, Mehrotra and Dutta 2009; Kasai 2018; Liu, Wang and Lan 2018; Hu and Wang 2016) |
| PVA/gelatin | Solution casting | (Maria 2008; Pawde and Deshmukh 2008a; Pawde, Deshmukh and Parab 2008b; Pal 2007; Ino 2013; Mendieta-Taboada 2008) |

In an extrusion process, the weighed amounts of polymers with other additives are blended at room temperature (i.e. dry blending) (Wang et al. 2015) or at an elevated temperature (i.e. melt blending) (Li, Chen and Wang 2014), which were then fed to a single-screw extruder (Mao et al. 2002; Zou, Qu and Zou 2007, 2008) or a twin-screw extruder (Wang et al. 2015; Zanela et al. 2015) with the sophisticated design for extrusion processing parameters such as screw speed and temperature profile from different zones starting from the feeder to the die (Wang et al. 2015; Zou, Qu and Zou 2008). The extruded pellets can be co-extruded to a flat die (Zanela et al. 2015), blowed (Wang et al. 2015) and cold pressed (Li, Chen and Wang 2014) to produce films. The screw extrusion is hard to use for processing PVA/ST blends due to their unique rheology in term of moisture content and processing temperature (Zou, Qu and Zou 2008, 2007). On the other hand, PVA is hard to be processed in extrusion because its processing temperature is very close to both degradation and melting temperatures (Chiellini et al. 2003). Consequently, solution casting is considered as the most suitable method for processing PVA blends.

Melt blending process is used to prepare products with their final form. Polymers are mixed in the dry form, and then blended together through mixers (e.g. Brabender mixer) (Restrepo et al. 2018) with a blade type rotary to melt them at a predefined temperature, rotating speed and time (Tănase et al. 2015). Then the molten blends are hot pressed in the mould at the specific temperature, pressure, time and dimensions (Yeh et al. 2008; Chai et al. 2009). Tănase et al. (2015) found that there was a relationship between material formulation of plasticised PVA/ST blends and melt processing parameters. Their results showed that increasing the ST content from 0 to 30 wt% in the blends increased the melt viscosity when compared with plasticised PVA blends leading to an increase in power consumption with much harder processability. Overall, PVA/ST blends at a low ST content are much easier to be processed in melt blending process.

### 2.2.7 Properties

As mentioned earlier, most PVA properties depend on molecular weight and HD (Baker et al. 2012; Tang and Alavi 2011). Moreover, these properties can be modified by using blending processes. Polymer blending is an effective method to produce a material system with better properties as opposed to their individual components in order to avoid inherent limitations of neat polymers (Gupta, Agarwal and Alam 2013). Therefore, blending PVA with other polymers particularly with polymers having similar solubility parameters can improve overall blend material performance owing to the formation of strong hydrogen bonds instead of weak van der Waals interaction (Rahmat et al. 2009).

Material morphological structures should be analysed carefully as a key indicator for many other material properties. SEM images of neat PVA films showed smooth and

homogenous surfaces with some irregularities along the cross section, reflecting typical semi-crystalline structures of PVA (Cano et al. 2015c, 2016), as depicted in Figure 2-10.

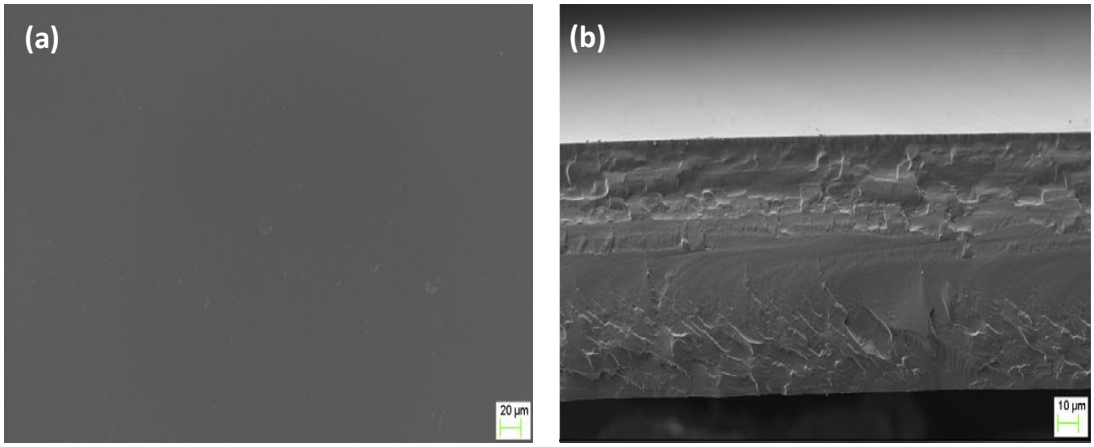


Figure 2-10. SEM images of neat PVA: (a) surface structure and (b) cross-sectional structure (Cano et al. 2015c)

Smooth and homogenous morphological structures disappear when PVA is blended with ST particularly when the PVA content is equal to or higher than the ST content due to their partial miscibility consisting of ST-rich phase that is distributed in PVA-rich phase (Cano et al. 2015b), Figure 2-11-(a). This structure is completely changed when plasticising PVA/ST blends with glycerol due to the enhanced compatibility between polymers (Cano et al. 2015b). Moreover, an excessive amount of plasticisers may form oily layers on the film surface, as evidenced by a blooming/blushing phenomenon under SEM examination (Ismail and Zaaba 2011), Figure 2-11-(b). The presence of GL helps to improve the compatibility between PVA and chitosan as well to produce smooth and homogenous blend surfaces (Grande, Pessan and Carvalho 2015; Grande and Carvalho 2011). As such, the presence of plasticisers is beneficial to increase the compatibility. However, a higher plasticiser content could also cause phase separation while the lower content induced hardening effect instead of the plasticisation.

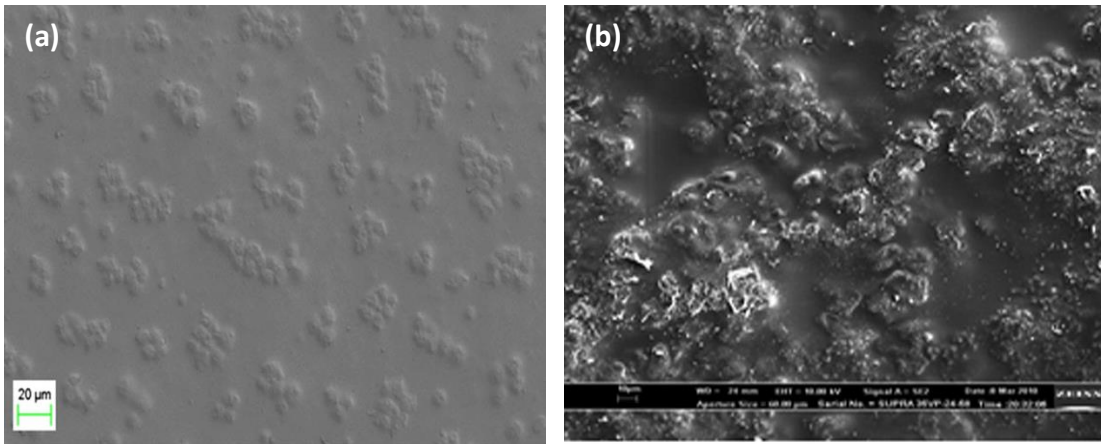


Figure 2-11. SEM images for (a) un-plasticised PVA/ST blends (Cano et al. 2015b), and (b) over-plasticised PVA/ST blends (Ismail and Zaaba 2011)

Neat full-hydrolysis PVA has maximum values of tensile strength, Young's modulus and elongation at break about 1.6 GPa, 48.0 GPa and 6.5%, respectively (Minus et al. 2009; Song et al. 2013; Gaaz et al. 2015), as opposed to 25.4 MPa, 27.6 MPa and 260% accordingly for partial-hydrolysis PVA (Loryuenyong et al. 2015). Blending PVA with PLA improved the tensile strength and water resistance compared with neat PVA counterparts (Restrepo et al. 2018; Gajria et al. 1996). Li, Chen and Wang (2014) reported that the tensile strength of plasticised PVA/PLA blends was increased by 11.86% as compared with that of plasticised PVA counterparts while the elongation at break was decreased by 14.81%. Furthermore, the water contact angle of blends increased slightly as a sign of the improvement of water resistance. Moreover, Liu et al. (2018) prepared PVA/PLA membranes with high miscibility between components leading to the improvement of Young's modulus by 170% as opposed to that of neat PVA, which have been successfully used as high-performance tissue scaffolds in biomedical areas. A similar behaviour of improving tensile strength and reducing elongation at break was also observed when blending PVA with chitosan due to the interactions between hydroxyl groups of PVA with $NH_2$ and hydroxyl groups of chitosan (Giannakas et al. 2016). For instance, Zhuang et al. (2012) prepared a series

of PVA/chitosan membranes with their weight blend ratios of 3:1, 2:1, 1:1, 1:2 and 1:3. Their results showed that tensile strength and flexibility improved linearly with increasing the PVA content. Whereas, cytotoxicity and microbial growth were decreased with increasing the chitosan content leading to potential applications of these blends in guided tissue regeneration (GTR). Furthermore, Bonilla et al. (2014) found that blending PVA with 20 wt% chitosan could significantly improve tensile strength and Young's modulus of PVA/chitosan by 86.95 and 428.51%, respectively due to the better interactions between them. Gelatine reflected similar effect on mechanical properties according to Hago and Li (2013). Their results showed that tensile strength and Young's modulus of PVA/gelatine blends were increased by 60.97 and 77.78%, respectively, as opposed to those of neat PVA due to the dense and rigid morphological structures of blends. On the other hand, blending PVA with ST improved Young's modulus and reduced the tensile strength and elongation at break owing to high brittleness and amorphous nature of ST regardless its sources (Chen et al. 2008). This behaviour appeared to be more pronounced with increasing ST content in the blends (Ramaraj 2007a; Azahari, Othman and Ismail 2011). Consequently, many studies have focused on using cross-linking agents like sodium benzoate, borax, citric acid, boric acid, glutaraldehyde and tetraethylene glycol diacrylate to improve mechanical properties of PVA/ST blends (Zhou et al. 2009; Das et al. 2010; Shi et al. 2008). These agents form strong intermolecular linkages between components by reacting with the hydroxyl groups of polymers leading to the enhancement of tensile strength (Zhou et al. 2009; Yoon, Cough and Park 2007). Besides, plasticisers like urea and different polyol based materials are used to enhance the flexibility and elongation at break for blends by penetrating between polymeric chains to improve their mobility and free volumes (Aydın and Ilberg 2016; Ismail and Zaaba 2011). In other words,

mechanical properties of blends depend on the properties of individual components as well as the interactions between them.

Thermal properties of neat PVA and its blends can be determined with the aid of thermogravimetric analysis (TGA) and DSC. The $T_m$ of neat PVA is determined to be 230ºC while the $T_g$ becomes a function of HD. A full-hydrolysis PVA has a $T_g$ around 85ºC as opposed to 58ºC for partial-hydrolysis PVA (Holland and Hay 2001). PVA can thermally degrade in both molten and solid states. The high flexibility and chain mobility of PVA in a molten state promotes the fragmentation and elimination of chain segments, which produces saturated and unsaturated volatile ketones and aldehydes as well as water (Holland and Hay 2001). While in the solid state, the side groups are eliminated and followed by the reduction of melting temperature and degree of crystallinity with the production of appreciable amounts of polyenes in isolated and conjugated forms, as well as small amounts of carboxyl groups (Holland and Hay 2001). Neat PVA films prepared by solution casting possess similar thermal degradation steps to those of PVA blends. The initial step includes 10% weight loss due to the loss of bonded water at around 100ºC. The second step lies in 70% weight loss as a result of the degradation process with dehydration, polymer scission and decomposition at a temperature range of 150-380ºC. Further, the third step comprises the formation of end products taking place at a temperature range of 380-500ºC (Cano et al. 2015b). In comparison with PVA/PLA blends and PVA/chitin blends (see sections 2.2.3 and 2.2.2), PVA/ST blends do not show a single and clear $T_g$ because of the partial miscibility of polymers in the absence of plasticisers (Cano et al. 2016). Furthermore, the presence of plasticisers decreases the $T_g$ and $T_m$, as well as degree of crystallinity and thermal enthalpy of both neat PVA and PVA blends (Aydın and Ilberg 2016). Generally, these plasticiser molecules are smaller than polymer molecules,

which makes them easier to penetrate polymeric chains and reduce cohesion forces between polymeric molecules leading to improve their chain mobility (Ramaraj 2007a).

Neat PVA is not a completely biodegradable polymer in all environments particularly in the absence of specific conditions such as relative humidity, temperature, pH level and types of microorganisms (Kopcilova et al. 2012). Neat PVA is completely biodegradable in activated sludge, whereas its degradation-rate range of 8-9% over the period of 74 days in soil, and was increased up to 13% in an aerobic condition on the 21st day (Kopcilova et al. 2012; Chiellini et al. 2003). Consequently, neat PVA is blended with other polymers like ST and chitin to improve the biodegradability in different environments. Lots of studies have showed that ST can be attacked and consumed first by the microorganisms in PVA/ST blends in soil burial biodegradation tests because it is a completely biodegradable polymer. Since porous residues of PVA films are left behind, weak structures can be fragmented easily (Shah et al. 2008; Siracusa et al. 2008; Bin-Dahman, Jose and Al-Harthi 2016; Spiridon et al. 2008). A similar behaviour can also be identified in PVA/chitin blends. Takasu et al. (1998) reported that the residual weight of soil burial films was decreased after 150 days from 89% for neat PVA films to 24% for PVA/chitin films. The biodegradation of PVA blend films depends on the blend components, miscibility of these components and types of biodegradation media (Shuai et al. 2000).

Neat PVA as a water soluble polymer has poor water resistance in terms of water solubility ($W_s$), water uptake ($W_a$), and water contact angle as well as water vapour permeability (*WVP*) (Chiellini et al. 2003). Whereas, it has good gas barrier properties due to dense, small and closely packed crystallites (Jang and Lee 2003). Moreover, barrier properties of PVA blends can be affected by temperature, relative humidity,

chemical contents such as plasticisers and cross-linking agents, as well as hydrophilicity of blend components (Bertuzzi et al. 2007). For instance, *WVP* and $W_s$ of most PVA/ST films were increased linearly with increasing the ST content in the blends because of high hydrophilicity of ST particularly in the presence of plasticisers (Cano et al. 2016; Azahari, Othman and Ismail 2011; Ismail and Zaaba 2011). Furthermore, PVA/chitin blends show higher hydrophilicity when compared with neat PVA , as evidenced by decreasing water contact angle (Takasu et al. 1998). According to Liu, Wang and Yi (2018), blending PVA with chitosan reduced the gas permeability due to strong interactions between the components that produced a strong packed structure. Whereas, the *WVP* of blends was increased as the hydrophilicity of blends was increased due to improve the diffusivity of water molecules within the films. As such, barrier properties of PVA are not significantly improved when blended with other biopolymers, however, it can be altered with the incorporation of hydrophobic fillers.

## 2.3 PVA nanocomposites

Polymer nanocomposites consist of nanoscaled reinforcement constituents uniformly dispersed in continuous polymer matrices (i.e. neat polymers or polymer blends) (Youssef 2013). such nanofillers can be categorised as one dimensional (nanoplatelets), two dimensional (nanotubes) and three dimensional (spherical nanofillers) (Youssef 2013). Superior improvement in material properties such as barrier, mechanical and thermal properties of polymer nanocomposites can be achieved at small nanofiller contents ($\leq$ 5 wt%) when compared with conventional polymer composites reinforced with 40-50 wt% conventional fillers (Rhim, Park and Ha 2013; Ray and Bousmina 2005). On the other hand, polymer nanocomposites still

face the limitations in relation to the dispersion of nanofillers during the processing as well as nanofiller agglomeration at high contents, as shown in Figure 2-12 (Julkapli, Bagheri and Sapuan 2015). Biopolymers are used widely as the matrices of polymer nanocomposites to enhance their relatively low mechanical and thermal properties as well as poor barrier properties as opposed to petroleum-based polymers (Dong et al. 2015a). In particular, PVA is regarded as good matrices for polymer nanocomposites when used in medical and packaging applications (Dong et al. 2015a).

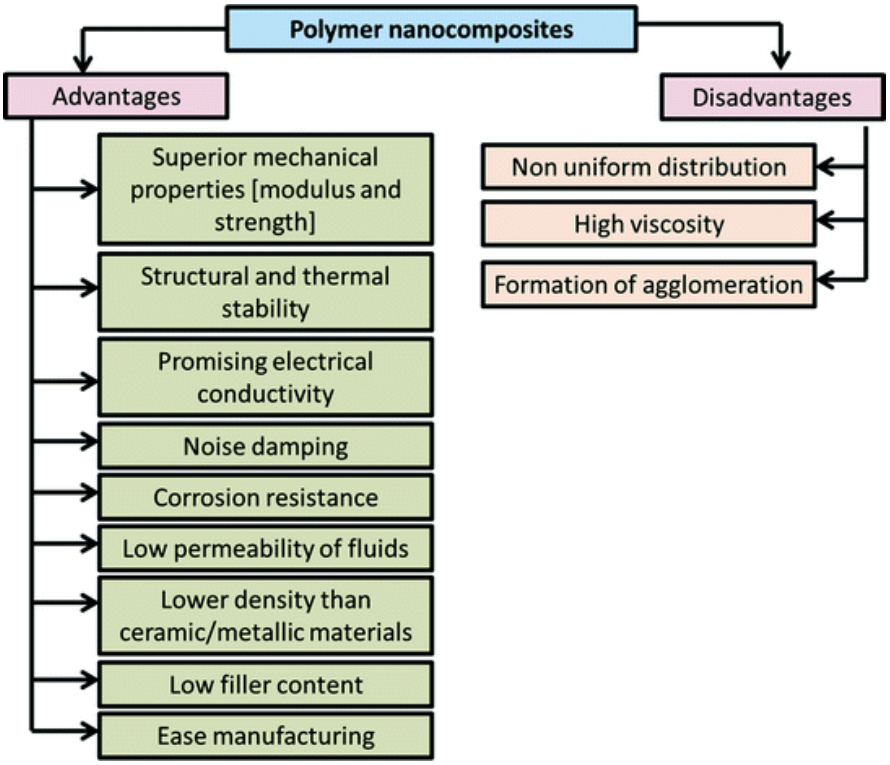


Figure 2-12. Advantages and disadvantages of polymer nanocomposites (Julkapli, Bagheri and Sapuan 2015)

### 2.3.1 PVA/montmorillonite (MMT) nanocomposites

MMTs are the most popular clays belonging to the family of layered silicates used as nanofillers in polymer nanocomposites (Youssef 2013). MMTs have a 2:1 layered structure consisting of one crystal sheet of alumina octahedron sandwiched between two crystal sheets of silica tetrahedron (Rhim and Ng 2007; Sapalidis, Katsaros and

Kanellopoulos 2011), Figure 2-13. These layers have the ability to organise themselves in stacks with regular van der Waals gaps, which are known as galleries or interlayers with the thickness of 1 nm and the length in range of 30 nm to several microns. These van der Waals forces are relatively weak, so small molecules like water, chemicals, and monomers as well as polymers could easily penetrate between them and expanded MMT interlayers (Sapalidis, Katsaros and Kanellopoulos 2011; Ray and Bousmina 2005; Ray et al. 2006). MMTs are inorganic materials with hydrophilic nature due to the presence of hydrated sodium and potassium ions to improve the miscibility with hydrophilic polymers such as PVA (Ray and Bousmina 2005; Rhim and Ng 2007). Unique characteristics of MMTs like high surface area (750 $m^2/g$) and high aspect ratio (50-1000) can greatly enhance mechanical and thermal properties of polymer/MMT nanocomposites (Rhim, Park and Ha 2013).

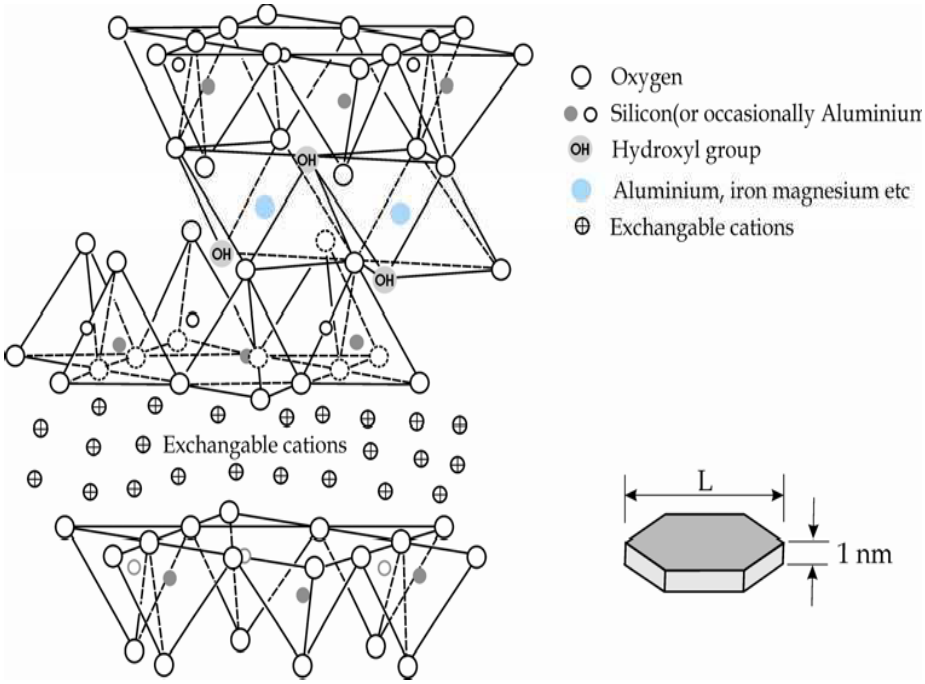


Figure 2-13. Chemical structure of MMTs (Sapalidis, Katsaros and Kanellopoulos 2011)

The resulting properties and structures of polymer/clay nanocomposites depend on nanoclay dispersibility within polymer matrices (Sapalidis, Katsaros and

Kanellopoulos 2011). Three different structures of polymer/clay nanocomposites can be produced based on material selection and preparation methods, as shown in Figure 2-14 (Ray et al. 2006; Rhim and Ng 2007):

- ***Tactoid structure***: also known as non-intercalated structure (Ray et al. 2006), non-mixing composites or microcomposites (Sapalidis, Katsaros and Kanellopoulos 2011). In this structure, polymeric molecules cannot diffuse between clay interlayers due to no interaction between them, generally resulting in conventional microcomposite structures (Arora and Padua 2010).
- ***Intercalated structure***: polymeric chains are intercalated between clay interlayers and expanded with *d*-spacing values of 2-5 nm to produce multilayered morphological structures consisting of alternative polymeric chains and clay layers (Sapalidis, Katsaros and Kanellopoulos 2011; Rhim and Ng 2007).
- ***Exfoliated structure***: the clay interlayers are expanded by more than 5-10 nm when individual and randomly-oriented clays are homogeneously dispersed within continuous polymer matrices to yield a completely exfoliated structure (Sapalidis, Katsaros and Kanellopoulos 2011; Rhim and Ng 2007).

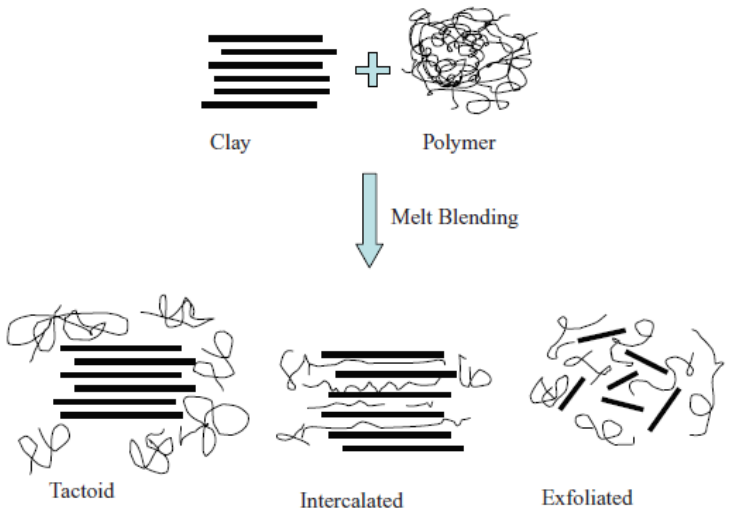


Figure 2-14. Polymer/clay nanocomposite structures (Arora and Padua 2010)

Both intercalated and exfoliated structures can be found in PVA/MMT nanocomposites (Sapalidis, Katsaros and Kanellopoulos 2011). Furthermore, XRD results showed that the *d*-spacing of MMTs within PVA/MMT nanocomposites was increased up to 1.92 nm when compared with pristine MMT counterparts, and the degree of intercalated structures was increased with increasing the MMT content. Moreover, associated results determined by transmission electron microscopy (TEM) demonstrated clear exfoliated structures at the MMT contents of 0.1 and 0.2 wt% though the degree of exfoliated structures was decreased with increasing the MMT content (Li et al. 2015). Furthermore, Majdzadeh-Ardakani and Nazari (2010a) reported that the tensile strength of PVA/ST/MMT nanocomposites was increased by 30.18% with the incorporation of 4 wt% MMTs when compared with that of neat polymers due to the formation of exfoliated/intercalated structures. Nonetheless, the tensile strength of such nanocomposites declined beyond 4 wt% MMTs in the absence of exfoliated clay structures particularly at high MMT content levels when typical MMT agglomeration took place. In short, the resulting structures of polymer/clay nanocomposites depends on nanofiller dispersion within polymer matrices. In other words, well dispersed nanofillers can produce exfoliated structures particularly at low nanofiller contents. Whereas, such exfoliated structures can be replaced by intercalated counterparts with increasing the nanofiller content.

### 2.3.2 PVA/halloysite nanotube (HNT) nanocomposites

HNTs are considered as the other popular nanoclays that were discovered first by Omalius d'Halloy in 1826 (Mousa, Dong and Davies 2016; Joussein et al. 2005). HNTs are naturally available nanoclays formed by the hydrothermal alteration of alumina silicate minerals. HNTs can exist in different forms depending on their

formations (Joussein et al. 2005). The tubular form of HNTs is more popular than spherical and plate-like counterparts with typical inner diameters of 5-20 nm, outer diameters of 10-50 nm and the length of 500 nm-1.2 µm depending on their sources (Khoo, Ismail and Ariffin 2011; Rawtani and Agrawal 2012). HNTs have a chemical formula $Al_2Si_2O_5(OH)_4.nH_2O$ similar to kaolin with a monolayer of water (Khoo, Ismail and Ariffin 2011; Rawtani and Agrawal 2012). The material classification of HNTs depends on *n* values with *n*=2 and *d*-spacing of 10 Å for hydrated HNTs, as well as *n* =0 and *d*-spacing of 7 Å for dehydrated HNTs (Tully, Fakhrullin and Lvov 2015; Zhang et al. 2016). HNTs have a unique 1:1 crystalline structure consisting of tetrahedral sheets with corner shared $SiO_4$ and octahedral sheets with edge shared $AlO_6$ with low hydroxyl groups on the outer surfaces to improve their dispersion and reduce tube to tube interactions (Gaaz et al. 2015; Rawtani and Agrawal 2012), as illustrated in Figure 2-15.

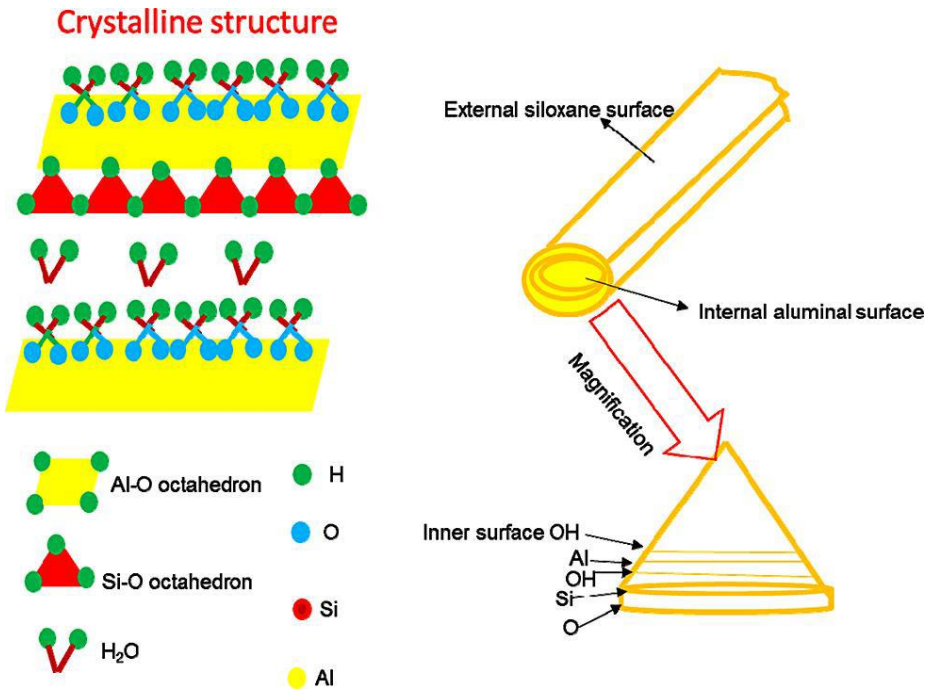


Figure 2-15. Chemical structure of HNTs (Kausar 2017)

As compared with other nanofillers with similar tubular structures like carbon nanotubes (CNTs), boron nitride nanotubes and metal oxide nanotubes, HNTs are

considered as relatively cheap nanofillers with abundant availability, and can be dispersed easily within polymer matrices (Tully, Fakhrullin and Lvov 2015; Zhang et al. 2016; Darie-Niţă and Vasile 2018). Furthermore, HNTs are a good nanofiller candidate for many nanocomposite systems due to their high aspect ratio, low hydroxyl density on the surfaces, as well as good mechanical properties and thermal stability (Zhang et al. 2016; Darie-Niţă and Vasile 2018). With high biocompatibility, non-carcinogenicity and non-toxicity, PVA/HNT nanocomposites can also be widely utilised in biomedical applications such as artificial heart surgery, drug delivery systems, contact lenses and wound dressing (Gaaz et al. 2015). Moreover, Khoo, Ismail and Ariffin (2011) found the addition of 0.5 wt% HNTs improved the tensile strength and tear strength as well as the swelling resistance of PVA/chitosan/HNT nanocomposites as favourable packaging materials.

### 2.3.3 PVA/graphene oxide (GO) nanocomposites

GOs were discovered for the first time by a British chemist B. C. Brodie with the chemical treatment of graphite in 1859. The original name of GOs was graphite oxides, but it was changed to graphene oxides in 2004 (Gao 2015; McDonald et al. 2015). Notwithstanding that there are many preparation methods for the bulk production of GOs, modified Hummer's method is still considered as the most popular with the higher oxidation degree (McDonald et al. 2015; Kim, Lee and Lee 2011). GOs in a chemical formula of $C_{11}H_4O_5$ are two-dimensional nanosheets with the thickness of 1 nm and lateral dimensions in range of a few nanometres to several microns with high aspect ratios (Gao 2015), as shown in Figure 2-16. GOs have various oxygen functional groups such as epoxide, hydroxyl, carboxyl and carbonyl groups on the edges and basal planes (McDonald et al. 2015; Xu et al. 2009; Huang et al. 2012).

These oxygen groups provide strong interactions to GOs with other polar-molecule based polymers to produce intercalated and/or exfoliated nanocomposite structures (Xu et al. 2009; Zhu et al. 2010). Moreover, polymer/GO nanocomposites yielded higher improvements in mechanical and barrier properties, electrical and thermal conductivities and acceptable transparency as compared with those of polymer matrices alone (Zhu, et al. 2010).

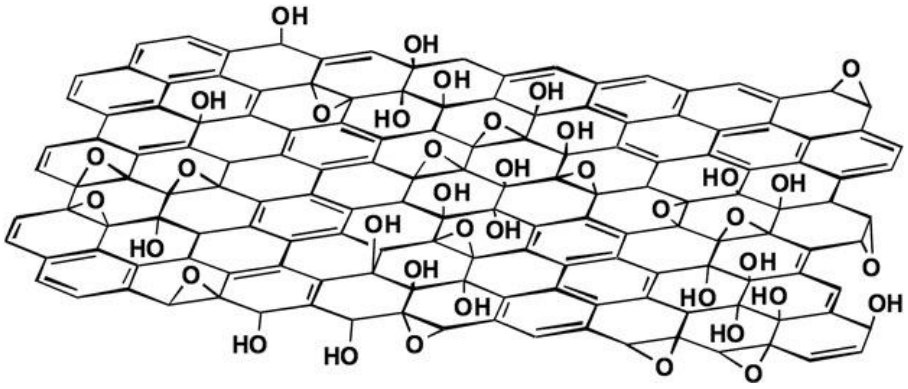

Figure 2-16. Chemical structure of GOs (Zhu, et al. 2010)

Huang et al. (2012) found that the oxygen permeability (*OP*) and *WVP* of PVA/GO nanocomposite films declined by 98.86 and 67.91%, respectively, with increasing the GO content from 0 to 1 wt%, which could be explained by full GO exfoliation in polymer/GO nanocomposites to generate tortuous paths. Accordingly, PVA/GO nanocomposites were proven to be used as effective packaging materials with good barrier properties (Kim, Lee and Lee 2011). Moreover, Sellam et al. (2015) and Liu at al. (2016a) reported remarkable improvements in tensile strength and Young's modulus of PVA/GO nanocomposites when compared with those of neat PVA due to inherent high Young's modulus of GOs as well as the strong interactions between functional groups of GOs with hydroxyl groups in polar PVA.

### 2.3.4 PVA/carbon nanotube (CNT) nanocomposites

Since the first discovery of CNTs in 1991, they become very popular one-dimensional carbon-based nanofillers in possession of high aspect ratios over 1000, excellent mechanical properties and high thermal and electrical conductivities (Lemes et al. 2015; Rafique et al. 2015; Myhra and Riviere 2013). CNTs are built up by using $sp^2$ carbon-carbon bonds in a layered structure with strong in-plane bonds and weak out-of-plane Van der Waals interactions (Mousa, Dong and Davies 2016). CNTs are available in three major forms: single-walled CNTs (SWCNTs), double-walled CNTs (DWCNTs) and multi-walled CNTs (MWCNTs), as depicted in Figure 2-17. SWCNTs consist of a single graphite crystal that can be rolled into a cylinder form while DWCNTs have two graphite crystals rolled concentrically. On the other hand, MWCNTs comprise concentric multi-graphite crystals that are rolled over around central hollow structures with interlayer spacing of 0.34 nm (Lemes et al. 2015; Karthik, Himaja and Singh 2014; Myhra and Rivieri 2013). CNTs are used widely to produce polymer/CNT nanocomposites in many applications, particularly for electromagnetic interface shielding with the combination of high electrical conductivity of CNTs and good flexibility of polymers (Kausar 2018; Lemes et al. 2015). Polymer/CNT nanocomposites possess good mechanical, thermal and electrical properties due to inherently high mechanical properties (50-100 GPa in tensile strength and 50-1000 GPa in Young's modulus), high thermal conductivity ($2\times10^3$ W/m·K for SWCNTs and $3\times10^3$ W/m·K for MWCNTs), high electrical conductivity ($10^4$ S/cm for SWCNTs and $1.85\times10^3$ S/cm for MWCNTs) as well as good fire retardancy and high barrier properties of CNTs (Rafique et al. 2015; Kausar 2018). There are many challenges encountered by using polymer/CNT nanocomposites due to high surface stability of CNTs resulting in the prevention of interactions between CNTs and

polymer matrices. Moreover, small sizes and high surface areas of CNTs increase the opportunities of CNT agglomeration as opposed to well-dispersed CNTs within polymer matrices. Chemical modifications of CNTs with the incorporation of functional groups can overcome some of these challenges by reducing van der Waals interactions (Kausar 2018; Lemes et al. 2015; Rafique et al. 2015).

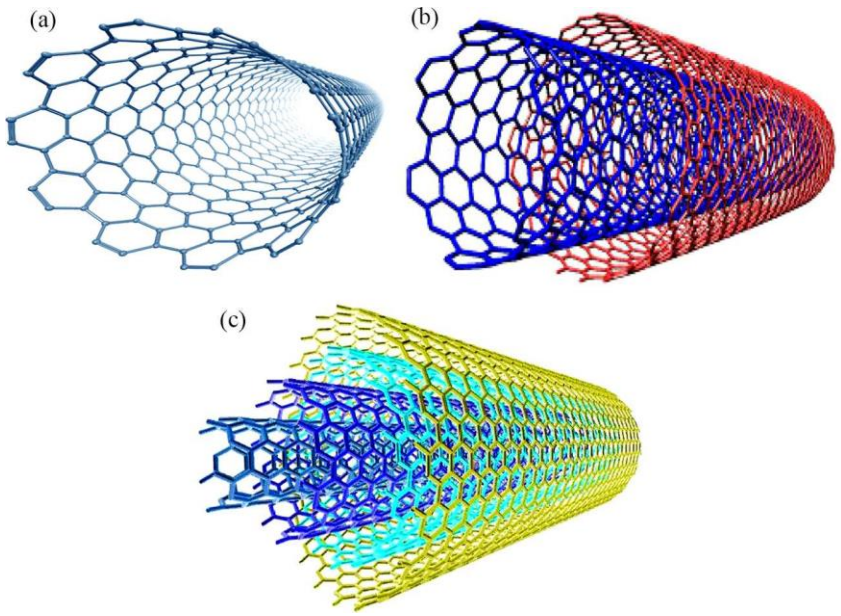


Figure 2-17. CNT structure configurations: (a) SWCNT, (b) DWCNT and (c) MWCNT (Rafique et al. 2015)

Liu et al. (2005) functionalised SWCNTs with multi-surface hydroxyl groups to improve their dispersion within PVA matrices. Single $T_g$ of PVA/functionalised SWCNT nanocomposites was indicative of improving the interactions between polymer matrices and SWCNTs. Moreover, tensile yield strength and Young's modulus as well as $T_g$ of PVA/functionalised SWCNT nanocomposites were found to be increased by 47.0%, 79.0% and 5.5ºC, respectively, when compared with those of neat PVA. Basiuk et al. (2009) reported that SWCNTs could be more easily dispersed within cross-linked PVA matrices in comparison with MWCNTs with relatively high

van der Waals interactions. In addition, Ryan et al. (2007) found that Young's modulus of PVA/ 1 wt% MWCNT nanocomposites was increased by 5.8 folds as opposed to that of neat PVA. However, with increasing the MWCNT content beyond 1 wt%, Young's modulus of such nanocomposites was decreased, which was ascribed to typical MWCNT agglomeration issue.

### 2.3.5 PVA/cellulose nanocomposites

Cellulose is a linear-chain polymer in polysaccharide family with abundant resources on earth (Mousa, Dong and Davies 2016; Moon et al. 2011). Cellulose with a chemical formula $(C_6H_{11}O_5)_n$ consists of ringed glucose molecules connected by β(1→4) linkages, as shown in Figure 2-18. The interactions between hydroxyl groups and oxygen of adjacent ring molecules via hydrogen bonding improve cellulose stability and build its liner configuration chains with the diameter of 2-20 nm and the length of a few microns (George, Sabapathi and Siddaramaiah 2015; Moon et al. 2011; Muhamad, Salehudin and and Salleh 2015). Consequently, cellulose is regarded as an insoluble polymer in water owing to its high density of hydrogen bonding networks. Soluble cellulose in water can be synthesised by the chemical functionalisation through the esterification or etherification process with full or partial replacement of hydroxyl groups in cellulose with ester or ether groups, respectively (George, Sabapathi and Siddaramaiah 2015).

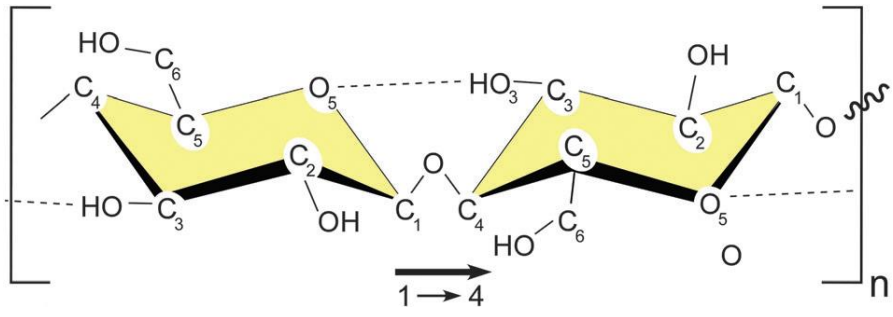


Figure 2-18. Chemical structure of cellulose (Moon et al. 2011)

Cellulose can be extracted from a wide range of natural resources such as bacteria, algae, tunicate and wood as well as plants like cotton, sisal, wheat straw, flax, potato tubers, etc. (Moon et al. 2011). Depending on the biosynthesis process used to extract cellulose from these resources, a range of cellulose forms can be achieved like cellulose nanocrystals (CNCs), nanofibril celluloses (NFCs) and cellulose nanowhiskers (CNWs) as well as cellulose microfibrils (CMFs) (Douglass et al. 2017). All these types of cellulose fillers are biodegradable, biocompatible, and cheap with abundant availability, low densities, high aspect ratios and large surface areas. Consequently, they can be deemed as effective nano-reinforcements in polymer nanocomposite systems (Douglass et al. 2017). Cai et al. (2016) discovered that there was an intimate interfacial interaction between NFCs and PVA associated with hydrogen bonding between hydroxyl groups for improving mechanical, thermal and optical properties. Chiekh et al. (2018) reported that good compatibility between PVA and NFCs led to exfoliated structures in nanocomposites. As a result, Young's modulus and tensile strength of PVA/10 wt% NFC nanocomposites were increased by 113 and 41%, respectively, as compared with those of neat PVA counterparts. Moreover, the decomposition temperature and $T_g$ of PVA/10 wt% NFC nanocomposites were increased by 66.5 and 3.6ºC, respectively, as opposed to those of neat PVA, which was believed to be caused by the restriction of chain mobility of PVA in the presence of NFCs. Ibrahim, El-Zawawy and Nassar (2010) showed that the incorporation of cellulose nanoparticles (CNPs) into PVA matrices increased the biodegradation rate of nanocomposite films thanks to the complete biodegradable nature of CNPs.

### 2.3.6 Manufacturing processes

Depending on nanocomposite constituents and processing steps, manufacturing methods of nanocomposites can be summarised as follows:

- ***In situ polymerisation***: it is also called interlamellar polymerisation. In this process, nanofillers (mostly nanoclays) are combined with the monomer solution or liquid monomers to swell prior to the polymerisation to produce exfoliated nanocomposites, Figure 2-19 (a). Radiation, heat and catalysts can be used as polymerisation initiators. This method can be restricted by the unavailability of suitable monomers (Rhim and Ng 2007; Ray et al. 2006; Ray and Bousmina 2005; Cui et al. 2015).
- ***Melt intercalation***: this method is known as direct melt intercalation as well. Nanofillers are melt compounded with polymer matrices (mostly thermoplastic polymers) above the softening point of polymers with the aid of extruders or other internal mixers. Polymeric molecules penetrate between nanofillers to produce intercalated and/or exfoliated nanocomposites, as demonstrated in Figure 2-19 (b) (Cui et al. 2015; Rhim and Ng 2007; Ray et al. 2006; Ray Bousmina 2005). This method is considered as an ecofriendly process in the absence of solvents (Youssef 2013). Although it becomes a standard manufacturing method at an industrial upscaling level for polymer/clay nanocomposites (Ray and Bousmina 2005), it is still restricted to thermoplastics polymers (Cui et al. 2015).
- ***Solution intercalation***: it is also known as solution processing or solution casting. The nanofillers are dispersed in water or other suitable chemical solvents with the aid of mechanical and magnetic mixing as well as sonication mixing. In the meantime, the polymer is dissolved in water or other solvents.

Then the suspension of nanofillers are mixed with polymer solution with continuous agitation, which is followed by casting in flat surfaces and drying to evaporate the solvents, Figure 2-19(c) (Ray and Bousmina 2005; Rhim and Ng 2007; Youssef 2013; Cui et al. 2015). This method is suitable for most nanofiller types such as nanoclays particularly HNTs as well as CNTs and GOs (Mousa, Dong and Davies 2016). In general, it is used to produce nanocomposites in thin films with intercalated structures at a laboratory scale. However, from an industrial point of view, solution intercalation is not ecofriendly and economically prohibitive with the existence of chemical solvents (Ray et al. 2006).

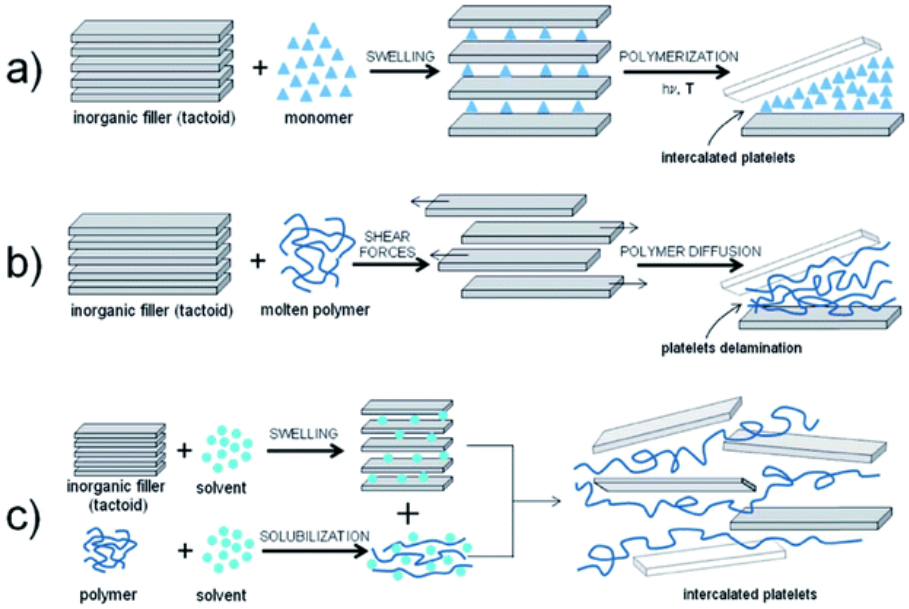


Figure 2-19. Typical preparation methods of polymer nanocomposites: (a) in-situ polymerisation, (b) melt intercalation, and (c) solution intercalation (Cui et al. 2015)

### 2.3.7 Properties

In view of packaging application, the improvements of mechanical, thermal and barrier properties of polymer nanocomposites are of a major concern, which highly depend on nanofiller content, nanofiller size and aspect ratio, nanofiller dispersibility within

polymer matrices, as well as filler-matrix interfacial bonding (Strawhecker and Manias 2000; Zagho and Khader 2016). Loryuenyong et al. (2015) found that the tensile strength and Young's modulus of PVA/GO nanocomposites were increased by 18.11 and 76.44%, respectively when incorporated with 1.5 wt% GOs owing to the inherently high strength of GOs. Nevertheless, such properties tended to diminish with increasing the GO content beyond 1.5 wt% due to the nanofiller agglomeration. Apparently, morphological structures of nanocomposites play an important role in their final resulting properties. Strawhecker and Manias (2000) demonstrated that exfoliated structures of PVA/MMT nanocomposites yielded the significant improvement of Young's modulus by 300% with the incorporation of 4 wt% MMTs when compared with that of neat PVA. Increasing the MMT content from 4 to 10 wt% induced the decrease in Young's modulus of such nanocomposites with the highly stacked and aggregated MMTs. Moreover, Khoo, Ismail and Ariffin (2011) stated that the agglomeration of HNTs could act as stress concentration sites leading to the reduction in tensile strength and Young's modulus as well as elongation at break for PVA/chitosan/HNT nanocomposite films beyond 0.5 wt% HNTs. The crystallinity level of nanofillers and their good compatibility with polymer matrices could alleviate the effect of agglomeration issues to a great extent. Liu et al. (2013) reported that tensile strength and Young's modulus of PVA/NFC nanocomposites were increased in a linear manner by 87.20 and 522.97%, respectively with increasing the NFC content from 0 to 60 wt% due to the high crystallinity level of NFCs and good compatibility with PVA matrices to yield overall rigid nanocomposite structures with the high load-bearing capacity.

The presence of nanofillers can also enhance the thermal stability of polymer nanocomposites due to the insulating effect and the role of nanofillers as a barrier

against the mass transfer in a decomposition process (Ray and Bousmina 2005). Based on the previous work mentioned by Nistor and Vasile (2012), exfoliated PVA/ST/modified MMT nanocomposites led to increasing the decomposition temperature and char residues as compared with intercalated MMT nanocomposites , which could be related to good dispersion of modified MMTs to hinder heat and mass transfer of nanocomposites. Qiu and Netravali (2013) stated that the inherent thermal stability of nanofillers could be the main reason for improving thermal stability of nanocomposites. Their TGA results showed that PVA had two decomposition temperatures detected at 266 and 276ºC. These temperatures were increased by 20 and 29ºC, respectively for PVA/10 wt% HNT nanocomposites, and then further increase was reported by 29 and 67ºC, respectively for PVA/20 wt% HNT nanocomposites. Moreover, Liu et al. (2013) reported that the $T_g$ and $T_m$ of PVA/NFC nanocomposites were increased dramatically from 77.4 to 83.2ºC and from 288 to 331ºC, respectively with increasing the NFC content from 0 to 60 wt%, which arose from strong interfacial bonding between nanofillers and polymer matrices to restrict the mobility of polymeric chains and further enhance their thermal stability.

Most nanocomposites are transparent materials with the incorporation of a small amount of nanofillers to minimise the light scattering in contrast with conventional composites (Zagho and Khader 2016). In particular, when such nanofillers are well dispersed within polymer matrices, the resulting nanocomposites can possess high optical clarity because of no light scattering points (Sapalidis, Katsaros and Kanellopoulos 2011). Zhou et al. (2010) reported that there were no significant changes in the light transparency of PVA/HNT nanocomposites when compared with that of PVA alone. This was because HNTs were uniformly dispersed within polymer matrices according to the AFM observation. Similar results were confirmed for

PVA/NFC nanocomposites by Cai et al. (2016). However, Loryuenyong et al. (2015) found that the light transparency of PVA/0.3 wt% GO nanocomposites was decreased by 13.18% relative to near PVA alone, and then changed to be completely opaque when increasing the GO content up to 2 wt%, which was attributed to GO aggregation resulting in blocking the light paths within polymer matrices. On the other hand, Cao et al. (2015b) reported that the reduction in light transparency in the UV-visible range of PVA/CNC nanocomposites could be used to protect the products from a light oxidative process for the purpose of food packaging.

Barrier properties of nanocomposites are important for many applications such as protective coating and material packaging particularly when in direct contact with foodstuffs (Rhim and Ng 2007; Cano et al. 2015a). Nanofiller content, aspect ratio and their dispersion within polymer matrices as well as their orientation relative to the diffusion direction are deemed as main factors to influence barrier properties of nanocomposites (Ray and Bousmina 2005; Choudalakis and Gotsis 2009). Nanofillers improve barrier properties of nanocomposites by creating "tortuous" paths within polymer matrices so that permeable molecules have to follow a zig-zag pathway with the diffusion delay in nanocomposites, and the reduction of free volumes of polymer matrices makes it inaccessible to permeable molecules (Ray and Bousmina 2005; Bhattacharya, Biswas and Bhowmick 2011). Consequently, the presence of nanofillers with good dispersion in polymer matrices improves barrier properties of nanocomposites by means of permeability reduction (Cui et al. 2015). Strawhecker and Manias (2000) found that well-dispersed MMTs (4-6 wt%) within PVA matrices gave rise to exfoliated nanocomposite structures with the reduction of *WVP* by 40% when compared with that of neat PVA. Moreover, Loryuenyong et al. (2015) concluded that the good dispersion of 2 wt% GO sheets into PVA matrices built

tortuous paths within nanocomposites, which reduced the *WVP* and oxygen permeability by 21 and 76%, respectively . Similarly, Aloui et al. (2016) reported that the *WVP* was decreased by 42% in PVA/5 wt% CNC/3 wt% HNT nanocomposites as opposed to that of PVA, as evidenced by SEM images illustrating well-dispersed CNCs and HNTs to generate much longer tortuous paths.

## 2.4 Permeability modelling of nanocomposites

The permeation process of gas or liquid molecules through polymer films has four major steps. It starts with the sorption of permeable molecules on the films, and is followed by the dissolution of these molecules inside the films, then the dissolved permeable molecules diffuse in films and finally are adsorbed on other film surfaces (Choudalakis and Gotsis 2009). Consequently, the permeability is completely determined by a diffusion/solubility mechanism that can be explained mathematically using the following equation (Picard et al. 2007; Choudalakis and Gotsis 2009; Cui et al. 2015).

$$P_o = D_o \times S_o \qquad (2\text{-}1)$$

where $P_o$, $D_o$ and $S_o$ are the permeability, diffusion and solubility coefficients of polymers, respectively (Picard et al. 2007; Choudalakis and Gotsis 2009). This equation can be used to describe the permeability of polymer nanocomposites with the assumption of no voids taking place at polymer/nanofiller interfaces due to strong filler-matrix interfacial bonding (Picard et al. 2007). The solubility of permeable molecules in nanocomposites can be given by (Choudalakis and Gotsis 2009; Cui et al. 2015; Picard et al. 2007):

$$S = (1 - \emptyset)S_o \qquad (2\text{-}2)$$

where $S$ and $S_o$ are the solubility coefficients in nanocomposites and polymer matrices (Choudalakis and Gotsis 2009), respectively and $\phi$ is the volume fraction of nanofillers (Picard et al. 2007; Chen and Evans 2006; Alexandre et al. 2009) expressed as:

$$\frac{1}{\emptyset} = 1 + \frac{\rho_i(1-\mu_i)}{\rho_p \mu_i} \qquad (2\text{-}3)$$

where $\rho_i$ and $\rho_p$ are the densities of nanofillers and polymer matrices, respectively, and $\mu_i$ is the weight fraction of nanofillers (Picard et al. 2007; Chen and Evans 2006; Alexandre et al. 2009). Moreover, the permeable molecules should follow tortuous paths in nanocomposite films for the diffusion through them. Therefore, the diffusion coefficient ($D$) of nanocomposites can be written as (Choudalakis and Gotsis 2009; Cui et al. 2015; Picard et al. 2007):

$$D = \frac{D_o}{\tau} \qquad (2\text{-}4)$$

where $D_o$ and $\tau$ are the diffusion coefficients in polymer matrices and the tortuosity, respectively ( Choudalakis and Gotsis 2009). The permeability of nanocomposites ($P_c$) relative to the permeability of polymer matrices can be calculated by combining eqs. 2-2 and 2-4 below (Choudalakis and Gotsis 2009; Cui et al. 2015; Picard et al. 2007):

$$\frac{P_c}{P_o} = \frac{(1-\emptyset)}{\tau} \qquad (2\text{-}5)$$

Consequently, the relative permeability of nanocomposites depends on the volume fraction and tortuosity factor defined by Nielsen's model as follows (Choudalakis and Gotsis 2009; Nielsen 1967):

$$\tau = \frac{l'}{l} \qquad (2\text{-}6)$$

where $l'$ and $l$ are the distances of zig-zag path in nanocomposite films and the straight path in polymer matrices films, respectively (Nielsen 1967). Several models have been developed to calculate $\tau$ depending on the nanofillers content, aspect ratio and

geometrical shape (Picard et al. 2007) according to Table 2-3. In most of these models, it is assumed that nanofillers have regular geometrical shapes in form of hexagonal flakes, ribbons and disks (Picard et al. 2007).

Table 2-3. Description of tortuosity factor according to different theoretical models

| **Model** | **Nanofiller geometry** | **Tortuosity formula ($\tau$)** | **Remark** | **Ref.** |
|---|---|---|---|---|
| Nielsen | Ribbon nanofillers | $1+\frac{\alpha\emptyset}{2}$ | $\alpha$: nanofiller aspect ratio | (Picard et al. 2007; Nielsen 1967) |
| Cussler | Ribbon nanofillers | $1+\frac{\alpha^2\emptyset^2}{4(1-\emptyset)}$ | Perpendicular alignment | (Cui et al. 2015; Picard et al. 2007) |
| | Ribbon nanofillers | $1+\frac{\alpha^2\emptyset^2}{8(1-\emptyset)}$ | Alignment and misalignment | |
| | Hexagonal nanofillers | $1+\frac{\alpha^2\emptyset^2}{54(1-\emptyset)}$ | | |
| Lape and Cussler | Ribbon nanofillers | $\left(1+\frac{\alpha\emptyset}{3}\right)^2$ | | (Picard et al. 2007) |
| Maxwell | Spherical nanofillers | $1+\frac{1+\left(\frac{\emptyset}{2}\right)}{1-\emptyset}$ | | (Cui et al. 2015) |
| | Cylindrical nanofillers | $\frac{1+\emptyset}{1-\emptyset}$ | | |
| Gusev and Lusti | Disk nanofillers | $exp\left[\left(\frac{\alpha\emptyset}{3.47}\right)^{0.71}\right]$ | | (Cui et al. 2015; Picard et al. 2007) |

| | | | |
|---|---|---|---|
| Fredrickson and Bicerano | Disk nanofillers | $4\left[\frac{1+x+0.1245x^2}{2+x}\right]^2$ $x=\frac{\pi\alpha\emptyset}{2}ln\frac{\alpha}{2}$ | (Picard et al. 2007) |

Some expressions in relation to $\tau$ are used to predict the relative permeability of nanocomposites with the consideration of nanofiller orientation when dispersed within polymer matrices (Choudalakis and Gotsis 2009), as listed in Table 2-4. The order parameter (*S*) provides a good expression for nanofiller orientation particularly with respect to ribbon-like and platelet-like nanofillers as follows (Bharadwaj 2001; Choudalakis and Gotsis 2009; Cui et al. 2015):

$$S=\frac{1}{2}(3cos^2\theta-1) \qquad (2\text{-}7)$$

where $\theta$ is the angle between the direction of preferred direction orientation (*n*) and normal unit vectors of nanofillers (*p*) (Bharadwaj 2001). As such, *S* has three different values including (i) *S*= -1/2 ($\theta$= 90º) for nanofillers without barrier effect against permeable molecules, (ii) *S*= 0 ($\theta$= 54.74º) for randomly-oriented nanofillers, and (iii) *S*= 1 ($\theta$=0º) for nanofillers with a regular arrangement (Bharadwaj 2001; Alexandre et al. 2009; Cui et al. 2015), Figure 2-20.

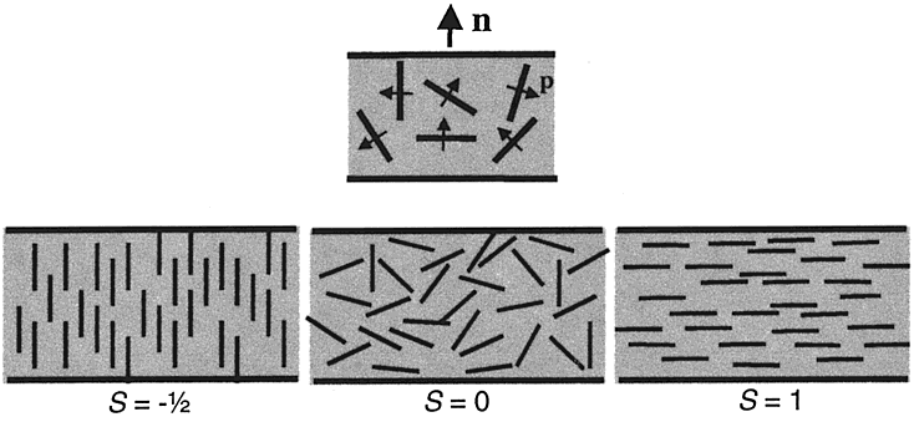


Figure 2-20. Relationship between nanofiller orientation and order parameters (Bharadwaj 2001)

Table 2-4. Description of relative permeability theoretical models

| Model | Nanofiller arrangement | Relative permeability formula ($P_c/P_o$) | Ref. |
|---|---|---|---|
| Nielsen | Regular arrangement | $\frac{1-\emptyset}{1+\left(\frac{\propto}{2}\right)\emptyset}$ | (Choudalakis and Gotsis 2009; Gusev and Lusti 2001; Takahashi et al. 2006; Tan and Thomas 2016) |
| | Random arrangement | $\frac{1-\emptyset}{1+\frac{1}{3}\left(\frac{\propto}{2}\right)\emptyset}$ | |
| Cussler | Regular arrangement | $\frac{1-\emptyset}{1+\left(\frac{\alpha\emptyset}{2}\right)^2}$ | (Choudalakis and Gotsis 2009; Takahashi et al. 2006) |
| | Random arrangement | $\frac{1-\emptyset}{\left(1+\frac{\alpha\emptyset}{3}\right)^2}$ | |
| Bharadwaj | Any arrangement | $\frac{1-\emptyset}{1+\frac{2}{3}\frac{\alpha\emptyset}{2}\left(S+\frac{1}{2}\right)}$ | (Choudalakis and Gotsis 2009; Tan and Thomas 2016) |
| Gusev and Lusti | Random arrangement | $\frac{1-\emptyset}{exp\left[\left(\frac{\alpha\emptyset}{3.47}\right)^{0.71}\right]}$ | (Gusev and Lusti 2001; Takahashi et al. 2006) |
| Fredrickson and Bicerano | Random arrangement | $\frac{1-\emptyset}{4\left[\frac{1+x+0.1245x^2}{2+x}\right]^2}$ | (Gusev and Lusti 2001; Takahashi et al. 2006; Tan and Thomas 2016) |

Tan and Thomas (2016) stated that Nielsen model could be used accurately for both *WVP* and gas permeability particularly for polymer/clay nanocomposites because of its dependence on the first-order formula when compared with other models.

Moreover, Bharadwaj model is used successfully for incomplete exfoliated polymer/clay nanocomposites and Cussler models are more applicable for nanocomposites with low volume fraction and aspect ratio of nanofillers (Tan and Thomas 2016). These findings were proven by Saritha et al. (2012) when the experimental permeability results of chlorobutyl rubber/modified MMT (Cloisite-15A) nanocomposites were compared with those obtained from theoretical models. Their results showed that experimentally determined gas permeabilities ($O_2$, $N_2$ and $CO_2$) for chlorobutyl rubber/Cloisite-15A nanocomposites had good agreement with Gusev and Lusti model and Nielsen model. Whereas, Cussler model revealed a much closer correlation with experimental results with low aspect ratio and volume fraction of Cloisite-15A clays. Nielsen model and Cussler model were used by Liu et al. (2016b) as well for the comparison with the experimental data for gas permeabilities of PVA/GO nanocomposites. Their results showed that the hydrogen permeabilities of PVA/GO nanocomposites and PVA/modified-GO nanocomposites were decreased in a linear manner by 90 and 94%, respectively with increasing the nanofiller content from 0 to 3 wt% in contrast with that of neat PVA. Moreover, the experimental data of PVA/GO nanocomposites were positioned between Nielsen model and Cussler model while PVA/modified-GO nanocomposites demonstrated better agreement with Cussler model for well-aligned nanofillers as the GO modification improved the overall dispersion within PVA matrices in nanocomposite systems ( Liu et al. 2016b).

## 2.5 Summary

In summary, biopolymers have received great attention nowadays to replace the petroleum-based polymers due to their availability, renewability, and ecofriendly characteristics that can help to reduce critical problems with respect to plastic wastes

for the following three sectors (Chandra and Rustgi 1998; Mensitieri et al. 2011; Avérous and Pollet 2012):

- ***Medical applications***: polymers used for medical applications should have good biocompatibility with biological systems. The most popular examples of these applications are drugs delivery systems, surgical sutures, scaffolds, bone fixation devices and artificial skins, etc. (Chandra and Rustgi 1998; Van de Velde and Kiekens 2002).
- ***Agricultural applications***: biodegradability and water solubility are two important material features that should be available in polymers used for these applications such as green house, agricultural planting containers and controlled release of agricultural chemicals (Chandra and Rustgi 1998).
- ***Packaging applications***: polymers have high barrier properties can be used successfully for food packaging applications (Chandra and Rustgi 1998; Van de Velde and Kiekens 2002; Mensitieri et al. 2011).

PVA is one of these polymers that have good mechanical properties and acceptable thermal properties with complete transparency as well as low gas permeability. PVA as a water-soluble polymer has good compatibility with a variety of polymers and nanofillers. PVA can be used as a base polymer or a part of polymer blends in nanocomposite systems (Baker et al. 2012). Using PVA as a neat polymer or a part of polymer blends for nanocomposites diminish its material demerits such as relatively high cost, poor biodegradability in some environments and weak water resistance (Tang and Alavi 2011). For example, PVA blends with polysaccharides polymers and/or nanofillers improve the biodegradability and cost-effectiveness (Rahmat et al. 2009; Ibrahim, El-Zawawy and Nassar 2010). Moreover, blending PVA with chitosan and gelatin enhanced antimicrobial and swelling resistance, respectively (Tripathi,

Mehrotra and Dutta 2009; Pawde, Deshmukh and Parab 2008b). On the other hand, reinforcing PVA with nanoclays highly increase mechanical, thermal and barrier properties, which is the main requirement for food packaging applications (Mensitieri et al. 2011). Additionally, the incorporation of carbonaceous nanofillers with PVA also gives rise to superior improvements in thermal and electrical properties (Kausar 2018).

Plasticised PVA/ST blends have been studied for decades due to their remarkable blend properties like good biodegradability, cost effectiveness and ductility compared with neat PVA as well as high strength and formability as opposed to neat ST (Chiellini et al. 2003; Li, Chen and Wang 2014). Such blends still have poor barrier properties due to their high water affinity of the components to restrict its applications on a wide scale (Zanela et al. 2015). The development of new bionanocomposite systems can overcome such limitations with the inclusion of nanofillers in possession of inherent barrier properties and nontoxicity in order to benefit their food packaging applications.

# Chapter 3: Materials, Manufacturing Processes and Characterisation Methods

## 3.1 Introduction

According to the definition of sustainable packaging (Sustainable Packaging Coalition 2011; Magnier and Crié 2015), sustainable packaging materials should be based on renewable or recycled resources of materials, clean production technologies, safe and healthy features throughout their life cycle as well as meeting the market requirements for cost and performance. Consequently, ecofriendly materials namely PVA, ST, GL and HNTs were used to prepare bionanocomposite films using solution casting method to design a sustainable material for food packaging with cost effectiveness. In this chapter, major chemical and physical properties of these materials were listed according to the data sheet given by their suppliers. Moreover, manufacturing procedures and conditions of neat PVA, PVA films and corresponding bionanocomposite films were explained in detail. Furthermore, material characterisation techniques and setup for these films were elaborated with their potential applications to be considered.

## 3.2 Materials

### 3.2.1 Polyvinyl Alcohol (PVA)

PVA is a popular synthetic water-soluble polymer. PVA has a wide range of applications in biochemical, biomedical, pharmaceutical and packaging sectors because of its good compatibility, water solubility and relatively high biodegradability in some environment like active sludge though it has poor thermal stability and barrier

properties (Sapalidis, Katsaros and Kanellopoulos 2011; Chiellini et al. 2003). Full-hydrolysis PVA with a hydrolysis degree of approximately 99% was used, which was purchased from Sigma-Aldrich Pty. Ltd, Australia with specific material properties listed in Table 3-1.

Table 3-1: Physical properties of materials used in this study (based on material data sheets from the supplier)

| **Polymer** | **Molecular weight (g/mol)** | **Colour** | **Relative density ($g/cm^3$)** | **Other properties (ºC)** |
|---|---|---|---|---|
| PVA | $89\times10^3$-$98\times10^3$ | colourless | 1.26 | Melting point: 200<br>Flash point: > 113 |
| ST | $166\times10^3$ | White | 1.55 | Gelatinisation point: 56-68 |
| GL | 92.09 | Colourless | 1.26 | Boiling point: 182<br>Flash point: 160 |

### 3.2.2 Potato Starch (ST)

ST is a completely biodegradable polymer being extracted from numerous resources like corn, rice, potato, wheat, barley, pea and so on (Avérous 2004; Corre, Bras and Dufresne 2010). It is rarely used as a neat polymer because of high brittleness and closeness between melting and degradation temperatures (Schmitt et al. 2012). ST from potato with 100% concentration was also supplied by Sigma-Aldrich Pty. Ltd, Australia with detailed properties given in Table 3-1.

### 3.2.3 Glycerol (GL)

GL is the best plasticiser and compatible agent that have been used with PVA/ST blends for many decades (Rahman et al. 2010). The presence of GL increases the

ductility and compatibility of PVA/ST blends by improving polymeric chain mobility and creating hydrogen bonds with the consumption of hydroxyl groups, respectively (Siddaramaiah, Raj and Somashekar 2003). GL was also provided by Sigma-Aldrich Pty. Ltd, Australia with the material specifications listed in Table 3-1.

### 3.2.4 Halloysite nanotubes (HNTs)

HNTs are natural nanoclays belonging to kaolin family with hollow and tubular structures. HNTs have high aspect ratios of 10-50 and specific surface areas of 22.1-81.6 $m^2/g$ (Liu et al. 2014; Mousa, Dong and Davies 2016; Idumah et al. 2018). Such nanofillers possess high thermal stability and moderate hydrophobicity, making them a good additive candidate to improve thermal and barrier properties (Xie et al. 2011; Zhang et al. 2016). HNTs were donated by Imerys Tableware Asia Ltd, New Zealand in the form of ultrafine particles with a relative density of 2.53 $g/cm^3$, which were used without any more purification.

### 3.2.5 Other reagents

Magnesium bromide hexahydrate, magnesium nitrate hexahydrate, strontium chloride hexahydrate and barium chloride dehydrate salts were all purchased from Sigma-Aldrich Pty. Ltd, Australia. Saturated solutions of these salts were used to maintain the relative humidity (RH%) at a given level (Wexler and Hasegawa 1954; Young 1967) when *WVTR* and *WVP* were evaluated. Chemical formulae and physical properties of these salts are summarised in Table 3-2:

Table 3-2: Chemical formulae and physical properties of salts

| Salt | Chemical formula | Molecular weight (g/mol) | Relative density ($g/cm^3$) | RH% at 25°C |
|---|---|---|---|---|
| Magnesium bromide hexahydrate | $MgBr_2 \cdot 6H_2O$ | 292.20 | 2.00 | 30 |
| Magnesium nitrate hexahydrate | $Mg(NO_3)_2 \cdot 6H_2O$ | 256.41 | 1.63 | 50 |
| Strontium chloride hexahydrate | $SrCl_2 \cdot 6H_2O$ | 266.62 | 1.93 | 70 |
| Barium chloride dehydrate | $BaCl_2 \cdot 2H_2O$ | 244.26 | 3.10 | 90 |

Furthermore, ethanol solution with 100% concentration (Rowe Scientific Pty. Ltd, Australia), nitric acid with 70% concentration (Sigma-Aldrich Pty. Ltd, Australia) and glacial acetic acid with 96% concentration (Merck Pty. Ltd, Australia) were used as food simulants in migration tests according to European Commission Regulation (EU) No 10/2011 (2011) and British Standard EN 1186-1 (2002). For the same tests, standard solutions of aluminium and silicon ions were prepared from aluminium stock solution with the concentration of 1000 mg/L (ThermoFisher Scientific Pty. Ltd, Australia) and silicon stock solution with the same concentration (High-Purity Standards, Inc.), respectively as control samples.

### 3.3 Manufacturing process

Solution casting process was used as a simple and straightforward processing method to manufacture neat PVA, PVA blends and PVA/ST/HNT bionanocomposite films.

### 3.3.1 Polymer blends

Neat PVA solution at the concentration of 5 wt%/v was prepared by dissolving 10 g PVA powder in 190 ml deionised water at 35ºC. This solution was heated gradually up to 85ºC for 3 h by continued stirring at 500 rpm with the aid of IKA®-RCT magnetic stirrer. Equal amounts of clear solutions were poured in glass petri-dishes (diameter: 15 cm). Samples were dried for 48 h at 50ºC in an oven. The same procedure was followed to prepare plasticised PVA film (i.e., PVA/GL blend). GL solution (30 wt% content relatives to the dry weight) was added to neat PVA solution by magnetic stirring during last 30 min of preparation process. Whereas, PVA/ST blend films were prepared by mixing 8 g PVA with 2 g ST as powders at room temperature, and then the mixture was further dissolved in 190 ml deionised water accordingly with the same procedure mentioned earlier. PVA/ST blend films were plasticised with 30 wt% GL to produce PVA/ST/GL films by adding GL solution at last 30 min in the preparation process for stirring. Completely dried films were removed carefully from petri-dishes and kept in a desiccator with silica gel underneath them to prevent humidity absorption for at least a week before material characterisation.

### 3.3.2 Bionanocomposites

PVA/ST/GL blends were adopted as the matrices for bionanocomposite films. HNT suspension was prepared by mixing weighted amounts of HNT powders (0.25, 0.50, 1, 3 and 5 wt%) in 100 ml deionised water using an IKA®RW20-mechanical mixer at 50ºC and 500 rpm for 2 h. Subsequently, the suspension was sonicated in an ultrasonicating bath ELMA Ti-H-5 model at 50ºC, with a 25-kHz frequency and a 90% power intensity for 1 h to get better HNT dispersion. Well dispersed HNT suspension was added in a dropwise manner to 100 ml PVA/ST/GL blend solution via mechanical

mixing at 500 rpm and 50ºC for 30 min. The prepared mixture solution was homogenised for 30 min with a magnetic stirrer at 50ºC and 350 rpm. Such a solution was sonicated again at the same condition previously mentioned for additional 30 min in order to remove any air bubbles. Equal amounts of bionanocomposite solutions were poured in petri-dishes to dry at 50ºC for 48 h. All samples were further dried in a desiccator after removed from the petri-dishes.

## 3.4 Experimental characterisation

### 3.4.1 Electron microscopic analysis

The holistic investigation of morphological structures of PVA/ST/GL blends and resulting bionanocomposite films was important to understanding the compatibility between PVA, ST and GL in addition to the HNT dispersion within blend matrices. Consequently, SEM was used to investigate the fracture morphology of tensile testing samples in order to evaluate their structure-property relationship. Furthermore, sample surfaces subjected to biodegradation tests were also examined with SEM observation before and after the tests. These samples were scanned during the period for the test progress as well at the first and third weeks, respectively. Moreover, the surface roughness of PVA/ST/GL blends and corresponding bionanocomposite films were investigated along with the determination of aspect ratios of both as-received HNT powders and those embedded HNTs in bionanocomposite films via AFM.

#### *3.4.1.1 SEM*

As-received HNT powders and fracture surfaces of neat PVA, PVA blends and PVA/ST/GL/HNT bionanocomposite films were investigated by a Tescan Mira 3 field emission scanning electron microscope (FE-SEM) at the accelerating voltage of 3 kV,

see Figure 3-1. All samples were coated with a layer of carbon (layer thickness: 10 nm) to improve the material contrast. Moreover, HNT dispersion within bionanocomposite films was evaluated by Oxford Instrument X-Max X-ray energy dispersive spectroscopic (EDS) with the aid of Aztec software.

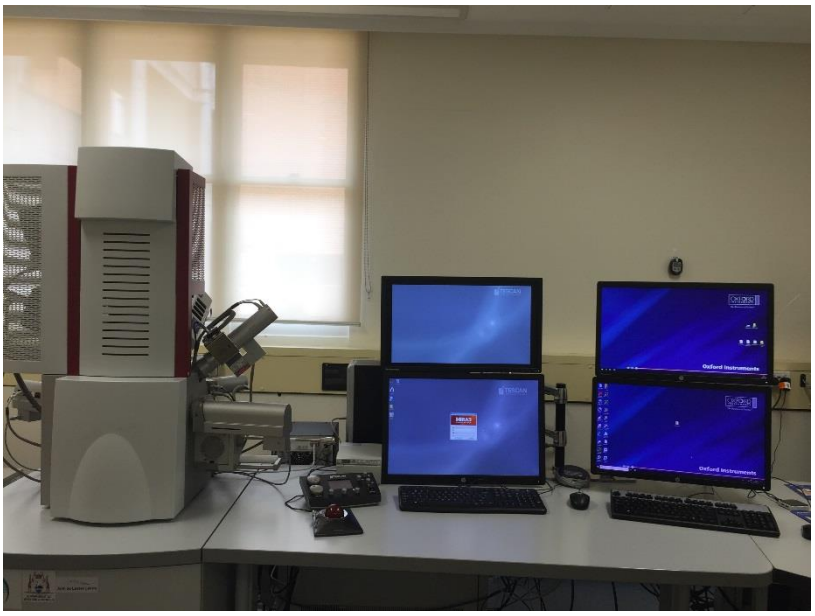

Figure 3-1. Tescan Mira 3 field emission scanning electron microscope

NEON-40EsB field emission scanning electron microscope (FS-SEM), as seen in Figure 3-2, was used to investigate the surface morphology of neat PVA, PVA blends and resulting bionanocomposite films at different HNT contents before, during and after biodegradation tests. FE-SEM was operated at an accelerating voltage of 2kV, and all samples were sputter coated with platinum layers (thickness: 3 mm) for improving the image contrast during scanning.

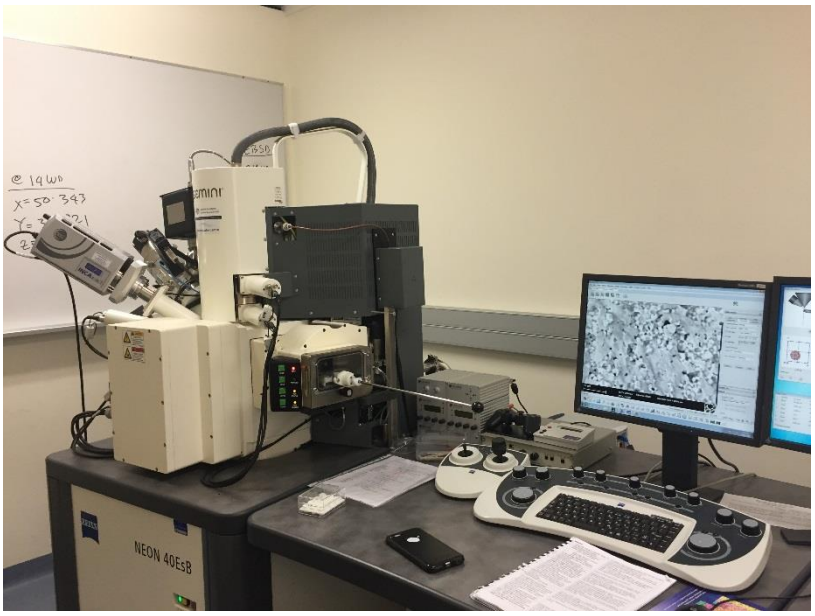


Figure 3-2. NEON-40EsB field emission scanning electron microscope

### *3.4.1.2 AFM*

Morphological structures and surface roughness of PVA/ST/GL blends and their bionanocomposite films at different HNT contents were also examined via a Bruker Dimension Fastscan AFM system, as presented in Figure 3-3. A drop of sonicated suspension of as-received HNT powders was deposited on the mica substrate for analysis. On the other hand, PVA/ST/GL blends and their bionanocomposite films were glued on glass substrates with a carbon tape. A tapping mode was used for AFM measurements with a TESPA probe at the scanning rate of 2 Hz, a nominal resonant frequency of 525 kHz with images being captured in the ambient condition. Surface roughness of bionanocomposite films and HNT aspect ratios for as-received powders and those embedded within bionanocomposite films were individually determined with the help of NanoScope Analysis 1.90 software.

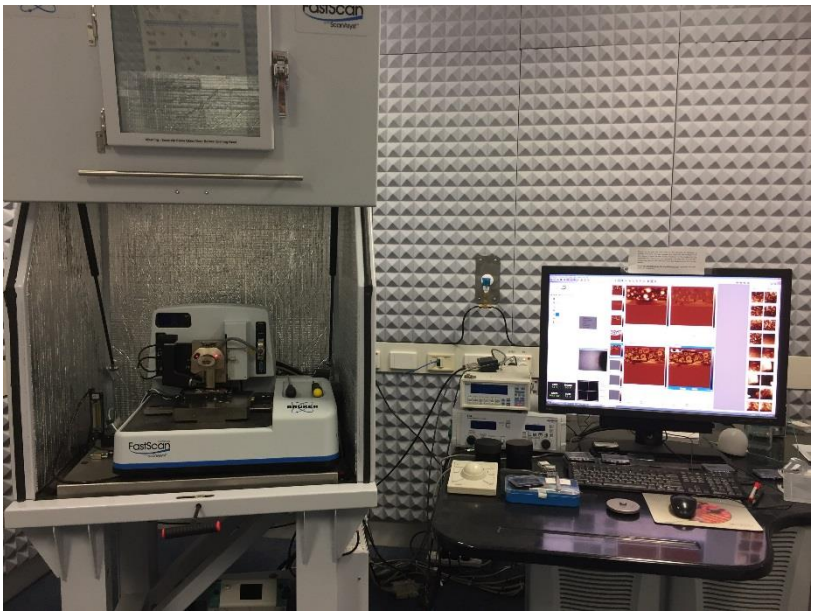


Figure 3-3. Bruker Dimension Fastscan AFM system

### 3.4.2 Mechanical properties

Tensile tests are used mostly to characterise mechanical properties of material such as tensile strength, Young's modulus and elongation at break. Lloyd-LR10K universal testing machine was employed to assess mechanical properties of neat PVA, PVA blends and resulting bionanocomposite films at different HNT contents according to ASTM standard D882, as shown in Figure 3-4. Rectangular samples of all material films were cut in size of 100 mm length, 20 mm width and 100-120 µm thickness. For each material composition, 5 to 8 samples were tested to get average data with reported standard deviations. Crosshead speed and gauge length of samples were set to 10 mm/min and 50 mm, respectively.

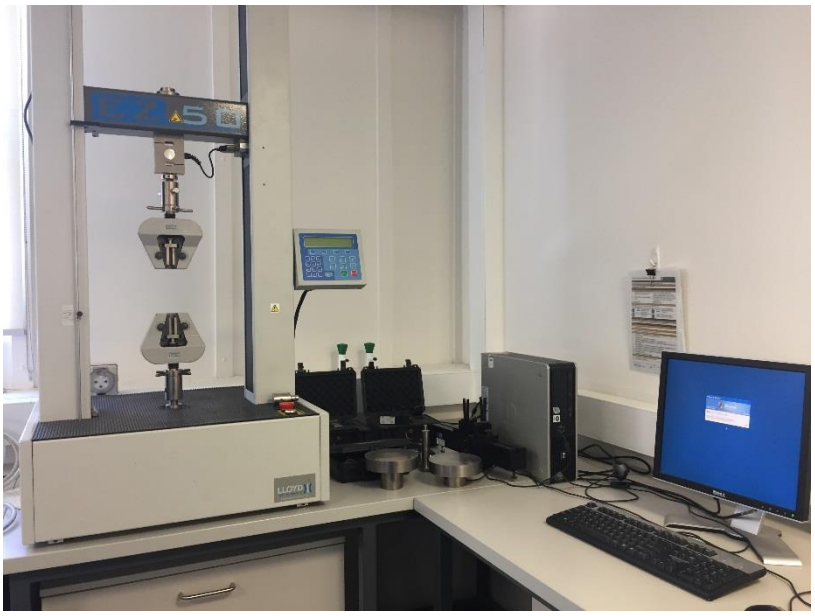

Figure 3-4. Lloyd-LR10K universal testing machine

### 3.4.3 Thermal properties

Thermal properties of neat materials (i.e., PVA, ST and HNTs), PVA blends and resulting bionanocomposites at different HNT contents were determined via thermogravimetric analysis (TGA) and differential scanning calorimetry (DSC) in the TGA/DSC 1 STAR$^e$ System, METTLER TOLEDO, Australia, as shown in Figure 3-5. The weighed samples of 5-15 mg were heated at the heating rate 10ºC/min from 35 to 600ºC in argon atmosphere (flow rate: 30 ml/min). The decomposition temperatures of materials were determined from TGA curves. These temperatures were detected at 5, 50 and 90% weight loss, which were referred to as $T_{5\%}$, $T_{50\%}$ and $T_{90\%}$, respectively. Whereas, the degradation temperatures were determined from derivative thermogravimetric (DTG) curves and represented by $T_{d1}$, $T_{d2}$, $T_{d3}$ and $T_{d4}$. Furthermore, $T_g$, $T_m$, crystallisation temperature ($T_c$), and crystallisation rate ($X_c$) were obtained from DSC thermograms during the heating scans. $X_c$ can be calculated according to the equation given below (Dong et al. 2015b):

$$X_c = \frac{\Delta H_m - \Delta H_c}{\Delta H_m^\circ} \times \frac{100}{1 - w_f} \qquad (3\text{-}1)$$

Where $\Delta H_m$ and $\Delta H_c$ are the melting and crystallisation enthalpies of polymer matrices in bionanocomposites, respectively, and $w_f$ is the weight fraction of nanofillers. In particular, $\Delta H^\circ_m$ is the melting enthalpy of 100% crystalline PVA (i.e. $\Delta H^\circ_m$=142 J/g (Sreekumar, Al-Harthi and De 2012)).


Figure 3-5. TGA/DSC 1 STAR$^e$ System for thermal analysis

### 3.4.4 X-ray diffraction (XRD)

The type of nanocomposite structures (i.e. intercalated and/or exfoliated) was investigated using XRD analysis. XRD patterns of as-received HNT powders and PVA/ST/GL/HNT bionanocomposite films at different HNT contents were investigated via a Bruker D8 advance diffractometer (Cu-Kα source, wave length λ=0.1541 nm), as depicted in Figure 3-6, at the accelerating voltage and current of 40 kV and 40 mA, respectively. The material samples were scanned in a diffraction-angle ($2\theta$) range of 5º-40º at the scan rate of 0.013º/s. Bragg's law was used to calculate *d*-spacing values for both as-received HNT powders and bionanocomposite films at

different HNT contents according to the following equation (Zagho and Khader 2016; Dong et al. 2013):

$$n\lambda = 2d\ sin\theta \qquad (3\text{-}2)$$

Where *n* is an integer used for incident X-ray beam.

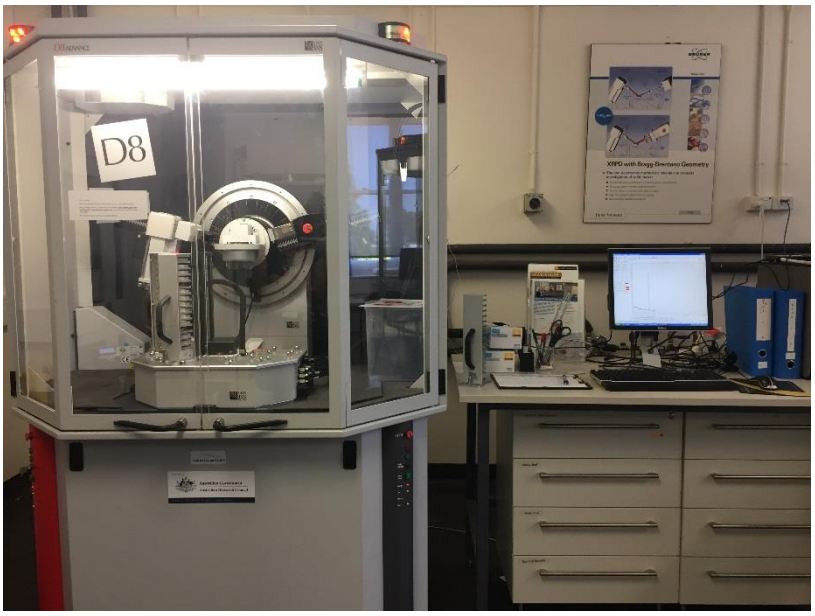


Figure 3-6. Bruker D8 advance X-ray diffractometer

### 3.4.5 Fourier transformation infrared (FTIR) spectroscopy

The investigation of molecular bonding interactions for neat materials (PVA, ST, GL and HNTs), PVA blends and PVA/ST/GL/HNT bionanocomposite films at different HNT contents was carried out using FTIR technique. All samples were tested via a Perkin-Elmer 100 FTIR spectrometer mounted with the attenuated total reflection (ATR) accessory, which enables samples to be examined directly in different states without further preparation in FTIR analysis, at the scanning resolution of 4/cm and a wave range of 4000-500/cm, illustrated in Figure 3-7.


Figure 3-7. FTIR spectrometer

### 3.4.6 UV-vis spectra

In food packaging applications, the transparency level of packaging materials is very important. The light transmittance of neat PVA, PVA blends and PVA/ST/GL/HNT bionanocomposite films at different HNT contents was determined with the aid of an ultraviolet-visible (UV-vis) spectrometer (Jasco-V670), as shown in Figure 3-8. Light transmittance (*T%*) was measured with a wavelength range of 200-800 nm to cover ultraviolet, visible and infrared wavelengths at a scan rate of 200 nm/min. In addition, a glass plate was utilised as a reference sample. Three samples were investigated for each material batch for testing reproducibility. Moreover, additional visual comparison in terms of transparency was made by using captured digital images of Curtin University logo.


Figure 3-8. Ultraviolet-visible (UV-vis) spectrometer

### 3.4.7 Barrier properties

One of the most important requirements for packaging materials is that they should possess good barrier properties. The incorporation of well dispersed nanofillers within polymer matrices may generate tortuous paths, which can produce a barrier structure against water vapour and gases. The high tortuosity means high barrier properties and lower permeability (Feldman 2013). Consequently, *WVTR* and *WVP* of neat PVA, PVA blends and PVA/ST/GL/HNT bionanocomposite films at different HNT contents were evaluated at a various range of temperatures and RH gradients. Furthermore, the gas permeabilities of these aforementioned films were also examined against oxygen and air.

#### *3.4.7.1 WVTR and WVP*

According to ASTM E96M-16 standard, the *WVTR* and *WVP* were determined for neat PVA, PVA blends and PVA/ST/GL/HNT bionanocomposite films at different HNT contents. The circular samples of these pre-dried films were cut and sealed on the

mouth of laboratory bottle of borosilicate glass filled with distilled water (100% RH). The gap between the surfaces of material samples and water in each bottle should be at least 20 mm to avoid any direct contact. These bottles were kept in an air-circulating oven at 25± 1ºC and 50%± 2% RH for two weeks. The weight loss of bottle was recorded daily to establish the relationship between weight loss and time for determining the slope of the steady-state period to calculate the *WVTR* according to the equation below:

$$WVTR = \frac{G/t}{A} \qquad (3\text{-}3)$$

where *G* is the weight loss of bottle (g), *t* is the time (h), *G/t* is the slope of linear regression (g/h) and *A* is the tested sample area ($m^2$). These data were further employed to calculate the *WVP* as follows:

$$WVP = \frac{WVTR \times l}{S \times \Delta RH} \qquad (3\text{-}4)$$

where *l* is the sample thickness (m) determined as the average thickness value in different positions when randomly selected on the sample surfaces, *S* is the saturated water vapour pressure (kPa) and $\Delta RH$ is the relative humidity gradient across the sample (50%), which is the different relative humidity from inside and outside permeability cells. All associated tests were conducted three times to obtain average data of *WVTR* and *WVP* with relevant standard deviations.

The temperature effect on the *WVTR* and *WVP* of neat PVA, PVA blends and bionanocomposite films at different HNT contents was examined by running the tests at different temperatures of 25, 35, 45 and 55ºC and a constant RH level of 50%± 2% according to the procedure mentioned previously. The RH gradient was maintained at a constant level of 50%± 2% by using the saturated salt solution of $Mg(NO_3)_2 \cdot 6H_2O$ (Wexler and Hasegawa 1954; Young 1967) in an open beaker inside the oven with

continuous monitoring of the temperature and humidity level in order to keep the RH level at 50%, as opposed to the RH level of 100% inside the bottle due to being filled with distilled water. The saturated salt solution was prepared by dissolving a sufficient amount of salt in distilled water at a boiling point, and then the solution was gradually cooled with additional salt for initialising the precipitation. This solution was kept to stabilise for 1-2 weeks before further use (Winston and Bates 1960).

The effect of RH level on the *WVTR* and *WVP* of neat PVA, PVA blends and PVA/ST/GL/HNT bionanocomposite films at different HNT contents was also investigated with RH gradients of 70, 50, 30 and 10%± 2% at a given temperature of 25ºC. The RH level remained at 100% inside the test bottle by filling it with distilled water. On the other hand, various RH levels were generated out of the test bottle by using saturated salt solutions, as described in earlier work (Wexler and Hasegawa 1954; Young 1967). The details of the salts used, as well as RH% and ΔRH% are summarised in Table 3-3:

Table 3-3. Saturated salt solutions with various RH% levels

| **Salt** | **RH% at 25 ºC** | **ΔRH% for permeability tests** |
|---|---|---|
| $MgBr_2 \cdot 6H_2O$ | 30 | 70 |
| $Mg(NO_3)_2 \cdot 6H_2O$ | 50 | 50 |
| $SrCl_2 \cdot 6H_2O$ | 70 | 30 |
| $BaCl_2 \cdot 2H_2O$ | 90 | 10 |

### *3.4.7.2 Gas permeability*

The dynamic method was used to assess the gas permeabilities of neat PVA, PVA blends and PVA/ST/GL/HNT bionanocomposite films at different HNT contents. This method depends on the gas diffusion through material films (Khwaldia et al. 2004;

Imran et al. 2012). The pre-conditioned samples at 25ºC with the RH level of 50% were tightly fixed between two Teflon rings of permeability cell (ThermoFisher Scientific Pty. Ltd, Australia). Gas permeability was determined for both oxygen and air. The tested gas was continuously circulated in one chamber of permeability cell (channels A and B) at a controlled flow rate to keep a constant pressure gradient at 80 kPa. Nitrogen carrier gas was used at the same flow rate through channel C of another permeability cell chamber. The channel D of the same chamber was used to collect the gas mixture (i.e., tested gas and carrier gas) and injected directly to the gas chromatograph (GC), as shown in Figure 3-9. GC (Shimadzu GC-2014 with 5 Å molecular sieve column) was equipped with thermal conductivity detector and operated at a column temperature of 50ºC and helium flow rate of 25 ml/min. The tested gas concentration in the mixture was calculated as a percentage of detected peaks. Subsequently, the gas permeability can be determined according to the following equation (Imran et al. 2012; Khwaldia et al. 2004):

$$Gas\ permeability = \frac{a \times x \times V}{S \times t \times \Delta P} \qquad (3\text{-}5)$$

where $a$ is the concentration percentage of tested gas, $x$ is the film thickness (m), $V$ is the volume of permeability cell ($m^3$), $S$ is the surface area of tested films ($m^2$), $t$ is the time of gas circulation in permeability cell (approximately 60 min) and $\Delta P$ is the gas pressure gradient (kPa).

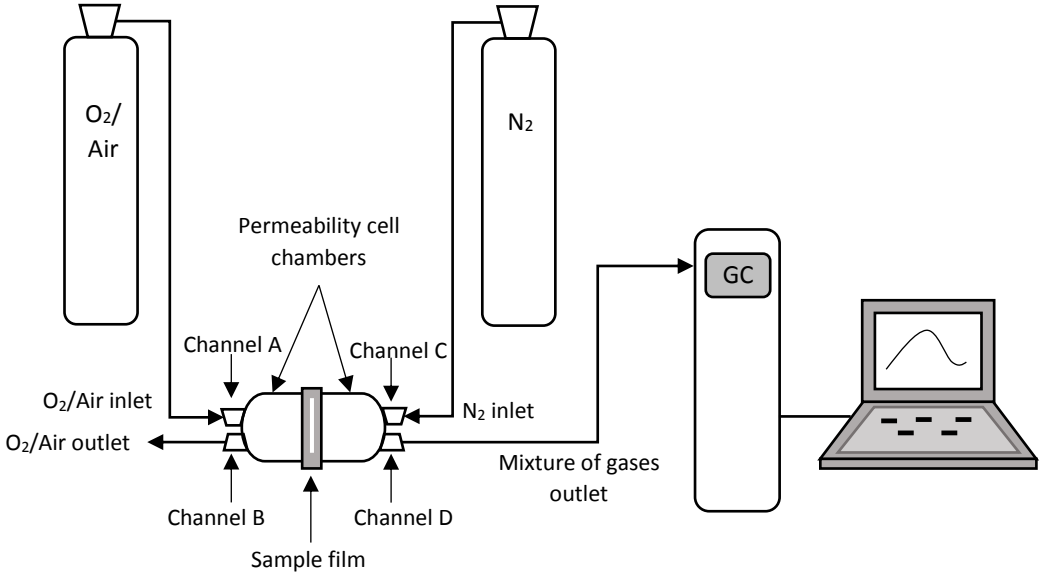


Figure 3-9. Gas permeability experiment setup

### 3.4.8 Water resistance

When nanocomposite materials are developed for food packaging applications, their interaction with water should be at a minimum level to improve the shelf life of packaged products. As such, water absorption capacity, water solubility and water contact angle were considered as key properties for the evaluation.

#### *3.4.8.1 Water absorption capacity ($W_a$)*

Water absorption capacity ($W_a$), also known as water uptake, was determined based on ASTM D570-98 standard. Square samples of neat PVA, PVA blends and PVA/ST/GL/HNT bionanocomposite films at different HNT contents in size of 2×2 $cm^2$ were pre-dried to remove any residual moisture at 50ºC for 24 h. The initial dry weight ($W_o$) of samples was recorded after cooled to room temperature in a desiccator filled with silica gel. These samples were immersed in 100 ml distilled water for 24 h to reach an equilibrium state at ambient conditions. The wetting samples were removed from water and dried gently with tissue papers to remove any excessive amount of

water on their surfaces. These samples were weighed again to record their weight with absorbing water ($W_t$). $W_a$ can be calculated according to the following equation:

$$Wa\ (\%) = \frac{W_t - W_o}{W_o} \times 100\% \qquad (3\text{-}6)$$

Three samples were tested for each material batch in order to obtain the average data with calculated standard deviations.

#### *3.4.8.2 Water solubility ($W_s$)*

The wetting samples from water absorption tests were used to measure the water solubility ($W_s$) according to ASTM D570-98 standard. Such samples were dried in a vacuum oven at 60ºC for 24 h to evaporate absorbed water. The dried samples were measured again to record the dry weight ($W_d$) after cooled to room temperature in a desiccator filled with silica gels as well. $W_s$ can be further calculated as follows:

$$Ws\ (\%) = \frac{W_t - W_d}{W_t} \times 100\% \qquad (3\text{-}7)$$

Average values with calculated standard deviations were recorded based on three repeated tests for each material batch.

#### *3.4.8.3 Water contact angle*

The wettability of materials can be generally characterised by water contact angle (Yuan and Lee 2013). A Tensiometer KSV-CAM 101 (KSV Instruments Ltd., Finland) was employed to measure water contact angles of neat PVA, PVA blends and PVA/ST/GL/HNT bionanocomposite films at different HNT contents, see Figure 3-10. The droplet of 2 µl deionised water was dropped on the film surface by using a Sessile Drop Half-Angle™ tangent line method (Alipoormazandarani, Ghazihoseini and Nafchi 2015; Sadegh-Hassani and Nafchi 2014) to determine the hydrophilicity of film

materials. Average values in relation to water contact angles were reported based on five droplets at randomly selected positions on different material films.

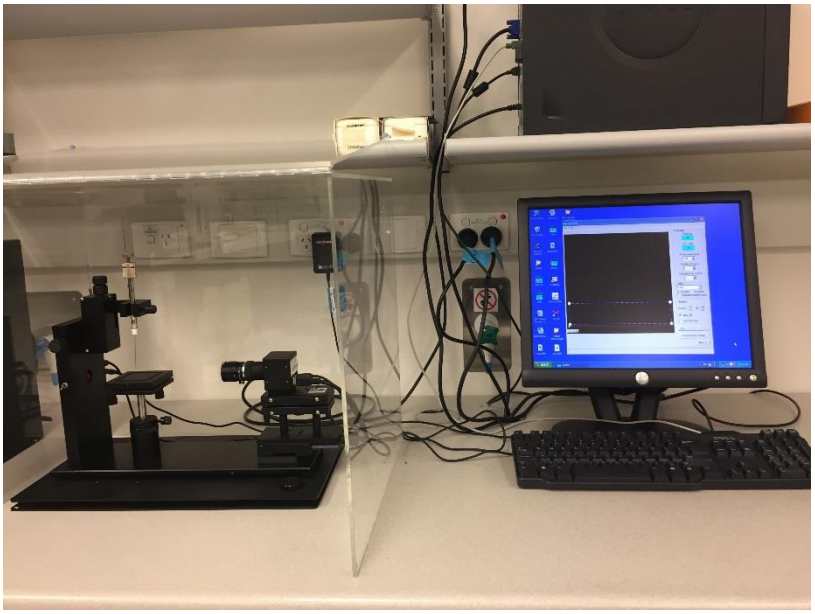

Figure 3-10. Tensiometer KSV-CAM 101 for water contact angle

### 3.4.9 Migration tests

When a packaging material gets in contact with foodstuffs, the migration of substances from packaging materials should be taken into account based on the criterion of an acceptable threshold of no more than 60 mg/kg of foodstuffs (European Commission Regulation (EU) No 10/2011). Consequently, the overall migration rate of PVA/ST/GL blends and their bionanocomposite films as well as the migration rate of HNTs from bionanocomposite films were studied together.

European Commission Regulation (EU) No 10/2011 (2011) was followed to evaluate the migration rates of PVA/ST/GL blends and their bionanocomposite films at different HNT contents. Three food simulants were selected to mimic hydrophilic, acidic and lipophilic foodstuff conditions, namely 10% (v/v) ethanol solution (simulant A), 3% (w/v) acetic solution (simulant B) and 50% (v/v) ethanol solution (simulant D1), respectively based on (European Commission Regulation (EU) No

10/2011). According to British Standard EN 1186-1 (2002), the material samples of PVA/ST/GL blends and their bionanocomposite films in size of 1 square decimetre ($dm^2$) were completely immersed in glass bottles filled with 100 ml of each food simulants. Three samples of each material batch and food simulants were prepared and kept in an air-circulating oven at 40ºC over the period of 10 days. After 10 days, the bottles containing samples were removed from the oven and all materials were cooled down to room temperature at ambient conditions before opening their covers for minimising the evaporation of food simulants. Samples were removed gently from bottles, and food simulants were evaporated, and their residual traces were dried completely overnight at 105ºC. The residues were cooled to room temperature, and then weighed with an analytical balance (±0.0001 g precision) to calculate the overall migration rate in comparison with the overall migration limit (OML) of 60 mg/kg (European Commission Regulation (EU) No 10/2011).

A similar procedure of overall migration rate was also performed to study the migration rate of HNTs. The dried residues of food simulants were analysed using Inductivity Coupled Plasma-Optical Emission Spectroscopy (ICP-OES), as illustrated in Figure 3-11, to identify the presence of aluminium ions ($Al^+$) and silicon ions ($Si^+$) as an indicator of the HNT migration from bionanocomposite films. At least three residue samples were utilised with ICP-OES after digested with 15 ml $HNO_3$ solution at the concentration of 3% for 2.5 h at 95ºC to convert Al and Si elements into an ionic state, which further diminished the effect of blend matrices and any other contaminations. PerkinElmer-Optima 8300 ICP-OES was employed for the corresponding analysis with the operation parameters summarised in Table 3-4. Two blank solutions were used for the calibration purpose consisting of distilled water and 3% $HNO_3$ solution. Furthermore, three controlled samples were prepared from a serial

dilution of standard stock solution for $Al^+$ and $Si^+$ for the comparison and calibration. 1000 mg/L concentrated solutions containing both $Al^+$ and $Si^+$ were diluted gradually to prepare $Al^+$ and $Si^+$ control samples at the concentrations of 10, 5 and 1 mg/L, respectively.

Table 3-4. Operation parameters of ICP-OES for HNT migration tests

| Parameter | Value |
|---|---|
| Plasma viewing mode | Radial and Axial |
| Plasms gas flow rate | 15.00 L/min |
| Auxiliary gas flow rate | 0.50 L/min |
| Nebuliser gas flow rate | 0.60 L/min |
| Pump flow rate | 1.50 mL/min |
| Radiofrequency | 1400 Watts |

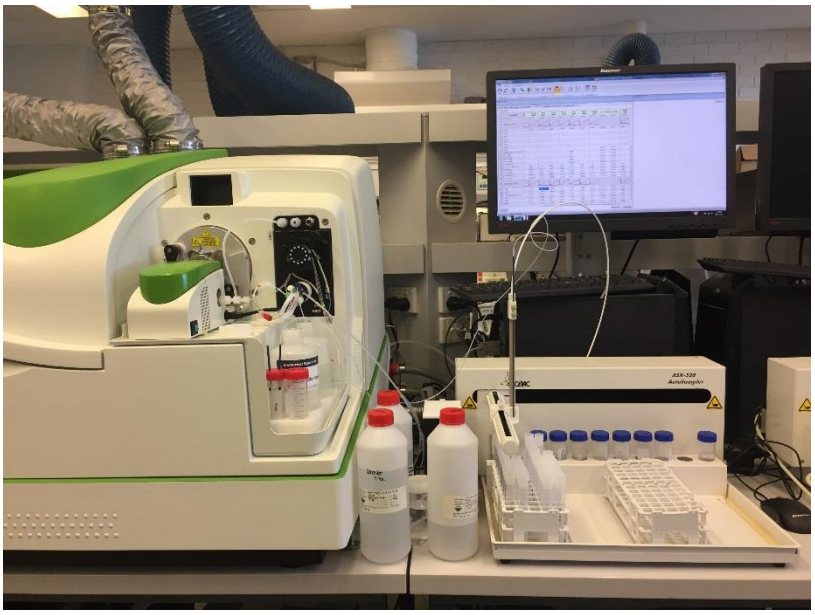

Figure 3-11. Inductivity coupled plasma-optical emission spectroscopic unit

### 3.4.10 Food packaging tests

Neat PVA, PVA/ST/GL blend and PVA/ST/GL/1 wt% HNT bionanocomposite films were used for food packaging tests. These films were manufactured in size of 23.0×24.0 cm according to the same procedure mentioned earlier in section 3.3. These films were double sealed (i.e. two sealing lines) with a hot sealing machine Pro-Line-C1 (Home and Commercial Heavy Duty) to avoid any gas leaking. Avocados with a lipid content of 20% (≈18.7/100g) (Seymour and Tucker 1993) and peaches with pH level ≤3.5 (Brady 1993) were purchased from local markets with similar size, colour and appearance as well as defect-free to minimise the differences between samples during the tests, as shown in Figure 3-12. Packaged fruits of peaches and freshly cut avocados were stored in a fridge at 8ºC with a RH level of 85% over the period of 14 days (Brady 1993; Seymour and Tucker 1993), which was subjected to the data recording of daily weight loss as an indicator for the shelf life of fruits (Hu et al. 2011).

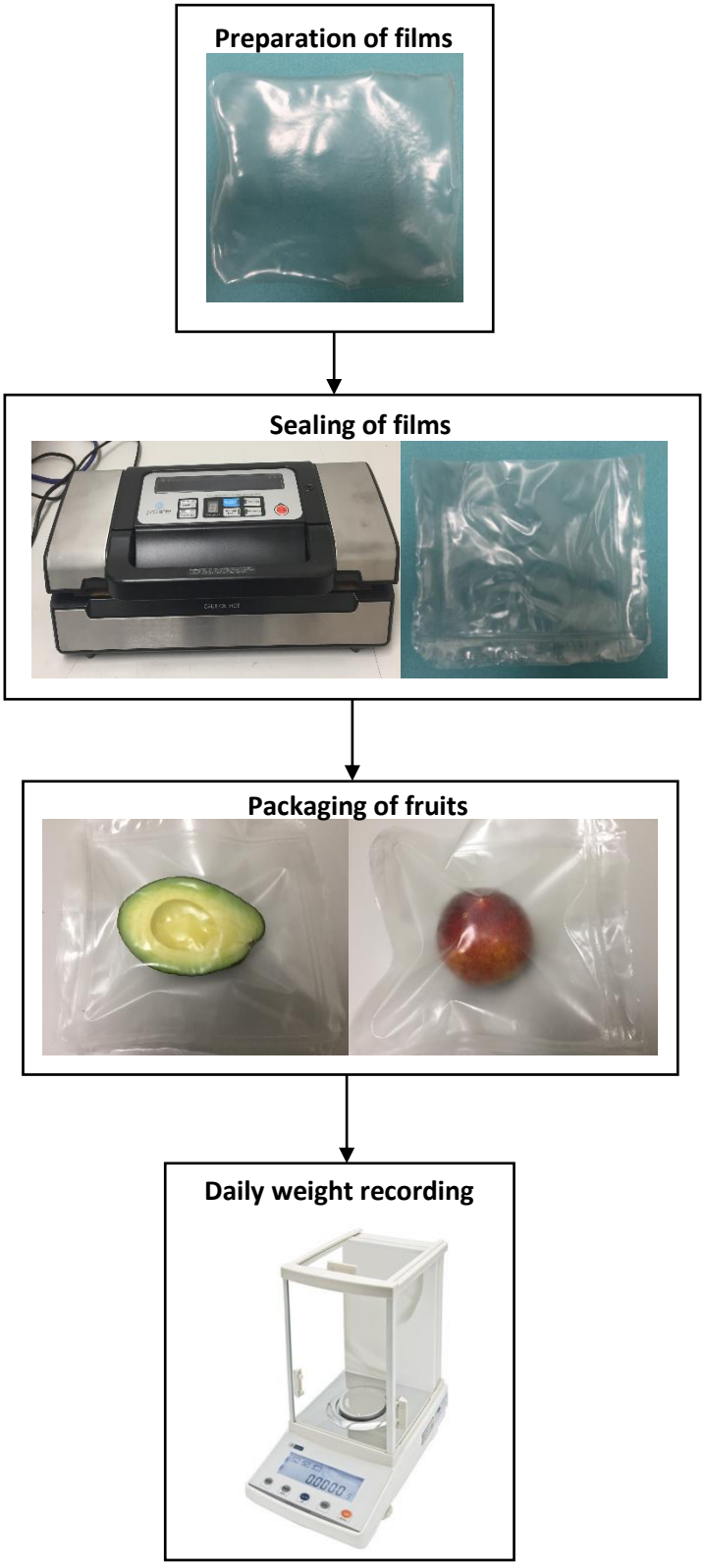


Figure 3-12. Flow chart of the food packaging test procedure

### 3.4.11 Soil burial tests

The biodegradability of material films was evaluated by means of soil burial degradation tests according to the procedure developed by Thakore et al. (2001). Square samples (3×3 $cm^2$) of neat PVA, PVA blends and PVA/ST/GL/HNT bionanocomposite films at different HNT contents were weighed with aid of an analytical balance to record their initial weights ($W_o$). These samples were buried at 5 cm under the surface in plastic containers of 2L capacity filled with sieved agricultural soil purchased from a local plant nursery. These containers were kept at room temperature with a RH level of 40-50% and using a humidity meter to monitor the RH at the same level by sprinkling water for the reduction of RH. The biodegradability results were recorded as a weight loss with time over a period of six months (i.e., 24-weeks). In the initial three months, the samples were removed from the containers on a weekly basis and gently washed with distilled water to remove soil from their surfaces. This routine was extended to be once every three weeks in the following three months. The clean samples were completely dried at 70ºC for 24 h to evaporate any moisture absorbed from the soil and/or in a washing process. The dried samples were weighed again to record the dry weight ($W_d$). Biodegradation rate can be calculated according to the following equation:

$$Biodegredation\ rate\ (\%) = \frac{W_o - W_d}{W_o} \times 100\% \qquad (3\text{-}8)$$

The weights of samples were measured in (g) and three samples were tested for each material composition for recording their average data along with associated standard deviations apart from the additional samples used for SEM observation.

# Chapter 4: Morphological, Mechanical and Thermal Properties of PVA/ST/GL/HNT Bionanocomposite Films

## 4.1 Introduction

Polymer nanocomposites offer the potential improvements in material properties like mechanical, thermal, optical and barrier properties at low nanofiller contents (Liu et al. 2006). A number of molecular changes can happen in nanocomposites due to the interactions between nanofillers with high surface areas and polymer matrices leading to the "non-classical" response of these nanocomposites reflected on the change of bulk material properties (Jancar et al. 2010). Consequently, the investigation of morphological structures of nanocomposites is important to understand the structure-property relationship. In this chapter, the morphological structures of as-received HNTs, PVA blends and PVA/ST/GL/HNT bionanocomposites were investigated by SEM and AFM. Moreover, the matrix-filler interactions, as well as bionanocomposite structures were evaluated via Fourier FTIR and XRD analyses, respectively. The effect of bionanocomposite structures and HNT dispersion was also studied on their mechanical, thermal and optical properties.

## 4.2 Morphological structures

### 4.2.1 SEM

Morphological structures of as-received HNT powders, neat PVA and PVA blends were illustrated in Figure 4-1. Whereas, morphological structures of PVA/ST/GL/HNT bionanocomposite films at different HNT contents were depicted

in Figure 4.2. A tubular structure of HNTs was clearly observed in Figure 4-1 (a). Moreover, typical HNT agglomeration was also noticeable as HNT nanoparticles naturally tended to agglomerate due to their weak Van Der Waals interactions. As seen from Figure 4-1 (b), fracture surfaces of neat PVA appeared to be smooth, brittle with the limited elongation and coexistence of crystalline and amorphous phases in the films, as mentioned earlier. However, more ductile material behaviour was clearly observed for PVA/GL blends owing to the GL plasticisation effect shown in Figure 4-1 (c). Whereas, fracture surfaces of PVA/ST blend films appeared to be much rougher and more brittle with the addition of ST (Figure 4-1-d). The further inclusion of GL depicted in Figure 4-1 (e) was found to diminish such brittleness nature. The constituents of PVA/ST/GL blends showed good compatibility with one another without apparent phase separation, which was in good agreement with the results obtained by Wu et al. (2017). Their field emission (FE)-SEM results showed that PVA/ST blends had homogenous and dense film structures in the presence of GL and citric acid with better binding improvements between different material components (Wu et al. 2017).

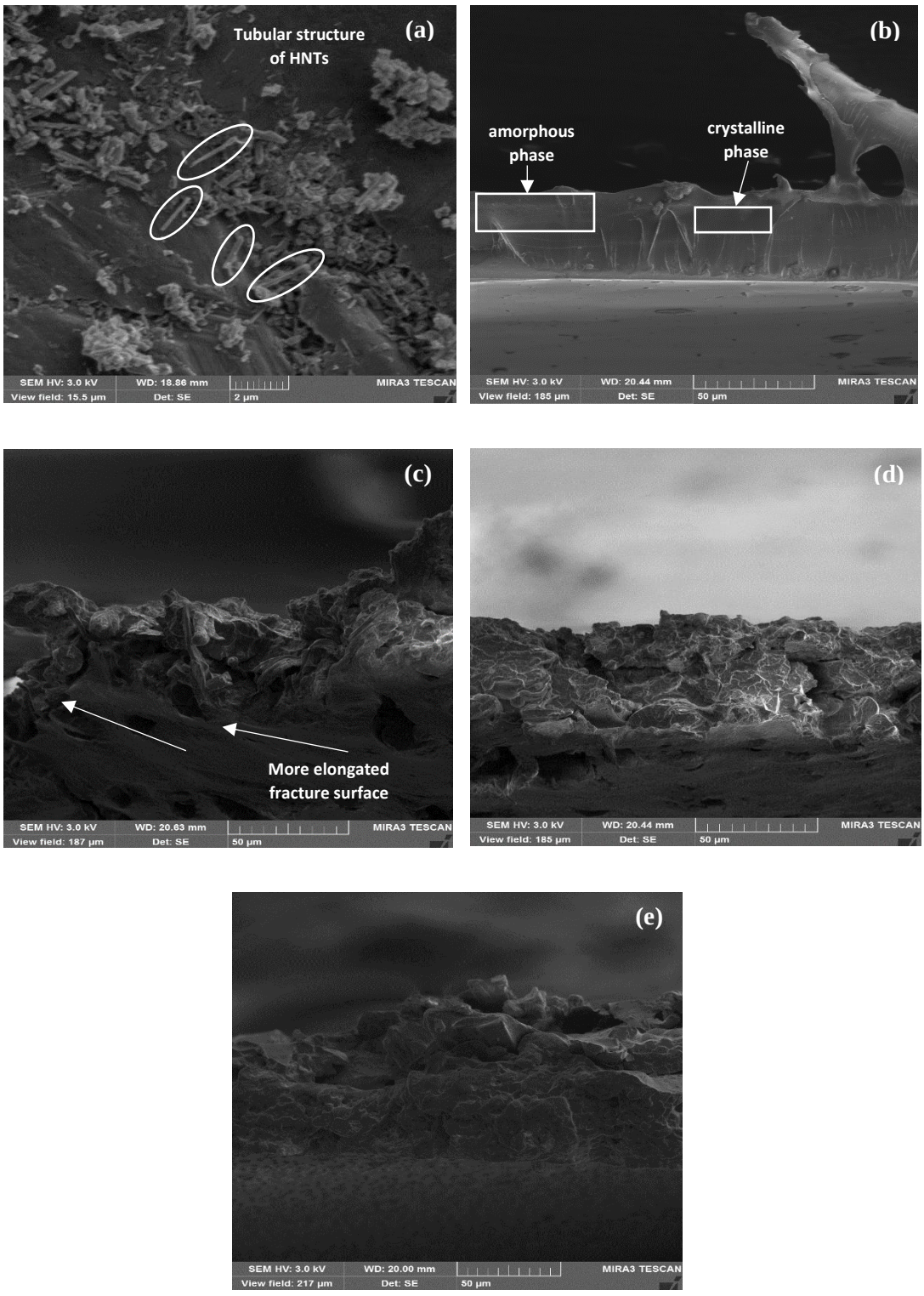


Figure 4-1. SEM micrographs: (a) as-received HNT powders, (b) pure PVA, (c) PVA/GL blends, (d) PVA/ST blends and (e) PVA/ST/GL blends

This identical compatibility appeared again in bionanocomposite films. In other words, the presence of HNTs did not affect the compatibility of PVA/ST/GL blends. Low HNT contents at 0.25 and 1 wt% yielded homogeneous HNT dispersion in bionanocomposites (as circled in white colour) with typical wavy-line structures (as circled in red colour) demonstrated in Figures 4-2 (a)-(c), which was also identified in previous studies carried out by Khoo, Ismail and Ariffin (2011) for PVA/chitosan/HNT nanocomposites at the HNT contents of 0.25 and 0.5 wt%, respectively. Such wavy-line structures were believed to showcase the enhancement of tensile strength of such bionanocomposite films when compared with their polymer blends alone due to improvement of tearing strength. On the other hand, a clear sign of HNT agglomeration was detected at the HNT contents of 3 and 5 wt% in PVA/ST/GL/HNT bionanocomposites, as illustrated in Figures 4-2 (d) and (e), as circulated with weight colour, which was consistent with previous work (Khoo, Ismail and Ariffin 2011). As such, the tendency of HNT agglomeration increased with increasing their weight fraction reported by Gaaz et al. (2017).

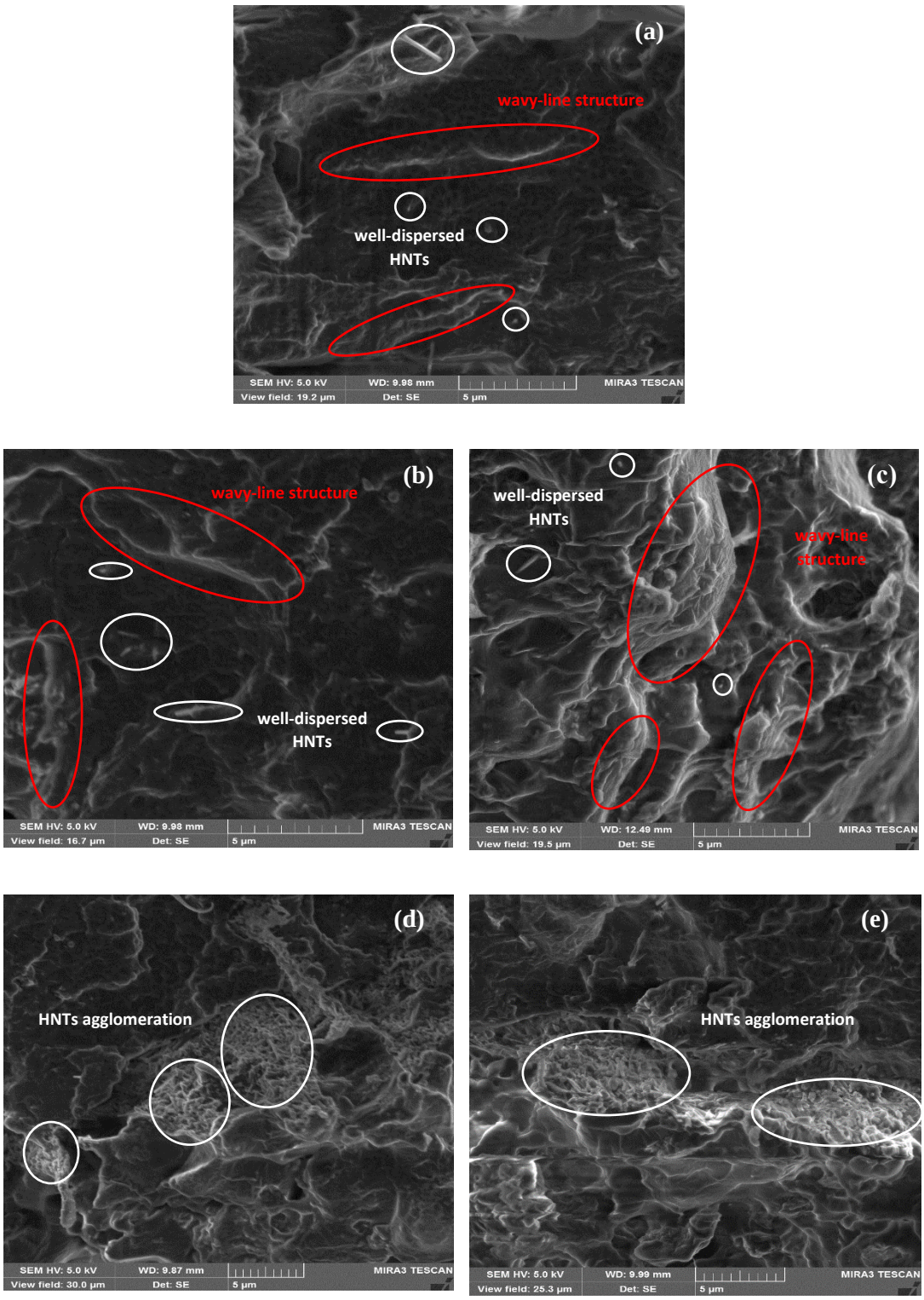


Figure 4-2. SEM micrographs of PVA/ST/GL/HNT bionanocomposites at different HNT contents: (a) 0.25 wt%, (b) 0.5 wt%, (c) 1 wt%, (d) 3 wt% and (e) 5 wt%

Energy-dispersive spectroscopic (EDS) tests were performed for bionanocomposite films at the HNT contents of 0.25 and 3 wt% to highlight two typical conditions of well-dispersed HNTs and HNT agglomerates, respectively, Figure 4-3. The presence of Al and Si elements in the chemical composition of bionanocomposite films was associated with dispersed HNTs within blend matrices as Al and Si are the major elements of HNT chemical structure (i.e., $Al_2Si_2O_5(OH)_4.nH_2O$) in good accordance with Dong et al. (2015b). The presence of carbon and oxygen elements was attributed to the existence of PVA/ST/GL blends with additional carbon contents derived from carbon-coating sample layers.

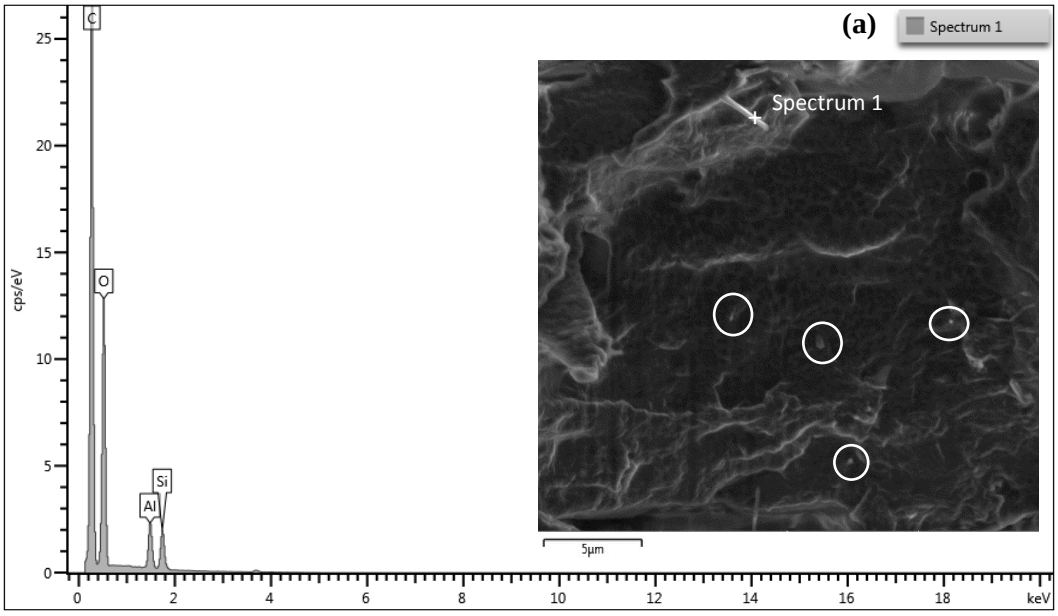

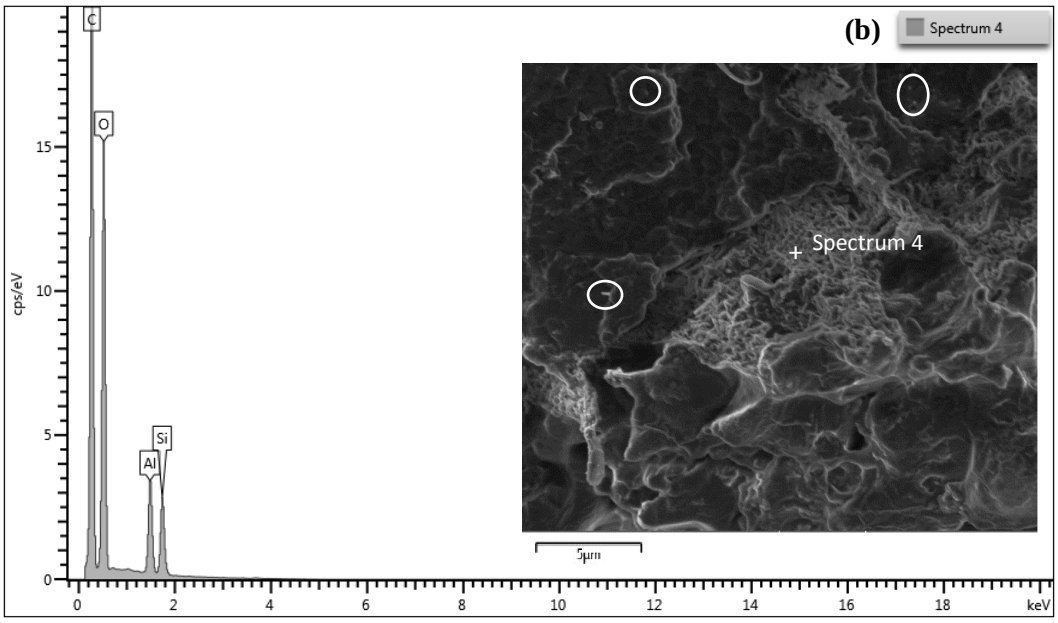


Figure 4-3. EDS spectra of PVA/ST/GL/HNT bionanocomposites at two typical HNT contents: (a) 0.25 wt% and (b) 3 wt%. Circled areas indicate dispersed HNT particles within polymer blend matrices.

### 4.2.2 AFM

The tubular morphology of as-received HNTs was observed again with the AFM images shown in Figure 4-4 (a). Moreover, the average dimensions of as-received HNTs were calculated as well based on the measurements of 173 individual particles despite the difficulty to overcome HNTs agglomeration. As-received HNTs had an average diameter $D$ = 18.63± 0.52 nm and an average length $L$= 730.75± 13.40 nm, as illustrated in Figure 4-4 (b). Consequently, the average aspect ratio ($L/D$) of as-received HNTs was 39.22, which was in good accordance with other studies (Yuan, Tan and Annabi-Bergaya 2015; Wagner, Cooper and Riedlinger 2005).

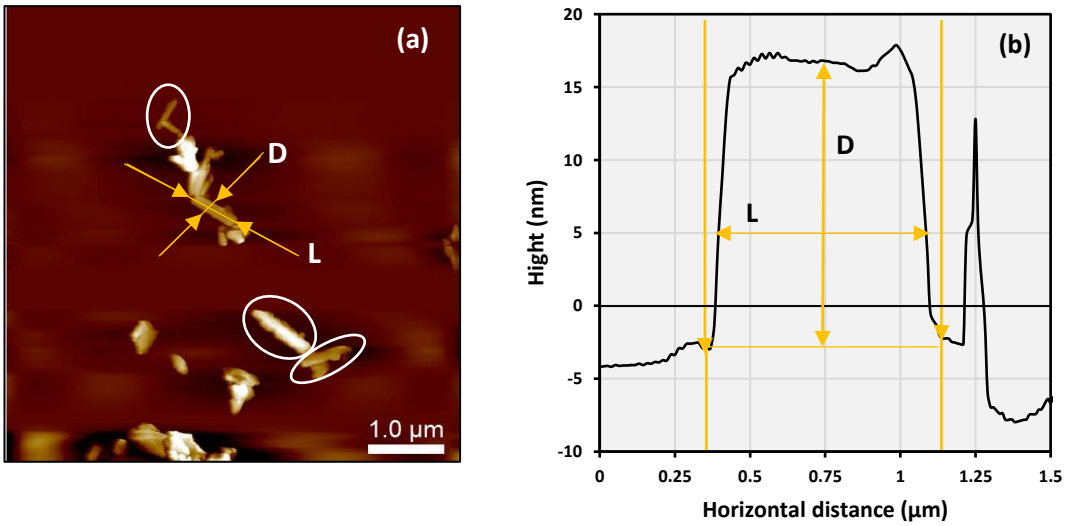


Figure 4-4. (a) AFM image of as-received HNTs and (b) height section profile of individual HNT.

AFM images of PVA/ST/GL blends and corresponding bionanocomposite films at different HNT contents clearly demonstrated three major areas including black areas to represent amorphous phase of polymer blend matrices, light and dark brown areas for their crystalline phase and interfacial phase between polymer blend matrices and HNTs as well as white and yellow areas for fully and partially embedded HNTs within polymer matrices, respectively (see Figure 4-5), which was based on the diversity of mechanical properties of each surface area in good accordance with previous literatures (Farhoodi et al. 2014; Voss, Stark and Dietz 2014).

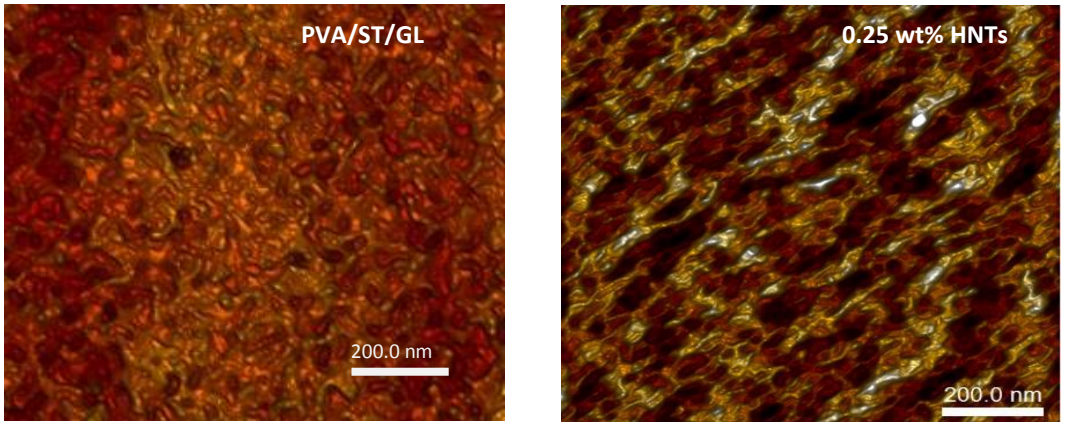

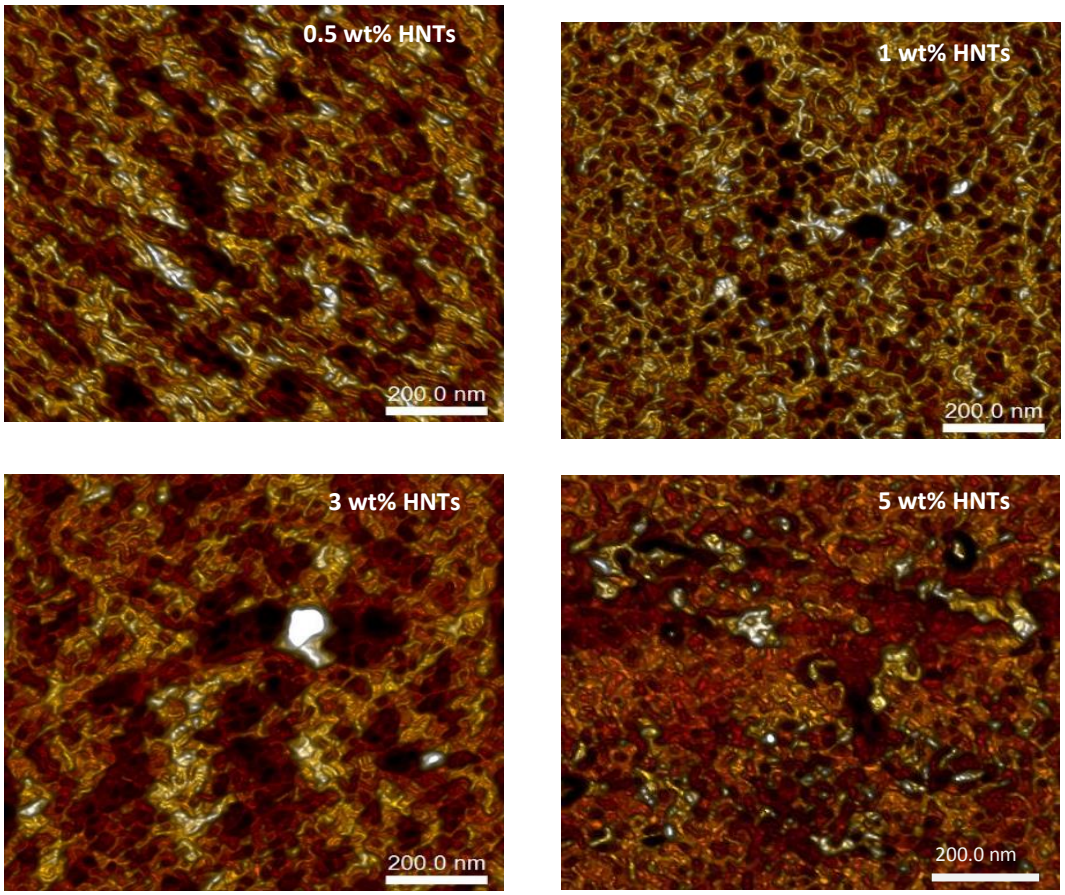


Figure 4-5. AFM images of PVA/ST/GL blends and corresponding bionanocomposite films at different HNT contents

The variation of surface mechanical properties can produce different contrasts under AFM corresponding to each area. The AFM technique in a Peak Force tapping mode can be used to evaluate these variations in mechanical properties like elastic modulus, adhesion and dissipation of each surface area. For example, PVA/ST/GL blends (Figure 4-6-a) were scanned along A-A1 section (Figure 4-6-b) to reflect the variation of elastic modulus for each area along the scanning section. As exhibited in Figure 4-6 (c), the light areas had relatively high elastic modulus of 103.7 ± 9.3 MPa related to crystalline phases. Whereas, the dark areas had much lower elastic modulus of 21.2 ± 4.1 MPa for amorphous phases.

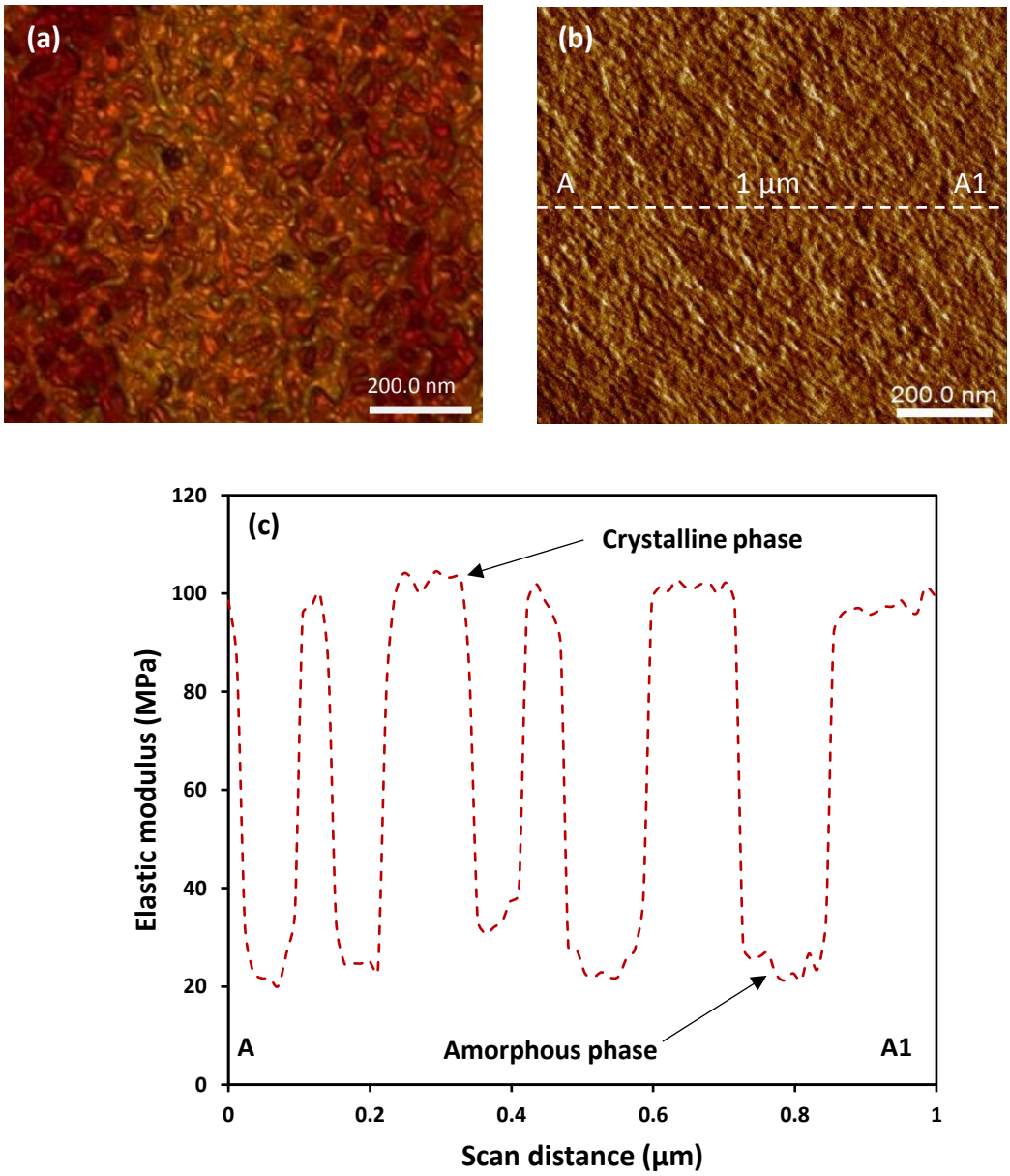


Figure 4-6. (a) 2D-AFM mapping image of PVA/ST/GL blend films, (b) DMT modulus image, and (c) DMT elastic modulus-scan distance curve for typical section A-A1 in (b).

Furthermore, bionanocomposite films at the HNT contents up to 1 wt% reflected good HNT dispersion within polymer matrices, beyond which, HNT agglomeration became more pronounced. These observations were supported by the evaluation of surface roughness of PVA/ST/GL blends and their bionanocomposite films. The surface roughness of bionanocomposite films increased with increasing the HNT content from 0 to 5 wt% in a more and less linear manner from 13.83 to 75.80 nm. This trend became

less pronounced beyond 1 wt% HNTs, as shown in Figure 4-7. The lower surface roughness of bionanocomposite films with the HNT inclusion up to 1 wt% could be attributed to uniform HNT dispersion within polymer matrices as well as homogenous structures that were built up by effective intermolecular bonding between different components (Monteiro et al. 2018). It is well known that aspect ratios of nanofillers can be remarkably reduced with increasing the nanofiller content (Choudalakis and Gotsis 2009; Sridhar and Tripathy 2006; Saritha et al. 2012), particularly resulting from their agglomeration at high content levels. This phenomenon was proven experimentally in this study by determining the aspect ratios of HNTs within bionanocomposite films at different HNT contents. HNT aspect ratios decreased in a monotonic manner from 39.27 to 14.87 with increasing HNT contents from 0.25 to 5 wt% illustrated in Figure 4-7. In short, the surface roughness of bionanocomposite films and embedded HNT aspect ratios completely reflected an opposite trend. In other words, increasing the HNT content could further increase the surface roughness of bionanocomposite films along with the reduction in HNT aspect ratios within films accordingly.

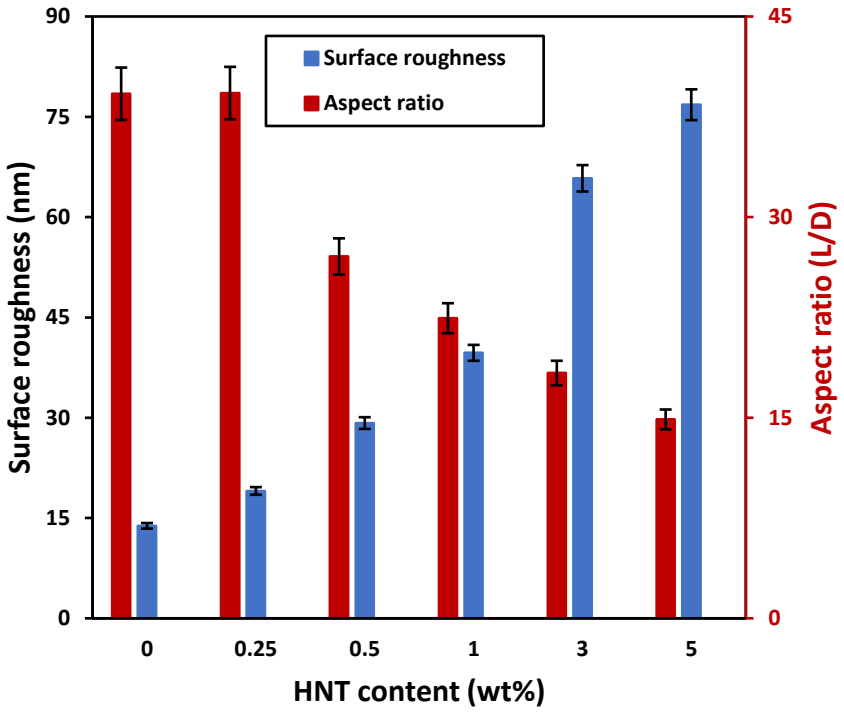


Figure 4-7. Effect of HNT content on surface roughness and aspect ratio of embedded HNTs in PVA/ST/GL/HNT bionanocomposite films

### 4.3 Mechanical properties

Mechanical properties of neat PVA, PVA/GL, PVA/ST and PVA/ST/GL blends were summarised in Figure 4-8. Plasticised PVA films with 30 wt% GL were prepared to improve the elasticity and reduce the brittleness of neat PVA. Significant reductions in tensile strength and Young's modulus of PVA/GL blend films were found to be 77.95 and 96.5%, respectively, as compared with those of neat PVA. Nonetheless, the elongation at break was shown to be increased drastically by 321.09% owing to typical GL plasticisation effect to improve the movement of polymeric chains, and thus increase free volume resulting in the ductile fracture surfaces in SEM results obtained. Moreover, PVA/ST blends had lower tensile strength and elongation at break than those of neat PVA by 28.32 and 51.66%, respectively, despite an increase in Young's modulus by 52.68% as opposed to that of neat PVA. This trend could be ascribed to amorphous nature and inherent brittleness of ST leading to the improvement of

stiffness at the expense of flexibility in good accordance with Azahari, Othman and Ismail (2011) and Ramaraj (2007b) as well as the rough fractured surfaces depicted in SEM images of this study. Additionally, PVA/ST/GL blends had increases in tensile strength and Young's modulus by 4.0 and 119.67% relative to those of PVA/ST blends in spite of being still lower than those of neat PVA and PVA/ST blends. Compared with both neat PVA and PVA/ST blends, PVA/ST/GL blends possessed excellent elongation at break which is regarded as one of key mechanical properties in relation to nanocomposite manufacturing processes. According to Wu et al. (2017), the elongation at break varied as a function of the GL content. GL with hydroxyl groups can form hydrogen bonds with polymers via the interaction with hydroxyl and carboxyl groups as well to effectively improve the free volume of the material system by reducing intermolecular forces and change polymer blends from typical brittle nature to good ductility. Overall, these findings were consistent with the morphological structures observed in SEM analysis.

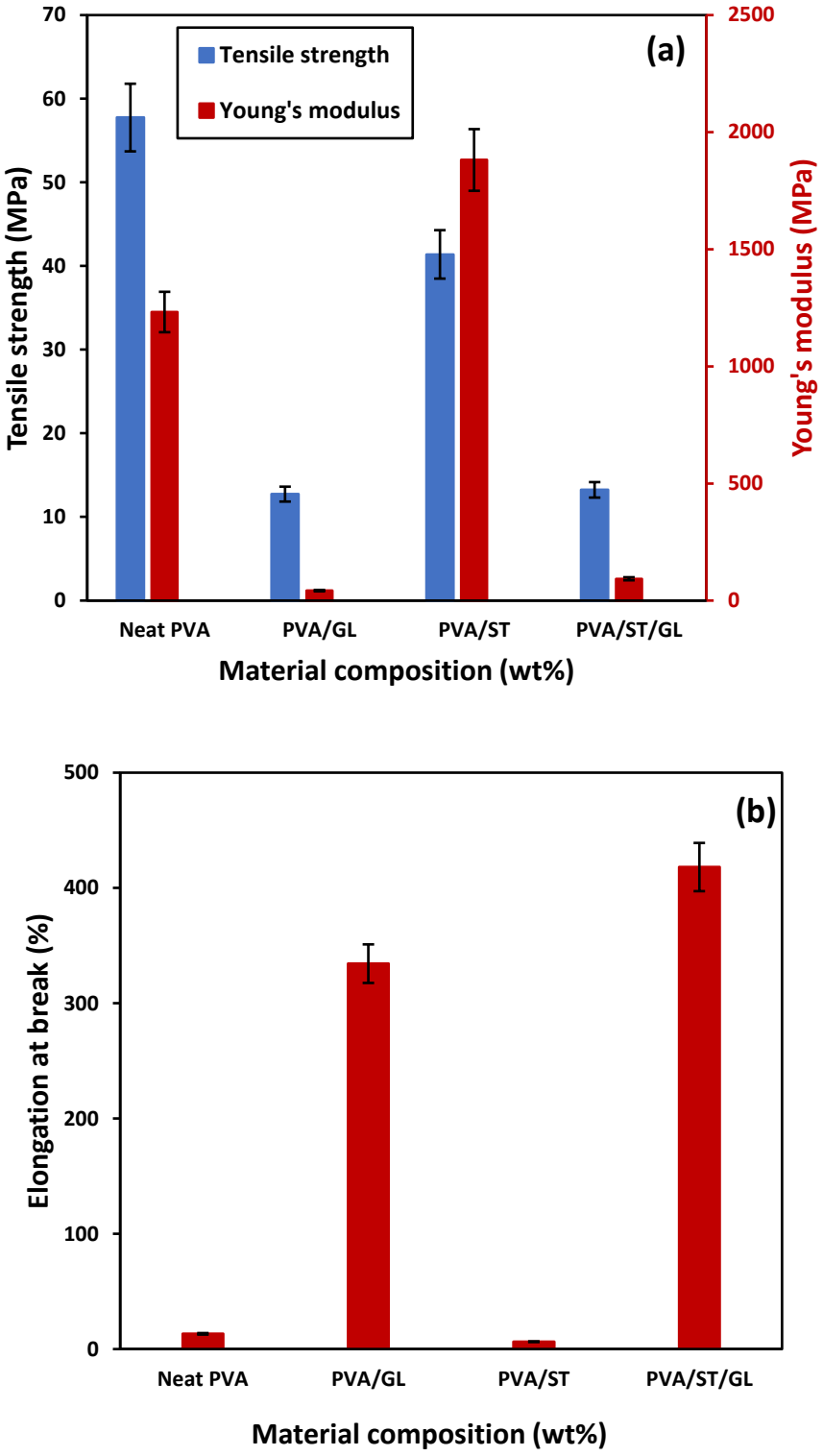


Figure 4-8. Mechanical properties of neat PVA, PVA/GL, PVA/ST and PVA/ST/GL blends: (a) tensile strength and Young's modulus and (b) elongation at break

PVA/ST/GL/HNT bionanocomposite films at the HNT contents of 0.25 and 0.5 wt% had higher tensile strength than that of PVA/ST/GL blends with an increasing level by

20.0 and 3.4%, respectively (see Figure 4-9). Moreover, the tensile strength of bionanocomposite films declined significantly beyond 1 wt% HNTs. This trend could be interpreted by HNT agglomeration beyond 1 wt% to induce detrimental effect on interfacial bonding between polymer blend matrices and nanofillers for effective load transfer, which was clearly demonstrated in the SEM and AFM results. Similar trends were also reported by Sadhu et al. (2014) for PVA/ST/Cloisite-30B clay nanocomposite films and Tang et al. (2008) for PVA/ST/nano-$SiO_2$ nanocomposite films. Moreover, Young's moduli of bionanocomposite films increased linearly with increasing the HNT content from 0 to 1 wt% up to 148.97% due to the inherent toughness of HNTs (Qiu and Netravali 2013). Although Young's moduli of bionanocomposite films reinforced with 3 and 5 wt% HNTs declined as compared to those with lower HNT contents, it was still higher than that of PVA/ST/GL blends. Accordingly, the elongation at break decreased remarkably with increasing the HNT content beyond 0.25 wt% due to the mobility restriction of polymeric chains in the presence of nanofillers (Tang et al. 2008). Nanofiller agglomeration arising from poor dispersion within polymer matrices can be the main reason associated with the similar behaviour, as evidenced by Heidarian, Behzad and Sadeghi (2017) for PVA/ST/cellulose nanofibril (CNF) nanocomposite films and Cano et al. (2015b) for PVA/ST/cellulose nanocrystal (CNC) nanocomposite films. Overall, the improvements in tensile strength and Young's modulus were related to nanofiller dispersion and nanofiller content while the elongation at break was influenced by the plasticiser contents in polymer blends, which was decreased with increasing the nanofiller content as well.

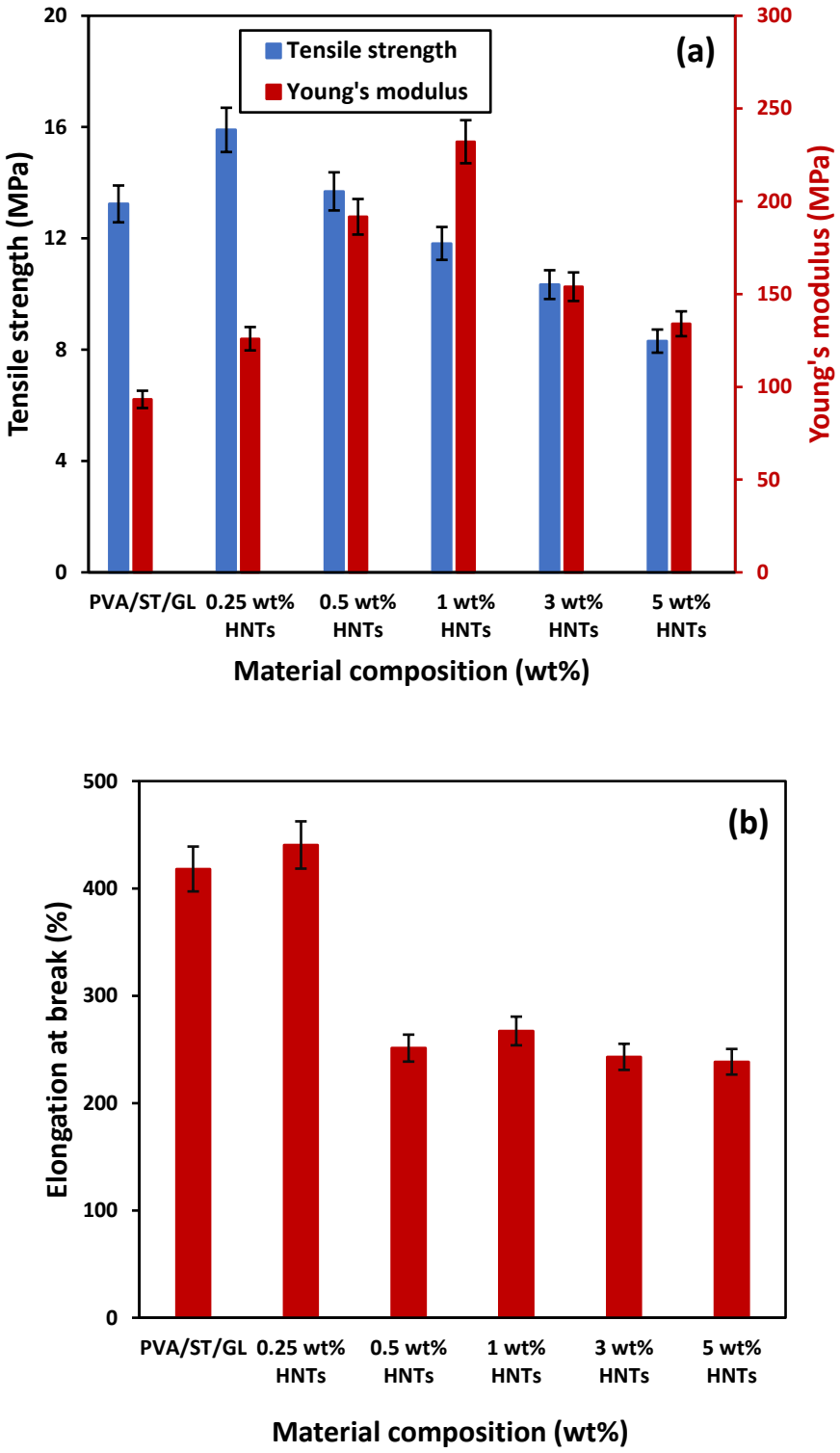


Figure 4-9. Mechanical properties of PVA/ST/GL blends and corresponding bionanocomposite films at different HNT contents: (a) tensile strength and Young's modulus and (b) elongation at break

## 4.4 Thermal properties

Thermogravimetric analysis (TGA) curves and derivative thermogravimetric (DTG) curves of neat PVA and neat ST as well as their blends were shown in Figure 4-10 (a) and (b), respectively. Additionally, the data of these curves were summarised in Table 4-1 accordingly. The thermal stability of PVA/GL blends was relatively low in comparison with that of neat PVA since GL plasticisation effect could weaken inter-and-intramolecular forces with the improvement of chain mobility leading to an increase in both heat and mass transfer. Similarly, Mohsin, Hossin and Haik (2011b) concluded that the plasticisers had low molecular weight compared with polymers, and easily penetrated between polymeric molecules to reduce their interactions. As such, chain mobility and free volume were increased resulting in the final reduction in their thermal stability. Such findings were clearly demonstrated with decreasing the decomposition temperatures of PVA/GL blends by 104.7, 32.8 and 7.8ºC at the weight losses of 5 ($T_{5\%}$), 50 ($T_{50\%}$) and 90% ($T_{90\%}$), respectively as opposed to that of neat PVA. In particular, higher thermal stability of PVA/ST blends compared with that of neat PVA could be explained by the inherent ST structures of thermal resistive cyclic hemiacetal (Aydın and Ilberg 2016). As a result, the $T_{50\%}$ and $T_{90\%}$ of PVA/ST blends were found to be increased by 44.2 and 57.8ºC, respectively, as opposed to those of neat PVA. Furthermore, the thermal stability of PVA/ST/GL blends was not comparable to those of PVA and ST alone in that such blends had complex polymeric components with plenty of hydroxyl and carboxyl groups that could be actively interacted for generating hydrogen bonds. In summary, thermal properties of PVA/ST/GL appeared to be between those of PVA/GL and PVA/ST blends.

On the other hand, the thermal stability of PVA/ST/GL/HNT bionanocomposites was even better than that of PVA/ST/GL blends, evidenced by increasing decomposition

temperatures and decreasing the weight loss, as illustrated in Figure 4-11 (a) and (b). At the HNT content of 1 wt%, $T_{5\%}$, $T_{50\%}$ and $T_{90\%}$ of bionanocomposites were mostly the highest among other bionanocomposites, which were increased by 20.5, 8.7 and 8.5ºC, respectively as opposed to those of PVA/ST/GL blends, Table 4-1. Notwithstanding that the thermal stability of bionanocomposites with the inclusion of 3 and 5 wt% HNTs slightly declined due to the HNT agglomeration, it still appeared to be better than those of PVA/ST/GL blends. The inherent characteristic of HNTs as a barrier material against heat and mass transfer was clearly shown because hollow tubular structures could trap volatile molecules for delaying the mass transfer during the thermal decomposition process, which was deemed as the main reason for improving the thermal stability of bionanocomposite films (Liu et al. 2014).

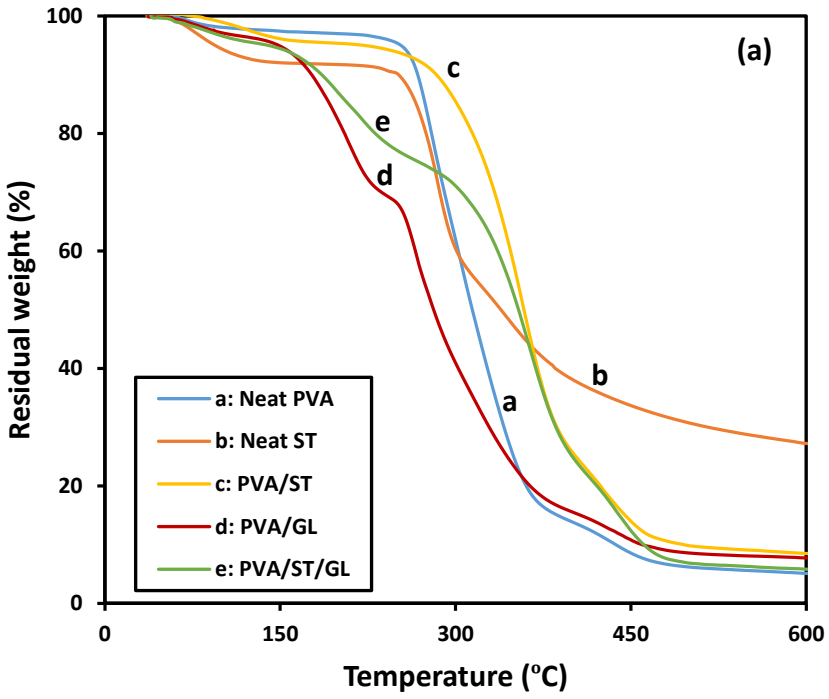

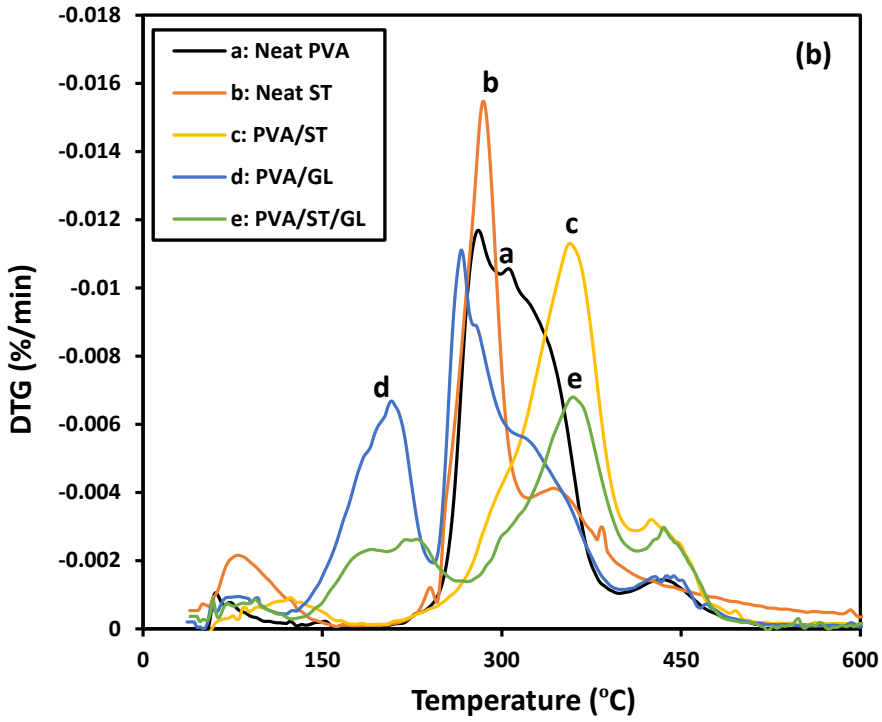


Figure 4-10. (a) TGA curves and (b) DTG curves of neat PVA, ST and their polymer blends

DTG curves of neat PVA and ST (Figure 4-10-b) depicted clear decomposition temperatures ($T_{d3}$) with associated sharp peaks taking place at 282.1 and 285.3ºC, respectively, which were related to the decomposition and dehydration of hydrogen bonds. Additionally, water loss and carbonisation of organic molecules gave rise to the other two unclear decomposition temperatures detected below 100ºC ($T_{d1}$) and above 400ºC ($T_{d4}$), respectively, as confirmed in previous work (Nistor and Vasile 2012; Sin et al. 2011). A new decomposition temperature ($T_{d2}$) at approximately 200ºC was attributed to the evaporation of volatile materials for PVA/GL blends. In a similar manner, PVA/ST blends had comparable decomposition temperatures to that of neat PVA with a slight increase in $T_{d1}$ relating to the moisture content within ST structures. PVA/ST/GL blends showed four decomposition temperatures similar to that of PVA/GL blends, namely $T_{d1}$ below 100ºC for water loss, $T_{d2}$ at about 225ºC due to the presence of GL as a plasticiser, $T_{d3}$ at approximately 360ºC arising from the

decomposition/dehydration of hydrogen bonds, as well as $T_{d4}$ at about 435ºC in relation to the carbonisation of organic molecules (Sreekumar, Al-Harthi and De 2012; Nistor and Vasile 2013). All decomposition temperatures of bionanocomposites increased when compared with those of corresponding polymer blends, which was ascribed to the incorporation of HNTs with a single decomposition temperature detected at 490.0ºC due to their higher thermal stability (Figure 4-11-b). $T_{d1}$, $T_{d2}$, $T_{d3}$ and $T_{d4}$ of bionanocomposites reinforced with 1 wt% HNTs increased by 6.4, 18.7, 14.7 and 7.8ºC, respectively when compared with those of PVA/ST/GL blends, which also appeared to decline slightly at HNT contents of 3 and 5 wt% owing to the HNT agglomeration at high content levels. In comparison, at the low HNT contents between 0.25 and 1 wt%, the enhanced thermal stability of bionanocomposites was believed to be associated with good HNT dispersion resulting in increasing the heterogeneity of polymer blends, which was consistent with Priya et al. (2014) for PVA/ST/CNF nanocomposites and Sadhu, Soni and Garg (2015) for PVA/ST/Cloisite-30B clay nanocomposites.

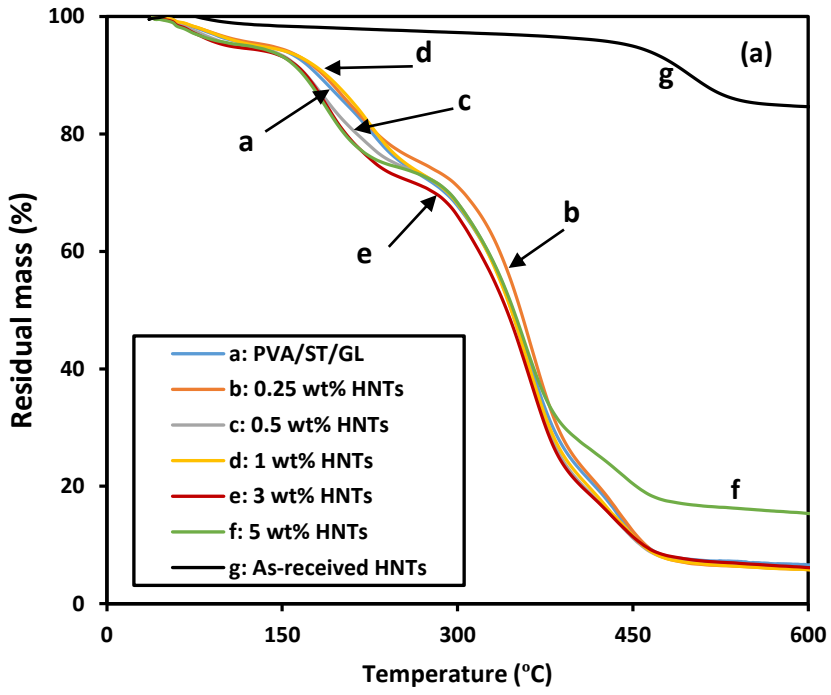

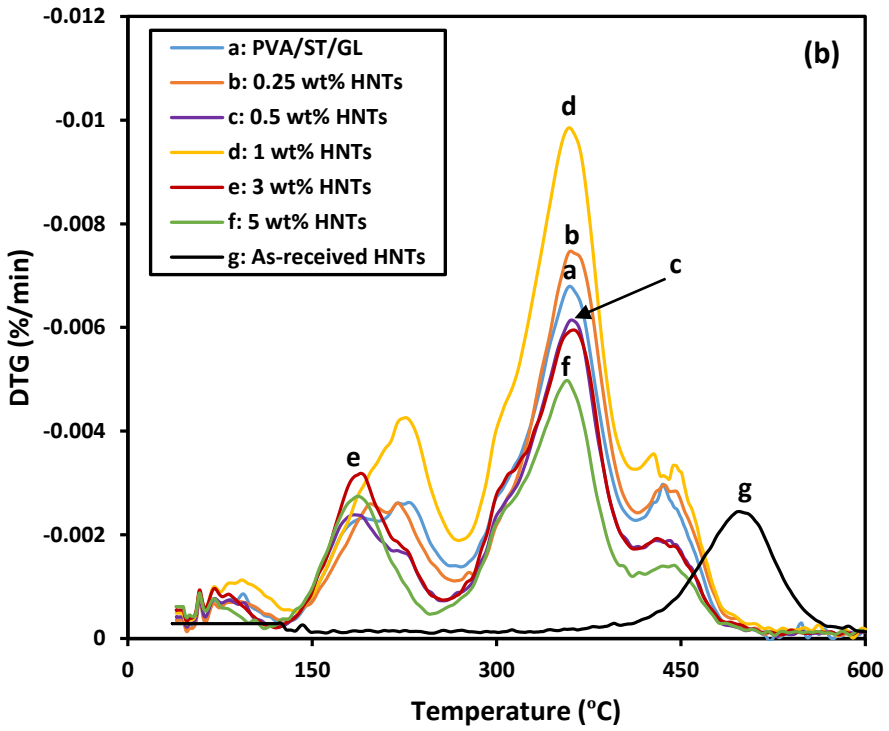


Figure 4-11. (a) TGA curves and (b) DTG curves for as-received HNTs, PVA/ST/GL blends and their corresponding bionanocomposites at different HNT contents

Differential scanning calorimetry (DSC) curves of neat PVA, neat ST and their blends were shown in Figure 4-12 (a). Moreover, the DSC curves of as-received HNTs, PVA/ST/GL blends and their bionanocomposites were exhibited in Figure 4-12 (b) along with associated thermal properties listed in Table 4-2. $T_g$ and $T_m$ of neat PVA was determined to be 70.7 and 244.6ºC, respectively, which was in good agreement with previous studies (Lim et al. 2015; Sreedhar et al. 2005; Strawhecker and Manias 2000). Whereas, the $T_g$ and $T_m$ of neat ST were relatively high reaching 80.4 and 263.3ºC, respectively. The good compatibility between PVA, ST and GL were indicated by a single $T_g$ for all PVA blends, which was supported by the SEM observation in section 4.2.1. The $T_g$ and $T_m$ of PVA/ST blends were improved by 3.4 and 43.7ºC, respectively, as opposed to those of neat PVA, which was ascribed to better stiffening effect of hydrogen bonds between PVA and ST with the addition of ST to induce new hydroxyl groups (Ramaraj 2007b; Jose et al. 2015). Conversely, $T_g$

and $T_m$ of PVA/GL blends were decreased by 23.0 and 15.6ºC, respectively relative to those of PVA due to GL plasticisation effect mentioned earlier.

On the other hand, $T_g$ and $T_m$ of bionanocomposites were increased with the inclusion of HNTs at different rates as opposed to those of PVA/ST/GL blends. For instance, the higher increasing rate of $T_g$ by 9.95ºC at 0.25 wt% HNTs and an increasing rate of $T_m$ by 14.48ºC at 5 wt% HNTs could be associated with high thermal stability of HNTs. It is well known that HNTs can act as heterogeneous nucleating agents when incorporated into polymer matrices in bionanocomposite material systems (Liu et al. 2014). Hence, the crystallisation temperature ($T_c$) of bionanocomposites tended to be decreased with the addition of HNTs while the related crystallisation rate ($X_c$) was enhanced with the incorporation of HNTs particularly at HNT contents between 0.25 and 1 wt% when compared with those of PVA/ST/GL blends counterparts. Furthermore, the melting enthalpy ($\Delta H_m$) of bionanocomposites improved as well with the addition of HNTs due to the thermal stability and barrier action of HNTs against heat and mass transfer (Liu et al. 2014; Liu et al. 2007), which also coincided with Tee et al. (2013) in PVA/ST/MMT nanocomposites.

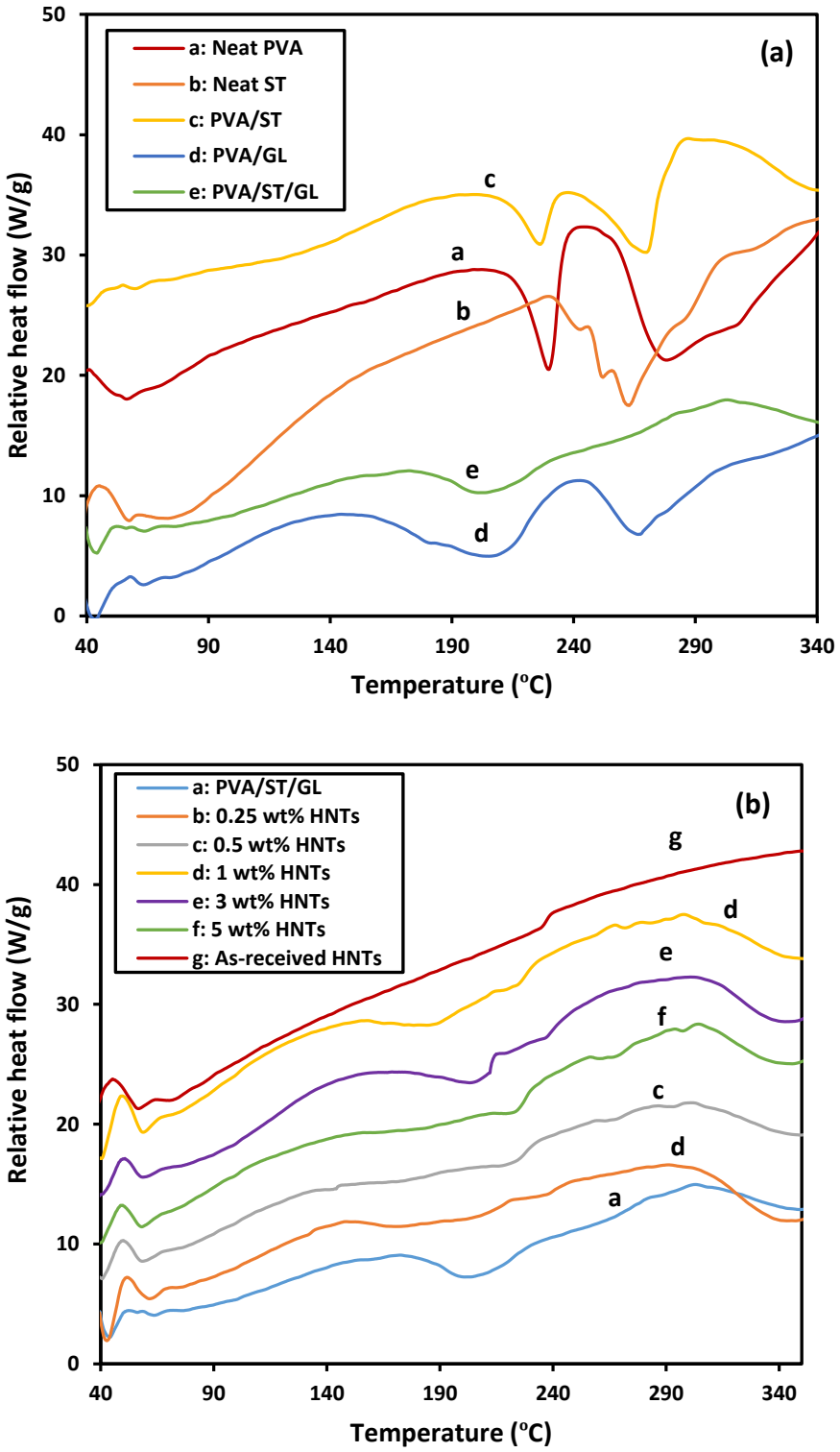


Figure 4-12. DSC thermograms: (a) neat PVA and ST and corresponding blends, and (b) as-received HNTs, PVA/ST/GL blend and their corresponding bionanocomposites at different HNT contents

Table 4-1. TGA and DTG data summary for neat materials, PVA blends and PVA/ST/GL/HNT bionanocomposites at different HNT contents

| **Sample** | $T_{5\%}$ **(ºC)** | $T_{50\%}$ **(ºC)** | $T_{90\%}$ **(ºC)** | $T_{d1}$ **(ºC)** | $T_{d2}$ **(ºC)** | $T_{d3}$ **(ºC)** | $T_{d4}$ **(ºC)** |
|---|---|---|---|---|---|---|---|
| Neat PVA | 253.2 | 314.3 | 436.9 | 76.1 | – | 282.1 | 432.0 |
| Neat ST | 94.1 | 338.6 | – | 81.1 | – | 285.3 | 349.8 |
| As-received HNT | – | – | 448.9 | – | – | – | 497.0 |
| PVA/GL | 148.5 | 281.1 | 429.1 | 80.9 | 211.0 | 267.7 | 440.0 |
| PVA/ST | 221.2 | 358.5 | 494.7 | 126.9 | – | 359.2 | 428.4 |
| PVA/ST/GL | 135.3 | 347.1 | 460.4 | 90.3 | 211.3 | 350.3 | 438.2 |
| PVA/ST/GL/0.25 wt% HNTs | 139.5 | 359.7 | 460.8 | 91.7 | 210.1 | 364.4 | 439.6 |
| PVA/ST/GL/0.5 wt% HNTs | 144.1 | 356.1 | 466.8 | 92.9 | 200.1 | 364.6 | 443.3 |
| PVA/ST/GL/1wt% HNTs | 155.8 | 355.8 | 468.9 | 96.7 | 230.0 | 365.0 | 446.1 |
| PVA/ST/GL/3 wt% HNTs | 153.3 | 345.9 | 468.0 | 91.4 | 195.5 | 362.4 | 443.0 |
| PVA/ST/GL/5 wt% HNTs | 137.5 | 347.7 | – | 93.2 | 190.5 | 359.2 | 445.8 |

Table 4-2. DSC data summary for neat materials, PVA blends and PVA/ST/GL/HNT bionanocomposites at different HNT contents

| **Sample** | $T_g$ (ºC) | $T_c$ (ºC) | $T_m$ (ºC) | $\Delta H_c$ (J/g) | $\Delta H_m$ (J/g) | $X_c$ (%) |
|---|---|---|---|---|---|---|
| Neat PVA | 70.71 | 229.90 | 244.69 | 8.64 | 30.14 | 15.14 |
| Neat ST | 80.49 | – | 263.30 | – | 30.52 | – |
| PVA/GL | 47.75 | 237.02 | 229.01 | 19.37 | 27.08 | 5.42 |
| PVA/ST | 74.12 | 269.7 | 288.41 | 10.18 | 21.29 | 7.82 |
| PVA/ST/GL | 56.88 | 204.28 | 290.04 | 6.45 | 20.32 | 9.76 |
| PVA/ST/GL/0.25%HNTs | 66.83 | 203.33 | 303.11 | 6.38 | 28.8 | 16.19 |
| PVA/ST/GL/0.5%HNTs | 66.56 | 200.39 | 301.72 | 5.25 | 25.46 | 14.98 |
| PVA/ST/GL/1%HNTs | 65.88 | 192.17 | 300.34 | 8.19 | 26.38 | 14.23 |
| PVA/ST/GL/3%HNTs | 65.45 | 202.80 | 304.36 | 7.41 | 23.46 | 11.65 |
| PVA/ST/GL/5%HNTs | 64.22 | 200.39 | 304.52 | 3.72 | 18.91 | 11.15 |

## 4.5 XRD

The XRD patterns of as-received HNTs and PVA/ST/GL/HNT bionanocomposites at different HNT contents were presented in Figure 4-13, and the related *d*-spacing values were summarised in Table 4-3. As-received HNTs had three major peaks at diffraction angles ($2\theta$) of 12º, 20º and 25º, respectively, which corresponded to (001), ((020), (110)) and (002) crystal planes, respectively. Based on Bragg's law, these peaks associated with *d*-spacing values about 0.73, 0.44 and 0.35 nm, respectively. PVA/ST/GL/HNT bionanocomposites reflected a slight peak shift from 12.12º to 11.54º and 11.21º with the addition of 0.25 and 0.5 wt% HNTs, respectively. These slight changes could be considered as minor intercalated clay structures with respect to (001) peak, which was in good agreement with Dong et al. (2013) in polylactic acid (PLA)/HNT nanocomposites. Furthermore, the other peaks at ((020), (110)) and (002) had a similar trend for intercalated structures with a slight peak shift as well. Nonetheless, XRD peaks completely disappeared for bionanocomposites beyond 1 wt% HNTs, which could be principally associated with the combination of well-dispersed and highly agglomerated HNTs in the disordered orientation.

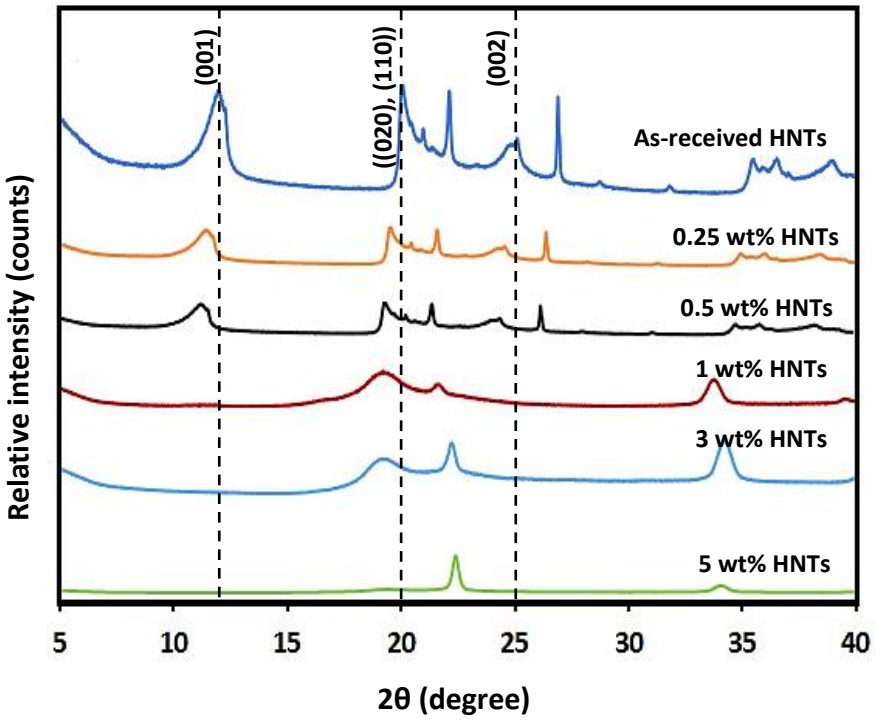


Figure 4-13. XRD patterns of as-received HNTs and PVA/ST/GL/HNT bionanocomposites at different HNT contents

Table 4-3. *d*-spacing values of as-received HNTs and HNTs embedded in PVA/ST/GL bionanocomposites

| **Sample** | ***2θ*** | $d_{001}$ **(nm)** | ***2θ*** | $d_{020/110}$ **(nm)** | ***2θ*** | $d_{002}$ **(nm)** |
|---|---|---|---|---|---|---|
| As-received HNTs | 12.12 | 0.73 | 20.01 | 0.44 | 24.98 | 0.35 |
| PVA/ST/GL/0.25 wt% HNTs | 11.54 | 0.76 | 19.22 | 0.46 | 24.00 | 0.37 |
| PVA/ST/GL/0.5 wt% HNTs | 11.21 | 0.79 | 19.02 | 0.46 | 23.57 | 0.38 |
| PVA/ST/GL/1 wt% HNTs | – | – | 18.95 | 0.47 | – | – |
| PVA/ST/GL/3 wt% HNTs | – | – | 18.40 | 0.48 | – | – |
| PVA/ST/GL/5 wt% HNTs | – | – | – | – | – | – |

### 4.6 FTIR spectra

Neat polymers of PVA, ST and GL, as-received HNTs, PVA blends and PVA/ST/GL/HNT bionanocomposites at different HNT contents were examined via FTIR analysis. As shown in Figure 4-14, many peaks could be observed from these spectra and each peak was related to predefined functional groups in polymeric chains. For neat PVA, ST, and GL, the evident peak detected at 3200-3300 $cm^{-1}$ was related to the O-H stretching due to the strong molecular hydrogen bonding. The other apparent peaks identified at 2900-2950, 1600-1650, 1414-1420, and 1000-1090 $cm^{-1}$ were associated with C-H, bonding water, $CH_2$ groups, and C-O stretching, respectively in good accordance with previous findings (Sreekumar, Al-Harthi and De 2012; Cano et al. 2015b; Wu et al. 2017; Akhavan, Khoylou and Ataeivarjovi 2017). PVA/ST, PVA/GL, and PVA/ST/GL blends had similar peaks with some changes taking place in their intensity and wavelength of O-H stretching due to their good compatibility to increase hydrogen bonding (Cano et al. 2015a). Nonetheless, slight changes in other peaks were manifested possibly resulting from inter-and-intramolecular bonding between blend components (Akhavan, Kholyou and Ataeivarovi 2017).

As-received HNTs showed two distinct peaks at 3692 and 3621 $cm^{-1}$, which were assigned to the O-H stretching vibration. According to Gaaz et al. (2017), the first peak was related to inner surface O-H groups in connection with the aluminium centred sheet while the second peak was ascribed to inner O-H groups. As-received HNTs had other peaks at 1004 and 907 $cm^{-1}$ assigned to Si-O and Al-OH stretchings, respectively (Dong et al. 2015b). The O-H stretching of as-received HNTs disappeared when embedded within polymer blend matrices in bionanocomposite films at HNT contents in range of 0.25-1 wt%. This phenomenon could be interpreted by the

emerging O-H stretching of HNTs within PAV/ST/GL blend matrices arising from good HNT dispersion at low nanofiller contents in bionanocomposite films. On the other hand, the O-H stretching was observed again for bionanocomposites with the inclusion of 3 and 5 wt% HNTs with a clear sign of HNT agglomeration, as confirmed in the XRD results. Moreover, with increasing the HNT content, Si-O and Al-OH stretchings became more pronounced while other peaks identified at 1650 and 1417 $cm^{-1}$ implied typical HNT-matrix interaction at the specific sites for bonding water and $CH_2$ stretching, respectively.

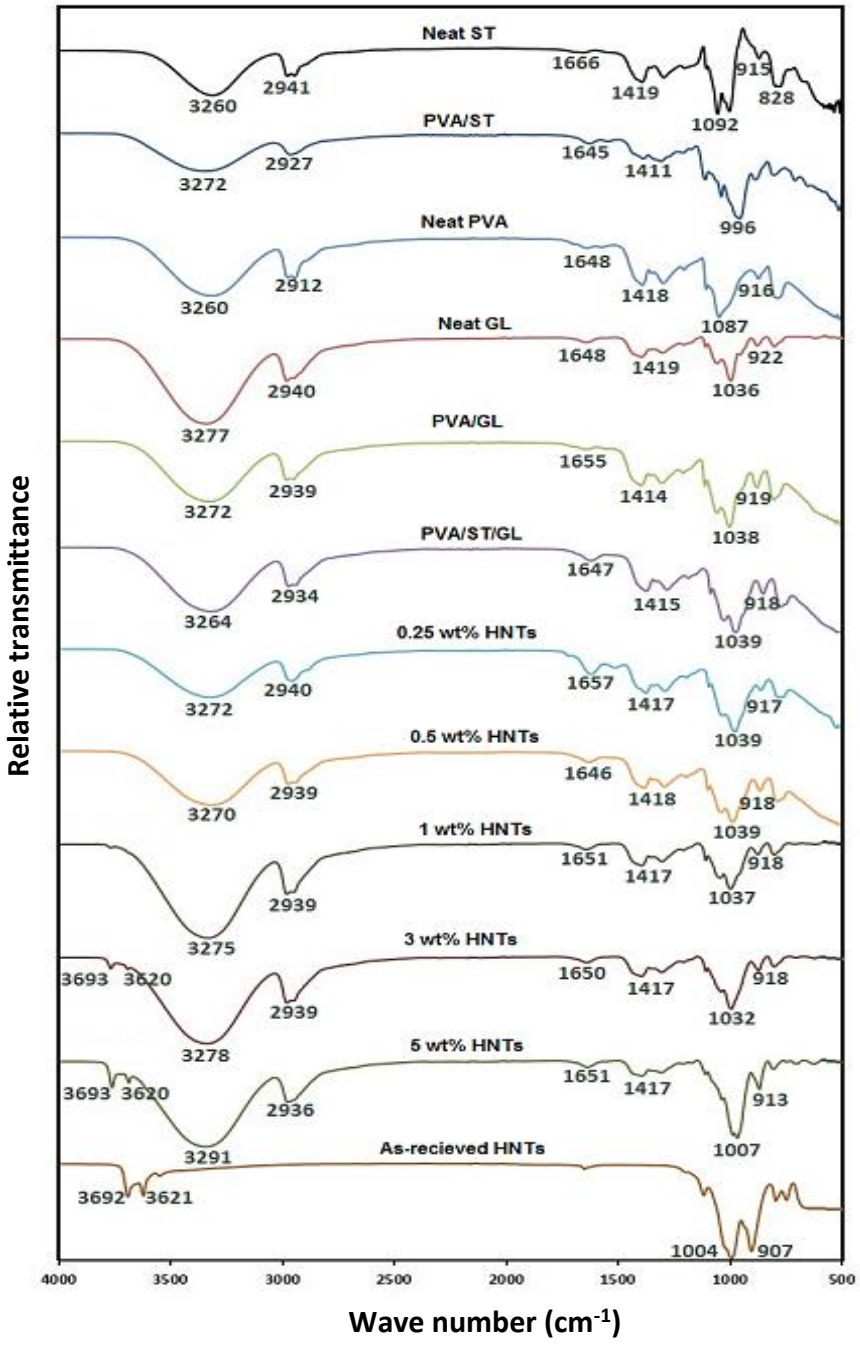


Figure 4-14. FTIR spectra of neat PVA, ST, GL, as-received HNTs, PVA blends and PVA/ST/GL/HNT bionanocomposites at different HNT contents

## 4.7 UV-vis spectra

Film transparency in term of light transmittance (*T%*) is an important material feature in food packaging applications. Consequently, neat PVA, PVA blends and PVA/ST/GL/HNT bionanocomposite films at different HNT contents were examined

under UV-visible light spectra as well as Curtin University's logo was observed through all these films, as displayed in Figure 4-15 (a) and (b), respectively.

The high crystallinity degree of neat PVA led to a high *T%* range of 99-100% in good agreement with previous results (Gupta, Agarwal and Alam 2013; Guohua et al. 2006), as summarised in Table 4-4. PVA/GL, PVA/ST and PVA/ST/GL blend films had relatively high *T%* in range of 95.23-98.72% because of the good component miscibility consistent with the SEM results obtained in section 4.2.1. Although these blends had good *T%*, it was still lower than that of neat PVA because the crystallinity rates of these films became relatively lower as opposed to that of neat PVA, which was demonstrated clearly in our DSC results (see Table 4-2). As shown from Curtin University's logo, there was no great difference in clarity between neat PVA and their blends.

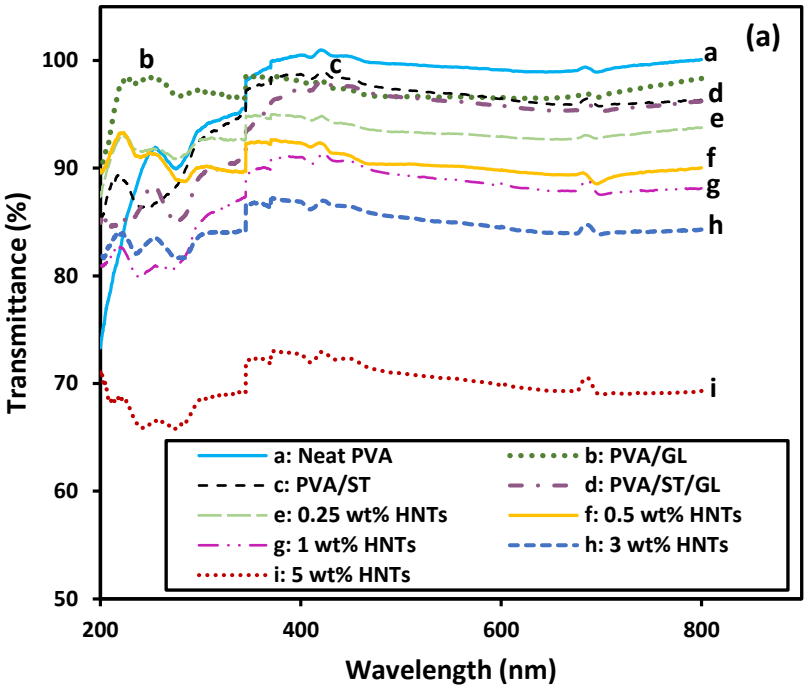

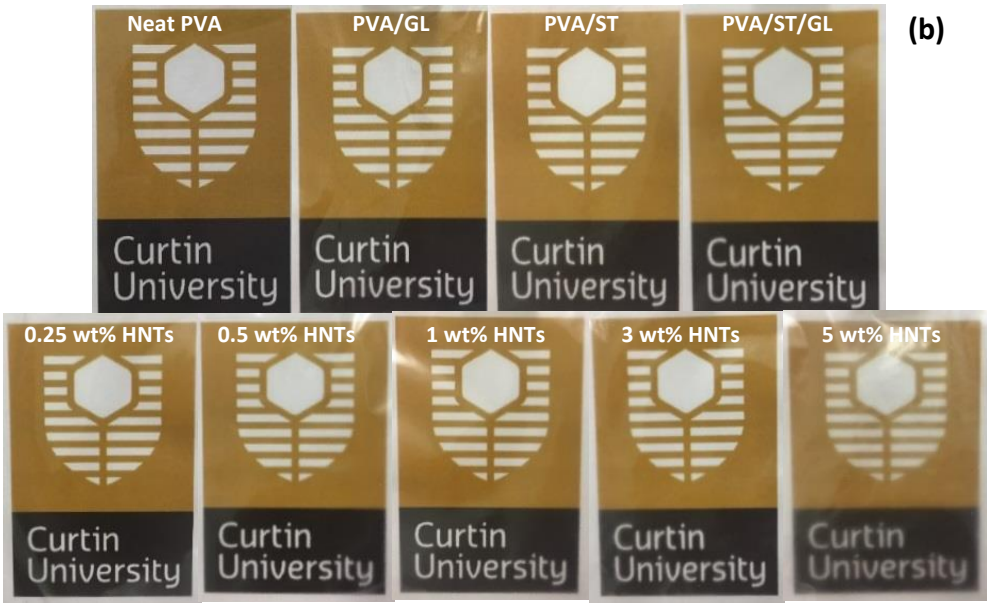


Figure 4-15. (a) UV-vis spectra curves, and (b) digital images for the film transparency of neat PVA, PVA blends and PVA/ST/GL/HNT bionanocomposite films at different HNT contents

The incorporation of HNTs within PVA/ST/GL blend matrices reduced the *T%* of bionanocomposite films when further compared with that of corresponding blends alone. Regardless of the wavelength used, the reduction of *T%* for bionanocomposite films increased linearly with increasing the HNT contents from 0.25 to 5 wt%, which was attributed to an increase in surface roughness of bionanocomposite films particularly at HNT contents of 3 and 5 wt%. As such, the number of light scattering sites could be increased accordingly (Grunlan et al. 2004), as reflected clearly by reducing the visibility of the Curtin University's logo particularly with the inclusion of 5 wt% HNTs. These results were consistent with the AFM results in term of surface roughness shown in section 4.2.2. Moreover, this decreasing trend of *T%* for PVA/ST/GL/HNT bionanocomposite films was confirmed by other studies in PVA/ST/nano-$SiO_2$ nanocomposites (Tang et al. 2008) and PVA/ST/ZnO nanocomposites (Akhavan, Khoylou and Ataeivarjovi 2017). On the other hand, Lee, Kim and Park (2018) considered the reduction of *T%* was advantageous when

analysing the UV-vis spectra for chitosan/clove essential oil/HNT nanocomposite films used for food packaging applications because UV-barrier properties were improved leading to better protection of foodstuffs against nutrient loss, decolourisation and lipid oxidation.

Table 4-4. Visible light transmittance data summary for neat PVA, PVA blends and PVA/ST/GL/HNT bionanocomposite films at different HNT contents

| **Material Composition** | ***T%* at a visible wavelength range** | | | |
|---|---|---|---|---|
| | **400 nm** | **500 nm** | **600 nm** | **700 nm** |
| Neat PVA | 100.00± 0.091 | 99.67± 0.30 | 99.13± 0.72 | 98.99± 0.48 |
| PVA/GL | 98.15± 0.56 | 96.66± 0.71 | 96.50± 0.24 | 96.67± 0.66 |
| PVA/ST | 98.72± 0.51 | 97.29± 0.18 | 96.43± 0.84 | 95.76± 0.69 |
| PVA/ST/GL | 97.43± 0.75 | 96.59± 0.86 | 95.73± 0.55 | 95.23± 0.72 |
| PVA/ST/GL/0.25 wt% HNTs | 89.79± 0.73 | 93.38± 0.67 | 92.91± 0.48 | 92.81± 0.50 |
| PVA/ST/GL/0.5 wt% HNTs | 85.32± 0.52 | 90.36± 0.77 | 89.79± 0.21 | 88.71± 0.17 |
| PVA/ST/GL/1 wt% HNTs | 81.02± 0.93 | 89.35± 0.97 | 88.38± 0.74 | 87.52± 0.89 |
| PVA/ST/GL/3 wt% HNTs | 86.90± 0.30 | 85.43± 0.79 | 84.48± 0.73 | 83.87± 0.27 |
| PVA/ST/GL/5 wt% HNTs | 72.76± 0.58 | 70.90± 0.80 | 69.87± 0.20 | 68.90± 0.31 |

## 4.8 Summary

This chapter investigated the effects of HNT content on morphological, mechanical, thermal and optical properties of PVA/ST/GL/HNT bionanocomposite films in comparison with those of neat PVA and its blends. Overall, blending PVA with GL substantially increased the elongation at break as compared with neat PVA at the expense of tensile strength and Young's modulus due to the improvement of polymeric chain mobility and free volume. A completely opposite behaviour was observed when blending PVA with ST due to the latter's inherent brittleness. Moreover, mechanical properties of PVA/ST/GL blends were found to range between those of PVA/GL and PVA/ST blends. The incorporation of HNTs in PVA/ST/GL/HNT bionanocomposite films at the HNT contents of 0.25 and 1 wt% improved both tensile strength and Young's modulus as opposed to those of corresponding polymer blends along with a slight reduction in elongation at break due to high stiffness of HNTs. These improvements declined beyond 1 wt% HNTs resulting from typical HNT agglomeration, which was confirmed by an increase in the surface roughness of bionanocomposite films, as well as decreasing aspect ratios of HNTs embedded within blend matrices.

Thermal properties of neat PVA in terms of $T_g$, $T_m$, $\Delta H_m$, and $X_c$ (%) declined with the addition of GL due to GL plasticisation effect. Such properties increased slightly for PVA/ST blends except $X_c$ (%) owing to amorphous structures of ST. Whereas, PVA/ST/GL blends possessed a relatively high $T_m$ as opposed to other polymer blends. The presence of HNTs enhanced most material properties determined for bionanocomposite films in study, as well as increased the decomposition temperatures when compared with those of corresponding blends. Such a finding was associated with the presence of HNTs acting as a barrier material against heat and mass transfer.

The *T%* of PVA blends declined slightly as opposed to that of neat PVA due to good compatibility of blended polymers. This decreasing tendency became more pronounced for bionanocomposite films owing to the presence of HNTs to increase surface roughness and the number of light scattering sites.

The property improvement for bionanocomposite films was manifested at the HNT content up to 1 wt%, beyond which a slight declining trend took place. Such a phenomenon could be explained by minor intercalated structures at the HNT contents of 0.25 to 1 wt% and typical HNT agglomeration beyond 1 wt%, accordingly.

# Chapter 5: Water Resistance and Biodegradation of PVA/ST/GL/HNT Bionanocomposite Films

## 5.1 Introduction

In general, water soluble polymers have poor water resistance that is reflected by high water uptake and high water solubility due to their free hydroxyl groups that can be easily interacted with water molecules (Chiellini et al. 2003). Several methods have been used to improve the water resistance of these polymers such as blending with other polymers (Gupta, Agarwal and Alam 2013), coating (Khwaldia, Tehrany and Desobry 2010), using cross-linking agents (Maiti, Ray and Mitra 2012), ionising rays like ultraviolet rays (UV) (Shahabi-Ghahfarrokhi, Goudarzi and Babaei-Ghazvini 2019) and nanotechnology (Abdollahi et al. 2013). All these methods based on consuming free hydroxyl groups and/or increased the surface hydrophobicity of polymers (Maiti, Ray and Mitra 2012). HNTs as a moderate hydrophobic nanofillers were used to improve the water resistance of PVA/ST/GL blends. On the other hand, many studies considered ST as a good candidate to enhance the biodegradability of PVA with good cost reduction (Jose et al. 2015; Sadhu, Soni and Garg 2015). Consequently, the effect of ST on the biodegradation rates of PVA blends and bionanocomposites were investigated in details.

## 5.2 Water absorption capacity ($W_a$)

Water absorption capacity or water uptake ($W_a$) is an important parameter for the evaluation of bionanocomposite materials particularly targeting food packaging applications (Sadegh-Hassani and Nafchi 2014; Aloui et al. 2016). $W_a$% of neat PVA, PVA blends and PVA/ST/GL/HNT bionanocomposite films were illustrated in Figure

5-1. As compared with neat PVA, PVA/GL blends had a slight decrease in $W_a$ by 10.21% due to good compatibility between PVA and GL leading to the consumption of more free hydroxyl groups, which was in good agreement with Follain et al. (2005). Whereas, PVA/ST blends had the highest $W_a$ owing to partial compatibility between PVA and ST in the absence of plasticiser leading to more free sites in the blends to be occupied by water molecules. Additionally, ST has high hydrophilicity leading to increasing $W_a$ of ST blends, which was associated with the hygroscopic nature of ST for the water gain or loss in order to achieve the equilibrium with the environment (Ali 2016; Ismail and Zaaba 2011; Azahari, Othman and Ismail 2011; Salleh et al. 2017). Nonetheless, the presence of GL reduced the $W_a$ of PVA/ST/GL blends by 23.92% as opposed to that of PVA/ST blend counterparts due to the improvement of compatibility and interactions between blend constituents. Similarly, Zou, Qu and Zou (2008) stated that the addition of GL reduced $W_a$ of PVA/ST blends by enhancing the compatibility between components.

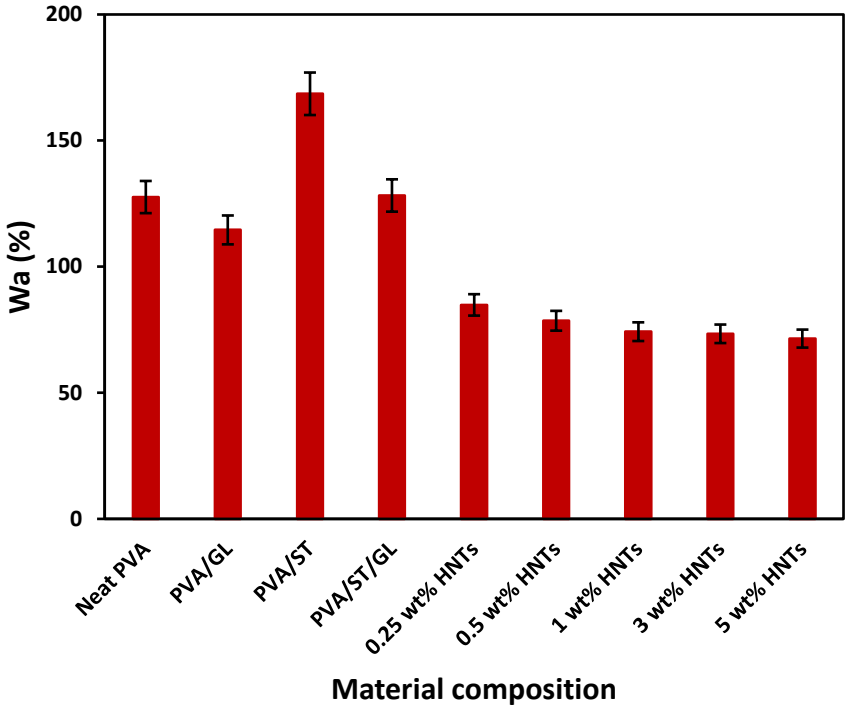


Figure 5-1. Water absorption capacity of neat PVA, PVA blends and PVA/ST/GL/HNT bionanocomposite films at different HNT contents

A further decrease in $W_a$ was achieved with the incorporation of HNTs in bionanocomposite films due to the typical restriction of water diffusion in the presence of HNTs resulting from the tortuous paths, as opposed to that of PVA/ST/GL blends. A remarkable reduction of $W_a$ by 42% was achieved for PVA/ST/GL/HNT bionanocomposites with increasing the HNT content from 0.25 to 1 wt% on account of good dispersion of nanofillers with the restriction to the diffusion of water molecules. Lee, Kim and Park (2018) reported similar effect of HNTs on the $W_a$ of chitosan/HNT nanocomposites and chitosan/clove essential oil (CEO)/HNT nanocomposites relative to their corresponding biopolymers or blends. The $W_a$ of chitosan/HNT nanocomposites and chitosan/CEO/HNT nanocomposites declined by 42.17 and 43.31%, respectively with the addition of 30 wt% HNTs as opposed to those of their matrices alone due to the presence of moderate hydrophobic nanofillers. Moreover, Abbasi (2012) concluded that the $W_a$ of PVA/ST/$SiO_2$ nanocomposites was

reduced by 50% with increasing $SiO_2$ nanofiller content from 1 to 5 wt%, which was ascribed to the strong physical interaction between components in order to consume more free hydroxyl groups that could bond with water molecules. Additionally, a slight reduction of $W_a$ by 4.04% was observed for bionanocomposites at the HNT contents beyond 1 wt% due to typical HNT agglomeration at 3 and 5 wt%, as evidenced in section 4.1, Chapter 4. These findings were consistent with other results based on PVA/ST/MMT nanocomposites (Tian et al. 2017b; Taghizadeh, Abbasi and Nasrollahzade 2011) and PVA/ST/nano-$SiO_2$ nanocomposites (Tang et al. 2008).

When compared with other nanofillers, HNTs produced a higher reduction in $W_a$ at small nanofiller contents up to 1 wt% due to their moderate hydrophobicity and morphological tubular structures, as shown in Figure 5-2. Whereas, this reduction became less pronounced beyond 1 wt% as compared with other nanofillers with similar behaviour at different nanofiller contents because of the nanofiller agglomeration issue. Overall, nanofiller content and dispersion are considered as major factors to affect the reduction in $W_a$ of nanocomposite films.

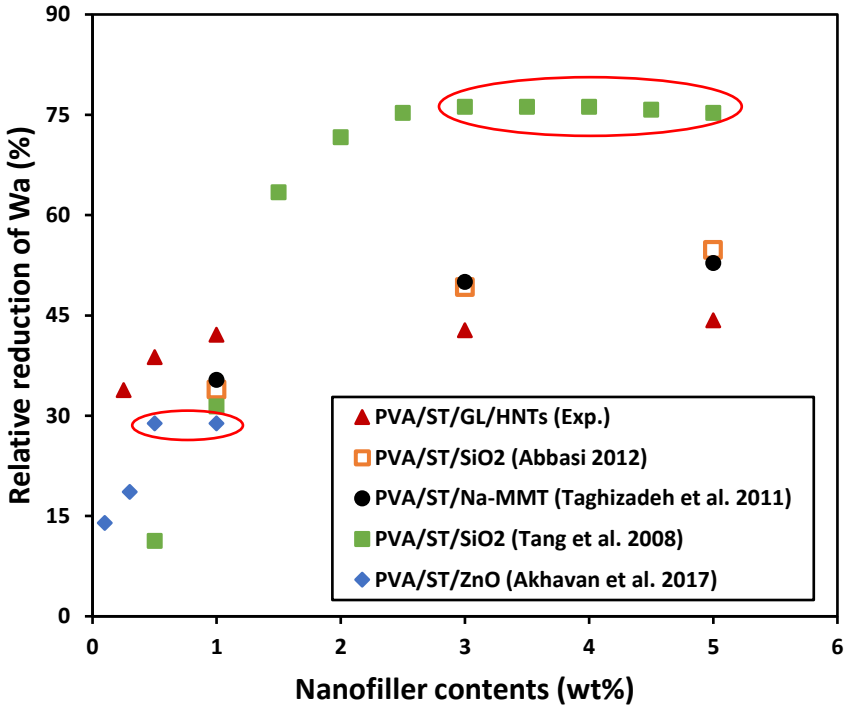


Figure 5-2. Data comparison for the relative reduction in $W_a$% of PVA/ST nanocomposite films reinforced with different nanofillers

### 5.3 Water solubility ($W_s$)

Water solubility ($W_s$) is one of critical material characteristics in relation to water resistance especially for water-soluble polymers like PVA. According to Azahari, Othman and Ismail (2011), when the material has high water absorption capacity, it possesses high water solubility as well because water molecules are absorbed onto hydroxyl groups particularly on hydrogen bonding sites leading to weak material structures and easier water dissolution. As such, $W_a$ and $W_s$ of neat PVA, PVA blends and PVA/ST/GL/HNT bionanocomposite films at different HNT contents showed a very similar trend despite their different magnitudes, as demonstrated in Figure 5-3. These films had a relatively high $W_s$ because of high hydrophilicity of all constituents like PVA, ST and GL, in good accordance with other studies (Zanela et al. 2015; Cano et al. 2015c). PVA/GL blend had a slight decrease in $W_s$ by 8.21% as compared with

that of neat PVA films because the number of free hydroxyl groups could decrease in polymer blends with the addition of GL. However, $W_s$ of PVA/ST blends increased by 4.69% as compared with that of neat PVA due to the increased hydrophilicity of blends with the addition of ST, as confirmed by Negim et al. (2014). Then $W_s$ of PVA/ST/GL blends was reduced by 14.89% as opposed to that of PVA/ST films with additional GL leading to the enhancement of compatibility and interfacial bonding between PVA and ST (Cano et al. 2015c; Zanela et al. 2015).

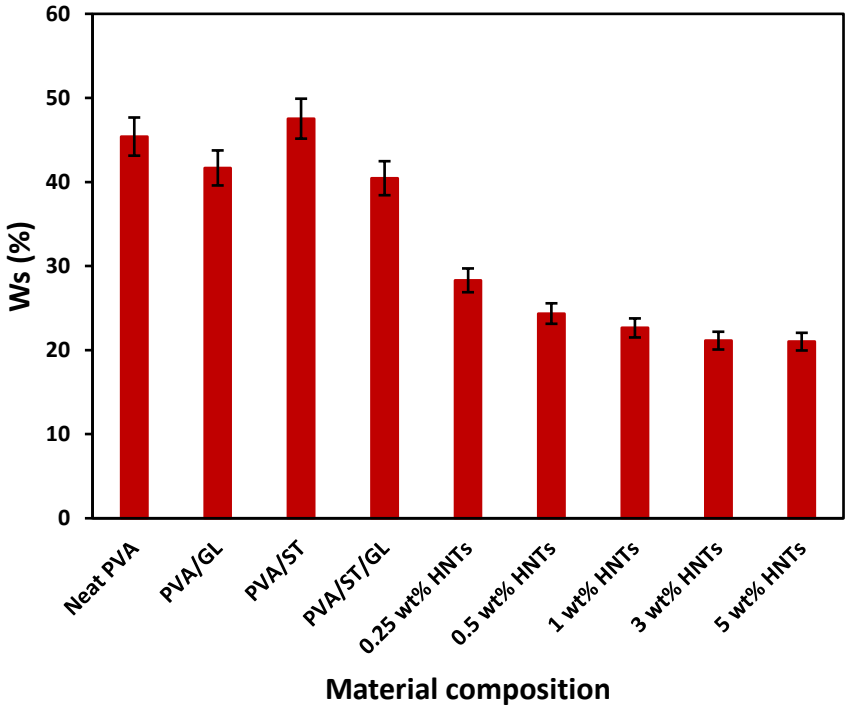


Figure 5-3. Water solubility of neat PVA, PVA blends and PVA/ST/GL/HNT bionanocomposite films at different HNT contents

When compared with corresponding polymer blends alone, PVA/ST/GL/HNT bionanocomposite films possessed a remarkable reduction in $W_s$ by 48.05% with increasing the HNT content from 0.25 to 5 wt%. This reduction may be interpreted by the moderate hydrophobicity of HNTs resulting from the low number of hydroxyl groups distributed on HNT surfaces (Liu et al. 2014). Additionally, the $SiO_2$ groups of HNTs have the ability to form numerous hydrogen bonds in nanocomposite films so

as to restrict mass transfer as well as consume the hydroxyl groups of polymer matrices leading to decreasing the number of free interaction sites occupied by water molecules (Sadegh-Hassani and Nafchi 2014). The good dispersion of HNTs up to 1 wt% gave rise to a remarkable reduction in $W_s$ of bionanocomposite films when compared with those films beyond 1 wt% HNTs with a slight reduction only by 7.20%, which was due to HNT agglomeration mentioned in section 5.1. These findings were in good agreement with those based on PVA/ST/nano-$SiO_2$ nanocomposites (Tang et al. 2008), PVA/ST/$CaCO_3$ nanocomposites (Kisku et al. 2014), and PVA/ST/nano-titania nanocomposites (Lin et al. 2018).

### 5.4 Water contact angle

The water contact angles of neat PVA, PVA blends and PVA/ST/GL/HNT bionanocomposite at different HNT contents were evaluated to understand the hydrophilicity of material surfaces, as illustrated in Figure 5-4. It is well known that water contact angle less than 90º means high material wettability while it is referred to as low wettability when greater than 90º instead (Yuan, and Lee 2013). In other words, the materials with low water contact angle may be associated with the high hydrophilicity of their surfaces and vice versa (Sadegh-Hassani and Nafchi 2014; Alipoormazandarani, Ghazihoseini and Nafchi 2015). Neat PVA, as a water-soluble polymer, had a low water contact angle of 28.35º measured in this study in good accordance with previous studies (Lim et al. 2015). In contrast with neat PVA, PVA/GL blends had slightly higher water contact angle by 0.33º primarily associated with the insignificant reduction in $W_a$ and $W_s$ for PVA/GL blends. Moreover, the water contact angle of PVA/ST blends decreased by 9.7º as opposed to that of neat PVA since the addition of ST could improve the hydrophilicity. Then a reduction of water contact angle by 2.78º was reported for PVA/ST/GL blends as opposed to that of neat

PVA films. As clearly shown in Figure 5-5, the water contact angles of PVA/ST and PVA/ST/GL blends were remarkably increased leading to the improvement of hydrophilicity when compared with that of neat PVA owing to more hydroxyl groups in PVA blends in the presence of ST. These findings can explain the further increase in $W_a$ and $W_s$ of these blends.

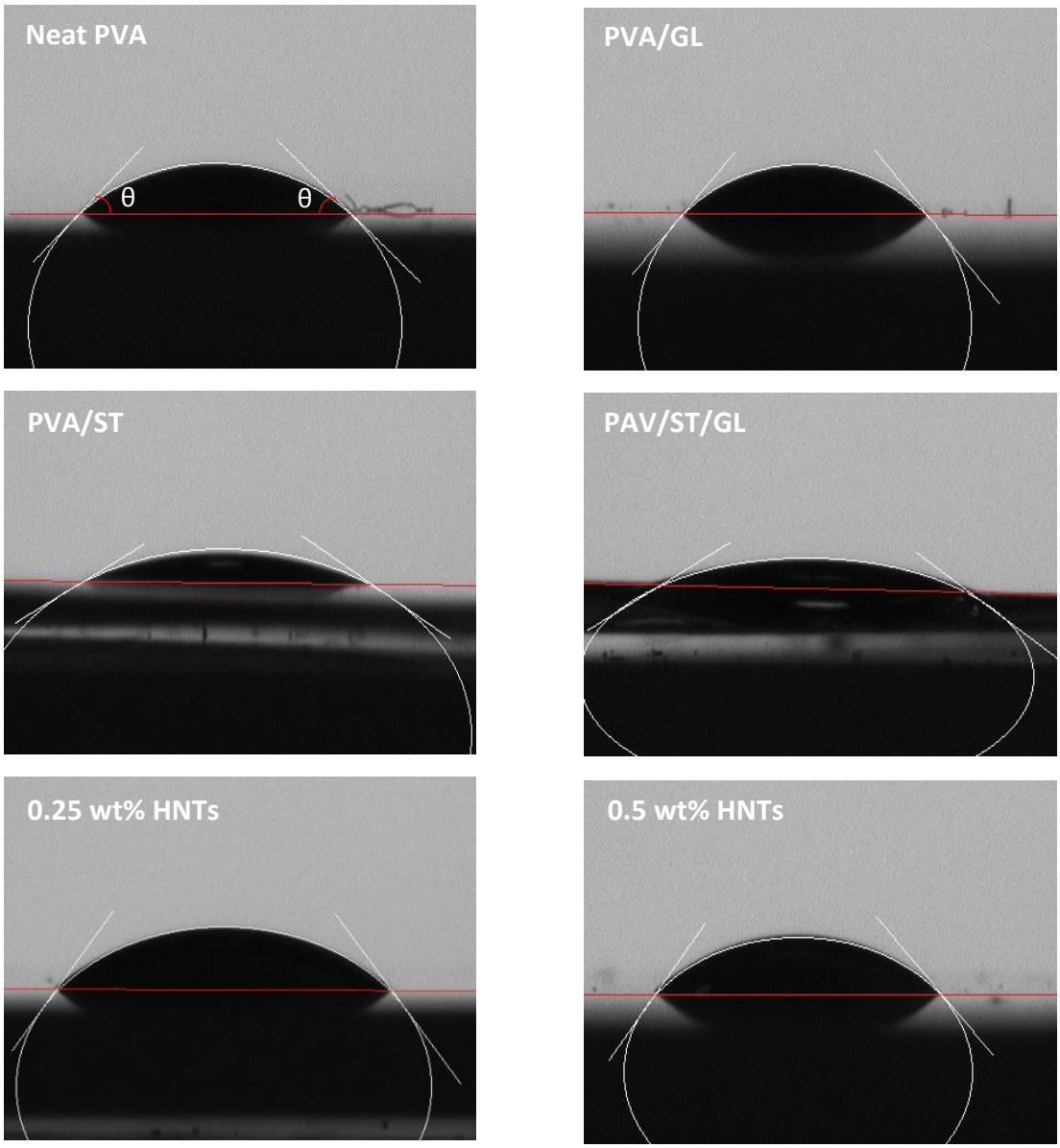

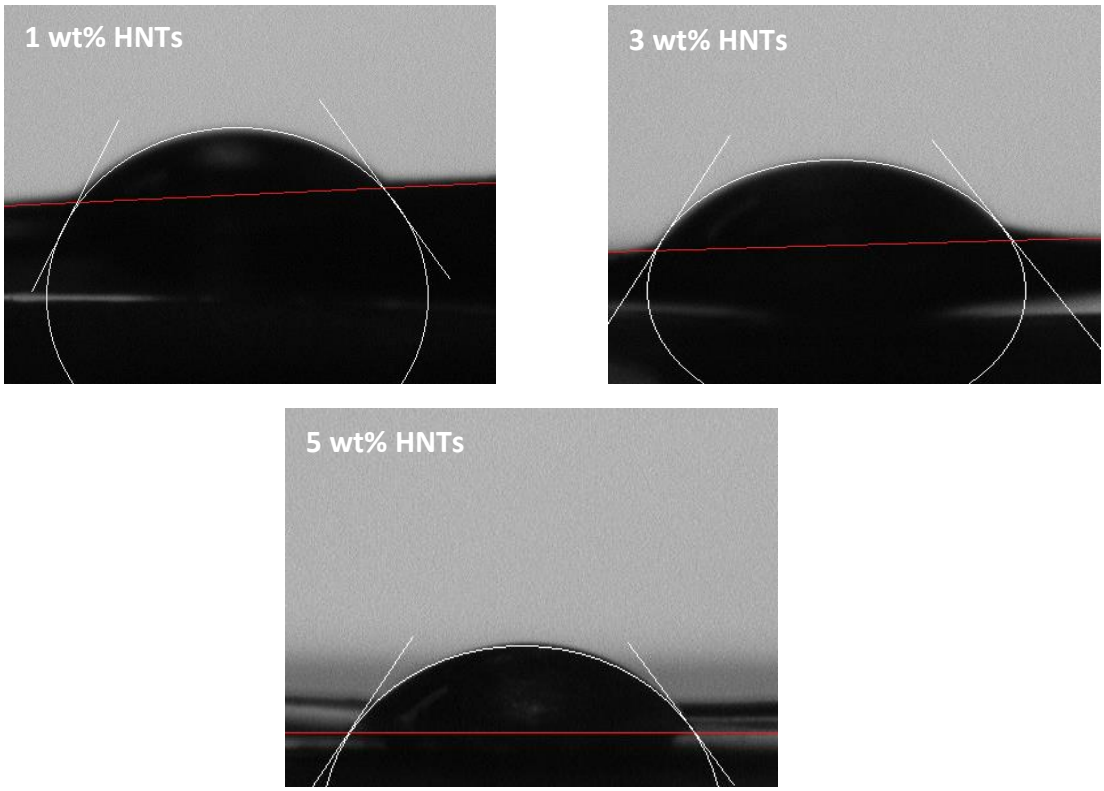


Figure 5-4. Images of water droplets on neat PVA, PVA blends and PVA/ST/GL/HNT bionanocomposite film surfaces for contact angle measurements

A linear increasing trend in water contact angle of bionanocomposite films was achieved from 25.57º to 46.93º with increasing the HNT content from 0 to 5 wt%. HNTs as moderate hydrophobic nanofillers have a low number of hydroxyl groups that could play an important role for the reduction in $W_a$ and surface hydrophilicity (Liu et al. 2014; Sadegh-Hassani and Nafchi 2014; Alipoormazandarani, Ghazihoseini and Nafchi 2015). Additionally, well-dispersed HNTs within polymer matrices could consume some free hydroxyl groups in nanocomposites in order to generate hydrogen bonding between components. It is well known that the incorporation of nanofillers can increase surface roughness of nanocomposites (Grunlan et al. 2004). Therefore, increasing surface roughness of nanocomposites in the presence of nanofillers can lead to a further increase in water contact angle according to Wenzel's theory (Wenzel

1949). As such, the surface hydrophobicity is increased with increasing the surface roughness based on the equation as follows (Kubiak et al. 2011):

$$cos\theta_m = r\ cos\theta \qquad (5\text{-}1)$$

where $\theta_m$ and $\theta$ are the measured and ideal water contact angles, respectively, which can be calculated from the perfect smooth surface like mirror, and $r$ is the surface roughness ratio where $r = 1$ for smooth surfaces and $r > 1$ for rough surfaces (Kubiak et al. 2011). Similarly, the water contact angle of pectin/HNT nanocomposite film surfaces was increased by 6º as compared with that of pectin counterparts due to the increase in surface roughness of nanocomposites in the presence of HNTs (Biddeci et al. 2016).

Although the water contact angles of PVA/ST/GL/HNT bionanocomposite films were increased by 21.36º compared with that of corresponding blends counterparts, the films could still be categorised within the range of hydrophilic materials (i.e., $\theta < 90º$). Overall, the moderate hydrophobicity of HNTs was the main reason for the increase in water contact angles of bionanocomposite film surfaces.

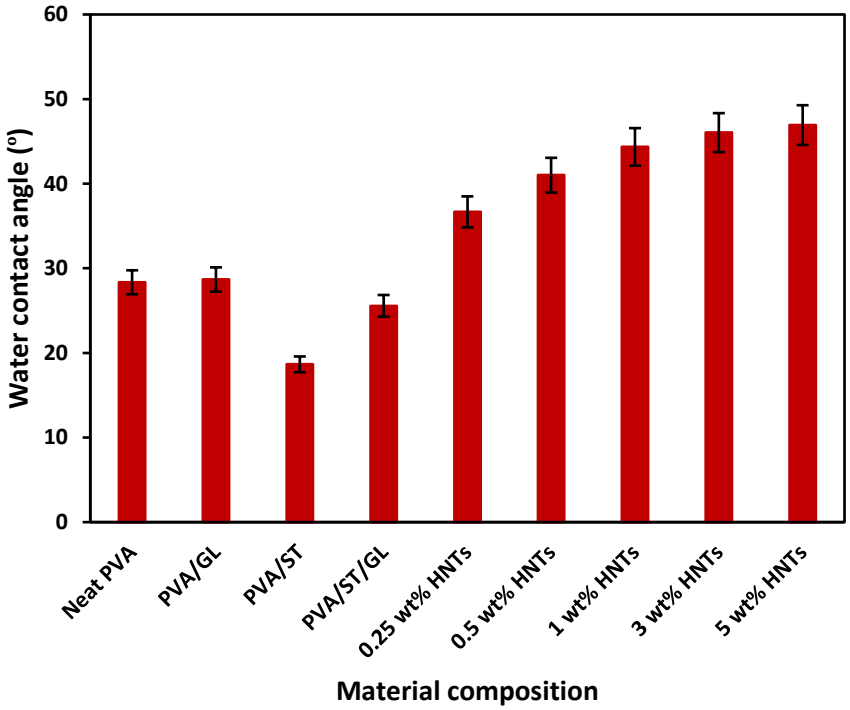


Figure 5-5. Water contact angles of neat PVA, PVA blends and PVA/ST/GL/HNT bionanocomposite films at different HNT contents

## 5.5 Soil burial biodegradation

In general, the biodegradability of most biopolymers depends on their $W_a$ and $W_s$ because the degradation process starts with water absorption on the material surfaces, which is then followed by the growth of microorganisms like bacteria and fungi to finish with cleavage particularly for soil burial biodegradation (Zanela et al. 2015; Guohua et al. 2006). The digital images of neat PVA, PVA blend and PVA/ST/GL/HNT bionanocomposite samples before and after soil burial biodegradation tests (24-week) were presented in Figure 5-6. Relative to neat PVA films, all other material films diminished in size after the test period and changed to more fragile and wrinkling films. Moreover, neat PVA and PVA/GL blend films sill had good transparency after biodegradation tests. Whereas, other material films showed great colour change and tended to be more yellowish rather than transparent after biodegradation tests. These changes were greatly related to the presence of

potato-based ST prone to the attack first by microorganisms as complete biodegradable materials when compared with PVA (Tănase et al. 2015).

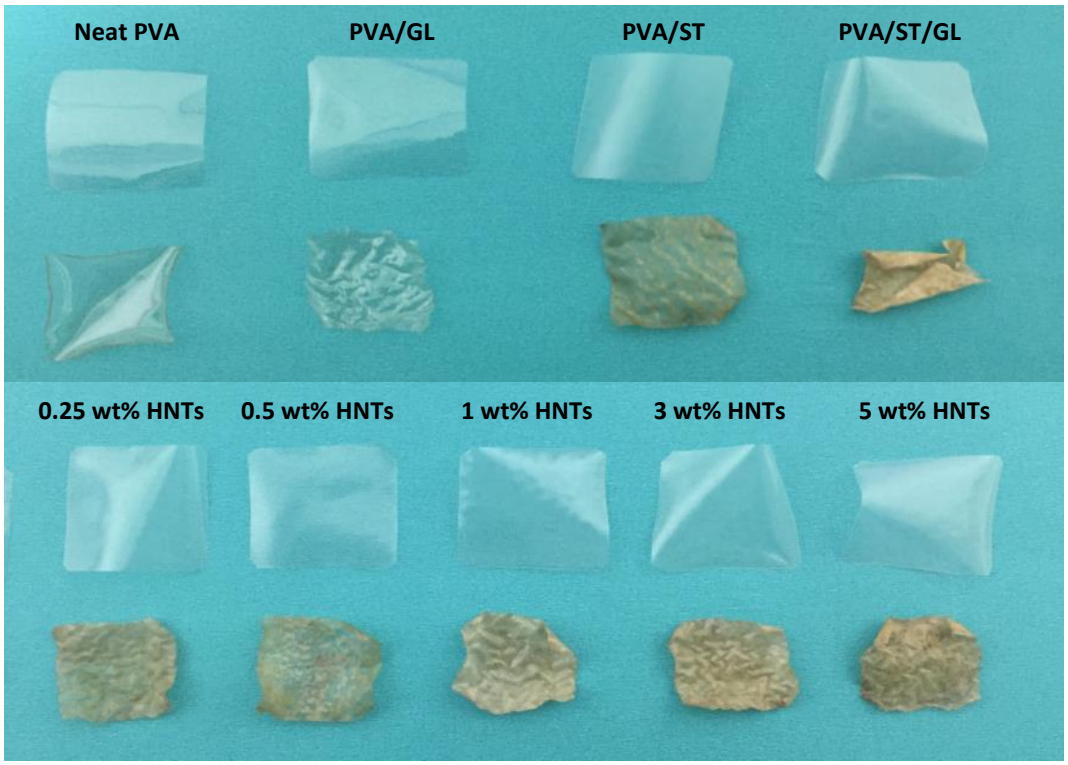


Figure 5-6. Digital images of neat PVA, PVA blends and PVA/ST/GL/HNT bionanocomposite films before (0 week) and after soil burial biodegradation tests (24 weeks)

Biodegradation rate of neat PVA, PVA blends and PVA/ST/GL/HNT bionanocomposite films at different HNT contents were determined as a function of time, as demonstrated in Figure 5-7. The biodegradation rates of all material films over 24 weeks could be characterised over an active-state period in first three weeks where the material samples degraded at a very rapid rate, which was followed by a steady-state period for the rest of time when the material samples degraded at a relatively slow rate to the end of tests, as evidenced by other studies (Guohua et al. 2006; Hejri et al. 2013; Singha and Kapoor 2014). According to Azahari, Othman and Ismail (2011), this phenomenon could be associated with a composting process consisting of two stages, namely “an active composting stage” and “a curing period”. The first stage

included increasing the temperature at an elevated level due to the microbial activities as long as oxygen was available. Further, the temperature decreased in stage two resulting from slower microbial activities despite continued slow degradation rates.

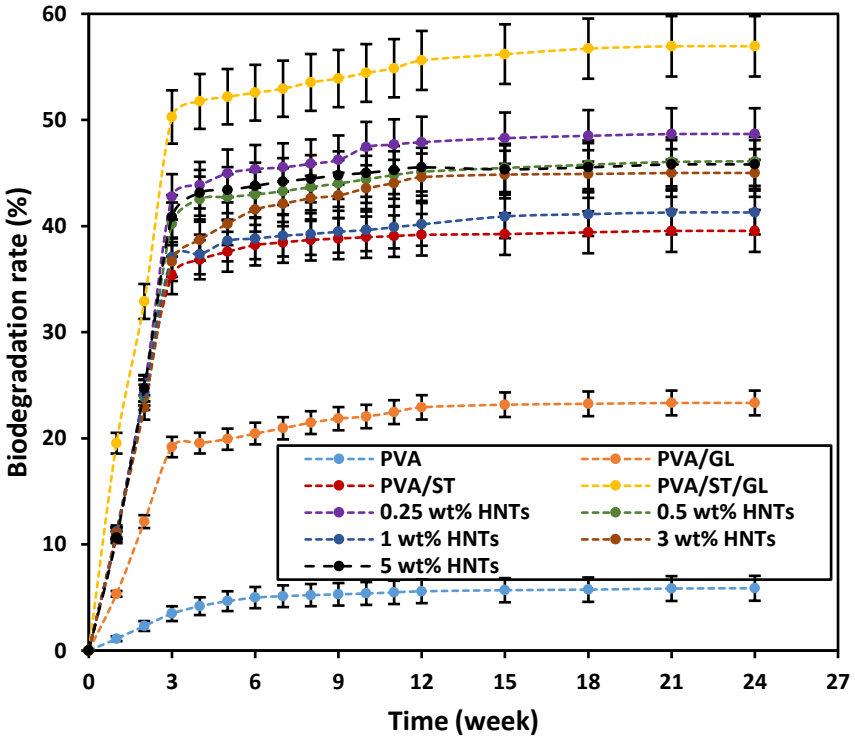


Figure 5-7. Biodegradation rates of neat PVA, PVA blends and PVA/ST/GL/HNT bionanocomposite films at different HNT contents

Neat PVA had the lowest biodegradation rates of 5.87% among all materials because of its high resistance to biodegradation in soil compared with other environments like sludge. Whereas, the slight weight loss was related to the hydrolysability of neat PVA (Guohua et al. 2006; Imam et al. 2005; Kopcilova et al. 2012). In general, carbon-only backbones polymers like most vinyl polymers are not susceptible to hydrolysis and biodegradation (Kale et al. 2007). However, hydroxyl groups (–OH) of PVA were oxidised by the enzymatic action into carbonyl groups (C=O), which was followed by the hydrolysis into two carbonyl groups (–CO–$CH_2$–CO–). This led to the cleavage of polymeric chains and decrease in molecular weight. Hence, these low molecular weight portions of neat PVA were consumed by microbes (Kale et al. 2007). On the

other hand, the biodegradation rate of PVA/GL blends was increased up to 23.33% as compared with that of neat PVA counterparts due to the presence of GL to improve the mobility of polymeric chains resulting in increasing the water diffusion through their molecular structures. Moreover, the biodegradation rate of PVA/ST blends was increased further up to 39.54% due to the addition of ST, which is regarded as a fully biodegradable polymer (Azahari, Othman and Ismail 2011; Guohua et al. 2006) whose material structures can be easily attacked by microorganisms (Hejri et al. 2013; Kale et al. 2007). The biodegradability of PVA/ST blends increased linearly with increasing the ST content, as reported in previous work (Tănase et al. 2015; Azahari, Othman and Ismail 2011; Jayasekara et al. 2003). Further improvement of biodegradation rate up to 56.94% was demonstrated in PVA/ST/GL blends due to the combination of complete biodegradability of ST with GL plasticisation effect to improve the rate of microorganism infiltration. Thus, PVA/ST/GL blends had a biodegradation rate comparable to those of other natural biopolymers shown in Figure 5-8.

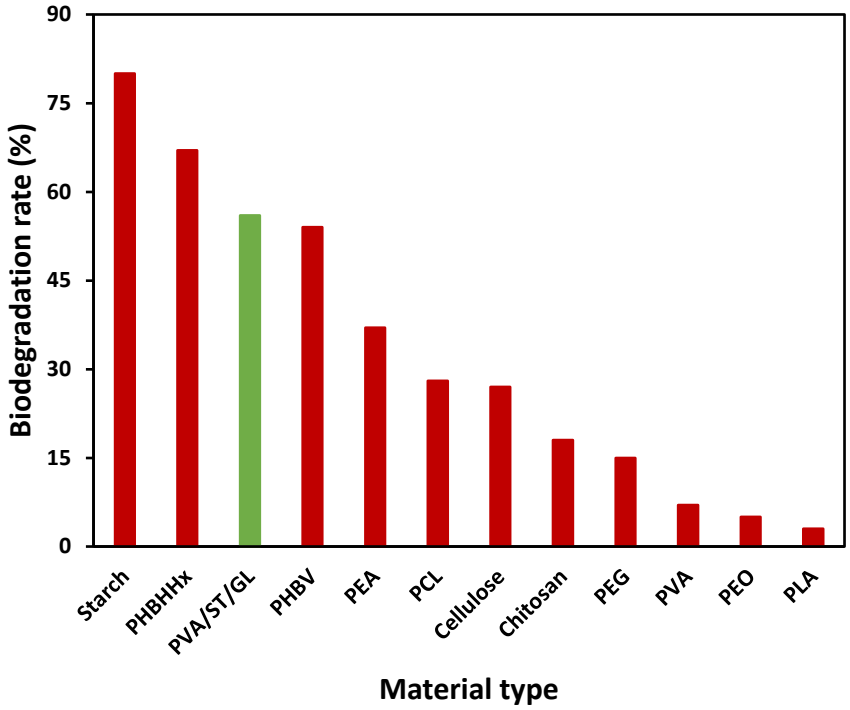


Figure 5-8. Comparisons for biodegradation rates of PVA/ST/GL blends with other different material types with the data collected from (Mangaraj et al. 2018)

The biodegradability of PVA/ST/GL/HNT bionanocomposite films declined significantly from 56.94 to 41.28% with increasing the HNT content from 0 to 1 wt%. This phenomenon was associated with good dispersion of HNTs within polymer blend matrices leading to strong hydrogen bonds between them to hinder water diffusion, mass transfer and rate of microorganism infiltration (Tang et al. 2008). Biodegradation rates of bionanocomposite films tended to increase slightly up to 45.0 and 45.80% at HNT contents of 3 and 5 wt%, respectively. Such results were attributed to HNT agglomeration even though these rates were still higher than those of neat PVA, as evidently shown in other studies (Tang et al. 2008; Imam et al. 2005; Heidarian, Behzad and Sadeghi 2017).

Well-dispersed HNTs clearly reduced the biodegradation rates of bionanocomposite films as opposed to other nanofillers at the same contents up to 1 wt% due to the strong interfacial bonding between HNTs and blend matrices. Whereas, HNT agglomeration

happening at the HNT contents of 3 and 5 wt% diminished these interactions and their effect on biodegradation rates, see Figure 5-9.

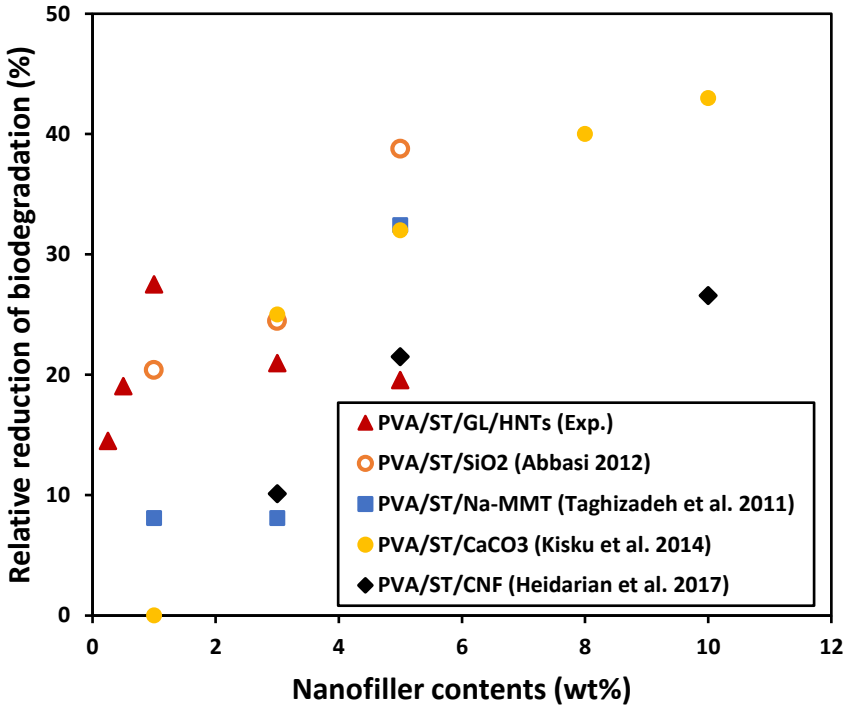


Figure 5-9. Effect of nanofiller content on the biodegradation rates of PVA/ST nanocomposite films reinforced with different nanofillers

## 5.6 SEM

In order to understand different morphological structures taking place in soil burial degradation tests, neat PVA, PAV blends and PVA/ST/GL/HNT bionanocomposite films at various HNT contents were examined via SEM. Moreover, the morphological structures of these samples were evaluated before the biodegradation tests in the initial week and during the active stage period after one and three weeks, as well as at the end of biodegradation tests after 24 weeks, as listed in Table 5-1.

At an initial week, both neat PVA and PVA/GL blend films showed similar smooth surface morphology in good accordance with (Cano et al. 2015b, 2015a). Such smooth structures were completely replaced with rough globular morphology for PVA/ST

blends due to the partial compatibility between PVA and ST in the absence of plasticisers (Cano et al. 2015a). As a result, two separate PVA-rich (continuous phase) and ST-rich (globular structure) phases were clearly observed. This partial compatibility reported in PVA/ST blends was considered as the main reason for their higher $W_a$ and $W_s$ in sections 5.2 and 5.3, respectively. Smooth surface morphology appeared again in PVA/ST/GL blends as a result of the addition of GL to promote the compatibility between components and meanwhile slightly reduce $W_a$ and $W_s$ when compared with those of PVA/ST blends. The addition of HNTs did not show phase separation of bionanocomposite films though the surface roughness was increased particularly with the inclusion of 3 and 5 wt% HNTs, which was in good agreement with the AFM results obtained in Chapter 4.

After one week of soil burial biodegradation tests, neat PVA film did not show clear surface changes, which was confirmed by low biodegradation rates in section 5.5. Whereas, branched traces known as "fungal hyphae" (Qiu and Netravali 2015) were slightly observed on PVA/GL blend surfaces and more clearly on surfaces of PVA/ST and PVA/ST/GL blend films. According to Qiu and Netravali (2015), these fungal hyphae was commonly generated during the progress in biodegradation process at appropriate temperature levels. Moreover, the number and extension of these fungal hyphae increased with time to cross each other and form grooves (Sang et al. 2002). Additionally, the presence of fungal hyphae was good evidence of high biodegradation rates during an active stage period of PVA blend films. Fungal hyphae did not appear on bionanocomposite films despite the increase in surface roughness because of the presence of HNTs, which reduced the rate of microorganism infiltration, as evidenced by Tang et al. (2008).

After three weeks, the surface roughness of neat PVA films was increased without sensible changes while clear alterations were observed on PVA/GL blend films like the pore formation with an average diameter in range of 0.12-1.64 μm. The addition of GL highly improved the mobility of polymeric chains (Ismail and Zaaba 2011; Talja et al. 2007) leading to increasing the rate of microorganism infiltration and biodegradation rate of PVA/GL blends. The fungal hyphae were connected to each other in PVA/ST and PVA/ST/GL blend films to generate small open pores with much faster biodegradation rates as opposed to that of neat PVA film counterparts. When compared with PVA/ST/GL blends alone, bionanocomposite films possessed a small number of pores with relatively large average diameters in range of 0.21-3.05 μm.

After 24 weeks of soil burial biodegradation tests, tiny pores with a small average diameter of 0.06-0.72 μm were revealed with more or less uniform distribution on the surfaces of neat PVA films, which reflected the low biodegradation rate of neat PVA. Nonetheless, the progressive deterioration from the external to internal layers was revealed in PVA blends and PVA/ST/GL/HNT bionanocomposite films. Overall, the addition of ST had remarkable effects on the biodegradation rate and morphological structures of PVA/ST blends, PVA/ST/GL blends and bionanocomposite films as opposed to neat PVA and PVA/GL blends.

Table 5-1. SEM micrographs of neat PVA, PVA blends and PVA/ST/GL/HNT bionanocomposites at different HNT contents at initial week, after one week, three weeks and 24 weeks in soil burial degradation tests

| Material | Initial week | After one week | After 3 weeks | After 24 weeks |
|---|---|---|---|---|
| **Neat PVA** | 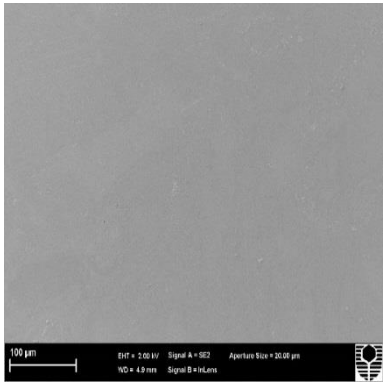 | 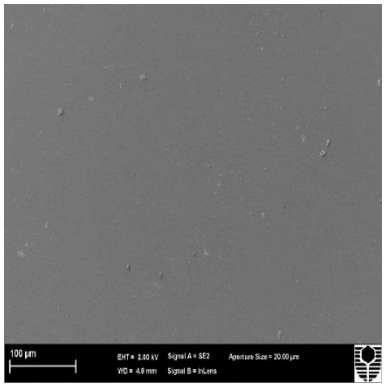 | 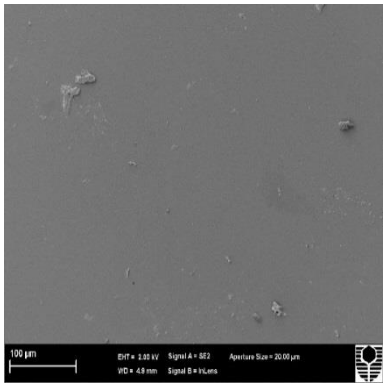 | 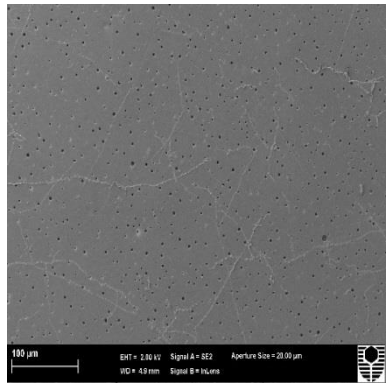 |
| **PVA/GL** | 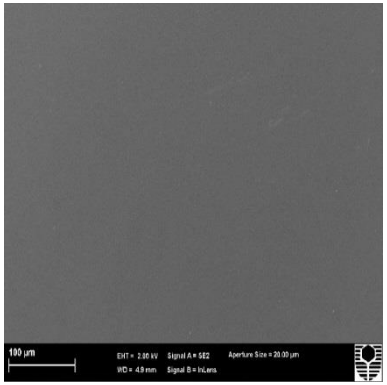 | 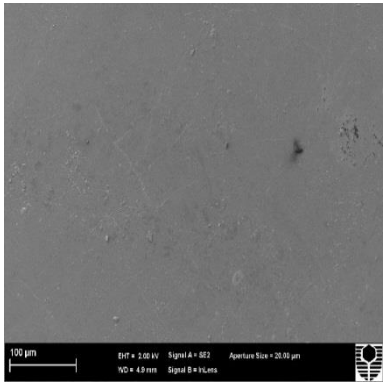 | 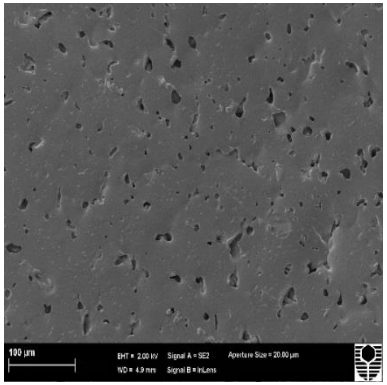 | 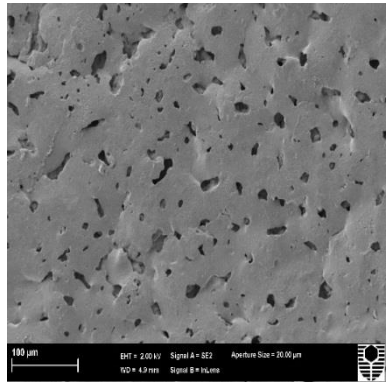 |

| | | | | |
|---|---|---|---|---|
| **PVA/ST** | 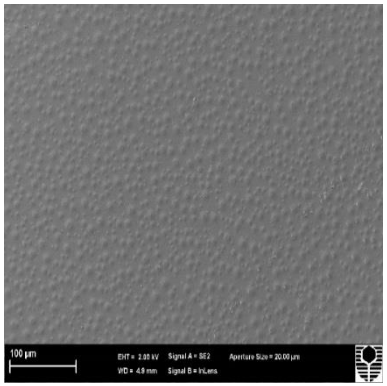 | 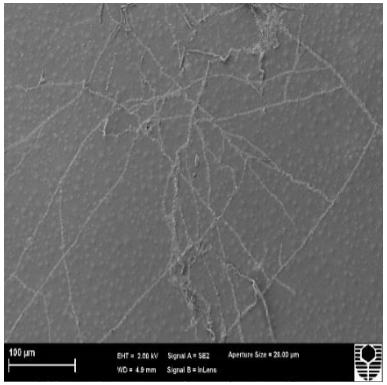 | 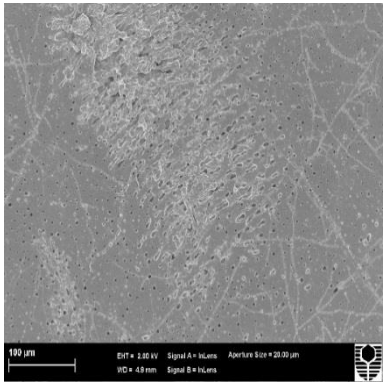 | 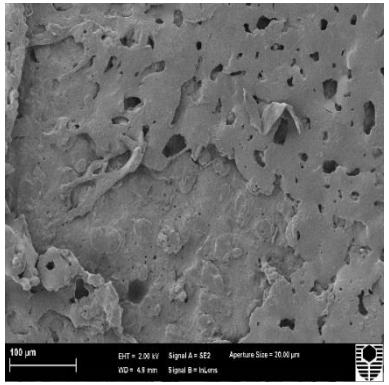 |
| **PVA/ST/GL** | 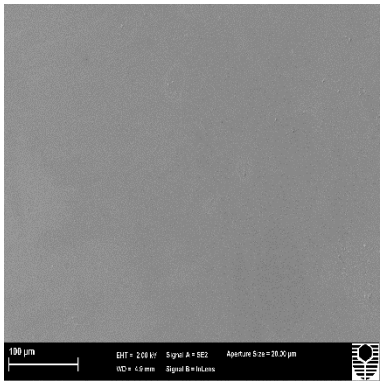 | 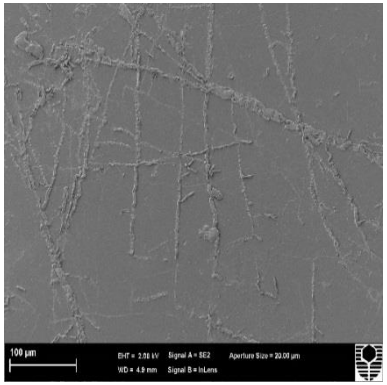 | 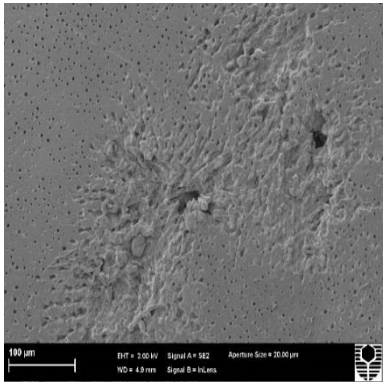 | 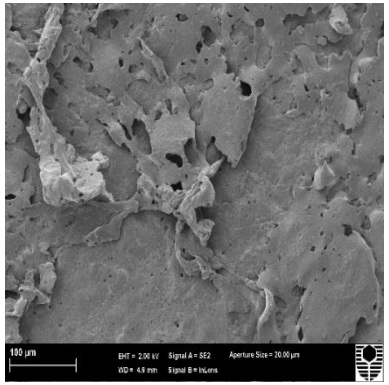 |

| | | | | |
|---|---|---|---|---|
| **0.25 wt% HNTs** | 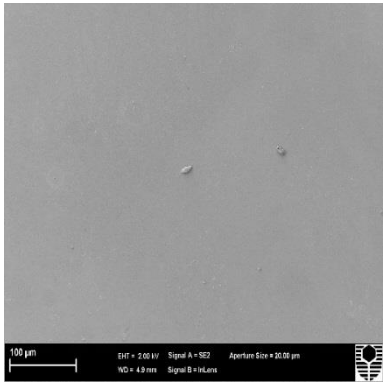 | 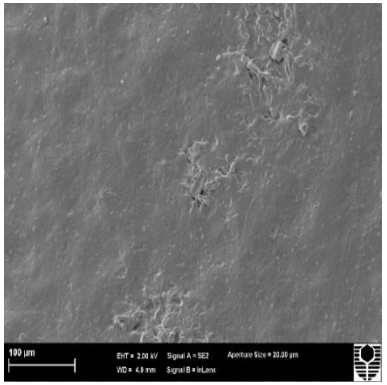 | 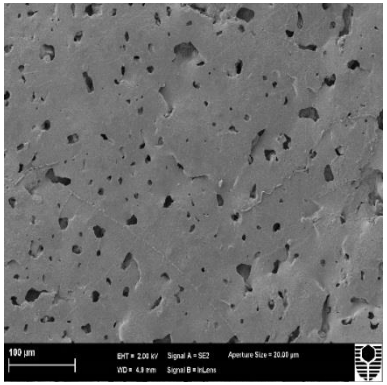 | 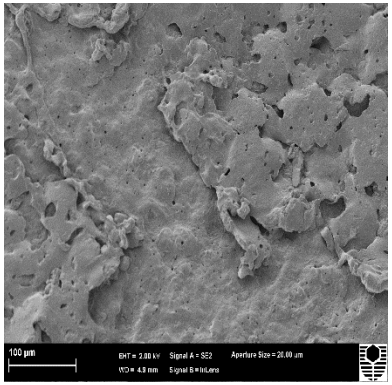 |
| **0.5 wt% HNTs** | 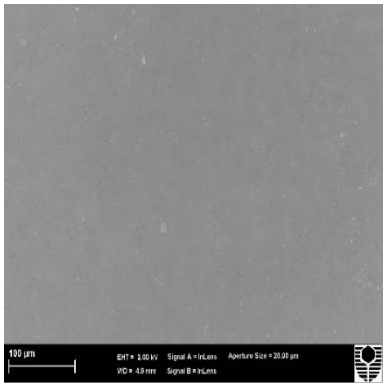 | 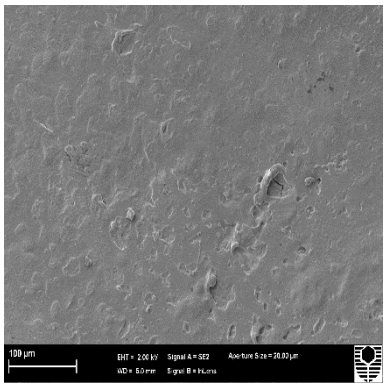 | 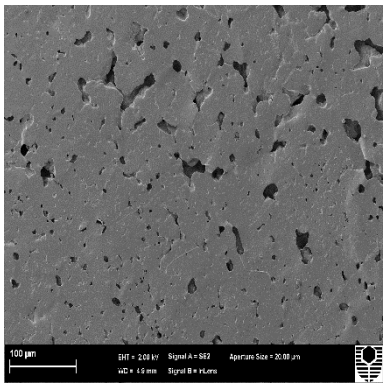 | 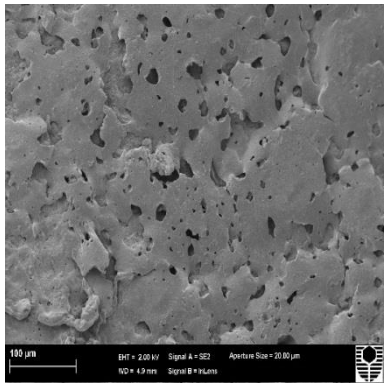 |

| | | | | |
|---|---|---|---|---|
| **1 wt% HNTs** | 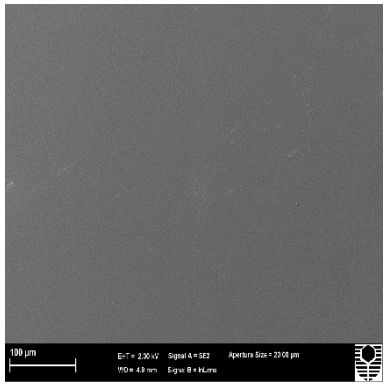 | 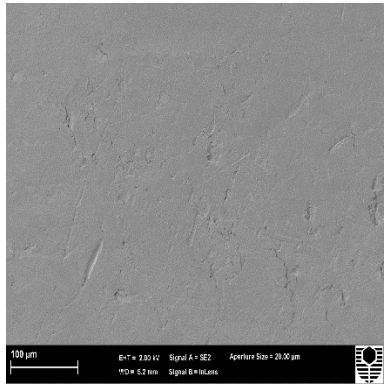 | 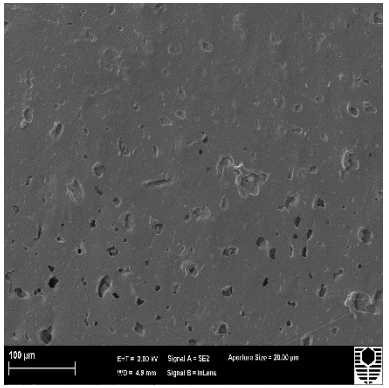 | 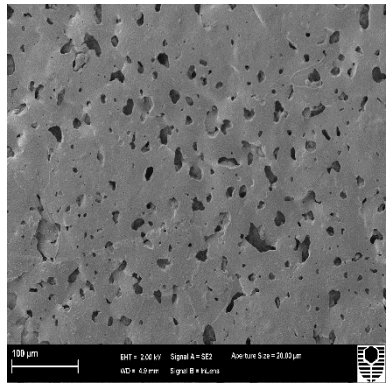 |
| **3 wt% HNTs** | 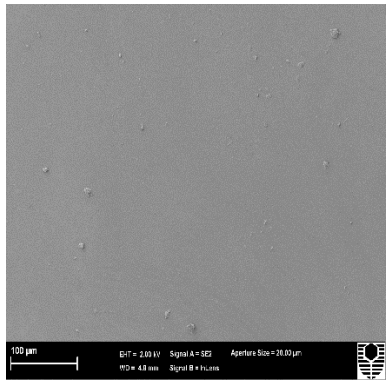 | 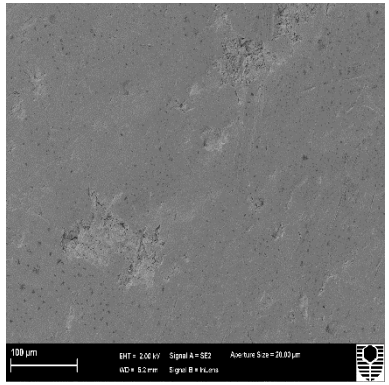 | 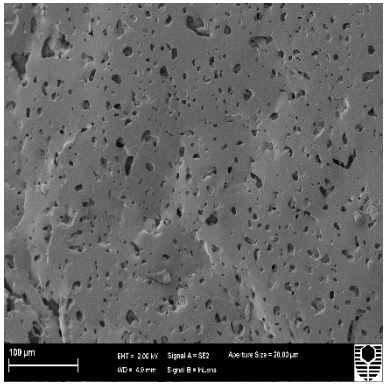 | 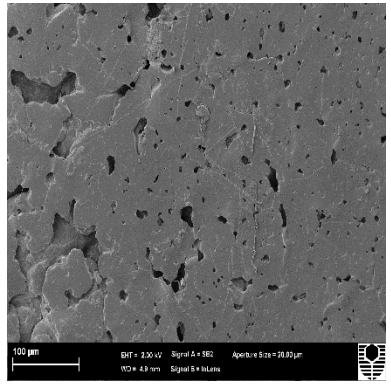 |

| | | | | |
|---|---|---|---|---|
| **5 wt% HNTs** | 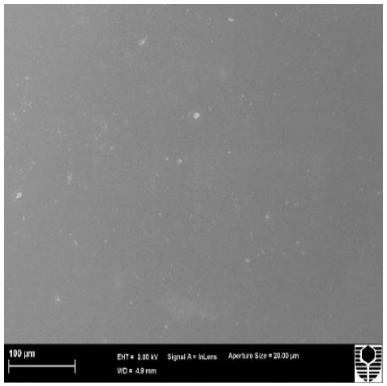 | 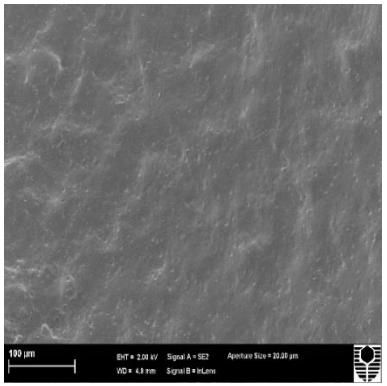 | 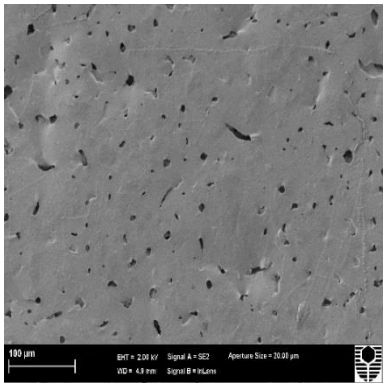 | 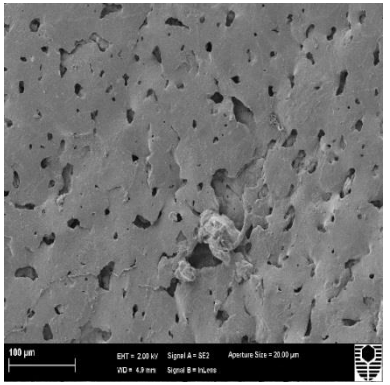 |

## 5.7 Summary

Neat PVA and ST are well known as hydrophilic polymers, so their blends and bionanocomposites had relatively high $W_a$ and $W_s$. When compared with neat PVA, PVA/GL blends had slightly lower $W_a$ and $W_s$ due to the consumption of some free hydroxyl groups by GL molecules to produce hydrogen bonds. A completely opposite trend was shown for PVA/ST blends because the partial compatibility between them made many free hydroxyl groups occupied by water molecules. This compatibility was promoted slightly with the addition of GL leading to the reduction in $W_a$ and $W_s$ of PVA/ST/GL blends. These findings have been further confirmed by the decreased water contact angles of PVA blend films as compared with that of neat PVA films.

A remarkable reduction in $W_a$ and $W_s$ was reported with the incorporation of HNTs within bionanocomposite films owing to moderate hydrophobicity of HNTs as well as the formation of strong hydrogen bonds between nanofillers and blend matrices to restrict the diffusion of water molecules and mass transfer. The presence of HNTs significantly increased the water contact angles of bionanocomposite films as a result of improving their hydrophobicity. The HNT agglomeration at the content levels of 3 and 5 wt% could restrict the reduction of $W_a$ and $W_s$ of bionanocomposite films despite being still better than those of PVA/ST/GL blends.

The poor biodegradability of PVA in some environments like soil was the main reason for lower biodegradation rate as well as slight morphological changes. This rate was increased for PVA/GL blends thanks to the enhanced mobility of polymeric chains to increase the rate of microorganism infiltration. This increasing tendency became more pronounced for PVA/ST blends with the addition of ST as a completely biodegradable polymer. Moreover, the combination of ST and GL highly promoted the biodegradation rate of PVA/ST/GL blends. This high biodegradation rate was reflected

by the growth of fungal hyphae over an active period and apparent damage at the steady state period.

The good dispersion of HNTs reduced the biodegradation rate of PVA/ST/GL/HNT bionanocomposite films with increasing the HNT content from 0.25 to 1 wt% in a linear manner because hydrogen bonding networks were established between nanofillers and blend matrices leading to the reduction in mass transfer. The biodegradation rate of bionanocomposite films was slightly increased beyond 1 wt% HNTs as a result of typical HNT agglomeration, which destabilised the molecular bonding between HNTs and the blend matrices.

# Chapter 6: Barrier Properties of PVA/ST/GL/HNT Bionanocomposite Films

## 6.1 Introduction

The shelf life of foodstuffs is associated with barrier properties of packaging materials in order to protect foodstuffs from the dehydration and oxidation (Othman 2014; Mangaraj et al. 2018). Consequently, barrier properties should be considered for biopolymers and their nanocomposites when considered as food packaging materials. Moreover, such properties of biopolymers and their nanocomposites can be affected by changing the temperature and relative humidity (RH) (Bertuzzi et al. 2007). Thus, the effects of temperature and RH gradient on the *WVP* was studied based on several material systems such as poly(hydroxy-butyrate) (PHB)/ organo-modified MMT nanocomposite films, poly(hydroxyl-butyrate-co-hydroxy-valerate) (PHBHV)/ organo-modified MMT nanocomposite films (Akin and Tihminlioglu 2017), PVA/MMT nanocomposite films (Huang et al. 2017), edible high amylose corn ST films (Bertuzzi et al. 2007), chitosan films (Wiles et al. 2000) and protein films (Gennadios et al. 1994). These investigations demonstrated that material permeability increased linearly with increasing the temperature and RH gradient. In this chapter, barrier properties of neat PVA, PVA blends and bionanocomposite films were evaluated at ambient conditions as well as the effects of temperature range between 25 and 55ºC and RH gradient between 10 to 70% on *WVTR* and *WVP* were thoroughly investigated. Furthermore, these results were compared with theoretical models of permeability based on typical aspect ratios of as-received HNTs as well as accurately

calculated aspect ratios of embedded HNTs in bionanocomposite films with the aid of AFM.

## 6.2 Water vapour transmission and water vapour permeability

The *WVTR* and *WVP* of neat PVA, PVA blends and PVA/ST/GL/HNT bionanocomposite films at different HNT contents were evaluated at 25ºC with a RH level of 50%±2%, as demonstrated in Figure 6-1. The average data related to *WVTR* and *WVP* of neat PVA and PVA blends showed relatively high values because of typical hydrophilic nature of such polymers with many hydroxyl groups, as mentioned in previous studies (Lim et al. 2015; Cano et al. 2015a). The presence of GL and ST was the main reason behind the high *WVTR* and *WVP* of PVA blends compared with those of neat PVA films, which was associated with the improvement of polymeric chain mobility and hydrophilicity, respectively (Cano et al. 2015a; Cano et al. 2015c). *WVTR* and *WVP* of PVA/GL blends increased by 7.08 and 16.72%, respectively, as opposed to those of neat PVA, in good accordance with other studies (Jiang 2016; Imam et al. 2005; Zhang and Han 2006; Arvanitoyannis, Nakayama and Aiba 1998). GL as a plasticiser could diminish the intermolecular interactions and promoted the mobility of polymeric chains leading to the improvement of both *WVTR* and *WVP* (Ismail and Zaaba 2011). Moreover, Talja et al. (2007) stated that the presence of plasticiser could improve the diffusion rate of water molecules within polymers resulting in higher *WVTR* and *WVP*. Additionally, PVA/ST blends revealed remarkable increases in *WVTR* and *WVP* by 21.27 and 30.96%, respectively, as opposed to those of neat PVA. Generally, the water solubility of PVA and water sensitivity of ST would produce water-sensitive and permeable blends (Cano et al. 2015a). The *WVTR* of PVA/ST/GL blends was lower than those of PVA/GL and PVA/ST blends while the *WVP* of PVA/ST/GL blends was between those of PVA/GL

and PVA/ST blends due to the presence of GL to enhance the compatibility between PVA and ST as well as consume some hydrogel groups to build up hydrogen bonds.

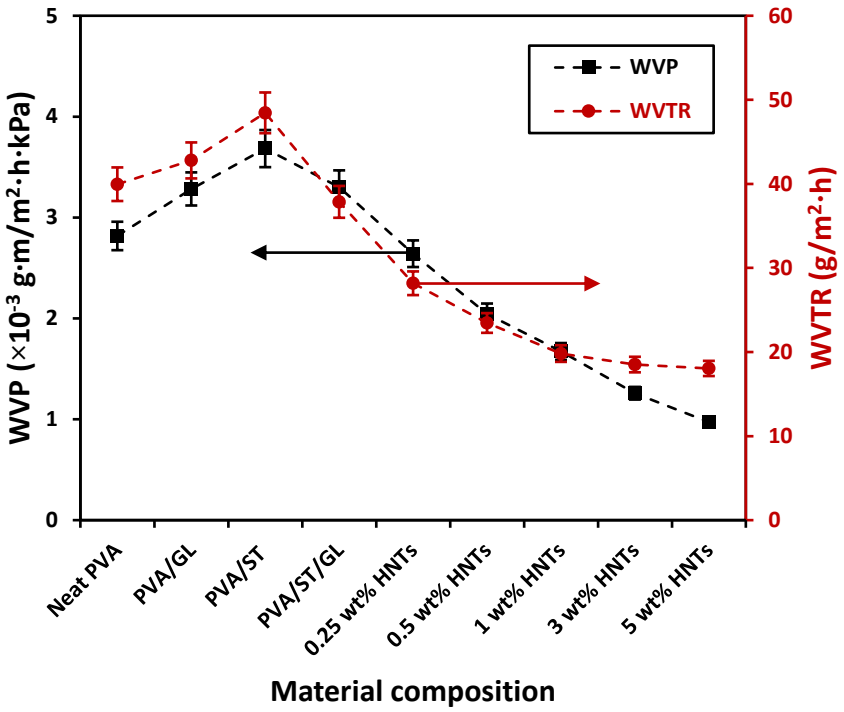


Figure 6-1. *WVTR* and *WVP* of neat PVA, PVA blends and PVA/ST/GL/HNT bionanocomposite films at 25ºC and 50% RH

*WVTR* and *WVP* of PVA/ST/GL/HNT bionanocomposite films were reduced as opposed to those of corresponding blend films since the addition of HNTs generated tortuous paths within bionanocomposite films (Noshirvani et al. 2016) to promote better water resistance (Sadegh-Hassani and Nafchi 2014). As such, *WVTR* and *WVP* of bionanocomposite films were decreased significantly by 52.34 and 73.59%, respectively, with increasing the HNT contents from 0 to 5 wt%. Lee, Kim and Park (2018) reported a similar reduction in *WVP* of chitosan/HNT nanocomposites and chitosan/clove essential oil (CEO)/HNT nanocomposites by 16.11 and 15.67%, respectively, as compared with their blends due to the presence of HNTs to consume free hydroxyl groups in nanocomposites and create hydrogen bonding with polymer matrices. Such decreases in *WVTR* and *WVP* became less pronounced between 1 and

5 wt% HNTs, resulting from typical HNT agglomeration, which was in good agreement with previous findings on plasticised PVA/ST nanocomposites (Guimarães Jr. et al. 2015; Heidarian, Behzad and Sadeghi 2017; Tang et al. 2008; Tang and Alavi 2012). In polymer/clay nanocomposites, the agglomeration of nanofillers could generate newly connected pathways for permeable molecules at the clay/polymer matrix interfaces instead of the touristy leading to the permeability improvement (Tan and Thomas 2016) shown in Figure 6-2.

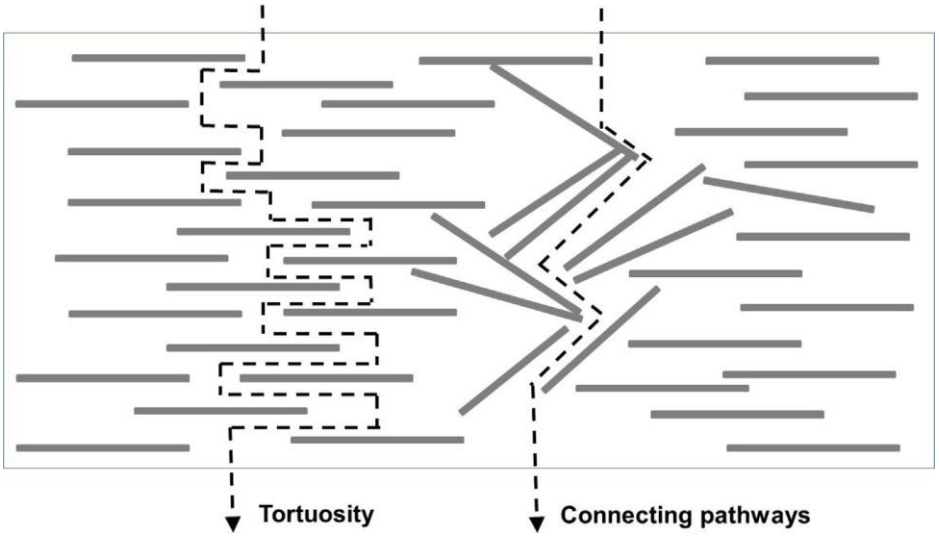


Figure 6-2. Schematic diagram of permeation through interfaces of polymer/clay nanocomposites (Tan and Thomas 2016)

It was clearly seen from Figure 6-3 that HNTs had significant effect on the *WVP* of PVA/ST blends as compared with other types of nanofillers due to their moderate hydrophobicity resulting from their lower number of hydroxyl groups on surfaces leading to reasonable water resistance, which was evidenced in the results of water contact angles previously mentioned in Chapter 5. Overall, the improvement rate in barrier properties of nanocomposites was determined by the dispersion of nanofillers to create tortuous paths for inhibiting the gas/liquid permeation (Choudalakis and Gotsis 2009; Ghanbarzadeh, Almasi and Entezami 2011).

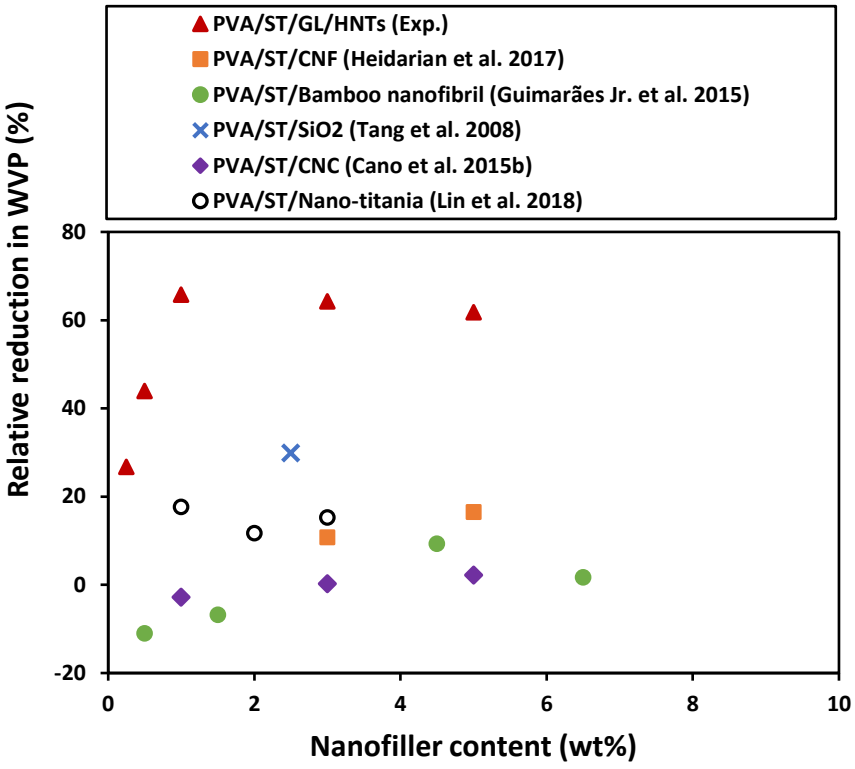


Figure 6-3. Effect of different nanofiller types on *WVP* of PVA/ST nanocomposite films

### 6.2.1 Effect of temperature

The food packaging materials may be used at different temperatures and RH levels during the transport and display processes. As such, *WVTR* and *WVP* of neat PVA, PVA blends and PVA/ST/GL/HNT bionanocomposite films were evaluated at 25, 35, 45 and 55ºC, as illustrated in Figure 6-4 (a) and (b), respectively. There exists a linearly increasing trend for *WVTR* and *WVP* of all material films when the temperature was increased from 25 to 55ºC. It is clearly known that the *WVP* values of polymers and corresponding nanocomposites were increased with increasing temperature owing to the enhancement of free volume and chain mobility of polymeric molecules, as well as the increase in the diffusion rate and energy level of permeable molecules (Bertuzzi et al. 2007; Rogers 1985; Poley et al. 2005). However, the *WVTR* and *WVP* of neat

PVA films were increased gradually with increasing the temperatures from 25 to 55ºC by 15.06 and 4.98%, respectively. The *WVTR* and *WVP* of neat PVA was less influenced by the temperature variation when compared with those of PVA blends because the selected temperature range of 25-55ºC was still less than the $T_g$ of PVA at 70.70ºC, as reported in section 4.3. For the same reason, *WVTR* and *WVP* of PVA/GL blends, PVA/ST/GL blends and PVA/ST/GL/HNT bionanocomposite films were moderately increased with increasing the temperature from 25 to 35ºC while such an increasing trend became more pronounced beyond 35ºC. For instance, *WVTR* and *WVP* of PVA/GL blends were increased slightly by 10.56 and 6.70%, respectively at 35ºC, which was followed by a remarkable increase with increasing the temperature from 35 to 55ºC. The significant increases in the *WVTR* and *WVP* of PVA/GL blends were related to the selected temperature range to be much closer to its $T_g$ of 47.70ºC. This was also the case for PVA/ST/GL blends and their corresponding bionanocomposite films. Whereas, *WVTR* and *WVP* of PVA/ST blends instead demonstrated a gradually increasing tendency over the selected temperature range despite being still less than the $T_g$ of 74.10ºC. At all temperature levels, PVA/ST/GL/HNT bionanocomposite films had lower *WVTR* and *WVP* than those of corresponding blends due to the presence of HNTs to undermine the temperature-dependent effect. In other words, the increasing rates in *WVTR* and *WVP* of bionanocomposite films in terms of temperature level were lower than those of blends. In a similar manner, Huang et al. (2017) reported that *WVP* of PVA/MMT bionanocomposite films was less dependent on the temperature level because the incorporation of nanofillers could restrict chain mobility of polymeric molecules and further reduce the diffusion rate of water molecules as the indicator for lower *WVTR* and *WVP*.

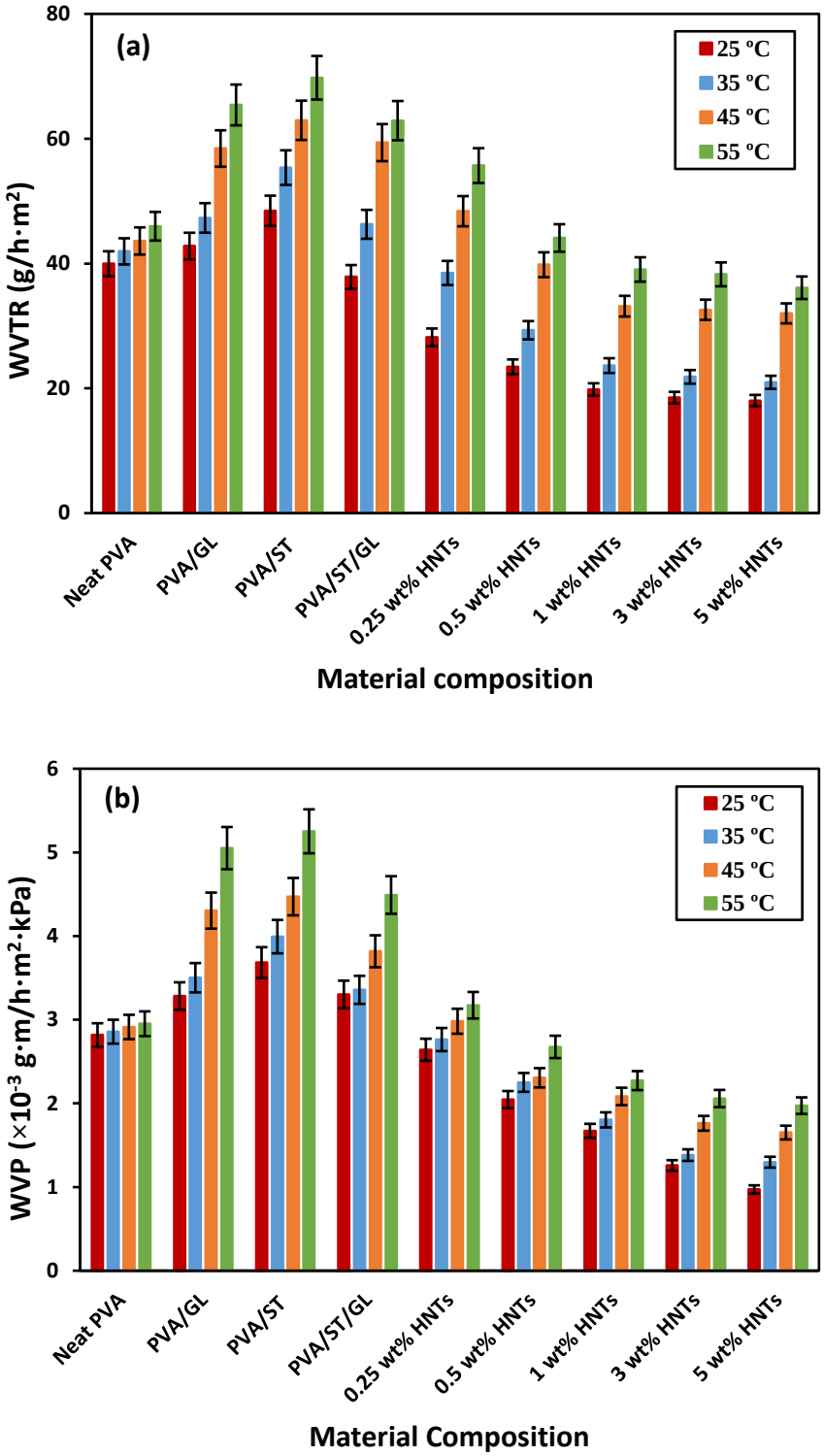


Figure 6-4. Temperature effect on (a) *WVTR* and (b) *WVP* of neat PVA, PVA blends and PVA/ST/GL/HNT bionanocomposite films at different HNT contents

This temperature dependence on *WVP* of PVA/ST/GL blends and their corresponding bionanocomposite films can be described according to Arrhenius equation as follows

(Arvanitoyannis, Nakayama and Aiba 1998; Rogers 1985; Ashley 1985; Siracusa 2012; Morillon et al. 2000):

$$WVP = P_a \, exp\left(\frac{-E_p}{RT}\right) \qquad (6\text{-}1)$$

where $P_a$ is the Arrhenius constant (i.e. pre-exponential constant), $E_p$ is the activation energy of permeability (kJ/mol), $R$ is the universal gas constant (8.314 kJ/mol·K) and $T$ is the absolute temperature (K). The logarithmic relationship between *WVP* values of PVA/ST/GL blends as well as their corresponding bionanocomposite films and *1/T* showed good line fitting with Arrhenius equation, as demonstrated in Figure 6-5. The linear gradient of this relationship means the high *WVP* of material depends on temperature, which was evident for PVA/ST/GL blends with their increasing line gradient when increasing the temperature level. Whereas, the high thermal stability of HNTs (Yuan, Tan and Annabi-Bergaya 2015) clearly reduced the effect of temperature dependence on bionanocomposite films at the HNT contents of 0.25 -1 wt% as compared with PVA/ST/GL blends alone in sign of less gradient lines. The lines gradient was increased again for bionanocomposites reinforced with 3 and 5 wt% HNTs due to the HNT agglomeration issue to hinder the effect of HNTs on *WVP*.

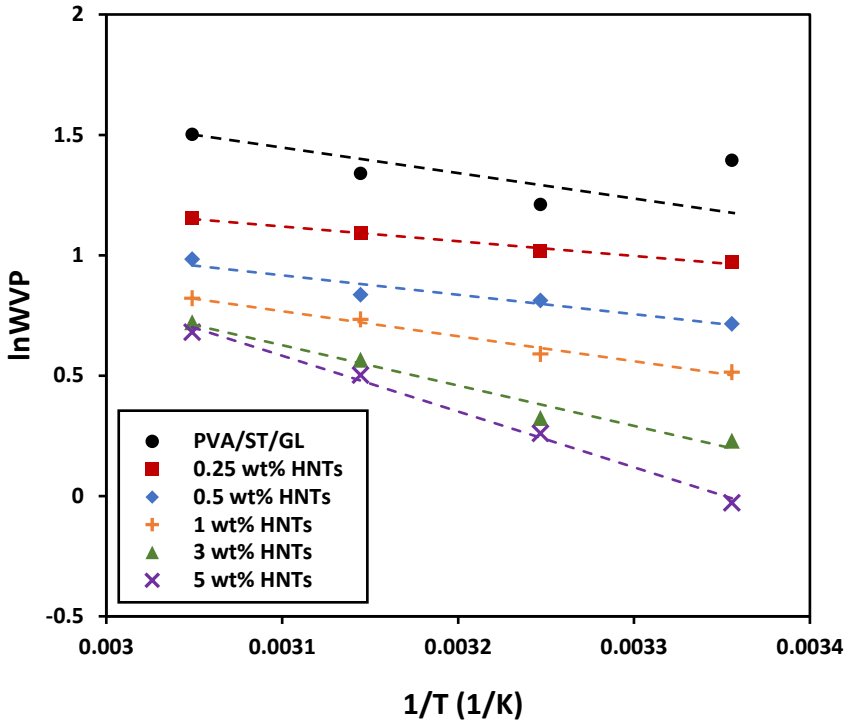


Figure 6-5. Arrhenius relationship between the *WVP* of PVA/ST/GL blends and corresponding bionanocomposite films at different HNT contents and temperature levels

According to Huang et al. (2017), $E_p$ is defined as the minimum energy required by permeable molecules to overcome interaction forces between material molecules and diffuse through the materials. Consequently, the high value of $E_p$ indicates that permeable molecules need higher energy to diffuse through the materials. In other words, a material possesses a low permeability rate at high $E_p$ value leading to less sensitivity to the temperature change (Gennadios et al. 1994; Gennadios, Weller and Testin 1993). It is clearly shown in Table 6-1 that PVA blends had lower $E_p$ than that of neat PVA. Accordingly, *WVP* of neat PVA was less sensitive to temperature change as opposed to its PVA blends counterparts. Additionally, PVA/ST/GL/HNT bionanocomposites had higher $E_p$ values compared with that of corresponding blends, and these values were increased in a monotonic manner with increasing the HNT content, as shown in other studies (Huang et al. 2017; Gennadios, Weller and Testin

1993; Akin and Tihminlioglu 2017). Overall, the incorporation of HNTs within PVA/ST/GL blends in bionanocomposite films greatly reduced *WVTR* and *WVP* of bionanocomposite films in the temperature range of 25-55ºC according to Arrhenius relationship.

Table 6-1. Activation energies of permeation and Arrhenius constants of neat PVA, PVA blends and PVA/ST/GL/HNT bionanocomposite films

| **Material composition** | $E_p$ **(kJ/mol)** | $P_a$ |
|---|---|---|
| Neat PVA | 11.27 | 2.97 |
| PVA/GL | 8.46 | 5.05 |
| PVA/ST | 7.97 | 5.47 |
| PVA/ST/GL | 10.84 | 4.52 |
| PVA/ST/GL/0.25 wt% HNTs | 12.01 | 3.26 |
| PVA/ST/GL/0.5 wt% HNTs | 12.98 | 2.71 |
| PVA/ST/GL/1 wt% HNTs | 13.04 | 2.43 |
| PVA/ST/GL/3 wt% HNTs | 14.13 | 2.48 |
| PVA/ST/GL/5 wt% HNTs | 14.16 | 2.22 |

### 6.2.2 Effect of RH gradient (ΔRH)

*WVTR* and *WVP* of neat PVA, PVA blends and PVA/ST/GL/HNT bionanocomposite films were evaluated at different RH gradients of 10, 30, 50 and 70%± 2% at the room temperature of 25ºC, as demonstrated in Figure 6-6 (a) and (b), respectively. According to Fick's first law of diffusion, the flux ($F_x$) in one direction ($\partial_x$) is proportional to the gradient of concentration ($\partial_c$) in the same direction shown below (Rogers 1985; Comyn 1985):

$$F_x = -D\left(\frac{\partial_c}{\partial_x}\right) \qquad (6\text{-}2)$$

Accordingly, the RH gradient is the driving force of permeation process across film thickness. It was evident that *WVTR* and *WVP* of neat PVA, PVA blends and

PVA/ST/GL/HNT bionanocomposites were increased remarkably with increasing the RH gradient, which was in good agreement with previous studies (Wiles et al. 2000; Talja et al. 2007). Consequently, the higher values of *WVTR* and *WVP* were recorded at the RH gradient of 70%± 2% as opposed to those recorded at 10%± 2%. According to Cuq et al. (1997), the plasticisation effect of water molecules could appear at the high RH level leading to the improvement of free volume of polymeric molecules as well as in order to improve the water molecules diffusion and transfer across the films. Moreover, Ashley (1985) and Mo et al. (2014) stated that hydrophilic polymers like PVA had increased *WVTR* and *WVP* with the RH level due to the interaction of water molecules with hydroxyl groups of polymers through hydrogen bonding resulting in the increase in water solubility coefficient (*S*). On the other hand, water diffusivity coefficient (*D*) may also be increased owing to the plasticisation effect of water molecules to enhance the permeability coefficient (*P*) as follows (Mo et al. 2014; Ashley 1985; Gennadios et al. 1994):

$$P = S \times D \qquad (6\text{-}3)$$

As such, *WVTR* and *WVP* of neat PVA were increased by 518.79 and 257.95%, respectively, with increasing the ΔRH from 10 to 70%± 2%. At different RH gradients, PVA blends had higher *WVTR* and *WVP* compared with those of neat PVA due to the presence GL and ST leading to better chain mobility of polymeric molecules and higher hydrophilicity of blends, as discussed earlier (Cano et al. 2015a; Cano et al. 2015c). At the same RH gradient of 10%± 2%, *WVTR* and *WVP* of PVA/GL, PVA/ST and PVA/ST/GL blends were evidently increased by 17.90 and 54.55%, 60.01 and 125.0% as well as 30.05 and 89.77%, respectively, as compared with those of neat PVA. A similar trend was recorded at other RH gradients (i.e. 30, 50 and 70%± 2%). These findings were in good accordance with other ST nanocomposites (Talja et al.

2007). Overall, *WVTR* and *WVP* of neat PVA were increased linearly with increasing RH gradient due to the plasticisation effect of water molecules. Additionally, this increasing trend becomes more pronounced for PVA blends due to the presence of GL and ST for better mobility of polymeric molecules and higher hydrophilicity of blends.

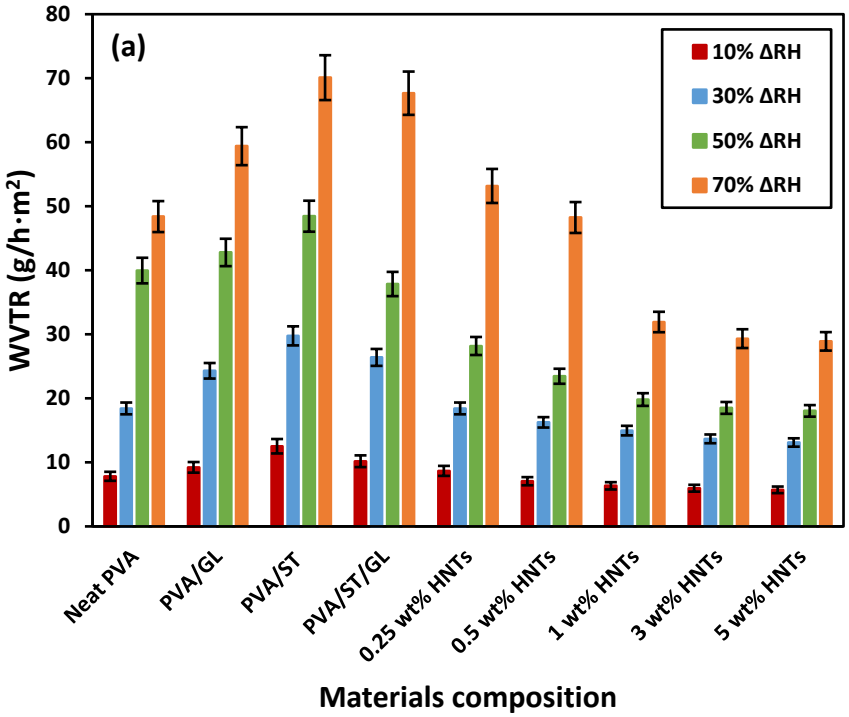

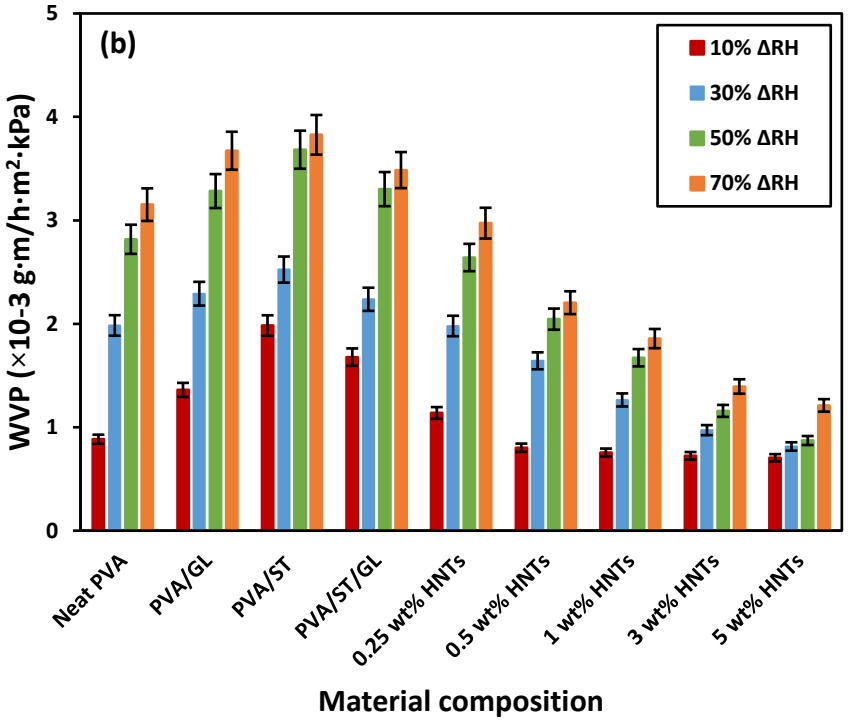


Figure 6-6. RH gradient effect on (a) *WVTR* and (b) *WVP* of neat PVA, PVA blends and PVA/ST/GL/HNT bionanocomposite films at different HNT contents

*WVTR* and *WVP* of PVA/ST/GL/HNT bionanocomposite films were greatly decreased at all RH gradients compared with those of corresponding blends, as illustrated in Figure 6-6 (a) and (b), respectively. The incorporation of HNTs within polymer matrices generated tortuous paths leading to the restriction to both diffusion of permeable molecules and mobility of polymeric chains (Noshirvani et al. 2016; Choudalakis and Gotsis 2009). *WVTR* and *WVP* of bionanocomposite films dropped remarkably by 57.28 and 65.26% with the increasing HNT content from 0 to 5 wt% as the RH gradient increasing from 10 to 70%±2%. Additionally, this improvement in barrier properties of bionanocomposite films diminished slightly beyond 1 wt% HNTs due to HNT agglomeration issue at the HNT contents of 3 and 5 wt% according to our predetermined SEM and AFM results in Chapter 4. However, barrier properties of bionanocomposite films reinforced with 3 and 5 wt% HNTs were still better than those of PVA/ST/GL blends at all RH gradients.

Depending on *WVP* data of PVA/ST/GL blends and corresponding bionanocomposite films, a clear linear relationship could be established between the *WVP* and RH gradient ($\Delta RH$) as follows (see Figure 6-7):

$$WVP = a\Delta RH + b \qquad (6\text{-}4)$$

where *a* and *b* are constants for line fitting. Furthermore, the slopes of these lines were decreased with increasing the HNT content. In other words, the *WVP* of bionanocomposite films became less sensitive to increasing the RH gradient as opposed to that of PVA/ST/GL blends. This phenomenon was ascribed to the improvement of relative surface hydrophobicity in the presence of HNTs in good accordance with the water contact angle results obtained in section 5.3.

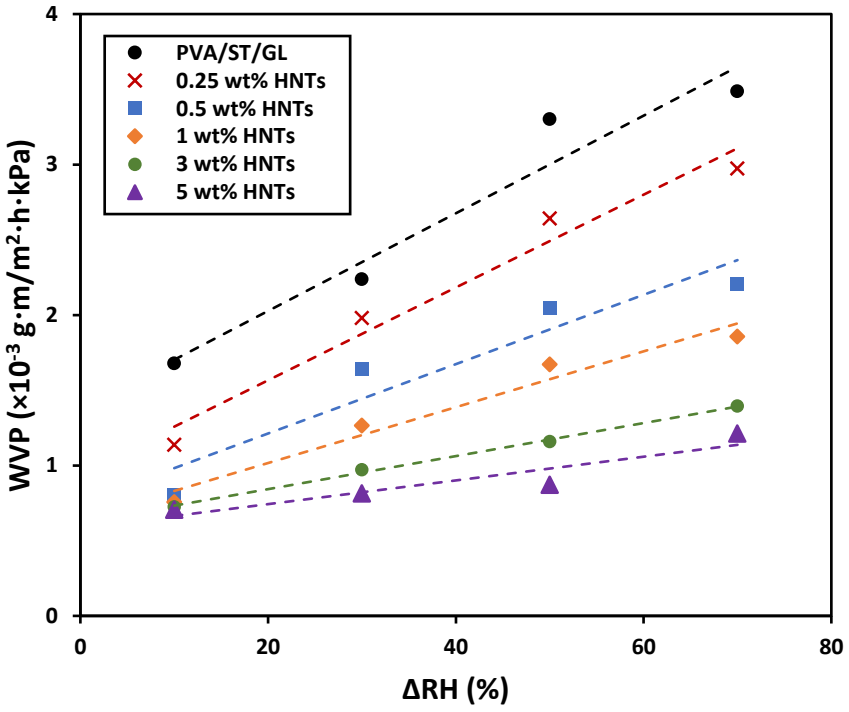


Figure 6-7. Relationship between *WVP* and *RH* gradient for PVA/ST/GL blends and corresponding bionanocomposite films at different HNT contents

## 6.3 Gas permeability

Gas permeability of neat PVA, PVA blends and PVA/ST/GL/HNT bionanocomposite films were evaluated by using oxygen and air, Figure 6-8. The good barrier properties mean lower permeability of materials (harder to permeate by permeable molecules) (Feldman 2013). It can be clearly seen that the gas permeability of all material films appeared to be lower than *WVP* because polar polymers like PVA have good gas barrier properties, but poor water resistance due to the presence of many hydroxyl groups while their gas barrier properties were decreased in the presence of plasticisers (Ashley 1985). Similarly, Lim et al. (2015) concluded that high crystallinity and strong intermolecular interactions of PVA gave rise to good oxygen barrier properties though lower water resistance arose from the presence of many hydroxyl groups. A similar trend was reported for oxygen and air permeabilities of all material films because there was no direct interaction between polymeric molecules and gas molecules, as evidenced in previous work (Sridhar and Tripathy 2006; Picard et al. 2007). The addition of GL increased oxygen and air permeabilities of PVA/GL blends by 77.59 and 75.88%, respectively, as opposed to those of neat PVA due to the plasticisation effect of GL. The presence of plasticisers improves the mobility of polymeric chains and increases the polymer-free volume that can be easily penetrated by permeable molecules with poor barrier properties. A further increase for oxygen and air permeabilities of PVA/ST blends by 91.25 and 99.29%, respectively, was also shown when compared with those of neat PVA owing to partial compatibility between PVA and ST in the absence of plasticiser. This resulted from the diffusion improvement of permeable molecules due to inhomogeneous morphological structures with several diffusion paths (Zou, Qu and Zou 2008) (see section 5.6). Consequently, oxygen and

air permeabilities of PVA/ST/GL blends dropped by 10.28 and 9.62%, respectively, relative to PVA/ST blends due to the addition of GL that improved their compatibility.

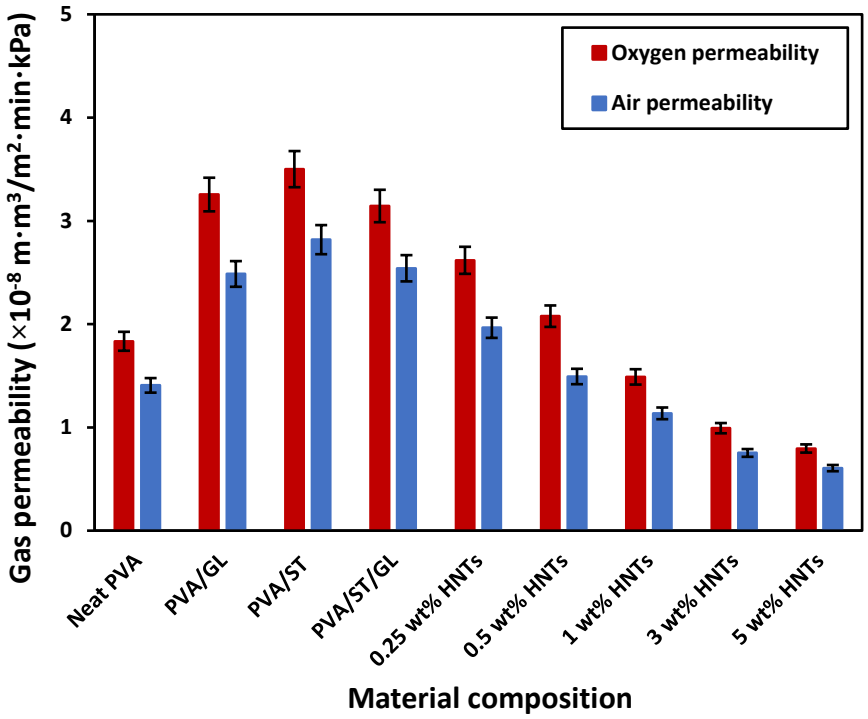


Figure 6-8. Oxygen and air permeabilities of neat PVA, PVA blends and PVA/ST/GL/HNT bionanocomposite films at different HNT contents

In general, when impermeable fillers are incorporated within polymer matrices, permeable molecules should travel around these fillers in much longer tortuous paths to be permeable through composites, particularly when there is no interaction between permeable molecules like oxygen and air, and matrix constituents (Liu et al. 2016b). Such tortuous paths can be described by tortuosity factor (τ) depending on simple Nielsen model given below (Sadegh-Hassani and Nafchi 2014; Alipoormazandarani, Ghazihoseini and Nafchi 2015; Picard et al. 2007; Nielsen 1967):

$$\frac{P_c}{P_o} = \frac{1 - \emptyset}{\tau} \qquad (6\text{-}5)$$

where $P_c$, $P_o$ and $\emptyset$ are the permeabilities of nanocomposites and polymer matrices, respectively, as well as the volume fraction of impermeable nanofillers (Nielsen 1967;

Picard et al. 2007). It was clearly revealed that τ values were increased in a monotonic manner with increasing the HNT content from 0 to 5 wt%, as listed in Table 6-2. This trend could be interpreted by the generation of tortuous paths within PVA/ST/GL/HNT bionanocomposite films leading to much better barrier properties

Table 6-2. Relative oxygen permeabilities and tortuosity factors of bionanocomposite films at different HNT contents

| **HNT content (wt%)** | $P_c/P_o$ | $\tau$ |
|---|---|---|
| 0 | 1.00 | 1.00 |
| 0.25 | 0.83 | 1.18 |
| 0.5 | 0.66 | 1.47 |
| 1 | 0.47 | 2.00 |
| 3 | 0.32 | 2.59 |
| 5 | 0.25 | 2.60 |

As such, oxygen and air permeabilities of bionanocomposite films were decreased significantly by 74.84 and 75.98%, respectively, with increasing the HNT content from 0 to 5 wt% in good accordance with other studies (Liu et al. 2016a; Huang et al. 2012; Sadegh-Hassani and Nafchi 2014; Alipoormazandarani, Ghazihoseini and Nafchi 2015). This reduction trend in oxygen and air permeabilities became less pronounced beyond 1 wt% HNTs owing to their agglomeration to generate direct paths for permeable molecules rather than tortuous paths mentioned previously (Heidarian, Behzad and Sadeghi 2017; Nafchi 2013). Such results coincided with other findings based on PVA/ST/nano-titania nanocomposites (Lin et al. 2018). It was manifested that morphological structures of nanocomposites in term of nanofiller dispersion played an important role in the improvement of barrier properties (Cui et al. 2015).

## 6.4 Comparison between experimental data and theoretical models

The most popular Nielsen model and Cussler model were considered to predict water vapour and gas permeabilities of polymer nanocomposites reinforced with ribbon-like nanofillers (Tan and Thomas 2016; Takahashi et al. 2006). There is no definite model for tubular nanofillers, and ribbon-like structures is the closest to HNTs in shape. Consequently, these two models based on ribbon-shape nanofillers in term of regular and random dispersion of nanofillers were used to predict water vapour, oxygen and air permeabilities of PVA/ST/GL/HNT bionanocomposite films in comparison with experimental data.

Nielsen model for regular and random nanofiller dispersion can be written in equations (6-6) and (6-7), respectively (Takahashi et al. 2006; Tan and Thomas 2016; Saritha et al. 2012; Choudalakis and Gotsis 2009):

$$\frac{P_c}{P_o} = \frac{1-\emptyset}{1+\left(\frac{\alpha}{2}\right)\emptyset} \qquad (6\text{-}6)$$

$$\frac{P_c}{P_o} = \frac{1-\emptyset}{1+\frac{1}{3}\left(\frac{\alpha}{2}\right)\emptyset} \qquad (6\text{-}7)$$

where $\alpha$ is aspect ratio of HNTs (i.e. $\alpha=L/D$). Ø can be calculated from the following equation (Picard et al. 2007; Alexandre et al. 2009):

$$\frac{1}{\emptyset} = 1 + \frac{\rho_i(1-\mu_i)}{\rho_p \mu_i} \qquad (6\text{-}8)$$

where $\rho_i$ and $\mu_i$ are the density (i.e. $\rho_i$ =2.53 g/cm$^3$ for HNTs) and weight fraction of impermeable phase (i.e., HNTs in this case), respectively. Whereas $\rho_p$ is the density of permeable phase (i.e., polymer blend matrices) that can be calculated as follows (Callister 2007):

$$\rho_p = \sum_{x=1}^{n} \rho_x V_x \qquad (6\text{-}9)$$

where $\rho_x$ and $V_x$ are the density and volume fraction of each component in polymer blend matrices (i.e., PVA, ST and GL) (Callister 2007). Typical aspect ratio of as-received HNTs (α=39.22) and variable aspect ratios of embedded HNTs in PVA/ST/GL/HNT bionanocomposite films were determined using AFM (see section 4.1.2) so that they could be further employed in Nielsen model and Cussler model for the best fitting with experimental data, as illustrated in Figure 6-9 (a) and (b), respectively. When the typical aspect ratio of as-received HNTs was considered, good agreement was detected between Nielsen model for regular nanofiller dispersion and relative permeability experimental data of bionanocomposites up to 1 wt% HNTs. This behaviour could be interpreted in term of significant reduction in relative permeabilities of bionanocomposites due to good dispersion of HNTs in the range of 0-1 wt%. Conversely, Nielsen model for random nanofiller dispersion fitted better beyond 1 wt% HNTs accordingly, which was believed to be associated with the HNT agglomeration according to our SEM and AFM images in section 4.1. In generally, most developed permeability models for nanocomposite films are based on regular shape and sizes of nanofillers within polymer matrices ( Choudalakis and Gotsis 2009). In fact, the shapes and sizes of nanofillers can be greatly altered during the manufacturing steps of nanocomposites. Additionally, nanofillers may be clustered or agglomerated particularly at the high contents due to their weak Van Der Waals interactions. As such, it is worthwhile to use experimentally determined aspect ratios of embedded HNTs in relation to their different nanofiller contents in bionanocomposites for more accurate modelling work. When variable aspect ratios of HNTs were taken into account, the results based on Nielsen model for regular

nanofiller dispersion were found to have better agreement with experimental permeability data with the consideration of HNT agglomeration, as depicted in Figure 6-9 (a) and lower error percentages listed in Table 6.3.

On the other hand, Cussler model for regular and random nanofiller dispersion can be written below according to equations, (6-10) and (6-11), respectively (Choudalakis and Gotsis 2009; Saritha et al. 2012; Takahashi et al. 2006):

$$\frac{P_c}{P_o} = \frac{1 - \emptyset}{1 + \left(\frac{\alpha\emptyset}{2}\right)^2} \qquad (6\text{-}10)$$

$$\frac{P_c}{P_o} = \frac{1 - \emptyset}{\left(1 + \frac{\alpha\emptyset}{3}\right)^2} \qquad (6\text{-}11)$$

It was clearly shown in Figure 6-9 (b) and Table 6.3 that Cussler model for regular and random dispersion of nanofillers reflected good fitting with permeability experimental data of bionanocomposites based on the aspect ratios of both as-received HNTs and embedded HNTs within polymer matrices in bionanocomposites at the HNT contents of 0-1 wt%. Nonetheless, beyond 1 wt% HNTs, Cussler model failed to fit experimental data of bionanocomposites owing to its applicability to nanocomposite systems at low nanofiller contents with high aspect ratios of nanofillers (Sadegh-Hassani et al. 2014; Cui et al. 2015). Overall, nanofiller content, nanofiller aspect ratio and nanofiller dispersion within polymer matrices in nanocomposite systems should be carefully considered for the effective prediction to permeabilities of bionanocomposite films.

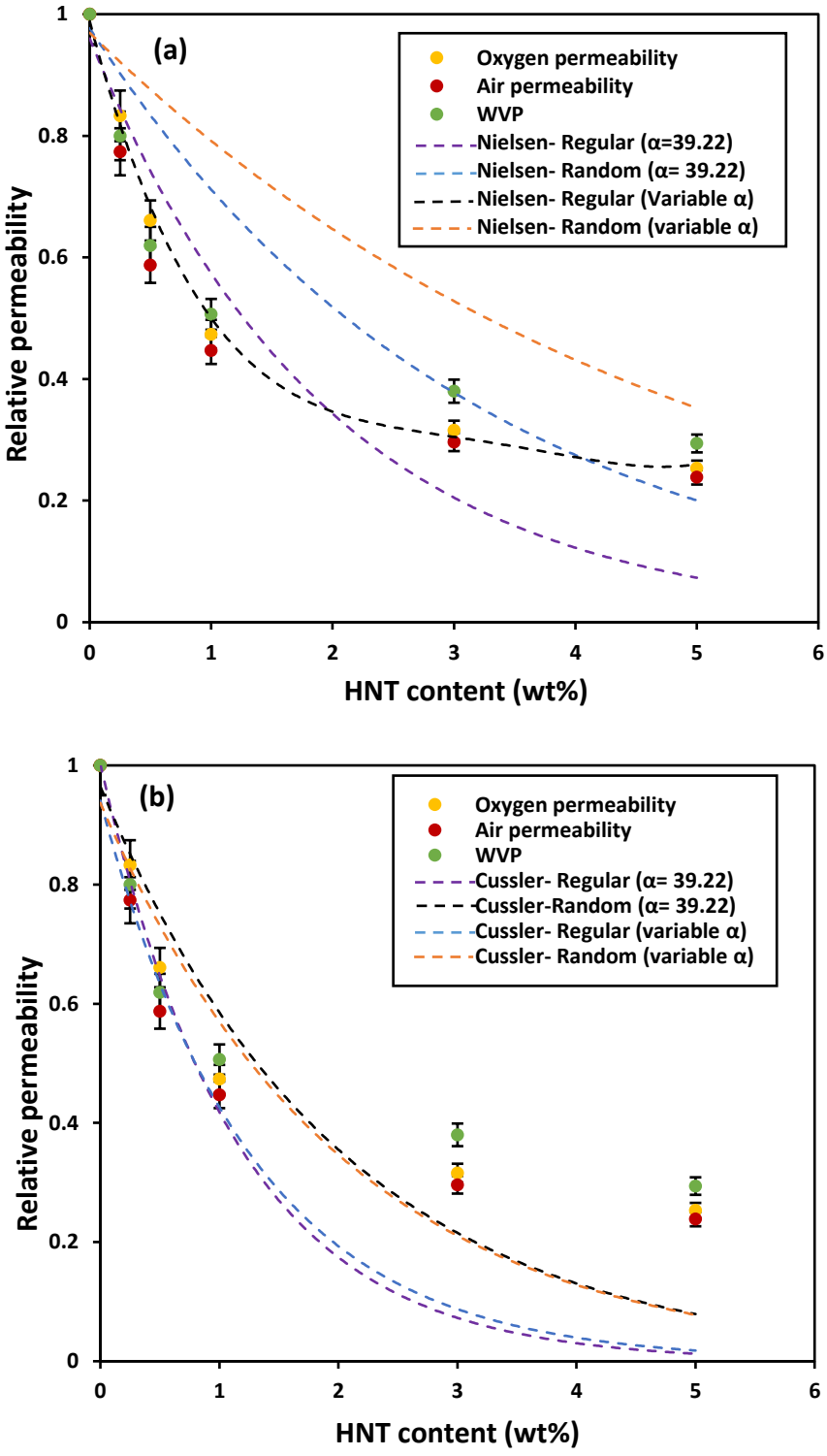


Figure 6-9. Prediction of relative permeabilities of bionanocomposites using (a) Nielsen model and (b) Cussler model

Table 6-3. Data comparison between experimental and theoretical permeabilities based on Nielsen models for regular and random dispersion

| WVP | | | | | | | | | |
|---|---|---|---|---|---|---|---|---|---|
| **HNTs (wt%)** | **Experimental WVP** | **Regular, α=39.22** | **Error %** | **Regular, variable α** | **Error %** | **Random, α=39.22** | **Error %** | **Random, variable α** | **Error %** |
| 0 | 1 | 1 | 0 | 1 | 0 | 1 | 0 | 1 | 0 |
| 0.25 | 0.79 | 0.78 | 2.01 | 0.78 | 2.14 | 0.90 | 11.91 | 0.90 | 11.91 |
| 0.5 | 0.61 | 0.63 | 3.08 | 0.71 | 13.38 | 0.82 | 25.29 | 0.86 | 28.73 |
| 1 | 0.50 | 0.45 | 11.29 | 0.49 | 2.71 | 0.69 | 27.24 | 0.78 | 35.49 |
| 3 | 0.38 | 0.17 | 113.48 | 0.30 | 24.59 | 0.37 | 2.15 | 0.52 | 27.48 |
| 5 | 0.29 | 0.08 | 245.88 | 0.26 | 13.07 | 0.20 | 44.82 | 0.35 | 17.18 |
| **Air permeability** | | | | | | | | | |
| **HNTs (wt%)** | **Experimental** | **Regular, α=39.22** | **Error %** | **Regular, variable α** | **Error %** | **Random, α=39.22** | **Error %** | **Random, variable α** | **Error %** |
| 0 | 1 | 1 | 0 | 1 | 0 | 1 | 0 | 1 | 0 |
| 0.25 | 0.77 | 0.78 | 1.31 | 0.78 | 1.18 | 0.90 | 14.79 | 0.90 | 14.79 |
| 0.5 | 0.58 | 0.63 | 8.05 | 0.71 | 17.83 | 0.82 | 29.13 | 0.86 | 32.39 |
| 1 | 0.44 | 0.45 | 1.73 | 0.49 | 9.31 | 0.69 | 35.76 | 0.78 | 43.04 |
| 3 | 0.29 | 0.17 | 66.40 | 0.30 | 2.88 | 0.37 | 20.37 | 0.52 | 43.47 |

| | | | | | | | | | |
|---|---|---|---|---|---|---|---|---|---|
| 5 | 0.23 | 0.08 | 180.47 | 0.26 | 8.30 | 0.20 | 17.43 | 0.35 | 32.84 |

**Oxygen permeability**

| HNTs (wt%) | Experimental | Regular, α=39.22 | Error % | Regular, variable α | Error % | Random, α=39.22 | Error % | Random, variable α | Error % |
|---|---|---|---|---|---|---|---|---|---|
| 0 | 1 | 1 | 0 | 1 | 0 | 1 | 0 | 1 | 0 |
| 0.25 | 0.83 | 0.78 | 6.22 | 0.78 | 6.36 | 0.90 | 8.28 | 0.90 | 8.28 |
| 0.5 | 0.66 | 0.63 | 3.39 | 0.71 | 7.59 | 0.82 | 20.30 | 0.86 | 23.97 |
| 1 | 0.47 | 0.45 | 4.10 | 0.49 | 3.91 | 0.69 | 31.93 | 0.78 | 39.65 |
| 3 | 0.31 | 0.17 | 77.35 | 0.30 | 3.50 | 0.37 | 15.13 | 0.52 | 39.75 |
| 5 | 0.25 | 0.08 | 197.78 | 0.26 | 2.64 | 0.20 | 24.68 | 0.35 | 28.69 |

Table 6-4. Data comparison between experimental and theoretical permeabilities based on Cussler models for regular and random dispersion

| WVP | | | | | | | | | |
|---|---|---|---|---|---|---|---|---|---|
| **HNTs (wt%)** | **Experimental** | **Regular, α=39.22** | **Error %** | **Regular, variable α** | **Error %** | **Random, α=39.22** | **Error %** | **Random, variable α** | **Error %** |
| 0 | 1 | 1 | 0 | 1 | 0 | 1 | 0 | 1 | 0 |
| 0.25 | 0.79 | 0.92 | 13.44 | 0.82 | 2.93 | 0.71 | 11.39 | 0.71 | 11.54 |
| 0.5 | 0.61 | 0.76 | 18.83 | 0.59 | 4.78 | 0.53 | 15.75 | 0.63 | 2.00 |
| 1 | 0.50 | 0.43 | 15.61 | 0.42 | 19.15 | 0.32 | 57.75 | 0.47 | 6.61 |
| 3 | 0.38 | 0.05 | 555.17 | 0.21 | 77.57 | 0.07 | 435.21 | 0.18 | 108.79 |
| 5 | 0.29 | 0.01 | 2000.0 | 0.08 | 237.93 | 0.02 | 1236.36 | 0.09 | 226.66 |
| **Air permeability** | | | | | | | | | |
| **HNTs (wt%)** | **Experimental** | **Regular, α=39.22** | **Error %** | **Regular, variable α** | **Error %** | **Random, α=39.22** | **Error %** | **Random, variable α** | **Error %** |
| 0 | 1 | 1 | 0 | 1 | 0 | 1 | 0 | 1 | 0 |
| 0.25 | 0.77 | 0.92 | 16.26 | 0.82 | 6.10 | 0.71 | 7.75 | 0.71 | 7.90 |
| 0.5 | 0.58 | 0.76 | 23.00 | 0.59 | 0.59 | 0.53 | 9.81 | 0.63 | 7.04 |
| 1 | 0.44 | 0.43 | 2.07 | 0.42 | 5.2 | 0.32 | 39.28 | 0.47 | 5.87 |

| | | | | | | | | | |
|---|---|---|---|---|---|---|---|---|---|
| 3 | 0.29 | 0.05 | 410.68 | 0.21 | 38.41 | 0.07 | 317.18 | 0.18 | 62.74 |
| 5 | 0.23 | 0.01 | 1602.85 | 0.08 | 174.02 | 0.02 | 983.63 | 0.09 | 164.88 |

**Oxygen permeability**

| **HNTs (wt%)** | **Experimental** | **Regular, α=39.22** | **Error %** | **Regular, variable α** | **Error %** | **Random, α=39.22** | **Error %** | **Random, variable α** | **Error %** |
|---|---|---|---|---|---|---|---|---|---|
| 0 | 1 | 1 | 0 | 1 | 0 | 1 | 0 | 1 | 0 |
| 0.25 | 0.83 | 0.92 | 9.87 | 0.82 | 1.06 | 0.71 | 15.98 | 0.71 | 16.72 |
| 0.5 | 0.66 | 0.76 | 13.40 | 0.59 | 11.79 | 0.53 | 23.49 | 0.63 | 33.93 |
| 1 | 0.47 | 0.43 | 8.15 | 0.42 | 11.45 | 0.32 | 47.57 | 0.47 | 52.63 |
| 3 | 0.31 | 0.05 | 444.31 | 0.21 | 47.52 | 0.07 | 344.64 | 0.18 | 68.43 |
| 5 | 0.25 | 0.01 | 1707.97 | 0.08 | 190.93 | 0.02 | 1050.53 | 0.09 | 74.68 |

## 6.5 Summary

Barrier properties in term of water vapour and gas permeabilities played an important role in the selection of nanocomposite systems for food packaging applications. Neat PVA as a typical water-soluble polymer possessed good gas barrier properties and poor water resistance. Furthermore, the addition of GL slightly reduced the *WVTR* and *WVP* owing to the consumption of some free hydroxyl groups through the hydrogen bonding. Clearly, the increases in both *WVTR* and *WVP* were reported for PVA/ST blends due to the hydrophilic characteristic of ST. It was worth mentioning that *WVTR* and *WVP* of PVA/ST/GL blends were ranging between those of PVA/GL blends and PVA/ST blends. On the other hand, a significant reduction in *WVTR* and *WVP* was observed for PVA/ST/GL/HNT bionanocomposites, which was ascribed to the inclusion of HNTs with moderate hydrophobicity to restrict the diffusion of water molecules. Increasing the temperature from 25 to 55ºC at 50% RH caused the increases in *WVTR* and *WVP* of neat PVA and PVA blends due to the chain mobility of polymeric molecules tended to be improved resulting in better diffusion of water molecules. On the other hand, bionanocomposite films became less sensitive to the increasing temperature according to Arrhenius relationship associated with the reduction of mass and heat transfer in the presence of HNTs. A similar increasing trend was clearly demonstrated as well in *WVTR* and *WVP* with increasing the ΔRH from 10 to 70% because the ΔRH was deemed as the driving force in the permeation process despite being less influential to bionanocomposite films as compared to blend matrices. A similar trend was reported for air and oxygen permeabilities with the clear reduction in gas permeability in the presence of HNTs due to a remarkable increase in tortuosity factor when incorporated with HNTs in bionanocomposite films. The experimental data of bionanocomposite permeabilities had the best agreement with

Nielsen model for regular dispersion of HNTs with variable aspect ratios. Whereas, Cussler model for regular and random dispersions of nanofillers can also fit the experimental data at HNT contents of 0-1 wt%.

# Chapter 7: Component Migration of PVA/ST/GL/HNT Bionanocomposite Films and Their Application as a Food Packaging Material

## 7.1 Introduction

When nanocomposite films start to be in contact with foodstuffs, the migration rate of constituents in bionanocomposite films should be considered. The migration process can be simply defined as the mass transfer of low-molecular-weight molecules from packaging materials to packaged products like foodstuffs (Huang, Li and Zhou 2015; Arvanitoyannis and Bosnea 2004). The migrated molecules may be plasticisers, nanofillers and other additives like surfactants (Arvanitoyannis and Bosnea 2004; Huang, Li and Zhou 2015). Furthermore, the migration rates of these molecules are deemed as a function of their molecular weight, concentration, solubility and diffusivity as well as other circumstance conditions like pH level, temperature and contact time between packaging materials and packaged products (Avella et al. 2005; Huang, Li and Zhou 2015). Migration process can be considered as a diffusion process according to Fick's second law (Souza and Fernando 2016). The European Commission Regulation (EU) No. 10/2011 (2011) specified the safety limits for the migrated molecules should not exceed the overall migration limit (OML) of 60 mg/kg onto foodstuffs, which is equivalent of 10 mg/dm$^2$ of packaging materials. Moreover, the European Commission Regulation (EU) No. 10/2011 (2011) had also specific limits for some elements like barium, copper, cobalt, iron, lithium, manganese and

zinc. Consequently, the migration process in term of overall migration rates and HNT migration rates was studied in this chapter, and their results can be implemented to utilise bionanocomposite films as food packaging materials.

## 7.2 Overall migration rate

The overall migration rates of PVA/ST/GL blends and their corresponding bionanocomposite films at different HNT contents were evaluated in three food simulants, as illustrated in Figure 7-1. These food simulants, including a 10% ethanol solution (simulant A), a 3% acidic acid solution (simulant B) at the pH level below 4.5 and a 50% ethanol solution (simulant D1), were selected to mimic hydrophilic, acidic and lipophilic foodstuffs, respectively. It can be clearly seen from Figure 7-1 that PVA/ST/GL blends and their bionanocomposite films had higher migration rates in food simulant A compared with other food simulants due to the hydrophilic nature of films constituents. The overall migration rate of these films exceeded the overall migration limits (OML) of 60 mg/kg ( European Commission Regulation (EU) No. 10/2011) in food simulant A except bionanocomposite films reinforced with 1 and 3 wt% HNTs. This behaviour could be interpreted depending on water solubility characteristics of blend matrices and their bionanocomposite films. In other words, PVA and ST are water soluble polymers and their blends have high solubility rates in hydrophilic media such as food simulant A. Furthermore, this solubility of polymer blends diminished in the presence of hydrophobic nanofillers like HNTs, which was reflected by the reduction in the overall migration rate of bionanocomposite films at different HNT contents in comparison with those of polymer blends (see Chapter 5, section 5.2). Moreover, the strong interfacial bonding between blend matrices and HNTs was another reason to reduce mass transfer when these films contacted

hydrophilic media. Consequently, remarkable reductions in overall migration rate by 47.41 and 45.85% were reported for PAV/ST/GL/HNT bionanocomposite films at the HNT contents of 1 and 3 wt%, respectively, as compared with that of blend matrices in food simulant A. When HNT contents increased up to 5 wt%, the overall migration rate of bionanocomposite films was increased by 30.97% as well due to the HNT agglomeration issue despite being still lower than those of blend matrices and bionanocomposite films reinforced with 0.25 and 0.5 wt% HNTs. Similar results were also reported by Cano et al. (2015b) based on PVA/ST/CNC nanocomposite films.

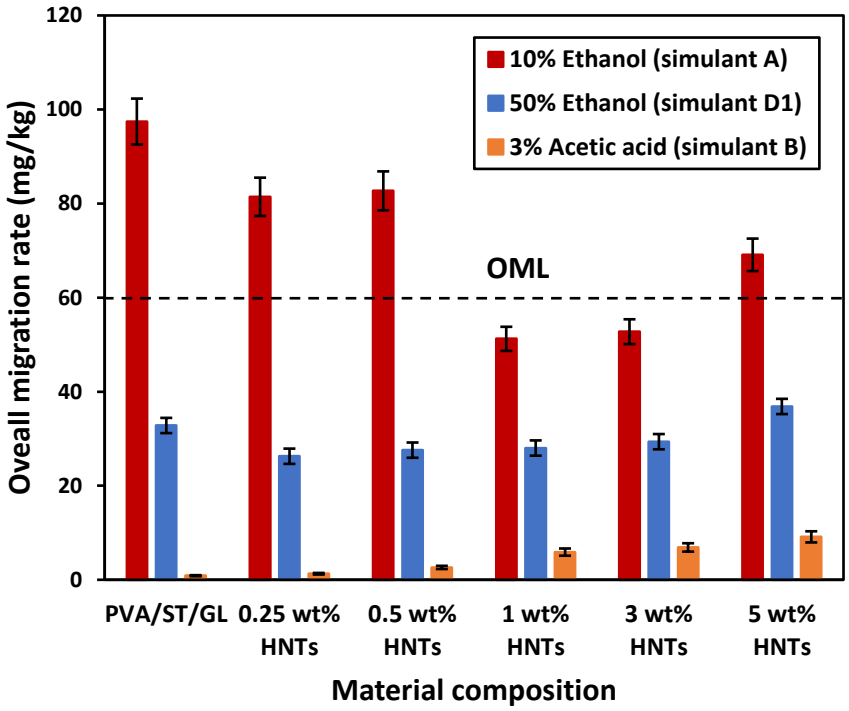


Figure 7-1. Overall migration rates of PVA/ST/GL blends and their corresponding bionanocomposite films at different HNT contents in three different food simulants

A completely different trend was observed in food simulant D1. The overall migration rate of PVA/ST/GL blends and their bionanocomposite films were lower than the OML of 60 mg/kg. A clear reduction in overall migration rate was reported for bionanocomposite films at HNT contents in range of 0.25-3 wt% as opposed to that of

corresponding blends. In particular, the maximum reduction was found to be 19.93% with the inclusion of 0.25 wt% HNTs in bionanocomposites.

The lowest overall migration rates of PVA/ST/GL blends and their bionanocomposite films were reported in food simulant B. Such a trend reflected the limited interactions between material films and acidic media like food simulant B. The overall migration rates were increased in a linear manner from 1.29 to 9.13 mg/kg with increasing the HNT content from 0 to 5 wt%. In short, the overall migration rates of blends and corresponding bionanocomposite films highly depended on the selection of food simulants. In other words, these films could be highly affected by hydrophilic foodstuffs, which was followed by lipidic foodstuffs along with the least impact by acidic foodstuffs. These overall lower rates of migration in lipidic and acidic foodstuffs could be associated with the good resistance of PVA to oil, grease, and solvents relative to the lower resistance of water.

### 7.3 HNT migration rate

The presence of $Al^+$ and $Si^+$ in migrated molecules was used to evaluate the migration rate of HNTs because of their chemical structure of $Al_2Si_2O_5(OH)_4.nH_2O$ (Khoo, Ismail and Ariffin 2011). Consequently, the migration rates of $Al^+$ and $Si^+$ from PVA/ST/GL blends and their bionanocomposite films at different HNT contents were depicted in Figure 7-2 (a) and (b), respectively. The migrated molecules from blend matrices did not show any traces of $Al^+$ and $Si^+$, which meant that the migrated molecules shown in the overall migration rate results completely reflected the quantities of migrated polymeric molecules in three different food simulants. The migration rate of $Al^+$ and $Si^+$ based on bionanocomposite films agreed with the overall migration rates in different food simulants (see Figure 7-1). In other words, higher

quantities of $Al^+$ and $Si^+$ were found in food simulant A, followed by food simulant D1 and finally food simulant B. This trend could be interpreted based on the hydrophilic nature of food simulant A, which worked as a plasticiser and solvent concurrently leading to the improvement of chain mobility of polymeric molecules and easy release of nanofillers from bionanocomposite films, respectively. Similar behaviour was observed by Lee, Kim and Park (2018) based on chitosan/clove essential oil (CEO)/HNT nanocomposite films. Their results showed that the release rate of CEO in lipidic food simulant was faster than those of hydrophilic and acidic food simulants in that food simulant molecules with oily nature diffused into the structures of nanocomposite films leading to weak bonding networks between constituents and easy release of active agents from film structures with similar nature. On the other hand, the migration rates of $Al^+$ and $Si^+$ were increased linearly with increasing the HNT content regardless of food simulants. For instance, the migration rates of $Al^+$ and $Si^+$ were increased by 766.67 and 424.82%, respectively with increasing the HNT content from 0 to 5 wt% in food simulant A. A similar increasing trend was reported in food simulant D1 by 381.82 and 202.87% for $Al^+$ and $Si^+$ as well as 162.79 and 290.38% in food simulant B, respectively. It was evident that the lower quantities of migrated $Al^+$ and $Si^+$ were detected in food simulant B due to weak interactions between bionanocomposite films and acidic media, which was in good accordance with the overall migration results mentioned earlier based on the dual sorption theory (Farhoodi et al. 2014; Huang et al. 2011). Because the *diffusion* process of food simulant molecules within bionanocomposite films took place at the faster pace than *embedding* process of intermolecular forces between penetrant molecules and bionanocomposite films, intermolecular spaces of polymeric chains as well as the release of HNTs from bionanocomposite films were improved. Apparently, the

diffusion of food simulant molecules within material films played an important role in the control of migration rates. In other words, the diffusion process of food simulant molecules would be faster when the material films and food simulants have the same characteristic (for example, both are hydrophilic materials) leading to increasing the release rate of active agents from the film materials.

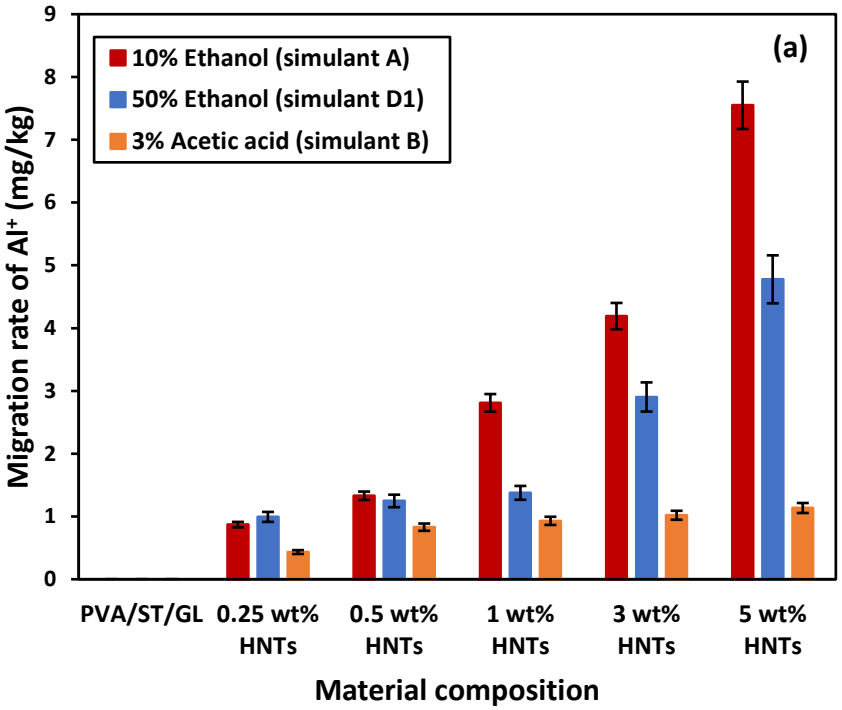

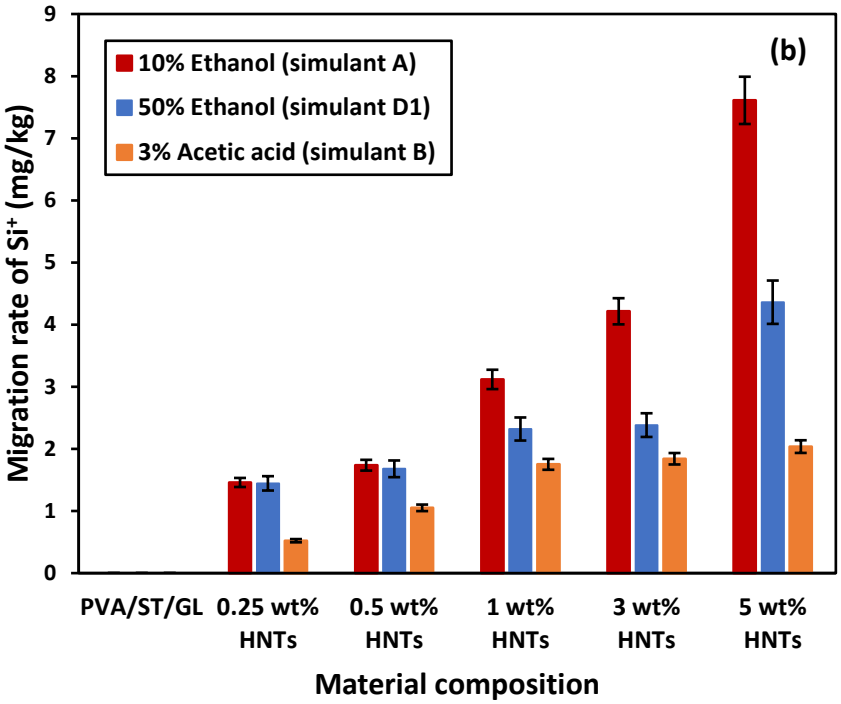


Figure 7-2. Migration rate of (a) $Al^+$ and (b) $Si^+$ from PVA/ST/GL blends and their bionanocomposite films at different HNT contents in three different food simulants

Unfortunately, there are no specific migration limits for $Al^+$ and $Si^+$ determined by the European Union Commission Regulation (EU) No 10/2011 (2011) for comparison purpose. However, HNTs as natural nanofillers are generally classified as a nontoxic, biocompatible and EPA-4A material (Kamble et al. 2012; Kryuchkova et al. 2016; Lvov, DeVilliers and Fakhrullin 2016). Consequently, HNTs are well-recognised as a good nanofiller candidate for several biomedical applications such as drug delivery for non-injectable drug formula, dentist resin, bone cement, tissue scaffolds and cosmetics (Lvov, DeVilliers and Fakhrullin 2016; Kamble et al. 2012; Fizir et al. 2018). The toxicity of HNTs has been studied over decades for *in-vitro* and *in-vivo* tests. Some of these studies showed that HNTs did not possess the toxicity up to 75 µg/mL while 90% of tested cells were still viable (Fizir et al. 2018; Santos et al. 2018; Vergaro et al. 2010). This safe concentration of HNTs was extended to 100 µg/mL based on other studies (Lvov, DeVilliers and Fakhrullin 2016), then further increased up to 200

μg/mL (Guo et al. 2012). When comparing the migrated rates of HNTs from PVA/ST/GL/HNT bionanocomposite films with these safe concentrations (based on part per million as a comparison scale), these migrated rates still remained within the safe limit without any toxic effect on human bodies.

It was clearly observed from Figure 7-2 (a) and (b) that there were no great differences between the migrated quantities of $Al^+$ and $Si^+$ for each of food simulant type due to similar element contents of Al (20.90%) and Si (21.76%) in as-received HNTs (Mousa, Dong and Davies 2016). Moreover, the agglomeration issue of HNTs at their content of 5 wt% clearly increased the migration rates of $Al^+$ and $Si^+$ due to the poor interfacial bonding between HNTs and blend matrices, which improved the releasing process of HNTs at high content levels from their films when compared with that at low HNT contents (see Figure 7-3).

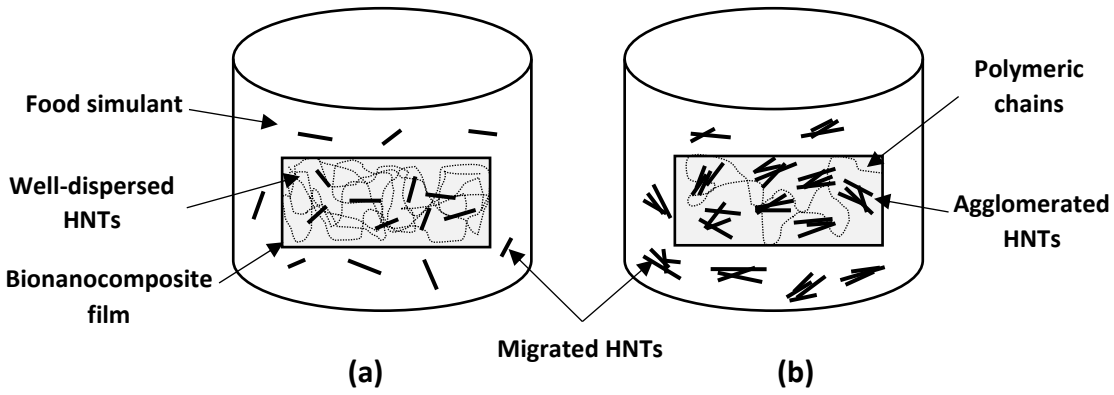


Figure 7-3. Schematic diagram of released HNTs from PVA/ST/GL/HNT bionanocomposite films in a typical food simulant based on (a) well-dispersed HNTs at low nanofiller contents and (b) agglomerated HNTs at high nanofiller contents

## 7.4 Food packaging tests

Based on migration rate results, PVA/ST/GL/HNT bionanocomposite films could be used as packaging materials for lipidic and acidic foodstuffs. Consequently, fresh cut avocados with a lipid content of 20% (≈18.7/100 g) (Seymour and Tucker 1993) and peaches with pH level ≤ 3.5 (Brady 1993) were selected to mimic lipidic and acidic foodstuffs, respectively. The weight loss rate of controlled avocados and peaches as well as packaged fruits in neat PVA, PVA/ST/GL blends and their corresponding bionanocomposite films reinforced with 1 wt% HNTs were summarised in Figure 7-4 (a) and (b), respectively. Packaged fruits with bionanocomposite films showed much lower rates of weight loss as opposed to those packaged with neat PVA and PVA blends due to lower water and gas permeabilities of bionanocomposite films as opposed to neat PVA and blends counterparts (see Chapter 6). Avocados and peaches packaged with bionanocomposite films had the weight losses of 25.24 and 18.05%, respectively in contrast to 35.15 and 25.93% for those packaged with PVA/ST/GL blends. Loryuenyong et al. (2015) concluded the similar results based on less fruits contact with air and oxygen due to enhanced barrier properties leading to the inhibition of the production and action of ethylene, which played an important role during the fruit ripening process. Moreover, fruits packaged with neat PVA showed lower weight loss rate than that of PVA/ST/GL blends due to the former's lower gas permeability. Nonetheless, the weight loss rate of fruits packaged with PVA/ST/GL blends appeared to be still better than those of controlled samples.

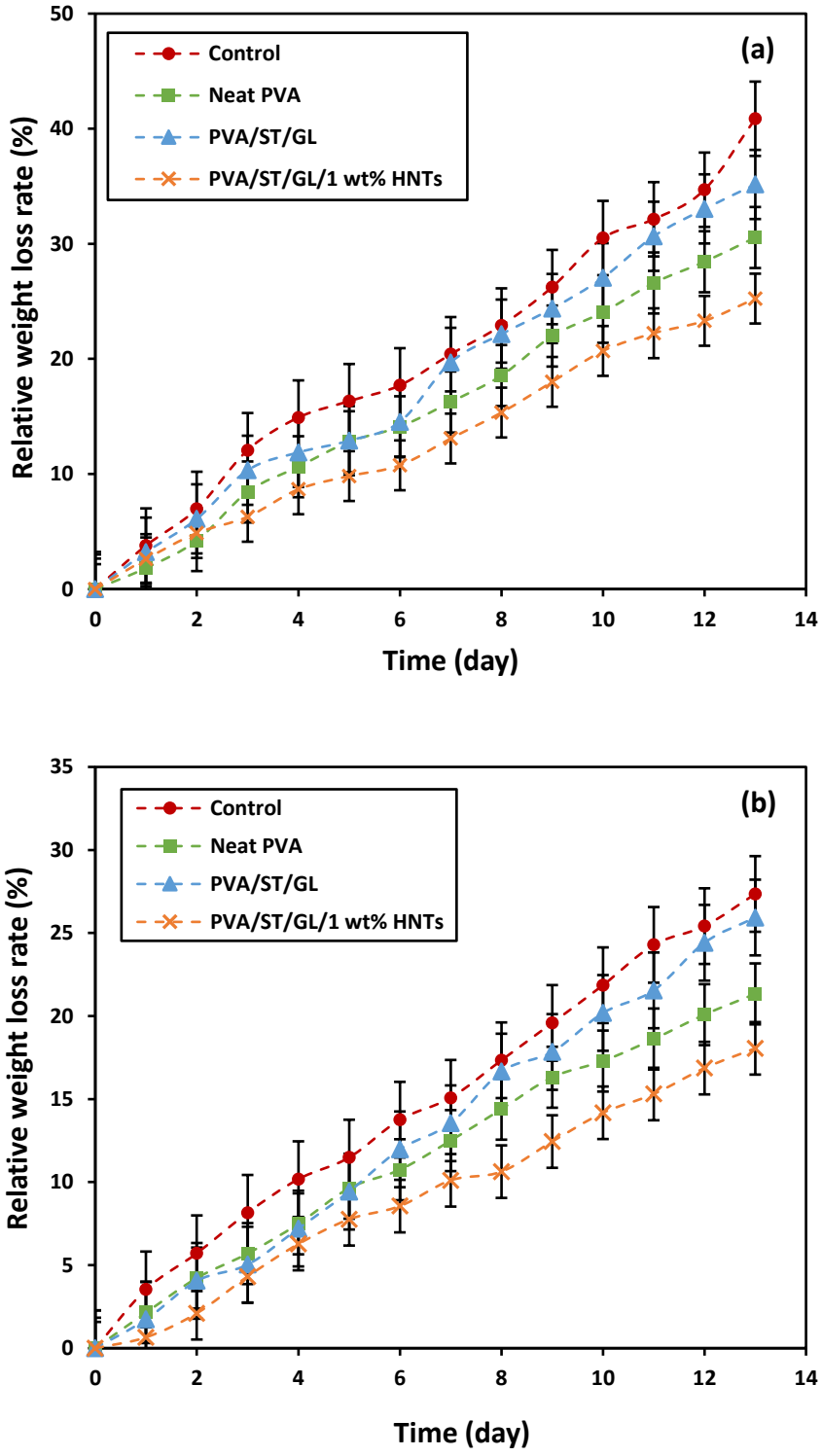


Figure 7-4. Weight losses of (a) avocados and (b) peaches versus storage time for different packaging materials

Moreover, fungi were found to grow on the external surfaces of avocados-controlled and peaches-controlled samples due to suitable environmental conditions of oxygen

availability and humidity level. Whereas, lower gas and water permeabilities were main reasons to restrict the fungi growth on packaged fruits, as shown in Figure 7-5. On the other hand, fruits packaged with bionanocomposite films gave rise to lower colour changes with the extended shelf life in contrast to those packaged with PVA/ST/GL blends. Accordingly, the improvement of barrier properties of PVA/ST/GL/HNT bionanocomposite films were more pronounced for the extension of fruit shelf life relative to that of PVA/ST/GL blends.

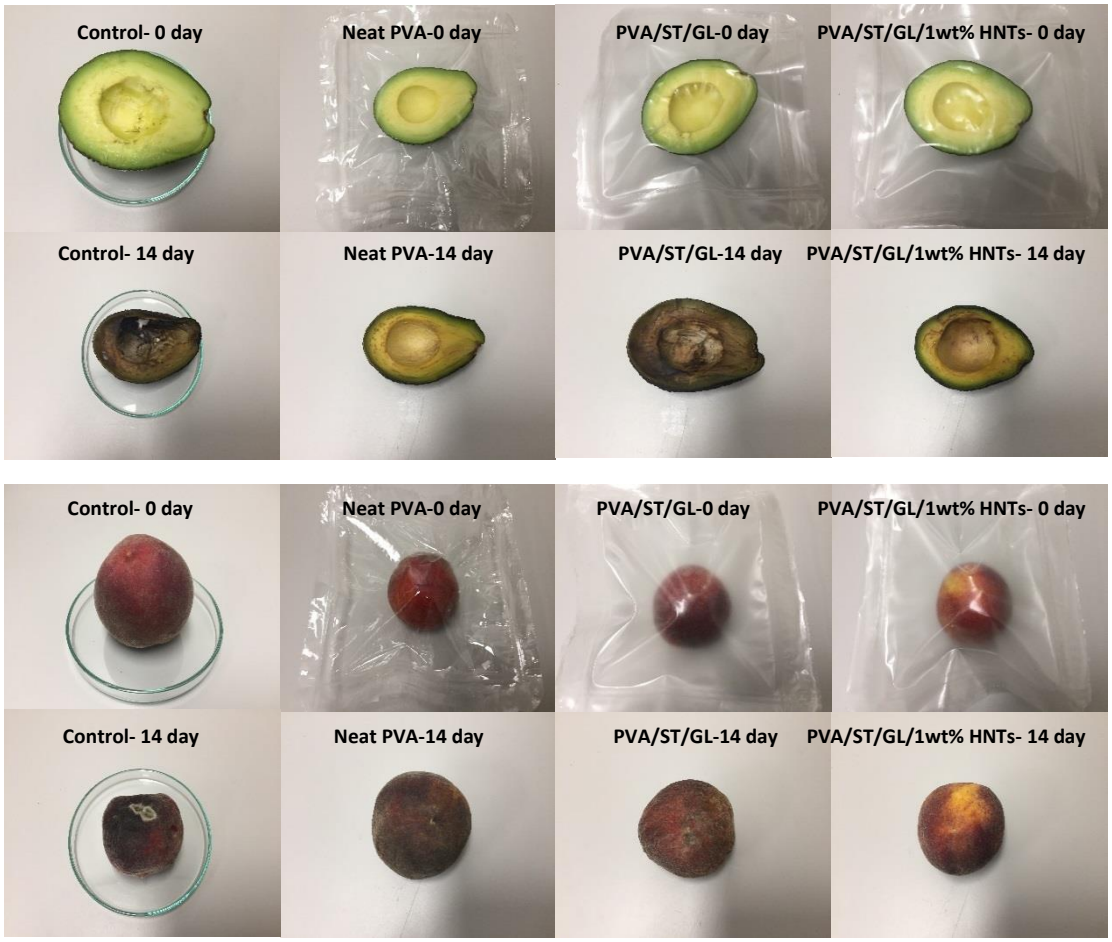


Figure 7-5. External appearance of (a) avocados and (b) peaches before and after packaging tests with different packaging materials

## 7.5 Summary

The migration of material constituents to the foodstuffs should be evaluated when considered as food packaging materials. Three different food simulant solutions of

10% ethanol (simulant A), 50% ethanol (simulant D1) and 3% acidic acid (simulant B) were used to study the overall migration rates as well as the migration rates of HNTs. For food simulant A, the overall migration rates of PVA/ST/GL blends and their bionanocomposite films, except those with the inclusion of 1 and 3 w% HNTs, exceeded the OML (60 mg/kg) due to the hydrophilic nature of food simulant A with better solubility of films. Whereas, the lower overall migration rates of PVA/ST/GL blends and corresponding bionanocomposite films were recorded in food simulant B though these migration rates were increased with increasing the HNT content, possibly resulting from poor interactions between material films and acidic foodstuffs. Moreover, the presence of HNTs reduced the overall migration rates of bionanocomposite films as compared with PVA/ST/GL blends in food simulant D1 despite being slightly increased at the HNT content of 5 wt%.

The quantities of $Al^+$ and $Si^+$ detected in migrated molecules were considered as an indicator for the migration rates of HNTs. The migration rates of HNTs were increased linearly with increasing the HNT content in three different food simulants due to the agglomeration issue of HNTs. This finding arose from weak interfacial bonding between blend matrices and nanofillers to assist in the release of HNTs from blend matrices. The migration rates of $Al^+$ and $Si^+$ had a similar trend to overall migration rates. In other words, the higher migration rates of $Al^+$ and $Si^+$ were reported in food simulant A resulting from the solubility of material films in hydrophilic media, which was followed by food simulant D1 and then food simulant B due to the limited interactions with material films.

Based on migration test results, PVA/ST/GL/HNT bionanocomposite films were more applicable as the packaging materials for lipidic and acidic foodstuffs. Neat PVA, PVA/ST/GL blend and bionanocomposite films reinforced with 1 wt% HNTs were

used to pack fresh cut avocados and peaches to mimic lipidic and acidic foodstuffs, respectively. The weight loss rates of packaged fruits with bionanocomposite films appeared to be lower than those of controlled fruits, and fruits packaged with neat PVA and PVA/ST/GL blends. This phenomenon could be interpreted by the improved barrier properties of bionanocomposite films with the incorporation of HNTs as opposed to those of neat PVA and PVA/ST/GL blends to restrict the effect of ethylene in the ripening process. Moreover, there was no noticeable fungi growth on the packed fruit surfaces as compared with controlled sample despite the change of colours, which was indicative of the improvement for fruit shelf life.

# Chapter 8: Conclusions and Future Work

## 8.1 Conclusions

In this work, novel PVA/ST/GL/HNT bionanocomposite films at HNT contents of 0.25, 0.5, 1, 3 and 5 wt% were manufactured via solution casting for sustainable food packaging applications. PVA as a water-soluble polymer was selected in this work based on its good mechanical and thermal properties as well as good oxygen barrier properties despite limited flexibility and biodegradability in some environments like soil as well as poor water barrier properties. Consequently, PVA was blended with GL and ST to improve its flexibility and biodegradability, respectively, then such blends were reinforced with HNTs to further enhance their barrier properties. Morphological structures of as-received HNTs, neat PVA, PVA blends (i.e., PVA/GL, PAV/ST and PVA/ST/GL) and PVA/ST/GL/HNT bionanocomposite films were studied by means of SEM and AFM. Moreover, mechanical, thermal and optical properties, biodegradability, water resistance as well as water and gas barrier properties were evaluated for all material films. The overall migration rates and migration rates of HNTs from bionanocomposite films were investigated when the materials came in contact with three different food simulants. The real application of PVA/ST/GL/1 wt% HNT bionanocomposite films as a food packaging material was carried out by using lipidic and acidic fruits compared with control fruits, as well as packaged fruits with neat PVA and PVA/ST/GL blends. The following conclusions can be drawn from this work:

- The tubular structures of as-received HNTs were clearly observed with the aspect ratio of 39.22. The aspect ratios of embedded HNTs within bionanocomposite

films were decreased from 39.27 to 14.87 with increasing HNT content from 0.25 to 5 wt%, respectively due to HNT agglomeration issue. Whereas, surface roughness of bionanocomposite films increased from 13.83 to 76.80 nm with increasing the HNT content from 0 to 5 wt%, respectively for the same aforementioned reason.

- The fracture surfaces of neat PVA were smooth and brittle as compared with those of PVA/GL blends that appeared to be more ductile due to the GL plasticisation effect. As compared with PVA/ST blends, PVA/ST/GL blends showed lower brittleness in spite of inherent brittleness of ST due to the presence of GL by improving the compatibility between material components. Moreover, good HNT dispersion was manifested for bionanocomposite films at the HNT contents between 0.25 and 1 wt% while apparent HNT agglomeration could be detected with the inclusion of 3 and 5 wt% HNTs.
- Slight intercalation structures became dominant in bionanocomposite films, as reflected by XRD spectra associated with the slight increases in *d*-spacing values. These results were confirmed with new FTIR peaks assigned at 1650 and 1417 $cm^{-1}$ relating to intercalated HNTs within blend matrices in bionanocomposites with water bonding and $CH_2$ stretching, respectively.
- Blending PVA with GL reduced tensile strength and Young's modulus by 77.95 and 96.5%, respectively, as well as increased elongation at break by 321.09% when compared with those of neat PVA counterparts Such phenomena could be attributed to the mobility enhancement of polymeric chains in the presence of a plasticiser. On the other hand, blending PVA with ST decreased tensile strength

and elongation at break by 28.32 and 51.66%, respectively while Young's modulus was increased by 52.68% as compared with those of neat PVA resulting from inherent brittleness and toughness of ST. Moreover, PVA/ST/GL blends possessed higher tensile strength and Young's modulus than those of PVA/GL blends by 4.0 and 119.67%, respectively as well as higher elongation at break than that of PVA/ST blends by 411.73%.

- The incorporation of 0.25 and 0.5 wt% HNTs improved the tensile strength of PVA/ST/GL/HNT bionanocomposite films by 20.0 and 3.4%, respectively compared with that of corresponding blends alone. These improvements declined beyond 1 wt% HNT due to typical HNT agglomeration issue. Similarly, Young's modulus was increased by 148.97% with increasing the HNT content up to 1 wt% resulting from higher toughness of HNTs though Young's modulus of bionanocomposites diminished with the inclusion of 3 and 5 wt% HNTs associated with HNT agglomeration. Although the elongation at break of bionanocomposite films decreased linearly with increasing the HNT content because of the enhanced stiffness of bionanocomposite films, it appeared to be still better than that of neat PVA.
- As compared with those of neat PVA, the decomposition temperatures $T_{5\%}$, $T_{50\%}$ and $T_{90\%}$ of PVA/GL blend were decreased by 104.7, 32.8 and 7.8ºC, which reflected lower thermal stability of PVA/GL blends resulting from the penetration of plasticiser molecules between those of polymeric chains leading to weak inter- and intramolecular bonding. Whereas, the $T_{50\%}$ and $T_{90\%}$ of PVA/ST blends were increased by 44.2 and 57.8ºC, respectively leading to much better thermal stability

as opposed to that of neat PVA. Moreover, PVA/ST/GL blends possessed moderate thermal stability between those of PVA/ST and PVA/GL blends.

- Thermal stability of PVA/ST/GL blends improved with the incorporation of HNTs up to 1 wt% by increasing the $T_{5\%}$, $T_{50\%}$ and $T_{90\%}$ of bionanocomposites by 20.5, 8.7 and 8.5ºC, respectively due to inherent barrier action of HNTs against heat and mass transfer. Although the thermal stability of bionanocomposite films when reinforced with 3 and 5 wt% HNTs declined due to the agglomeration of nanofillers, they were still better than that of PVA/ST/GL blends.
- PVA/GL blends had lower $T_g$ and $T_m$ by 23.0 and 15.6ºC, respectively when compared with those of neat PVA due to GL plasticisation effect. Whereas, the $T_g$ and $T_m$ of PVA/ST blends were increased by 3.4 and 43.7ºC, respectively as opposed to those of neat PVA. Further improvements were achieved in $T_g$ and $T_m$ of bionanocomposite films by 10.0 and 10.3ºC, respectively with incorporation of 1 wt% HNTs owing to good interfacial bonding between blend matrices and well-dispersed HNTs at lower nanofiller contents.
- Neat PVA had the light transmittance (*T%*) of 99.40% at 550 nm (in a mid-visible wavelength range). This *T%* was decreased to 96.64, 96.94 and 96.01% for PVA/GL, PVA/ST and PVA/ST/GL blends, respectively, owing to the change in compatibility and crystallinity of blends. The further reduction in *T%* was reported for bionanocomposite films due to increasing the surface roughness leading to more generated light scattering sites on the surfaces.
- Blending PVA with GL slightly reduced $W_a$ and $W_s$ by 10.21 and 8.21%, respectively due to the consumption of some of free hydroxyl groups in the blends.

Whereas, blending PVA with ST provided many free hydroxyl groups because of the partial compatibility in the absence of plasticiser leading to increasing $W_a$ and $W_s$ of PVA/ST blends by 30.08 and 4.69%, respectively as compared with those of neat PVA. Further, $W_a$ and $W_s$ of PVA/ST/GL blends dropped by 23.92 and 14.89%, respectively as opposed to those of PVA/ST blends resulting from the addition of GL. $W_a$ and $W_s$ were further reduced by 44.24 and 48.05%, respectively, which was achieved with the incorporation of HNTs resulting from moderate hydrophobicity of nanofillers with a low number of hydroxyl groups. This reduction was less pronounced beyond 1 wt% HNTs due to their agglomeration to deteriorate morphological structures of bionanocomposites.

- The low water contact angle of neat PVA at 28.23º increased slightly by 0.33º with the addition of GL. Then, it dropped by 9.70º for PVA/ST blends compared with that of neat PVA counterparts, which was followed by a slight increase by 2.78º for PVA/ST/GL blends for the same aforementioned reason associated with the variations of $W_a$ and $W_s$. A remarkable increasing trend in water contact angle was observed by 21.36º for bionanocomposite films reinforced with 5 wt% HNTs as opposed to that of PVA/ST/GL blends. Bionanocomposite films were still within the hydrophilic material range though the improvement in water contact angles were evident owing to the hydrophilic nature of all material constituents.
- Neat PVA had limited biodegradation rate of 5.87% because it could not biodegrade in the soil. This biodegradation rate increased up to 23.33, 39.54 and 56.94% for PVA/GL, PVA/ST and PVA/ST/GL blends, respectively due to the presence of GL to facilitate the microorganism infiltration as well as the use of

completely biodegradable ST. A significant reduction in biodegradation rate up to 41.28% was reported for bionanocomposite films reinforced with 1 wt% HNTs due to the good dispersion of nanofillers in order to restrict the microorganism infiltration through the films. The slight improvement of biodegradation rate by 3.72 and 4.52%, respectively for bionanocomposite films when incorporated with 3 and 5 wt% HNTs, resulted from typical agglomeration of nanofillers.

- *WVTR* and *WVP* were increased by 7.08 and 16.72%, respectively for PVA/GL blends and 21.27 and 30.96%, respectively for PVA/ST blends as opposed to those of neat PVA due to the mobility enhancement of polymeric chains in the presence of GL leading to higher diffusivity of water molecules within films as well as the enhancement of hydrophilicity in the presence of ST. Relatively good hydrophobic nature of HNTs was the main reason behind the reduction of *WVTR* and *WVP* of bionanocomposite films by 52.34 and 73.59%, respectively as opposed to those of PVA/ST/GL blends.
- The *WVTR* and *WVP* of neat PVA, PVA blends and bionanocomposite films were increased with increasing the temperatures from 25 to 55ºC as well as ΔRH from 10 to 70% since higher temperature levels could lead to the enhancement of free polymeric volume and diffusivity of permeable molecules as well as the ΔRH that was considered as the driving force of the permeation process. The temperature effect on *WVP* became less pronounced for bionanocomposite films as opposed to PVA/ST/GL blends due to the high thermal stability of HNTs according to the Arrhenius equation. A clear linear relationship was achieved between *WVP* and ΔRH of bionanocomposite films to reflect the less dependence on RH levels.

- The addition of GL and ST increased oxygen permeabilities by 77.59 and 91.25%, respectively as well as the air permeabilities by 75.88 and 99.25% accordingly as opposed to those of neat PVA due to the GL plasticisation effect and partial compatibility with ST. Whereas, the tortuosity factor of bionanocomposite films was increased by 160% as opposed to that of PVA/ST/GL blends leading to the reductions in oxygen and air permeabilities of bionanocomposite films by 74.84 and 75.98%.
- Nielsen model for regular nanofillers dispersion showed good agreement with experimental data of water vapour and gases when accurately calculated aspect ratios of HNTs were implemented via AFM. Additionally, Cussler model for regular HNT dispersion was in good accordance with experimental data in relation to water vapour and gas permeabilities of bionanocomposite films with the inclusion of HNTs up to 1 wt%.
- The higher overall migration rates of PVA/ST/GL blends and corresponding bionanocomposite films were reported in hydrophilic food simulants, which exceeded the OML, followed by lipidic food simulants and then acidic food simulants due to the high solubility of materials in the hydrophilic media, However, a clear reduction in migration rates of bionanocomposites was manifested when compared with that of PVA/ST/GL blends. A similar trend was also observed in migration rates of $Al^{+}$ and $Si^{+}$ as the indicator of HNT migration. Moreover, the migration rates of $Al^{+}$ and $Si^{+}$ were increased with increasing the HNT content regardless of used food simulant type in this study.

- Fresh cut avocados and peaches fruits packaged with bionanocomposite films showed lower weight losses by 38.22 and 34.0%, respectively as opposed to that of controlled fruits. Furthermore, packaged avocados with bionanocomposite films showed lower weight losses by 17.35 and 28.19%, respectively compared with those fruits packaged with neat PVA and PVA/ST/GL blend films. On the other hand, a similar trend by 15.37 and 30.38% was also found when peaches were used, accordingly due to the lower water vapour and gas permeabilities of bionanocomposite films compared with other films.

## 8.2 Future work

Based on the results achieved in this study, several recommendations can be given for the future work on a similar bionanocomposite system targeting material packaging applications as follows:

- Studying the biodegradation rates of neat PVA, PVA blends and corresponding bionanocomposite films in other environments like compost and enzymes media, and then comparing these rates with the biodegradation rates in soil.
- Developing experimental and/or theoretical studies to establish the relationship between the migrated rates of nanofillers from PVA/ST/GL/HNT bionanocomposite films and their aspect ratios.
- Exploring the overall migration rates as well as the migration of HNTs from PVA/ST/GL/HNT bionanocomposite films in other conditions according to different temperature levels and storage time periods.

# References


Abbasi, Zahra. 2012. "Water Resistance, Weight Loss and Enzymatic Degradation of Blends Starch/Polyvinyl Alcohol Containing Sio2 Nanoparticle." *Journal of the Taiwan Institute of Chemical Engineers* 43 (2): 264-268. doi.org/10.1016/j.jtice.2011.10.007.

Abdollahi, Mehdi, Mehdi Alboofetileh, Rabi Behrooz, Masoud Rezaei, and Reza Miraki. 2013. "Reducing Water Sensitivity of Alginate Bio-Nanocomposite Film Using Cellulose Nanoparticles." *International Journal of Biological Macromolecules* 54: 166-73. doi: 10.1016/j.ijbiomac.2012.12.016.

Akhavan, Azam, Farah Khoylou and Ebrahim Ataeivarjovi. 2017. "Preparation and Characterization of Gamma Irradiated Starch/PVA/ZnO Nanocomposite Films." *Radiation Physics and Chemistry* 138: 49-53. doi: 10.1016/j.radphyschem.2017.02.057.

Akin, Okan and FundaTihminlioglu. 2017. "Effects of Organo-Modified Clay Addition and Temperature on the Water Vapor Barrier Properties of Polyhydroxy Butyrate Homo and Copolymer Nanocomposite Films for Packaging Applications." *Journal of Polymers and the Environment* 26 (3): 1121-1132. doi: 10.1007/s10924-017-1017-2.

Alexandre B., D. Langevin, P. Médéric,T.Aubry, H. Couderc, Q.T. Nguyen, A. Saiter, and S. Marais. 2009. "Water Barrier Properties of Polyamide 12/Montmorillonite Nanocomposite Membranes: Structure and Volume Fraction Effects." *Journal of Membrane Science* 328 (1-2): 186-204. doi: 10.1016/j.memsci.2008.12.004.

Ali, Malek 2016. "Synthesis and Study the Effect of Hnts on PVA/Chitosan Composite Material." *International Journal of Chemical, Molecular, Nuclear, Materials and Metallurgical Engineering* 10 (2): 234-240.

Alipoormazandarani, Niloofar, Seyedehzahra Ghazihoseini, and Abdorreza Mohammadi Nafchi. 2015. "Preparation and Characterization of Novel Bionanocomposite Based on Soluble Soybean Polysaccharide and Halloysite Nanoclay." *Carbohydrate Polymers* 134: 745-51. doi: 10.1016/j.carbpol.2015.08.059.

Aloui, Hajer, Khaoula Khwaldia, Moktar Hamdi, Elena Fortunati, Jose M. Kenny, Giovanna G. Buonocore, and Marino Lavorgna. 2016. "Synergistic Effect of Halloysite and Cellulose Nanocrystals on the Functional Properties of PVA Based Nanocomposites." *ACS Sustainable Chemistry & Engineering* 4 (3): 794-800. doi: 10.1021/acssuschemeng.5b00806.

Aoi, Keigo, Akinori Takasu, and Masahiko Okada. 1997. "New Chitin-Based Polymer Hybrids. 2. Improved Miscibility of Chitin Derivatives Having Monodisperse Poly(2-Methyl-2-Oxazoline) Side Chains with Poly(Vinyl Chloride) and Poly(Vinyl Alcohol)." *Macromolecules Rapid Communecation* 30: 6134-6138.

Aoi, Keigo, Akinori Takasu, Masahiko Okada. 1995. "New Chitin-Based Polymer Hybrids, 1. Miscibility of Poly(Viny1 Alcohol) with Chitin Derivatives." *Macromolecules Rapid Communecation* 16: 757-761.

Arora, Amit and G.W. Padua. 2010. "Review: Nanocomposites in Food Packaging." *Journal of Food Science* 75 (1): R43-9. doi: 10.1111/j.1750-3841.2009.01456.x.

Arvanitoyannis, Ioannis, Atsuyoshi Nakayama, Sei-ichi Aiba. 1998. "Edible Films Made from Hydroxypropyl Starch and Gelatin and Plasticized by Polyols and Water." *Carbohydrate Polymers* 36: 105-119.

Arvanitoyannis, Ioannis S. and Loulouda Bosnea. 2004. "Migration of Substances from Food Packaging Materials to Foods." *Critical Reviews in Food Science and Nutrition* 44 (2): 63-76. doi: 10.1080/10408690490424621.

Ashley, R.J. 1985. "Permeability and Plastics Packaping." In *Polymer Permeability*, ed. J. Comyn, 269-308. London: Elsevier Applied Science Publishers.

Avella, Maurizio, Jan J. De Vlieger, Maria Emanuela Errico, Sabine Fischer, Paolo Vacca and Maria Grazia Volpe. 2005. "Biodegradable Starch/Clay Nanocomposite Films for Food Packaging Applications." *Food Chemistry* 93 (3): 467-474. doi: 10.1016/j.foodchem.2004.10.024.

Avérous, Luc 2004. "Biodegradable Multiphase Systems Based on Plasticized Starch: A Review." *Journal of Macromolecular Science, Part C* 44 (3). doi: 10.1081/MC-200029326.

Averous L. and N. Boquillon 2004. "Biocomposites Based on Plasticized Starch: Thermal and Mechanical Behaviours."*Carbohydrate Polymers* 56: 111-122. doi: 10.1016/j.carbpol.2003.11.015.

Avérous, Luc and Eric Pollet. 2012. "Biodegradable Polymers." In *Environmental Silicate Nano-Biocomposites*, eds L. Avérous and E. Pollet, 13-39. London: Springer.

Avérous, Luc and Peter J. Halley. 2009. "Biocomposites Based on Plasticized Starch." *Biofuels, Bioproducts and Biorefining* 3 (3): 329-343. doi: 10.1002/bbb.135.

Aydın, Ahmet Alper and Vladimir Ilberg. 2016. "Effect of Different Polyol-Based Plasticizers on Thermal Properties of Polyvinyl Alcohol:Starch Blends." *Carbohydrate Polymers* 136: 441-8. doi: 10.1016/j.carbpol.2015.08.093.

Azahari, N. A., N. Othman and H. Ismail. 2011. "Biodegradation Studies of Polyvinyl Alcohol/Corn Starch Blend Films in Solid and Solution Media." *Journal of Physical Science* 22 (2): 15-31.

Baker, Maribel I., Steven P. Walsh, Zvi Schwartz and Barbara D. Boyan. 2012. "A Review of Polyvinyl Alcohol and Its Uses in Cartilage and Orthopedic Applications." *Journal of Biomedical Materials Ressearch B Applied Biomaterials* 100 (5): 1451-7. doi: 10.1002/jbm.b.32694.

Basiuka, Elena V., Arfat Anis, Sri Bandyopadhyay, Edgar Alvarez-Zauco, Sammy L.I. Chan, Vladimir A. Basiuk. 2009. "Poly(Vinyl Alcohol)/CNT Composites: An Effect of Cross-Linking with Glutaraldehyde." *Superlattices and Microstructures* 46 (1-2): 379-383. doi: 10.1016/j.spmi.2008.10.007.

Bertuzzi, M.A., E.F. Castro Vidaurre, M. Armada, J.C. Gottifredi. 2007. "Water Vapor Permeability of Edible Starch Based Films." *Journal of Food Engineering* 80 (3): 972-978. doi: 10.1016/j.jfoodeng.2006.07.016.

Bharadwaj, R.K. 2001. "Notes." *Macromolecules* 34: 9189-9192. doi: 10.1021/ma010780b.

Bhattacharya, Mithun, Subharanjan Biswas, and Anil K. Bhowmick. 2011. "Permeation Characteristics and Modeling of Barrier Properties of Multifunctional Rubber Nanocomposites." *Polymer* 52 (7): 1562-1576. doi: 10.1016/j.polymer.2011.01.055.

Biddeci, G., G. Cavallaro, F. Di Blasi, G. Lazzara, M. Massaro, S. Milioto, F. Parisi, S. Riela, and G. Spinelli. 2016. "Halloysite Nanotubes Loaded with Peppermint Essential Oil as Filler for Functional Biopolymer Film." *Carbohydrate Polymers* 152: 548-557. doi: 10.1016/j.carbpol.2016.07.041.

Bin-Dahman, Osamah A., Jobin Jose and Mamdouh A. Al-Harthi. 2016. "Effect of Natural Weather Aging on the Properties of Poly(Vinyl Alcohol)/Starch/Graphene Nanocomposite." *Starch* 69: 1-8. doi: 10.1002/star.201600005].

Bonilla, J., E. Fortunati, L. Atarés, A. Chiralt, and J.M. Kenny. 2014. "Physical, structural and antimicrobial properties of poly vinyl alcoholechitosan biodegradable films." *Food Hydrocolloids* 35: 463-470. doi: 10.1016/j.foodhyd.2013.07.002.

Brady, C. J. 1993. "Stone Fruit." In *Biochetnistry of Fruit Ripening*, eds G. B. Seymour, J. E. Taylor and G. A. Tucker, 379-397. Malaysia: Springer.

British Standard. EN. 1186-1:2002. "Materials and Articles in Contact with Foodstuffs-Plastics. Part 1: Guide to the Selection of Conditions and Test Methods for Overall Migration." *European Committee Standard*: 1-52.

Cai, Jie, Jingyao Chen, Qian Zhang, Miao Lei, Jingren He, Anhong Xiao, Chengjie Ma, Sha Li, Hanguo Xiong. 2016. "Well-Aligned Cellulose Nanofiber-Reinforced Polyvinyl Alcohol Composite Film: Mechanical and Optical Properties." *Carbohydrate Polymers* 140: 238-45. doi: 10.1016/j.carbpol.2015.12.039.

Callister, William D. Jr. 2007. *Materials Science and Engineering: An Introduction*. Edited by Murphy. K. Seven Edition ed. USA: John Wiley & Sons.

Cano, A., E. Fortunati b,M.Chafer, J.M. Kenny, A. Chiralt, C. Gonzalez-Martínez. 2015a. "Properties and Ageing Behaviour of Pea Starch Films as Affected by Blend with

Poly(Vinyl Alcohol)." *Food Hydrocolloids* 48: 84-93. doi: 10.1016/j.foodhyd.2015.01.008.

Cano, A., E. Fortunati, M. Cha´fer, C. Gonza´lez-Martı´nez, A. Chiralt, J. M. Kenny. 2015b. "Effect of Cellulose Nanocrystals on the Properties of Pea Starch–Poly(Vinyl Alcohol) Blend Films." *Journal of Materials Science* 50 (21): 6979-6992. doi: 10.1007/s10853-015-9249-9.

Cano, Amalia I., Maite Cháfer, Amparo Chiralt, Chelo González-Martínez. 2015c. "Physical and Microstructural Properties of Biodegradable Films Based on Pea Starch and PVA." *Journal of Food Engineering* 167: 59-64. doi: 10.1016/j.jfoodeng.2015.06.003.

Cano, Amalia I., Maite Cháfer, Amparo Chiralt, and Chelo González-Martínez. 2016. "Biodegradation Behavior of Starch-PVA Films as Affected by the Incorporation of Different Antimicrobials." *Polymer Degradation and Stability* 132: 11-20. doi: 10.1016/j.polymdegradstab.2016.04.014.

Castro-Aguirre, E., F. Iñiguez-Franco, H.Samsudin, X. Fang, and R. Auras. 2016. "Poly(Lactic Acid)-Mass Production, Processing, Industrial Applications, and End of Life." *Advanced Drug Delivery Reviews* 107: 333-366. doi: 10.1016/j.addr.2016.03.010.

Cerqueira, Miguel A., António A. Vicente and Lorenzo M. Pastrana. 2018. "Nanotechnology in Food Packaging: Opportunities and Challenges." In *Nanomaterials for Food Packaging: Materials, Processing Technologies, and Safety Issues*, ed. Jose Maria Lagaron Miguel Ângelo Parente Ribeiro Cerqueira,

Lorenzo Miguel Pastrana Castro, António Augusto Martins de Oliveira Soares Vicente, 1-11. Elesvier.

Chai, Wan-Lan, Jing-Dong Chow, Chien-Chung Chen, Fu-Sheng Chuang and Wei-Chuan Lu. 2009. "Evaluation of the Biodegradability of Polyvinyl Alcohol/Starch Blends: A Methodological Comparison of Environmentally Friendly Materials." *Journal of Polymers and the Environment* 17 (2): 71-82. doi: 10.1007/s10924-009-0123-1.

Chandra, R. and Renu Rustgi. 1998. "Biodegradable Polymers." *Progress in Polymer Science* 23: 1273-1335.

Cheikh, Salma Ben, Ridha Ben Cheikh, Eunice Cunha, Paulo E. Lopes and Maria C. Paiva. 2018. "Production of Cellulose Nanofibers from Alfa Grass and Application as Reinforcement for Polyvinyl Alcohol." *Plastics, Rubber and Composites* 47 (7): 297-305. doi: 10.1080/14658011.2018.1479822.

Chen, Biqiong and Julian R. G. Evans. 2006. "Nominal and Effective Volume Fractions in Polymer-Clay Nanocomposites." *Macromolecules* 39: 1790-1796. doi: 10.1021/ma0522460.

Chen, Yun, Xiaodong Cao, Peter R. Chang, and Michel A. Huneault. 2008. "Comparative Study on the Films of Poly(Vinyl Alcohol)/Pea Starch Nanocrystals and Poly(Vinyl Alcohol)/Native Pea Starch." *Carbohydrate Polymers* 73 (1): 8-17. doi: 10.1016/j.carbpol.2007.10.015.

Chiellini, Emo, Andrea Corti, Salvatore D'Antone and Roberto Solaro. 2003. "Biodegradation of Poly (Vinyl Alcohol) Based Materials." *Progress in Polymer Science* 28: 963-1014. doi: 10.1016/S0079-6700(02)00149-1.

Chiou, Bor-Sen, Emma Yee, Greg M. Glenn, and William J. Orts. 2005. "Rheology of Starch–Clay Nanocomposites." *Carbohydrate Polymers* 59 (4): 467-475. doi: 10.1016/j.carbpol.2004.11.001.

Choudalakis G. and A.D. Gotsis. 2009. "Permeability of Polymer/Clay Nanocomposites: A Review." *European Polymer Journal* 45 (4): 967-984. doi: 10.1016/j.eurpolymj.2009.01.027.

Comyn, J. 1985. "Introduction to Polymer Permeability and the Mathmatics of Diffusion." In *Polymer Permeability*, ed. J. Comyn, 1-10. London: Elsevier Applied Science Publishers.

Corre, Deborah Le, Julien Bras, and Alain Dufresne. 2010b. "Starch Nanoparticles: A Review." *Biomacromolecules* 11: 1139-1153.

Cui, Yanbin, S. Kumar, Balakantha Rao Konac and Daniel van Houcke. 2015. "Gas Barrier Properties of Polymer/Clay Nanocomposites." *RSC Advances* 5 (78): 63669-63690. doi: 10.1039/c5ra10333a.

Cuq, Bernard, Nathalie Gontard, Christian Aymard and Stephane Guilbert. 1997. "Relative Humidity and Temperature Effects on Mechanical and Water Vapor Barrier Properties of Myofibrillar Protein-Based Films." *Polymer Gels and Networks* 5 (1-15).

Darie-Niţă, Raluca Nicoleta and Cornelia Vasile. 2018. "Halloysite Containing Composites for Food Packaging Applications." In *Composites Materials for Food Packaging*, ed. G.; Kozlowski Cirillo, M. A., Spizzirri, U. G., 73-122. USA: John Wiley & Sons.

Das, Kunal, Dipa Ray, N. R. Bandyopadhyay, Anirudhha Gupta, Suparna Sengupta, Saswata Sahoo, Amar Mohanty, and Manjusri Misra. 2010. "Preparation and Characterization of Cross-Linked Starch/Poly(Vinyl Alcohol) Green Films with Low Moisture Absorption." *Industrial & Engineering Chemistry Research* 49: 2176-2185.

Devi, Nirmala, Mandip Sarmah,Bably Khatun, and Tarun K.Maji. 2017. "Encapsulation of Active Ingredients in Polysaccharide-Protein Complex Coacervates." *Advances in Colloid and Interface Science* 239: 136-145. doi: 10.1016/j.cis.2016.05.009.

Djagny, Kodjo Boady, Zhang Wang and Shiying Xu. 2001. "Gelatin: A Valuable Protein for Food and Pharmaceutical Industries: Review." *Critical Reviews in Food Science and Nutrition* 41 (6): 481-92. doi: 10.1080/20014091091904.

Dong, Pei, Raghavan Prasanth, Fangbo Xu, Xifan Wang, Bo Li and Ravi Shankar. 2015a. "Eco-Friendly Polymer Nanocomposite—Properties and Processing." In *Eco-Friendly Polymer Nanocomposites: Processing and Properties*, ed. Vijay Kumar Thakur and Manju Kumari Thakur, 1-15. New Delhi: Springer India.

Dong, Yu, Jordan Marshall, Hazim J. Haroosh, Soheila Mohammadzadehmoghadam, Dongyan Liu, Xiaowen Qi and Kin-Tak Lau. 2015b. "Polylactic Acid (PLA)/Halloysite Nanotube (HNT) Composite Mats: Influence of Hnt Content and Modificatio." *Composites: Part A* 76: 28-36. doi: 10.1016/j.compositesa.2015.05.011.

Dong, Yu, Thomas Bickford, Hazim J. Haroosh, Kin-Tak Lau and Hitoshi Takagi. 2013. "Multi-Response Analysis in the Material Characterisation of Electrospun Poly (Lactic Acid)/Halloysite Nanotube Composite Fibres Based on Taguchi Design of

Experiments: Fibre Diameter, Non-Intercalation and Nucleation Effects." *Applied Physics A* 112: 747-757. doi: 10.1007/s00339-013-7789-x.

Douglass, Eugene F., Huseyin Avci, Ramiz Boy, Orlando J. Rojas and Richard Kotek. 2017. "A Review of Cellulose and Cellulose Blends for Preparation of Bio-Derived and Conventional Membranes, Nanostructured Thin Films, and Composites." *Polymer Reviews* 58 (1): 102-163. doi: 10.1080/15583724.2016.1269124.

Duncan, Timothy V. 2011. "Applications of nanotechnology in food packaging and food safety: Barrier materials, antimicrobials and sensors." *Journal of Colloid and Interface Science* 363 (1-24). doi: 10.1016/j.jcis.2011.07.017.

European Union Commission regulation (EU) No 10/2011 of 14 January. 2011. "On Plastic Materials and Articles Intended to Come into Contact with Food." *Official Journal of the European Union*: L12:1–89.

Farhoodi, Mehdi, Seyed Mohammad Mousavi, Rahmat Sotudeh-Gharebagh, Zahra Emam-Djomeh and Abdolrasul Oromiehie. 2014. "Migration of Aluminum and Silicon from Pet/Clay Nanocomposite Bottles into Acidic Food Simulant." *Packaging Technology and Science* 27 (2): 161-168. doi: 10.1002/pts.2017.

Feldman, Dorel 2013. "Polymer Nanocomposite Barriers." *Journal of Macromolecular Science, Part A* 50 (4): 441-448. doi: 10.1080/10601325.2013.768440.

Fizir, Meriem, Pierre Dramou, Nasiru Sintali Dahiru, Wang Ruya, Tao Huang and Hua He. 2018. "Halloysite Nanotubes in Analytical Sciences and in Drug Delivery: A Review." *Mikrochimica Acta* 185 (8): 389. doi: 10.1007/s00604-018-2908-1.

Follain, N., C. Joly, P. Dole, and C. Bliard. "Properties of Starch Based Blends. Part 2. "Influence of Polyvinyl alcohol addition and photocrosslinking on starch based materials mechanical properties." *Carbohydrate Polymers* 60, no. 2 (2005): 185-92. doi:10.1016/j.carbpol.2004.12.003.

Gaaz, Tayser Sumer, Abu Bakar Sulong, Abdul Amir H. Kadhum , Ahmed A. Al-Amiery, Mohamed H. Nassir and Ahed Hameed Jaaz. 2017. "The Impact of Halloysite on the Thermo-Mechanical Properties of Polymer Composites." *Molecules* 22 (5). doi: 10.3390/molecules22050838.

Gaaz, Tayser Sumer, Abu Bakar Sulong, Majid Niaz Akhtar, Abdul Amir H. Kadhum, Abu Bakar Mohamad, and Ahmed A. Al-Amiery. 2015. "Properties and Applications of Polyvinyl Alcohol, Halloysite Nanotubes and Their Nanocomposites." *Molecules* 20 (12): 22833-47. doi: 10.3390/molecules201219884.

Gajria, Ajay M., Vipul Dave, Richard A. Gross and Stephen P. McCarthy. 1996. "Miscibility and Biodegradability of Blends of Poly(Lactic Acid) and Poly(Vinyl Acetate)." *Polymer* 37 (3): 437-444.

Gao, Wei. 2015. "Synthesis, Structure, and Characterizations." In *Graphene Oxide-Reduction Recipes, Spectroscopy, and Applications*, ed. Wei Gao, 1-28. Switzerland: Springer.

García, N.L., L. Famá, N.B. D'Accorso and S. Goyanes. 2015. "Biodegradable Starch Nanocomposites." In *Eco-Friendly Polymer Nanocomposites: Processing and Properties*, ed. Vijay Kumar Thakur and Manju Kumari Thakur, 17-77. New Delhi: Springer India.

Gennadios, A., C.L. Weller, and R.F. Testin. 1993. "Temperature Effect on Oxygen Permeability of Edible Protein-Based Films." *Journal of Food Science* 58 (1): 212-214.

Gennadios, Aristippos, Alice H. Brandenburg, Jang W. Park, Curtis L. Weller, and Robert F. Testin. 1994. "Water Vapor Permeability of Wheat Gluten and Soy Protein Isolate Films." *Industrial Crops and Products* 2: 189-195.

George, Johnsy, S.N. Sabapathi and Siddaramaiah. 2015. "Water Soluble Polymer-Based Nanocomposites Containing Cellulose Nanocrystals." In *Eco-Friendly Polymer Nanocomposites: Processing and Properties*, ed. Vijay Kumar Thakur and Manju Kumari Thakur, 259-293. New Delhi: Springer India.

Geyer, Roland, Jenna R. Jambeck and Kara Lavender Law. 2017. "Plastocs: Production, Use, and Fate of All Plastics Ever Made." *Science Advances* 3: 1-5.

Ghanbarzadeh, Babak, Hadi Almasi, and Ali A. Entezami. 2011. "Improving the Barrier and Mechanical Properties of Corn Starch-Based Edible Films: Effect of Citric Acid and Carboxymethyl Cellulose." *Industrial Crops and Products* 33 (1): 229-235. doi: 10.1016/j.indcrop.2010.10.016.

Giannakas, Aris, Maria Vlacha, Constantinos Salmas, Areti Leontiou, Petros Katapodis, Haralambos Stamatis, Nektaria-Marianthi Barkoula, and Athanasios Ladavos. 2016. "Preparation, Characterization, Mechanical, Barrier and Antimicrobial Properties of Chitosan/PVOH/Clay Nanocomposites." *Carbohydrate Polymers* 140: 408-15. doi: 10.1016/j.carbpol.2015.12.072.

Gohil, J. M., A. Bhattacharya and P. Ray. 2006. "Studies on the Cross-Linking of Poly(Vinyl Alcohol)." *Journal of Polymer Research* 13: 161-169. doi: 10.1007/s10965-005-9023-9.

Grande, Rafael and Antonio J. F. Carvalho. 2011. "Compatible Ternary Blends of Chitosan/Poly(Vinyl Alcohol)/Poly(Lactic Acid) Produced by Oil-in-Water Emulsion Processing." *Biomacromolecules* 12 (4): 907-14. doi: 10.1021/bm101227q.

Grande, Rafael, Luiz A. Pessan, and Antonio J.F. Carvalho. 2015. "Ternary Melt Blends of Poly(Lactic Acid)/Poly(Vinyl Alcohol)-Chitosan." *Industrial Crops and Products* 72: 159-165. doi: 10.1016/j.indcrop.2014.12.041.

Grunlan, Jaime C., Ani Grigorian, Charles B. Hamilton, and Ali R. Mehrabi. 2004. "Effect of Clay Concentration on the Oxygen Permeability and Optical Properties of a Modified Poly(Vinyl Alcohol)." *Journal of Applied Polymer Science* 93 (3): 1102-1109. doi: 10.1002/app.20564.

Guimarães Jr., Mario, Vagner Roberto Botaro, Kátia Monteiro Novack, Fábio Gomes Teixeira, Gustavo Henrique Denzin Tonoli. 2015. "Starch/PVA-Based Nanocomposites Reinforced with Bamboo Nanofibrils." *Industrial Crops and Products* 70: 72-83. doi: 10.1016/j.indcrop.2015.03.014.

Guo, Mingyi, Aifei Wang, Faheem Muhammad, Wenxiu Qi, Hao Ren, Yingjie Guo, and Guangshan Zhu. 2012. "Halloysite Nanotubes, a Multifunctional Nanovehicle for Anticancer Drug Delivery." *Chinese Journal of Chemistry* 30 (9): 2115-2120. doi: 10.1002/cjoc.201200657.

Guohua, Zhao, Liu Ya, Fang Cuilan, Zhang Min, Zhou Caiqiong, and Chen Zongdao. 2006. "Water Resistance, Mechanical Properties and Biodegradability of Methylated-Cornstarch/Poly(Vinyl Alcohol) Blend Film." *Polymer Degradation and Stability* 91 (4): 703-711. doi: 10.1016/j.polymdegradstab.2005.06.008.

Gupta, Bhuvanesh, Roopali Agarwal, and M. Sarwar Alam. 2013. "Preparation and Characterization of Polyvinyl Alcohol-Polyethylene Oxide-Carboxymethyl Cellulose Blend Membranes." *Journal of Applied Polymer Science* 127 (2): 1301-1308. doi: 10.1002/app.37665.

Hago, Eltjani-Eltahir, and Xinsong Li. 2013. "Interpenetrating Polymer Network Hydrogels Based on Gelatin and PVA by Biocompatible Approaches: Synthesis and Characterization." *Advances in Materials Science and Engineering*, Article ID 328763, 8 pages. doi: 10.1155/2013/328763.

He, Zeqiang and Lizhi Xiong. 2012. "Evaluation of Physical and Biological Properties of Polyvinyl Alcohol/Chitosan Blend Films." *Journal of Macromolecular Science, Part B* 51 (9): 1705-1714. doi: 10.1080/00222348.2012.657584.

Heidarian, Pejman, Tayebeh Behzad, and Mohsen Sadeghi. 2017. "Investigation of Cross-Linked PVA/Starch Biocomposites Reinforced by Cellulose Nanofibrils Isolated from Aspen Wood Sawdust." *Cellulose* 24 (8): 3323-3339. doi: 10.1007/s10570-017-1336-4.

Hejri, Zahra, Ali Akbar Seifkordi, Ali Ahmadpour, Seyed Mojtaba Zebarjad, and Abdolmajid Maskooki. 2013. "Biodegradable Starch/Poly (Vinyl Alcohol) Film Reinforced with Titanium Dioxide Nanoparticles." *International Journal of*

*Minerals, Metallurgy, and Materials* 20 (10): 1001-1011. doi: 10.1007/s12613-013-0827-z.

Holland, B. J. and J. N. Hay. 2001. "The Thermal Degradation of Poly(Vinyl Alcohol)." *Polymer* 42: 6775-6783.

Hu, Dongying and Lijuan Wang. 2016. "Fabrication of Antibacterial Blend Film from Poly (Vinyl Alcohol) and Quaternized Chitosan for Packaging." *Materials Research Bulletin* 78: 46-52. doi: 10.1016/j.materresbull.2016.02.025.

Hu, Qiuhui, Yong Fang, Yanting Yang, Ning Ma and Liyan Zhao. 2011. "Effect of Nanocomposite-Based Packaging on Postharvest Quality of Ethylene-Treated Kiwifruit (Actinidia Deliciosa) During Cold Storage." *Food Research International* 44 (6): 1589-1596. doi: 10.1016/j.foodres.2011.04.018.

Hu, Yingmo, Qingling Wang and Mingru Tang. 2013. "Preparation and Properties of Starch-G-PLA/Poly(Vinyl Alcohol) Composite Film." *Carbohydrate Polymers* 96 (2): 384-8. doi: 10.1016/j.carbpol.2013.04.011.

Huang, Hua-Dong, Peng-Gang Ren, Jun Chen, Wei-Qin Zhang, Xu Ji and Zhong-Ming Li. 2012. "High Barrier Graphene Oxide Nanosheet/Poly(Vinyl Alcohol) Nanocomposite Films." *Journal of Membrane Science* 409-410: 156-163. doi: 10.1016/j.memsci.2012.03.051.

Huang, Jen-Yi, Janelle Limqueco, Yu Yuan Chieng, Xu Li and Weibiao Zhou. 2017. "Performance Evaluation of a Novel Food Packaging Material Based on Clay/Polyvinyl Alcohol Nanocomposite." *Innovative Food Science & Emerging Technologies* 43: 216-222. doi: 10.1016/j.ifset.2017.08.012.

Huang, Jen-Yi, Xu Li and Weibiao Zhou. 2015. "Safety Assessment of Nanocomposite for Food Packaging Application." *Trends in Food Science & Technology* 45 (2): 187-199. doi: 10.1016/j.tifs.2015.07.002.

Huang, Yanmin, Shuxiang Chen, Xin Bing, Cuiling Gao, Tian Wang and Bo Yuan. 2011. "Nanosilver Migrated into Food-Simulating Solutions from Commercially Available Food Fresh Containers." *Packaging Technology and Science* 24 (5): 291-297. doi: 10.1002/pts.938.

Huang, Yanping, HanghangWei, ZhenWang , Qian Li and Nan Tian. 2018. "Simultaneous Enhancement of Strength and Toughness of Pla Induced by Miscibility Variation with PVA." *Polymers* 10 (10): 1178. doi: 10.3390/polym10101178.

Ibrahim, Maha M., Waleed K. El-Zawawy, Mona A. Nassar. 2010. "Synthesis and Characterization of Polyvinyl Alcohol/Nanospherical Cellulose Particle Films." *Carbohydrate Polymers* 79 (3): 694-699. doi: 10.1016/j.carbpol.2009.09.030.

Idumah, Christopher Igwe, Azman Hassan, James Ogbu, J.U Ndem and Iheoma Chigoziri Nwuzor. 2018. "Recently Emerging Advancements in Halloysite Nanotubes Polymer Nanocomposites." *Composite Interfaces*. doi: 10.1080/09276440.2018.1534475.

Imam, S. H., P. Cinelli, S. H. Gordon, and E. Chiellini. 2005. "Characterization of Biodegradable Composite Films Prepared from Blends of Poly(Vinyl Alcohol), Cornstarch, and Lignocellulosic Fiber." *Journal of Polymers and the Environment* 13 (1): 47-55. doi: 10.1007/s10924-004-1215-6.

Imran, Muhammad, Anne-Marie Revol-Junelles, Noémie René, Majid Jamshidian, Muhammad Javeed Akhtar, Elmira Arab-Tehrany, Muriel Jacquot, and Stéphane

Desobry. 2012. "Microstructure and Physico-Chemical Evaluation of Nano-Emulsion-Based Antimicrobial Peptides Embedded in Bioactive Packaging Film." *Food Hydrocolloids* 29: 407-419. doi: 10.1016/j.foodhyd.2012.04.010.

Ino, Julia M., Ervi Sju, Veronique Ollivier, Evelyn K.F. Yim, Didier Letourneur, Catherine Le Visage. 2013. "Evaluation of Hemocompatibility and Endothelialization of Hybrid Poly(Vinyl Alcohol) (PVA)/Gelatin Polymer Films." *Journal of Biomedical Material Research B Applied Biomaterial* 101 (8): 1549-59. doi: 10.1002/jbm.b.32977.

Ismail, H. and N. F. Zaaba. 2011. "Effect of Additives on Properties of Polyvinyl Alcohol (PVA)/Tapioca Starch Biodegradable Films." *Polymer-Plastics Technology and Engineering* 50 (12): 1214-1219. doi: 10.1080/03602559.2011.566241.

Jancar, J., J.F. Douglas, F.W. Starr, S.K. Kumar, P. Cassagnau, A.J. Lesser, S.S. Sternstein, and M.J. Buehler. 2010. "Current Issues in Research on Structure–Property Relationships in Polymer Nanocomposites." *Polymer* 51 (15): 3321-3343. doi: 10.1016/j.polymer.2010.04.074.

Jang, Jyongsik and Dong Kweon Lee. 2003. "Plasticizer Effect on the Melting and Crystallization Behavior of Polyvinyl Alcohol." *Polymer* 44: 8139-8146. doi: 10.1016/j.polymer.2003.10.015.

Jayasekara, R., I. Harding, I. Bowater, G.B.Y. Christie, and G.T. Lonergan. 2004. "Preparation, Surface Modification and Characterisation of Solution Cast Starch PVA Blended Films." *Polymer Testing* 23 (1): 17-27. doi: 10.1016/s0142-9418(03)00049-7.

Jayasekara, Ranjith, Ian Harding, Ian Bowater, Gregor B. Y. Christie, and Greg T. Lonergan. 2003. "Biodegradation by Composting of Surface Modified Starch and PVA Blended Films." *Journal of Polymers and the Environment* 11 (2): 49-56.

Jiang, Xiancai, Yong Luo, Linxi Hou, Yulai Zhao. 2016. "The Effect of Glycerol on the Crystalline, Thermal, and Tensile Properties of $CaCl_2$-Doped Starch/PVA Films." *Polymer Composites* 37 (11): 3191-3199. doi: 10.1002/pc.23517.

Jose, Jobin, Mamdouh A. Al-Harthi, Mariam Al-Ali AlMa'adeed, Jolly Bhadra Dakua, and Sadhan K. De. 2015. "Effect of Graphene Loading on Thermomechanical Properties of Poly(Vinyl Alcohol)/Starch Blend." *Journal of Applied Polymer Science* 132 (16): n/a-n/a. doi: 10.1002/app.41827.

Joussein, E., S. Petit, J. Churchman, B. Theng, D. Richi and B. Delvaux. 2005. "Halloysite Clay Minerals- a Review." *Clay minerals* 40: 383-426.

Julkapli, Nurhidayatullaili Muhd, Samira Bagheri and S.M. Sapuan. 2015. "Multifunctionalized Carbon Nanotubes Polymer Composites: Properties and Applications." In *Eco-Friendly Polymer Nanocomposites-Processing and Properties*, ed. Vijay Kumar Thakur and Manju Kumari Thakur. New Delhi: Springer India.

Kale, Gaurav, Thitisilp Kijchavengkul, Rafael Auras, Maria Rubino, Susan E. Selke, and Sher Paul Singh. 2007. "Compostability of Bioplastic Packaging Materials: An Overview." *Macromolecular Bioscience* 7 (3): 255-77. doi: 10.1002/mabi.200600168.

Kamble, Ravindra, Manasi Ghag, Sheetal Gaikawad, and Bijoy Kumar Panda. 2012. "Halloysite Nanotubes and Applications: A Review." *Journal of Advanced Scientific Research* 3 (2): 25-29.

Karthik, P.S., A.L. Himaja and Surya Prakash Singh. 2014. "Carbon-Allotropes: Synthesis Methods, Applications and Future Perspectives." *Carbon letters* 15 (4): 219-237. doi: 10.5714/cl.2014.15.4.219.

Kasai, Deepak, Ravindra Chougale, Saraswati Masti, Raju Chalannavar, Ravindra B. Malabadi, and Ramesh Gani. 2018. "Influence of Syzygium Cumini Leaves Extract on Morphological, Thermal, Mechanical, and Antimicrobial Properties of PVA and PVA/Chitosan Blend Films." *Journal of Applied Polymer Science* 135 (17): 46188. doi: 10.1002/app.46188.

Kausar, Ayesha. 2017. "Review on Polymer/Halloysite Nanotube Nanocomposite." *Polymer-Plastics Technology and Engineering*, 57: 6, 548-564, doi:10.1080/03602559.2017.1329436

Kausar, Ayesha. 2018. "Eco-Polymer and Carbon Nanotube Composite: Safe Technology." In *Handbook of Ecomaterials*, ed. L.M.T. Martinez, 1-16. Springer International Publishing.

Khoo, W. S., H. Ismail, and A. Ariffin. 2011. "Tensile and Swelling Properties of Polyvinyl Alcohol/Chitosan/Halloysite Nanotubes Nanocomposite." In *National Postgraduate Conference*. IEEE. doi: 978-1-4577-1884-7/11.

Khwaldia, Khaoula, Elmira Arab-Tehrany, and Stephane Desobry. 2010. "Biopolymer Coatings on Paper Packaging Materials." *Comprehensive Reviews in Food Science and Food Safety* 9 (1): 82-91.

Khwaldia, Khaoula, Sylvie Banon, Ste´phane Desobry and Joel Hardy. 2004. "Mechanical and Barrier Properties of Sodium Caseinate–Anhydrous Milk Fat Edible Films." *International Journal of Food Science and Technology* 39: 403-411. doi: 10.1111/j.1365-2621.2004.00797.x.

Kim, Hye Min, Jung Kyoo Lee, Heon Sang Lee. 2011. "Transparent and High Gas Barrier Films Based on Poly(Vinyl Alcohol)/Graphene Oxide Composites." *Thin Solid Films* 519 (22): 7766-7771. doi: 10.1016/j.tsf.2011.06.016.

Kisku, Sudhir K., Niladri Sarkar, Satyabrata Dash, and Sarat K. Swain. 2014. "Preparation of Starch/PVA/$CaCO_3$ nanobiocomposite Films: Study of Fire Retardant, Thermal Resistant, Gas Barrier and Biodegradable Properties." *Polymer-Plastics Technology and Engineering* 53 (16): 1664-1670. doi: 10.1080/03602559.2014.919650.

Kopcilova, Martina, Jitka Huba´cˇkova´, Jan Ru°zˇicˇka, Marie Dvorˇa´cˇkova´, Marke´ta Julinova´, Marek Koutny´, Miroslava Tomalova´, Pavol Alexy, Peter Bugaj and Jaroslav Filip. 2012. "Biodegradability and Mechanical Properties of Poly(Vinyl Alcohol)-Based Blend Plastics Prepared through Extrusion Method." *Journal of Polymers and the Environment* 21 (1): 88-94. doi: 10.1007/s10924-012-0520-8.

Kryuchkova, Marina, Anna Danilushkina, Yuri Lvovab and Rawil Fakhrullin. 2016. "Evaluation of Toxicity of Nanoclays and Graphene Oxide in Vivo: A Paramecium Caudatum Study." *Environmental Science: Nano* 3 (2): 442-452. doi: 10.1039/c5en00201j.

Kubiak, K.J., M.C.T. Wilson, T.G. Mathia, and Ph. Carval. 2011. "Wettability Versus Roughness of Engineering Surfaces." *Wear* 271 (3-4): 523-528. doi: 10.1016/j.wear.2010.03.029.

Lee, Min Hyeock, Seong Yeon Kim, and Hyun Jin Park. 2018. "Effect of Halloysite Nanoclay on the Physical, Mechanical, and Antioxidant Properties of Chitosan Films Incorporated with Clove Essential Oil." *Food Hydrocolloids* 84: 58-67. doi: 10.1016/j.foodhyd.2018.05.048.

Lemes, A.P., T.L.A. Montanheiro, F.R. Passador and N. Durán. 2015. "Nanocomposites of Polyhydroxyalkanoates Reinforced with Carbon Nanotubes: Chemical and Biological Properties." In *Eco-Friendly Polymer Nanocomposites: Processing and Properties*, ed. Vijay Kumar Thakur and Manju Kumari Thakur, 79-108. New Delhi: Springer India.

Li, Hong-Zhen, Si-Chong Chen, and Yu-Zhong Wang. 2014. "Thermoplastic PVA/PLA Blends with Improved Processability and Hydrophobicity." *Industrial & Engineering Chemistry Research* 53: 17355-17361. doi: 10.1021/ie502531w.

Li, Yan, Huafeng Tian, Qingqing Jia, Ping Niu, Aimin Xiang, Di Liu, Yanan Qin. 2015. "Development of Polyvinyl Alcohol/Intercalated Mmt Composite Foams Fabricated by Melt Extrusion." *Journal of Applied Polymer Science* 132 (43): 42706. doi: 10.1002/app.42706.

Lim, L. Y. and Lucy S. C. Wan. 2008. "The Effect of Plasticizers on the Properties of Polyvinyl Alcohol Films." *Drug Development and Industrial Pharmacy* 20 (6): 1007-1020. doi: 10.3109/03639049409038347.

Lim, Mijin, Hyok Kwon, Dowan Kim, Jongchul Seo, Haksoo Han, Sher Bahadar Khan. 2015. "Highly-Enhanced Water Resistant and Oxygen Barrier Properties of Cross-Linked Poly(Vinyl Alcohol) Hybrid Films for Packaging Applications." *Progress in Organic Coatings* 85: 68-75. doi: 10.1016/j.porgcoat.2015.03.005.

Lin, Derong, Yichen Huang, Yuanqiang Liu, Tingting Luo, Baoshan Xing, Yuanmeng Yang, Zhengfang Yang, Zhijun Wu, Hong Chen, Qing Zhang and Wen Qin. 2018. "Physico-Mechanical and Structural Characteristics of Starch/Polyvinyl Alcohol/Nano-Titania Photocatalytic Antimicrobial Composite Films." *LWT-Food Science and Technology* 96: 704-712. doi: 10.1016/j.lwt.2018.06.001.

Liu, Dagang, Xun Sun, Sonakshi Maiti, Huafeng Tian and Zhongshi Ma. 2013. "Effects of Cellulose Nanofibrils on the Structure and Properties on PVA Nanocomposites." *Cellulose* 20 (6): 2981-2989. doi:10.1007/s10570-013-0073-6.

Liu, Di, Qibo Bian, Yan Li, Yaru Wang, Aimin Xiang and Huafeng Tian. 2016a. "Effect of Oxidation Degrees of Graphene Oxide on the Structure and Properties of Poly (Vinyl Alcohol) Composite Films." *Composites Science and Technology* 129: 146-152. doi: 10.1016/j.compscitech.2016.04.004.

Liu, Hongyu, Parthasarathi Bandyopadhyay, Nam Hoon Kim, Bongho Moon and Joong Hee Lee. 2016b. "Surface Modified Graphene Oxide/Poly(Vinyl Alcohol) Composite for Enhanced Hydrogen Gas Barrier Film." *Polymer Testing* 50: 49-56. doi: 10.1016/j.polymertesting.2015.12.007.

Liu, J.; Boo, W. J.; Clearfield, A.;Sue, H. J. 2006. "Intercalation and Exfoliation: A Review on Morphology of Polymer Nanocomposites Reinforced by Inorganic

Layer Structures." *Materials and Manufacturing Processes* 21 (2): 143-151. doi: 10.1080/amp-200068646.

Liu, Luqi, Asa H. Barber, Shahar Nuriel and H. Daniel Wargner. 2005. "Mechanical Properties of Functionlised Single-Walled Carbon Nantubes/Poly(Vinyl Alcohol) Nanocomposites." *Advanced Functional Materials* 15: 975-980.

Liu, M., B. Guo, M. Du and D. Jia. 2007. "Drying Induced Aggregation of Halloysite Nanotubes in Polyvinyl Alcohol/Halloysite Nanotubes Solution and Its Effect on Properties of Composite Film." *Applied Physics A* 88 (2): 391-395. doi: 10.1007/s00339-007-3995-8.

Liu, Mingxian, Zhixin Jia, Demin Jia and Changren Zhou. 2014. "Recent Advance in Research on Halloysite Nanotubes-Polymer Nanocomposite." *Progress in Polymer Science* 39 (8): 1498-1525. doi: 10.1016/j.progpolymsci.2014.04.004.

Liu, Yanging, Hanghang Wei, Zhen Wang, Qian Li and Nan Tian. 2018. "Simultaneous Enhancement of Strength and Toughness of PLA Induced by Miscibility Variation with PVA." *Polymers* 10: 1178. doi: 10.3390/polym10101178.

Liu, Yaowen, Shuyao Wang and Wenting Lan. 2018. "Fabrication of Antibacterial Chitosan-PVA Blended Film Using Electrospray Technique for Food Packaging Applications." *Int J Biol Macromol* 107 (Pt A): 848-854. doi: 10.1016/j.ijbiomac.2017.09.044.

Liu, Yurong, Luke M. Geever, James E. Kennedy, Clement L. Higginbotham, Paul A. Cahill and Garrett B. McGuinness. 2010. "Thermal Behavior and Mechanical Properties of Physically Crosslinked PVA/Gelatin Hydrogels." *Journal of*

*Mechanical Behavior of Biomedical Materials* 3 (2): 203-209. doi: 10.1016/j.jmbbm.2009.07.001.

Liu, Zhiqiang, Yi Feng and Xiao-Su Yi. 1999. "Thermoplastic Starch/PVAl Compounds: Preparation, Processing, and Properties." *Journal of Applied Polymer Science* 74: 2667-2673. doi: 0021-8995/99/112667-07.

Loryuenyong, Vorrada, Charinrat Saewong, Chaiyud Aranchaiya and Achanai Buasri1. 2015. "The Improvement in Mechanical and Barrier Properties of Poly(Vinyl Alcohol)/Graphene Oxide Packaging Films." *Packaging Technology and Science* 28 (11): 939-947. doi: 10.1002/pts.2149.

Lucas, Nathalie, Christophe Bienaime, Christian Belloy, Michèle Queneudec, Françoise Silvestre, and José-Edmundo Nava-Saucedo. 2008. "Polymer Biodegradation: Mechanisms and Estimation Techniques." *Chemosphere* 73 (4): 429-42. doi: 10.1016/j.chemosphere.2008.06.064.

Luo, Xuegang, Jiwei Li, Xiaoyan Lin. 2012. "Effect of Gelatinization and Additives on Morphology and Thermal Behavior of Corn Starch/PVA Blend Films." *Carbohydrate Polymers* 90 (4): 1595-600. doi: 10.1016/j.carbpol.2012.07.036.

Lvov, Yuri M., Melgardt M. DeVilliers and Rawil F. Fakhrullin. 2016. "The Application of Halloysite Tubule Nanoclay in Drug Delivery." *Expert Opinion on Drug Delivery* 13 (7): 977-86. doi: 10.1517/17425247.2016.1169271.

Magnier, Lise and Dominique Crié. 2015. "Communicating Packaging Eco-Friendliness." *International Journal of Retail & Distribution Management* 43 (4/5): 350-366. doi: 10.1108/ijrdm-04-2014-0048.

Maiti, Sonakshi, Dipa Ray and Debarati Mitra. 2012. "Role of Crosslinker on the Biodegradation Behavior of Starch/Polyvinylalcohol Blend Films." *Journal of Polymers and the Environment* 20 (3): 749-759. doi:10.1007/s10924-012-0433-6.

Majdzadeh-Ardakani K. and B. Nazari 2010a. "Improving the Mechanical Properties of Thermoplastic Starch/Poly(Vinyl Alcohol)/Clay Nanocomposites." *Composites Science and Technology* 70 (10): 1557-1563. doi: 10.1016/j.compscitech.2010.05.022.

Majdzadeh-Ardakani, Kazem, Amir H. Navarchian, Farhad Sadeghi. 2010b. "Optimization of Mechanical Properties of Thermoplastic Starch/Clay Nanocomposites." *Carbohydrate Polymers* 79 (3): 547-554. doi: 10.1016/j.carbpol.2009.09.001.

Mangaraj, S., Ajay Yadav, Lalit M. Bal, S. K. Dash, Naveen K. Mahanti. 2018. "Application of Biodegradable Polymers in Food Packaging Industry: A Comprehensive Review." *Journal of Packaging Technology and Research* 3 (1): 77-96. doi: 10.1007/s41783-018-0049-y.

Mao, Lijun, Syed Imam, Sherald Gordon, Patrizia Cinelli, and Emo Chiellini. 2002. "Extruded Cornstarch–Glycerol–Polyvinyl Alcohol Blends: Mechanical Properties, Morphology, and Biodegradability." *Journal of Polymers and the Environment* 8 (4): 205-211.

Maria, Thaı´s M.C., Rosemary A. de Carvalho, Paulo J.A. Sobral, Ana Moˆnica B.Q. Habitante, Javier Solorza-Feria. 2008. "The Effect of the Degree of Hydrolysis of the PVA and the Plasticizer Concentration on the Color, Opacity, and Thermal and

Mechanical Properties of Films Based on PVA and Gelatin Blends." *Journal of Food Engineering* 87 (2): 191-199. doi: 10.1016/j.jfoodeng.2007.11.026.

McDonald, Matthew P., Yurii Morozov, Jose H. Hodak, and Masaru Kuno. 2015. "Spectroscopy and Microscopy of Graphene Oxide and Reduced Graphene Oxide." In *Graphene Oxide- Reduction Recipes, Spectroscopy, and Applications*, ed. Wei Gao, 29-60. Switzerland: Springer.

Mendieta-Taboada, Oscar, Paulo Jose´ do A. Sobral, Rosemary A. Carvalho, Ana Monica B.Q. Habitante. 2008. "Thermomechanical Properties of Biodegradable Films Based on Blends of Gelatin and Poly(Vinyl Alcohol)." *Food Hydrocolloids* 22 (8): 1485-1492. doi: 10.1016/j.foodhyd.2007.10.001.

Mensitieri, Giuseppe, Ernesto Di Maio,Giovanna G. Buonocore, Irma Nedi, Maria Oliviero and Lucia Sansone and Salvatore Iannace. 2011. "Processing and Shelf Life Issues of Selected Food Packaging Materials and Structures from Renewable Resources." *Trends in Food Science & Technology* 22: 72-80. doi: 10.1016/j.tifs.2010.10.001.

Minus, Marilyn L., Han Gi Chae, and Satish Kumar. 2009. " Interfacial Crystallization in Gel-Spun Poly(vinyl alcohol)/Single-Wall Carbon Nanotube Composite Fibers." *Macromolecular Chemistry and Physics* 210: 1799–1808. doi: 10.1002/macp.200900223.

Mishra, Rachna and Kalya J. Rao. 1999. "On the Formation of Poly(Ethylenoxide)-Poly(Vinylalcohol) Blends." *European Polymer Journal* 35: 1883-1894.

Mishra, Raghvendra Kumar, Sung Kyu Ha, Kartikey Verma and Santosh K. Tiwari. 2018. "Recent Progress in Selected Bio-Nanomaterials and Their Engineering

Applications: An Overview." *Journal of Science: Advanced Materials and Devices* 3 (3): 263-288. doi: 10.1016/j.jsamd.2018.05.003.

Mo, Chen, Wang Yuan, Wang Lei, Yin Shijiu. 2014. "Effects of Temperature and Humidity on the Barrier Properties of Biaxially-Oriented Polypropylene and Polyvinyl Alcohol Films." *Journal of Applied Packaging Research* 6 (1): 40-46. doi: 10.14448/japr.01.0004.

Mohsin, Mahmood, Asiful Hossin and Yousef Haik. 2011a. "Thermal and Mechanical Properties of Poly(Vinyl Alcohol) Plasticized with Glycerol." *Journal of Applied Polymer Science* 122 (5): 3102-3109. doi: 10.1002/app.34229.

Mohsin, Mahmood, Asiful Hossin and Yousef Haik. 2011b. "Thermomechanical Properties of Poly(Vinyl Alcohol) Plasticized with Varying Ratios of Sorbitol." *Materials Science and Engineering A* 528: 925-930. doi: 10.1016/j.msea.2010.09.100.

Monteiro, M.K.S., V.R.L. Oliveira, F.K.G. Santos, E.L. Barros Neto, R.H.L. Leite, E.M.M. Aroucha, R.R. Silva, K.N.O. Silva. 2018. "Incorporation of Bentonite Clay in Cassava Starch Films for the Reduction of Water Vapor Permeability." *Food Res Int* 105: 637-644. doi: 10.1016/j.foodres.2017.11.030.

Moon, Robert J., Ashlie Martini, John Nairn, John Simonsen and Jeff Youngblood. 2011. "Cellulose Nanomaterials Review: Structure, Properties and Nanocomposites." *Chemical Society Reviews* 40 (7): 3941-94. doi: 10.1039/c0cs00108b.

Morillon, V., F. Debeaufort, G. Blond, and A. Voilley. 2000. "Temperature Influence on Moisture Transfer through Synthetic Film." *Journal of Membrane Science* 168: 223-231.

Mousa, Mohanad Hashim, Yu Dong and Ian Jeffery Davies. 2016. "Recent Advances in Bionanocomposites: Preparation, Properties, and Applications." *International Journal of Polymeric Materials and Polymeric Biomaterials* 65 (5): 225-254. doi: 10.1080/00914037.2015.1103240.

Muhamad, Ida Idayu, Mohd Harfiz Salehudin and Eraricar Salleh. 2015. "Cellulose Nanofiber for Eco-Friendly Polymer Nanocomposites." In *Eco-Friendly Polymer Nanocomposites: Processing and Properties*, ed. Vijay Kumar Thakur and Manju Kumari Thakur, 323-365. New Delhi: Springer India.

Mujtaba, Muhammad, Rania E. Morsi, Garry Kerch, Maher Z. Elsabee , Murat Kaya, Jalel Labidi, and Khalid Mahmood Khawar. 2019. "Current Advancements in Chitosan-Based Film Production for Food Technology; a Review." *Int J Biol Macromol* 121: 889-904. doi: 10.1016/j.ijbiomac.2018.10.109.

Myhra, S. and J. C. Riviere. 2013. *Characterisations of Nanostructures*. London: Taylor and Francis group.

Nafchi, Abdorreza Mohammadi, Roghayeh Nassiri, Samira Sheibani, Fazilah Ariffin, A.A. Karim. 2013. "Preparation and Characterization of Bionanocomposite Films Filled with Nanorod-Rich Zinc Oxide." *Carbohydrate Polymers* 96 (1): 233-9. doi: 10.1016/j.carbpol.2013.03.055.

Nakagaito, Antonio Norio, Kohei Fujii, Hitoshi Takagi and Yu Dong. 2019. "Strength Improvement of Poly(Vinyl Alcohol) (PVA) Reinforced by Halloysite Nanotube (HNT) Treated with Sulfuric Acid." *Journal of Functionally Graded Materials* 33: 16-22. doi: 10.14957/fgms.33.16.

Negim, E.S.M., Rakhmetullayeva, R.K., Yeligbayeva, G.Zh., Urkimbaeva, P.I., Primzharova, S.T., Kaldybekov, D.B., Khatib, J.M., Mun, G.A., and Craig, W. 2014. "Improving Biodegradability of Polyvinyl Alcohol/Starch Blend Films for Packaging Applications." *International Journal of Basic and Applied Sciences* 3 (3). doi: 10.14419/ijbas.v3i3.2842.

Nielsen, Lawrence E. . 1967. "Models for the Permeability of Filled Polymer Systems." *Journal of Macromolecular Science: Part A - Chemistry* 1 (5): 929-942. doi: 10.1080/10601326708053745.

Nistor, Manuela-Tatiana and Cornelia Vasile. 2012. "Influence of the Nanoparticle Type on the Thermal Decomposition of the Green Starch/Poly(Vinyl Alcohol)/Montmorillonite Nanocomposites." *Journal of Thermal Analysis and Calorimetry* 111 (3): 1903-1919. doi: 10.1007/s10973-012-2731-6.

Nistor, Manuela-Tatiana and Cornelia Vasile. 2013. "TG/FTIR/MS Study on the Influence of Nanoparticles Content Upon the Thermal Decomposition of Starch/Poly(Vinyl Alcohol) Montmorillonite Nanocomposites." *Iranian Polymer Journal* 22 (7): 519-536. doi: 10.1007/s13726-013-0152-4.

Noshirvani, Nooshin, Babak Ghanbarzadeh, Hadi Fasihi and Hadi Almasi. 2016. "Starch–PVA Nanocomposite Film Incorporated with Cellulose Nanocrystals and Mmt: A Comparative Study." *International Journal of Food Engineering* 12 (1). doi: 10.1515/ijfe-2015-0145.

Othman, Siti Hajar 2014. "Bio-Nanocomposite Materials for Food Packaging Applications: Types of Biopolymer and Nano-Sized Filler." *Agriculture and Agricultural Science Procedia* 2: 296-303. doi: 10.1016/j.aaspro.2014.11.042.

Pal, Kunal, Ajit K. Banthia, and Dipak K. Majumdar. 2007. "Preparation and Characterization of Polyvinyl Alcohol–Gelatin Hydrogel Membranes for Biomedical Applications." *AAPS PharmSciTech* 8 (1): E1-E5.

Pawde, S. M. and Kalim Deshmukh. 2008a . "Characterization of Polyvinyl Alcohol/Gelatin Blend Hydrogel Films for Biomedical Applications." *Journal of Applied Polymer Science* 109 (5): 3431-3437. doi: 10.1002/app.28454.

Pawde, Kalim Deshmukh, and Sanmesh Parab. 2008b. "Preparation and Characterization of Poly(Vinyl Alcohol) and Gelatin Blend Films." *Journal of Applied Polymer Science* 109 (2): 1328-1337. doi: 10.1002/app.28096.

Picard, E., A. Vermogen, J.-F. G´erard, and E. Espuche. 2007. "Barrier Properties of Nylon 6-Montmorillonite Nanocomposite Membranes Prepared by Melt Blending: Influence of the Clay Content and Dispersion Stateconsequences on Modelling." *Journal of Membrane Science* 292 (1-2): 133-144. doi: 10.1016/j.memsci.2007.01.030.

Poley, Luiz H., Marcelo G. da Silva, Helion Vargas, Marcelo O. Siqueira, Rubén Sánchez. 2005. "Water and Vapor Permeability at Different Temperatures of Poly (3-Hydroxybutyrate) Dense Membranes." *Polímeros* 15 (1): 22-26.

Priya, Bhanu, Vinod Kumar Gupta, Deepak Pathania, and Amar Singh Singha. 2014. "Synthesis, Characterization and Antibacterial Activity of Biodegradable Starch/PVA Composite Films Reinforced with Cellulosic Fibre." *Carbohydrate Polymers* 109: 171-9. doi: 10.1016/j.carbpol.2014.03.044.

Qiu, Kaiyan and Anil N. Netravali. 2013. "Halloysite Nanotube Reinforced Biodegradable Nanocomposites Using Noncrosslinked and Malonic Acid

Crosslinked Polyvinyl Alcohol." *Polymer Composites* 34 (5): 799-809. doi: 10.1002/pc.22482.

Qiu, Kaiyan and Anil N. Netravali. 2015. "Polyvinyl Alcohol Based Biodegradable Polymer Nanocomposites." In *Biodegradable Polymers*, ed. Chih-Chang Chu, 325-379. New York: Nova Science.

Rafique, Irum, Ayesha Kausar, Zanib Anwar and Bakhtiar Muhammad. 2015. "Exploration of Epoxy Resins, Hardening Systems, and Epoxy/Carbon Nanotube Composite Designed for High Performance Materials: A Review." *Polymer-Plastics Technology and Engineering* 55 (3): 312-333. doi: 10.1080/03602559.2015.1070874.

Rahman, W.A.W.A., Lee Tin Sin, A.R. Rahmat, and A.A. Samad. 2010. "Thermal Behaviour and Interactions of Cassava Starch Filled with Glycerol Plasticized Polyvinyl Alcohol Blends." *Carbohydrate Polymers* 81: 805-810. doi: 10.1016/j.carbpol.2010.03.052.

Rahmat, Abdul Razak, Wan Aizan Wan Abdul Rahman, Lee Tin Sin, A.A. Yussuf. 2009. "Approaches to Improve Compatibility of Starch Filled Polymer System: A Review." *Materials Science and Engineering: C* 29 (8): 2370-2377. doi: 10.1016/j.msec.2009.06.009.

Ramaraj, B. 2007a. "Crosslinked Poly(Vinyl Alcohol) and Starch Composite Films. Ii. Physicomechanical, Thermal Properties and Swelling Studies." *Journal of Applied Polymer Science* 103 (2): 909-916. doi: 10.1002/app.25237.

Ramaraj, B. 2007b. "Crosslinked Poly(Vinyl Alcohol) and Starch Composite Films: Study of Their Physicomechanical, Thermal, and Swelling Properties." *Journal of Applied Polymer Science* 103 (2): 1127-1132. doi: 10.1002/app.24612.

Ramos, Óscar L., Ricardo N. Pereira, Miguel A. Cerqueira, Joana R. Martins, José A. Teixeira, F. Xavier Malcata and António A. Vicente. 2018. "Bio-Based Nanocomposites for Food Packaging and Their Effect in Food Quality and Safety." In *Food Packaging and Preservation*, ed. Alexandru Mihai Grumezescu and Alina Maria Holban, 271-306. London, UK: Elsevier.

Rawtani, Deepak and Y.K. Agrawal. 2012. "Multifarious Applications of Halloysite Nanotubes: A Review." *Reviews on Advanced Material Science* 30: 282-295.

Ray, Sudip, Siew Young Quek, Allan Easteal and Xiao Dong Chen. 2006. "The Potential Use of Polymer-Clay Nanocomposites in Food Packaging." *International Journal of Food Engineering* 2 (4). doi: 10.2202/1556-3758.1149.

Ray, Suprakas Sinha and Mosto Bousmina. 2005. "Biodegradable Polymers and Their Layered Silicate Nanocomposites: In Greening the 21st Century Materials World." *Progress in Materials Science* 50: 962-1079. doi: 10.1016/j.pmatsci.2005.05.002.

Restrepo, Iván, Carlos Medina, Viviana Meruane, Ali Akbari-Fakhrabadi, Paulo Floresand Saddys Rodríguez-Llamazares. 2018. "The Effect of Molecular Weight and Hydrolysis Degree of Poly(Vinyl Alcohol)(PVA) on the Thermal and Mechanical Properties of Poly(Lactic Acid)/PVA Blends." *Polímeros* 28 (2): 169-177. doi: 10.1590/0104-1428.03117.

Rhim, Jong-Whan and Perry K.W. Ng. 2007. "Natural Biopolymer-Based Nanocomposite Films for Packaging Applications." *Critical Reviews in Food Science and Nutrition* 47 (4): 411-33. doi: 10.1080/10408390600846366.

Rhim, Jong-Whan, Hwan-Man Park and Chang-Sik Ha. 2013. "Bio-Nanocomposites for Food Packaging Applications." *Progress in Polymer Science* 38: 1629-1652. doi: 10.1016/j.progpolymsci.2013.05.008.

Robyt, John F. 2008. "Starch: Structure, Properties, Chemistry, and Enzymology." In *Glycoscience: Chemistry and Chemical Biology*, ed. Tatsuta K. Fraser-Reid B., Thiem J., 1437-1472. Berlin, Heidelberg: Springer Berlin Heidelberg.

Rogers, C. E. 1985. "Permeation of Gases and Vapours in Polymers." In *Polymer Permeability*, ed. J. Comyn, 11-73. Londaon: Elsevier Applied Science Publishers.

Roohani, Mehdi, Youssef Habibi, Naceur M. Belgacem, Ghanbar Ebrahim, Ali Naghi Karimi, and Alain Dufresne. 2005. "Cellulose Whiskers Reinforced Polyvinyl Alcohol Copolymers Nanocomposites." *European Polymer Journal* 44: 2489-2498. doi: 10.1016/j.eurpolymj.2008.05.024.

Ryan, Kevin P., Martin Cadek, Valeria Nicolosi, David Blond, Manuel Ruether, Gordon Armstrong, Harry Swan, Antonio Fonseca, Janos B. Nagy, Wolfgang K. Maser, Werner J. Blau, Jonathan N. Coleman. 2007. "Carbon Nanotubes for Reinforcement of Plastics? A Case Study with Poly(Vinyl Alcohol)." *Composites Science and Technology* 67 (7-8): 1640-1649. doi: 10.1016/j.compscitech.2006.07.006.

Sadegh-Hassani, Fatemeh and Abdorreza Mohammadi Nafchi. 2014. "Preparation and Characterization of Bionanocomposite Films Based on Potato Starch/Halloysite

Nanoclay." *International Journal of Biological Macromolecules* 67: 458-62. doi: 10.1016/j.ijbiomac.2014.04.009.

Sadhu, Susmita Dey, Anshuman Soni and Meenakshi Garg. 2015. "Thermal Studies of the Starch and Polyvinyl Alcohol Based Film and Its Nano Composites." *Journal of Nanomedicine & Nanotechnology* 01 (s7). doi: 10.4172/2157-7439.s7-002.

Sadhu, Susmita Dey, Anshuman Soni, Shivani G. Varmani, and Meenakshi Garg. 2014. "Preparation of Starch-Poly Vinyl Alcohol (PVA) Blend Using Potato and Study of Its Mechanical Properties." *International Journal of Pharmaceutical Science Invention* 3 (3): 33-37.

Salleh, M. S. N., N. N. Mohamed Nor, N. Mohd, and S. F. Syed Draman. 2017. "Water Resistance and Thermal Properties of Polyvinyl Alcohol-Starch Fiber Blend Film." In *AIP Conference Proceedings 1809,*, 020045. American Institute of Physics. doi: 10.1063/1.4975460.

Sang, B.-I. , K. Hori, Y. Tanji, and H. Unno. 2002. "Fungal Contribution to in Situ Biodegradation of Poly(3-Hydroxybutyrate- Co -3-Hydroxyvalerate) Film in Soil." *Applied Microbiology and Biotechnology* 58 (2): 241-247. doi: 10.1007/s00253-001-0884-5.

Santos, Ana C., Carolina Ferreira, Francisco Veiga, António J. Ribeiro, Abhishek Panchal, Yuri Lvov, and Anshul Agarwal. 2018. "Halloysite Clay Nanotubes for Life Sciences Applications: From Drug Encapsulation to Bioscaffold." *Advance in Colloid Interface Science* 257: 58-70. doi: 10.1016/j.cis.2018.05.007.

Sapalidis, Andreas A., Fotios K. Katsaros and Nick K. Kanellopoulos. 2011. "PVA/Montmorillonite Nanocomposites: Development and Properties." In

*Nanocomposites and Polymers with Analytical Methods*, ed. J. Cuppoletti. China: InTech.

Saritha, A., Kuruvilla Joseph, Sabu Thomas, and R. Muraleekrishnan. 2012. "Chlorobutyl Rubber Nanocomposites as Effective Gas and VOC Barrier Materials." *Composites Part A: Applied Science and Manufacturing* 43 (6): 864-870. doi: 10.1016/j.compositesa.2012.01.002.

Saxena, S. K. . 2004. "Polyvinyl Alcohol (PVA)- Chemical and Technical Assessment (CTA)." *JECFA* 61: 1-3.

Schmitt, H., K. Prashantha, J. Soulestin, M.F. Lacrampe and P. Krawczak. 2012. "Preparation and Properties of Novel Melt-Blended Halloysite Nanotubes/Wheat Starch Nanocomposites." *Carbohydrate Polymers* 89 (3): 920-7. doi: 10.1016/j.carbpol.2012.04.037.

Schmitt, Helene, Nicolas Creton, Kalappa Prashantha, Jeremie Soulestin, Marie-France Lacrampe and Patricia Krawczak. 2015. "Preparation and Characterization of Plasticized Starch/Halloysite Porous Nanocomposites Possibly Suitable for Biomedical Applications." *Journal of Applied Polymer Science* 132 (4): 1-9. doi: 10.1002/app.41341.

Sellam, Charline, Zhi Zhai, Hediyeh Zahabi, Olivier T. Picot, Hua Deng, Qiang Fu, Emiliano Bilotti & Ton Peijs. 2015. "High Mechanical Reinforcing Efficiency of Layered Poly(Vinyl Alcohol)–Graphene Oxide Nanocomposites." *Nanocomposites* 1 (2): 89-95. doi: 10.1179/2055033215y.0000000001.

Seymour, G.B. and G.A. Tucker. 1993. "Avocado." In *Biochetnistry of Fruit Ripening*, ed. J. E. Taylor G. B. Seymour, G. A.Tucker, 53-82. Malaysia: Springer.

Shah, Aamer Ali, Fariha Hasan, Abdul Hameed and Safia Ahmed. 2008. "Biological Degradation of Plastics: A Comprehensive Review." *Biotechnology Advances* 26 (3): 246-65. doi: 10.1016/j.biotechadv.2007.12.005.

Shahabi-Ghahfarrokhi, I.; Goudarzi, V.; and Babaei-Ghazvini, A. 2019. "Production of Starch Based Biopolymer by Green Photochemical Reaction at Different UV Region as a Food Packaging Material: Physicochemical Characterization." *International Journal of Biological Macromolecules* 122: 201-209. doi: 10.1016/j.ijbiomac.2018.10.154.

Shi, Rui, Jingliang Bi, Zizheng Zhang, Aichen Zhu, Dafu Chen, Xinhua Zhou, Liqun Zhang and Wei Tian. 2008. "The Effect of Citric Acid on the Structural Properties and Cytotoxicity of the Polyvinyl Alcohol/Starch Films When Molding at High Temperature." *Carbohydrate Polymers* 74 (4): 763-770. doi: 10.1016/j.carbpol.2008.04.045.

Shi, Rui, Zizheng Zhang, Quanyong Liu, Yanming Han, Liqun Zhang, Dafu Chen and Wei Tian. 2007. "Characterization of Citric Acid/Glycerol Co-Plasticized Thermoplastic Starch Prepared by Melt Blending." *Carbohydrate Polymers* 69 (4): 748-755. doi: 10.1016/j.carbpol.2007.02.010.

Shuai, Xinto, Yong He, Naoki Askawa, and Yoshio Inoue. 2000. "Miscibility and Phase Structure of Binary Blends of Poly(L-Lactide) and Poly(Vinyl Alcohol)." *Journal of Applied Polymer Science* 81: 762-772.

Siddaramaiah, Baldev Raj, and R. Somashekar. 2003. "Structure–Property Relation in Polyvinyl Alcohol/Starch Composites." *Journal of Applied Polymer Science* 91: 630-635.

Silvestre, Clara, Donatella Duraccio and Sossio Cimmino. 2011. "Food Packaging Based on Polymer Nanomaterials." *Progress in Polymer Science* 36 (12): 1766-1782. doi: 10.1016/j.progpolymsci.2011.02.003.

Sin, Lee Tin, A.R. Rahmat, W.A.W.A. Rahman, Zhao-Yan Sun, and A.A. Samad. 2010a. "Rheology and Thermal Transition State of Polyvinyl Alcohol–Cassava Starch Blends." *Carbohydrate Polymers* 81 (3): 737-739. doi: 10.1016/j.carbpol.2010.03.044.

Sin, Lee Tin, W.A.W.A. Rahman, A.R. Rahmat, and M.I. Khan. 2010b. "Detection of Synergistic Interactions of Polyvinyl Alcohol–Cassava Starch Blends through Dsc." *Carbohydrate Polymers* 79 (1): 224-226. doi: 10.1016/j.carbpol.2009.08.003.

Sin, Lee Tin, W.A.W.A. Rahman, A.R. Rahmat, and M. Mokhtar. 2011. "Determination of Thermal Stability and Activation Energy of Polyvinyl Alcohol–Cassava Starch Blends." *Carbohydrate Polymers* 83 (1): 303-305. doi: 10.1016/j.carbpol.2010.07.049.

Singha, A. S. and Himanshu Kapoor. 2014. "Effects of Plasticizer/Cross-Linker on the Mechanical and Thermal Properties of Starch/PVA Blends." *Iranian Polymer Journal* 23 (8): 655-662. doi: 10.1007/s13726-014-0260-9.

Siracusa, Valentina 2012. "Food Packaging Permeability Behaviour: A Report." *International Journal of Polymer Science* 2012: 1-11. doi: 10.1155/2012/302029.

Siracusa, Valentina, Pietro Rocculi, Santina Romani and Marco Dalla Rosa. 2008. "Biodegradable Polymers for Food Packaging: A Review." *Trends in Food Science and Technology* 19: 634-643. doi: 10.1016/j.tifs.2008.07.003.

Song, Kenan, Yiying Zhang, Jiangsha Meng, Emily C. Green, Navid Tajaddod, Heng Li and Marilyn L. Minus. 2013. "Structural Polymer-Based Carbon Nanotube Composite Fibers: Understanding the Processing–Structure–Performance Relationship". *Materials 6*: 2543-2577. doi:10.3390/ma6062543

Sorrentino, Andrea, Giuliana Gorrasi and Vittoria Vittoria. 2007. "Potential Perspectives of Bio-Nanocomposites for Food Packaging Applications." *Trends in Food Science & Technology* 18 (2): 84-95. doi: 10.1016/j.tifs.2006.09.004.

Souza, Victor Gomes Lauriano and Ana Luisa Fernando. 2016. "Nanoparticles in Food Packaging: Biodegradability and Potential Migration to Food—a Review." *Food Packaging and Shelf Life* 8: 63-70. doi: 10.1016/j.fpsl.2016.04.001.

Spiridon, Iuliana, Maria Cristina Popescu, Ruxanda Bodarlau, and Cornelia Vasile. 2008. "Enzymatic Degradation of Some Nanocomposites of Poly(Vinyl Alcohol) with Starch." *Polymer Degradation and Stability* 93 (10): 1884-1890. doi: 10.1016/j.polymdegradstab.2008.07.017.

Sreedhar, B., D. K. Chattopadhyay, M. Sri Hari Karunakar, and A. R. K. Sastry. 2006. "Thermal and Surface Characterization of Plasticized Starch Polyvinyl Alcohol Blends Crosslinked with Epichlorohydrin." *Journal of Applied Polymer Science* 101 (1): 25-34. doi: 10.1002/app.23145.

Sreedhar, B., M. Sairam, D. K. Chattopadhyay, P. A. Syamala Rathnam, and D. V. Mohan Rao. 2005. "Thermal, Mechanical, and Surface Characterization of Starch-Poly(Vinyl Alcohol) Blends and Borax-Crosslinked Films." *Journal of Applied Polymer Science* 96 (4): 1313-1322. doi: 10.1002/app.21439.

Sreekumar, P. A., Mamdouh A. Al-Harthi, and S. K. De. 2012. "Effect of Glycerol on Thermal and Mechanical Properties of Polyvinyl Alcohol/Starch Blends." *Journal of Applied Polymer Science* 123: 135-142. doi: 10.1002/app.3446510.1002/app.

Sridhar, V. and D. K. Tripathy. 2006. "Barrier Properties of Chlorobutyl Nanoclay Composites." *Journal of Applied Polymer Science* 101 (6): 3630-3637. doi: 10.1002/app.22722.

Strawhecker, K. E. and E. Manias. 2000. "Structure and Properties of Poly(Vinyl Alcohol)/$Na^+$Montmorillonite Nanocomposites." *Chemistry of Materials* 12: 29432949.

Sustainable Packaging Coalition. 2011. "Definition-of-Sustainable-Packaging." *Available online at: https://sustainablepackaging.org/wp-content/uploads/2017/09/ Definition-of-Sustainable-Packaging.pdf (Accessed 1 October, 2011).* 2: 1-10.

Taghizadeh, Mohammad Taghi, Zahra Abbasi, and Zainab Nasrollahzade. 2011. "Study of Enzymatic Degradation and Water Absorption of Nanocomposites Starch/Polyvinyl Alcohol and Sodium Montmorillonite Clay." *Journal of the Taiwan Institute of Chemical Engineers*. doi: 10.1016/j.jtice.2011.07.006.

Takahashi, S., H.A. Goldberg, C.A. Feeney, D.P. Karim, M. Farrell, K. O'Leary and D.R. Paul. 2006. "Gas Barrier Properties of Butyl Rubber/Vermiculite Nanocomposite Coatings." *Polymer* 47 (9): 3083-3093. doi: 10.1016/j.polymer.2006.02.077.

Takasu, Akinori, Keigo Aoi, Maki Tsuchiya, Masahiko Okada. 1998. "New Chitin-Based Polymer Hybrids, 4: Soil Burial Degradation Behavior of Poly(Vinyl Alcohol)/Chitin Derivative Miscible Blends." *Journal of Applied Polymer Science* 73: 1171-1179.

Talja, Riku A., Harry Hele´n , Yrjo¨ H. Roos, and Kirsi Jouppila. 2007. "Effect of Various Polyols and Polyol Contents on Physical and Mechanical Properties of Potato Starch-Based Films." *Carbohydrate Polymers* 67 (3): 288-295. doi: 10.1016/j.carbpol.2006.05.019.

Tănase, Elisabeta Elena, Mona Elena Popa, Maria Rapa, and Ovidiu Popa. 2015. "Preparation and Characterization of Biopolymer Blends Based on Polyvinyl Alcohol and Starch." *Romanian Biotechnological Letters* 20 (20): 10306-10315.

Tânase, Elisabeta Elena, Vlad Ioan Popa, Mona ElenaPopa, Maria Râpâ and Ovidiu Popa. 2016. "Biodegradation Study of Some Food Packaging Biopolymers Based on PVA." *Bulletin UASVM Animal Science and Biotechnologies* 73 (1): 1-5. doi: 10.15835/buasvmcn-asb.

Tan B. and N.L. Thomas. 2016. "A Review of the Water Barrier Properties of Polymer/Clay and Polymer/Graphene Nanocomposites." *Journal of Membrane Science* 514: 595-612. doi: 10.1016/j.memsci.2016.05.026.

Tang, Shangwen, Peng Zou, Hanguo Xiong and Huali Tang. 2008. "Effect of Nano-Sio2 on the Performance of Starch/Polyvinyl Alcohol Blend Films." *Carbohydrate Polymers* 72 (3): 521-526. doi: 10.1016/j.carbpol.2007.09.019.

Tang, Xiaozhi and Sajid Alavi. 2011. "Recent Advances in Starch, Polyvinyl Alcohol Based Polymer Blends, Nanocomposites and Their Biodegradability." *Carbohydrate Polymers* 85: 7-16. doi: 10.1016/j.carbpol.2011.01.030.

Tang, Xiaozhi and Sajid Alavi. 2012. "Structure and Physical Properties of Starch/Poly Vinyl Alcohol/Laponite Rd Nanocomposite Films." *Journal of Agricultural and Food Chemistry* 60 (8): 1954-62. doi: 10.1021/jf2024962.

Tee, Tiam-Ting, Lee Tin Sin, R. Gobinath, Soo-Tueen Bee, David Hui, A.R. Rahmat, Ing Kong, and QingHong Fang. 2013. "Investigation of Nano-Size Montmorillonite on Enhancing Polyvinyl Alcohol–Starch Blends Prepared Via Solution Cast Approach." *Composites Part B: Engineering* 47: 238-247. doi: 10.1016/j.compositesb.2012.10.033.

Teodorescu, Mirela, Maria Bercea and Simona Morariu. 2018. "Biomaterials of Poly(Vinyl Alcohol) and Natural Polymers." *Polymer Reviews* 58 (2): 247-287. doi: 10.1080/15583724.2017.1403928.

Thakore, I. M., Sonal Desai, B. D Sarawade and Surekha Devi. 2001. "Studies on Bioderadability, Morphology and Theromechanical Properties of Ldpe/Modified Starch Blend." *European Polymer Journal* 37.

Tian, Huafeng, Jiaan Yan, A. Varada Rajulu, Aimin Xiang and Xiaogang Luo. 2017a. "Fabrication and Properties of Polyvinyl Alcohol/Starch Blend Films: Effect of Composition and Humidity." *International Journal of Biological Macromolecules* 96: 518-523. doi: 10.1016/j.ijbiomac.2016.12.067.

Tian, Huafeng, Kai Wang, Di Liu, Jiaan Yan, Aimin Xiang and A. Varada Rajulu. 2017b. "Enhanced Mechanical and Thermal Properties of Poly (Vinyl Alcohol)/Corn Starch Blends by Nanoclay Intercalation." *International Journal of Biological Macromolecules* 101: 314-320. doi: 10.1016/j.ijbiomac.2017.03.111.

Tripathi, S., G.K. Mehrotra, and P.K. Dutta. 2009. "Physicochemical and Bioactivity of Cross-Linked Chitosan-PVA Film for Food Packaging Applications." *International Journal of Biological Macromolecules* 45 (4): 372-6. doi: 10.1016/j.ijbiomac.2009.07.006.

Tudorachi, N., C.N. Cascaval, M. Rusu, M. Pruteanu. 2000. "Testing of Polyvinyl Alcohol and Starch Mixtures as Biodegradable Polymeric Materials." *Polymer Testing* 19: 785-799.

Tully, Joshua, Rawil Fakhrullin, and Yuri Lvov. 2015. "Halloysite Clay Nanotube Composites with Sustained Release of Chemicals." In *Nanomaterials and Nanoarchitectures*, ed. T. Wagner M. Bardosova, 87-118. Dordrecht: Springer Netherlands.

Van de Velde, K. and P. Kiekens. 2002. "Biopolymers: Overview of Several Properties and Consequences on Their Applications." *Polymer Testing* 21: 433-442.

Van den Broek, Lambertus A.M., Rutger J.I. Knoop, Frans H.J. Kappen, and Carmen G. Boeriu. 2015. "Chitosan Films and Blends for Packaging Material." *Carbohydrate Polymers* 116: 237-42. doi: 10.1016/j.carbpol.2014.07.039.

Vergaro, Viviana, Elshad Abdullayev, Yuri M. Lvov, Ross Rinaldi, Andre Zeitoun, and Stefano Leporatti. 2010. "Cytocompatibility and Uptake of Halloysite Clay Nanotubes." *Biomacromolecules* 11: 820-826.

Visakh, P.M. 2015. " Starch: State-of-the-Art, New Challenges and Opportunities." In *Starch-Based Blends, Composites and Nanocomposites*, ed. Visakh P.M. and Long Yu, 1-16. Royal Society of Chemistry.

Voss, Agnieszka, Robert W. Stark, and Christian Dietz. 2014. "Surface Versus Volume Properties on the Nanoscale: Elastomeric Polypropylene." *Macromolecules* 47 (15): 5236-5245. doi: 10.1021/ma500578e.

Wagner, Aaron L., Sarah Cooper, and Michael Riedlinger. 2005. "Natural Nanotubes Enhance Biodegradable and Biocompatible Nanocomposites." *Industrial Biotechnology* 1 (3): 190-193.

Wang, Wentao, Hui Zhang, Yangyong Dai, Hanxue Hou and Haizhou Dong. 2015. "Effects of Low Poly(Vinyl Alcohol) Content on Properties of Biodegradable Blowing Films Based on Two Modified Starches." *Journal of Thermoplastic Composite Materials* 30 (7): 1017-1030. doi: 10.1177/0892705715614080.

Wenzel, Robert N. . 1949. "Surface Roughness and Contact Angle." *The Journal of Physical and Colloid Chemistry* 53 (9): 1466-1467 doi: DOI: 10.1021/j150474a015.

Wexler, Arnold and Saburo Hasegawa. 1954. "Relative Humidity-Temperature Relationships of Some Saturated Solutions in the Temperature Range 0 to 50 ºC." *Journal of Resarch of the National Bureau of Standards* 53 (1): 19-26.

Whistler, Roy L. and James Daniel. 2000. "Starch." In *Encyclopedia of Chemical Technology*, ed. Kirk-Othmer, 1-18. John Wiley and Sons, Inc.

Wiles, J. L., P. J. Vergano, F. H. Barron, J. M. Bunn and R. F. Testin. 2000. "Water Vapor Transmission Rates and Sorption Behavior of Chitosan Films." *Journal of Food Science* 65 (7).

Winston, Paul W. and Donald Bates. 1960. "Saturated Solutions for the Control of Humidity in Biological Research." *Ecology* 41 (1): 232-237.

Wu, Zhijun, Jingjing Wu, Tingting Peng , Yutong Li, Derong Lin, Baoshan Xing, Chunxiao Li, Yuqiu Yang, Li Yang, Lihua Zhang, Rongchao Ma, WeixiongWu, Xiaorong Lv, Jianwu Dai and Guoquan Han. 2017. "Preparation and Application

of Starch/Polyvinyl Alcohol/Citric Acid Ternary Blend Antimicrobial Functional Food Packaging Films." *Polymers* 9 (12): 102. doi: 10.3390/polym9030102.

Xie, Yanfang, Peter R. Chang, Shujun Wang, Jiugao Yu, and Xiaofei Ma. 2011. "Preparation and Properties of Halloysite Nanotubes/Plasticized Dioscorea Opposita Thunb. Starch Composites." *Carbohydrate Polymers* 83: 186-191. doi: 10.1016/j.carbpol.2010.07.039.

Xu, Yuxi, Wenjing Hong, Hua Bai, Chun Li, and Gaoquan Shi. 2009. "Strong and Ductile Poly(Vinyl Alcohol)/Graphene Oxide Composite Films with a Layered Structure." *Carbon* 47 (15): 3538-3543. doi: 10.1016/j.carbon.2009.08.022.

Yeh, Jen-Taut, Ming-Chien Yang, Ching-Ju Wu, Xiong Wu and Chin-San Wu. 2008. "Study on the Crystallization Kinetic and Characterization of Poly(Lactic Acid) and Poly(Vinyl Alcohol) Blends." *Polymer-Plastics Technology and Engineering* 47 (12): 1289-1296. doi: 10.1080/03602550802497958.

Yin, Yeping, Jianfang Li, Yingchun Liu and Zhong Li. 2005. "Starch Crosslinked with Poly(Vinyl Alcohol) by Boric Acid." *Journal of Applied Polymer Science* 96 (4): 1394-1397. doi: 10.1002/app.21569.

Yoon, Soon-Do, Sung-Hyo Chough, and Hye-Ryoung Park. 2006. "Properties of Starch-Based Blend Films Using Citric Acid as Additive. Ii." *Journal of Applied Polymer Science* 100 (3): 2554-2560. doi: 10.1002/app.23783.

Yoon, Soon-Do, Sung-Hyo Chough, and Hye-Ryoung Park. 2007. "Preparation of Resistant Starch/Poly(Vinyl Alcohol) Blend Films with Added Plasticizer and Crosslinking Agents." *Journal of Applied Polymer Science* 106 (4): 2485-2493. doi: 10.1002/app.26755.

Young, J. F. . 1967. "Humidity Control in the Laboratory Using Salt Solutions- Areview." *Journal of Applied Chemistry* 17: 241-245.

Youssef, Ahmed M. 2013. "Polymer Nanocomposites as a New Trend for Packaging Applications." *Polymer-Plastics Technology and Engineering* 52 (7): 635-660. doi: 10.1080/03602559.2012.762673.

Youssef, Ahmed M., Samah. M. El-Sayed. 2018. "Bionanocomposites Materials for Food Packaging Applications: Concepts and Future Outlook." *Carbohydrate Polymers* 193: 19-27. doi: 10.1016/j.carbpol.2018.03.088.

Yuan, Peng, Daoyong Tan, and Faïza Annabi-Bergaya. 2015. "Properties and Applications of Halloysite Nanotubes: Recent Research Advances and Future Prospects." *Applied Clay Science* 112-113: 75-93. doi: 10.1016/j.clay.2015.05.001.

Yuan, Yuehua and T. Randall Lee. 2013. "Contact Angle and Wetting Properties." In *Surface Science Techniques*, ed. G. Bracco and B. Holst, 3-34. Berlin Heidelberg: Springer.

Zagho, Moustafa M., Mahmoud M. Khader. 2016. "The Impact of Clay Loading on the Relative Intercalation of Poly(Vinyl Alcohol)-Clay Composites." *Journal of Materials Science and Chemical Engineering,* 4: 20-31. doi: 10.4236/msce.2016.410003.

Zanela, Juliano, Ana Paula Bilck, Maira Casagrande, Maria Victória Eiras Grossmann and Fabio Yamashita. 2018. "Polyvinyl Alcohol (PVA) Molecular Weight and Extrusion Temperature in Starch/PVA Biodegradable Sheets." *Polímeros* 28 (3): 256-265. doi: 10.1590/0104-1428.03417.

Zanela, Juliano, Juliana Bonametti Olivato, Adriana Passos Dias, Maria Victoria Eiras Grossmann and Fabio Yamashita. 2015. "Mixture Design Applied for the Development of Films Based on Starch, Polyvinyl Alcohol, and Glycerol." *Journal of Applied Polymer Science* 132 (43): n/a-n/a. doi: 10.1002/app.42697.

Zhang, Ruiyun, Wenyu Xu, and Fuqing Jiang. 2012. "Fabrication and Characterization of Dense Chitosan/Polyvinyl-Alcohol/Poly-Lactic-Acid Blend Membranes." *Fibers and Polymers* 13 (5): 571-575. doi: 10.1007/s12221-012-0571-4.

Zhang, Yachuan and J. H. Han. 2006. "Mechanical and Thermal Characteristics of Pea Starch Films Plasticized with Monosaccharides and Polyols." *Journal of Food Science* 71 (2): 109-118.

Zhang, Yi, Aidong Tang, Huaming Yang and Jing Ouyang. 2016. "Applications and Interfaces of Halloysite Nanocomposites." *Applied Clay Science* 119: 8-17. doi: 10.1016/j.clay.2015.06.034.

Zhou, Jiang, Yunhai Ma, Lili Ren, Jin Tong, Ziqin Liu and Liang Xie. 2009. "Preparation and Characterization of Surface Crosslinked TPS/PVA Blend Films." *Carbohydrate Polymers* 76 (4): 632-638. doi: 10.1016/j.carbpol.2008.11.028.

Zhou, Wen You, Baochun Guo, Mingxian Liu, Ruijuan Liao, A. Bakr M. Rabie and Demin Jia. 2010. "Poly(Vinyl Alcohol)/Halloysite Nanotubes Bionanocomposite Films: Properties and in Vitro Osteoblasts and Fibroblasts Response." *Journal of Biomedical Materials Research A* 93 (4): 1574-87. doi: 10.1002/jbm.a.32656.

Zhuang, Peng-Yu, You-Liang Li, Li Fan, Jun Linb, and Qiao-Ling Hu. 2012. "Modification of chitosan membrane with poly(vinyl alcohol) and

biocompatibility evaluation". *International Journal of Biological Macromolecules* 50: 658– 663. doi: 10.1016/j.ijbiomac.2012.01.026.

Zhu, Yanwu, Shanthi Murali, Weiwei Cai, Xuesong Li, Ji Won Suk, Jeffrey R. Potts, and Rodney S. Ruoff. 2010. "Graphene and Graphene Oxide: Synthesis, Properties, and Applications." *Advanced Materials* 22 (35): 3906-24. doi: 10.1002/adma.201001068.

Zou, Guo-Xiang, Jin-Ping Qu, and Xin-Liang Zou. 2007. "Optimization of Water Absorption of Starch/PVA Composites." *Polymer Composites* 28 (5): 674-679. doi: 10.1002/pc.20333.

Zou, Guo-Xiang, Jin Ping-Qu and Xin Liang-Zou. 2008. "Extruded Starch/PVA Composites: Water Resistance, Thermal Properties, and Morphology." *Journal of Elastomers & Plastics* 40 (4): 303-316. doi: 10.1177/0095244307085787.

# APPENDIX I: Summary of Research Data

Table I-1: Mechanical properties of neat PVA, PVA blends and PVA/ST/GL/HNT bionanocomposites at different HNT contents

| Material composition | Tensile strength (MPa) | Elongation at break (%) | Young's modulus (MPa) |
|---|---|---|---|
| Neat PVA | 57.75± 3.86 | 13.24± 2.36 | 1232.17± 21.91 |
| PVA/GL | 12.73± 1.27 | 334.33± 10.46 | 42.44± 7.35 |
| PVA/ST | 41.39± 5.37 | 6.4± 1.37 | 1881.36± 15.37 |
| PVA/ST/GL | 13.24± 0.87 | 418.13± 9.05 | 93.23± 10.23 |
| PVA/ST/GL/0.25 wt% HNTs | 15.9± 1.26 | 440.49± 12.39 | 125.93± 5.73 |
| PVA/ST/GL/0.5 wt% HNTs | 13.69± 0.99 | 251.21± 8.74 | 191.66± 4.28 |
| PVA/ST/GL/1 wt% HNTs | 11.82± 1.83 | 267.21± 6.72 | 232.12± 7.69 |
| PVA/ST/GL/3 wt% HNTs | 10.34± 0.67 | 243.07± 10.07 | 153.98± 1.45 |
| PVA/ST/GL/5 wt% HNTs | 8.31± 0.75 | 238.50± 4.67 | 134.00± 2.47 |

Table I-2: Water resistance of neat PVA, PVA blends and PVA/ST/GL/HNT bionanocomposites at different HNT contents

| **Material composition** | **$W_a$ (%)** | **$W_s$ (%)** | **Water contact angle (º)** |
|---|---|---|---|
| Neat PVA | 127.61± 4.39 | 45.4± 2.09 | 28.35± 1.90 |
| PVA/GL | 114.58± 5.12 | 41.67± 3.057 | 28.68± 3.46 |
| PVA/ST | 168.56± 5.65 | 47.53± 4.15 | 18.65± 2.71 |
| PVA/ST/GL | 128.23± 3.27 | 40.45± 5.73 | 25.57± 1.08 |
| PVA/ST/GL/0.25 wt% HNTs | 84.85± 1.97 | 28.3± 3.18 | 36.67± 2.16 |
| PVA/ST/GL/0.5 wt% HNTs | 78.56± 4.29 | 24.35± 1.09 | 41.01± 1.97 |
| PVA/ST/GL/1 wt% HNTs | 74.23± 3.46 | 22.64± 2.47 | 44.35± 2.04 |
| PVA/ST/GL/3 wt% HNTs | 73.39± 4.51 | 21.13± 1.36 | 46.04± 2.10 |
| PVA/ST/GL/5 wt% HNTs | 71.49± 2.31 | 21.01± 3.21 | 46.93± 1.28 |

Table I-3: Biodegradation rates of neat PVA, PVA blends and PVA/ST/GL/HNT bionanocomposites at different HNT contents

| Time (week) | Neat PVA | PVA blends | | | PVA/ST/GL/HNT bionanocomposites | | | | |
|---|---|---|---|---|---|---|---|---|---|
| | | PVA/GL | PVA/ST | PVA/ST/GL | 0.25 wt% | 0.5 wt% | 1 wt% | 3 wt% | 5 wt% |
| 0 | 0 | 0 | 0 | 0 | 0 | 0 | 0 | 0 | 0 |
| 1 | 1.12± 0.62 | 5.34± 0.79 | 11.03± 1.82 | 19.54± 0.36 | 10.78± 0.22 | 11.09± 0.61 | 11.23± 0.32 | 11.07± 0.61 | 10.65± 0.86 |
| 2 | 2.31± 0.94 | 12.15± 0.53 | 24.33± 0.28 | 32.90± 0.18 | 24.73± 1.19 | 23.86± 0.26 | 24.27± 0.85 | 22.90± 0.55 | 24.69± 0.39 |
| 3 | 3.48± 0.31 | 19.18± 0.15 | 35.35± 0.61 | 50.28± 0.21 | 42.76± 0.76 | 40.21± 0.16 | 37.06± 0.11 | 36.65± 0.74 | 40.87± 0.93 |
| 4 | 4.18± 0.58 | 19.5± 0.51 | 36.83± 1.27 | 51.74± 0.75 | 43.85± 0.49 | 42.53± 0.82 | 37.32± 0.83 | 38.68± 0.91 | 43.13± 0.70 |
| 5 | 4.6± 0.589 | 19.92± 0.89 | 37.58± 0.20 | 52.19± 0.33 | 44.97± 0.30 | 42.74± 0.73 | 38.61± 0.71 | 40.21± 0.97 | 43.39± 0.41 |
| 6 | 4.99± 0.69 | 20.45± 0.54 | 38.20± 0.41 | 52.56± 0.84 | 45.37± 0.34 | 42.97± 0.46 | 38.82± 0.46 | 41.55± 0.67 | 43.78± 0.87 |
| 7 | 5.12±0.51 | 20.94± 0.84 | 38.46± 0.60 | 52.94± 0.35 | 45.53± 0.24 | 43.28± 0.62 | 39.09± 1.93 | 42.09± 0.95 | 44.19± 0.92 |
| 8 | 5.22± 0.83 | 21.48± 0.38 | 38.69± 0.44 | 53.53± 0.79 | 45.87± 0.20 | 43.67± 0.49 | 39.25± 0.23 | 42.61± 0.65 | 44.46± 0.47 |
| 9 | 5.30± 0.66 | 21.85± 0.38 | 38.82±0.51 | 53.90± 0.58 | 46.22± 0.78 | 44.05± 0.99 | 39.46± 0.62 | 42.88± 0.98 | 44.80± 0.28 |
| 10 | 5.38± 0.31 | 22.05± 0.92 | 38.95± 0.58 | 54.42± 0.95 | 47.44± 0.68 | 44.40± 0.47 | 39.62± 0.65 | 43.55± 0.40 | 45.00± 0.80 |
| 11 | 5.48± 0.63 | 22.47± 0.46 | 39.05± 0.40 | 54.87± 0.53 | 47.67± 0.93 | 44.81± 1.07 | 39.89± 0.40 | 44.04± 0.36 | 45.28± 0.57 |

| | | | | | | | | | |
|---|---|---|---|---|---|---|---|---|---|
| 12 | 5.58± 0.95 | 22.92± 0.40 | 39.18± 0.47 | 55.61± 0.12 | 47.91± 1.86 | 45.12± 0.32 | 40.16± 1.33 | 44.60± 0.72 | 45.53± 0.91 |
| 15 | 5.69± 0.27 | 23.17± 1.01 | 39.24± 0.98 | 56.20± 0.56 | 48.28± 0.71 | 45.48± 0.25 | 40.91± 0.22 | 44.85± 0.74 | 45.34± 0.56 |
| 18 | 5.74± 0.43 | 23.25± 0.33 | 39.41± 0.36 | 56.72± 0.21 | 48.50± 0.55 | 45.77± 0.58 | 41.12± 0.41 | 44.90± 0.68 | 45.53± 0.87 |
| 21 | 5.80± 0.75 | 23.29± 0.56 | 39.49± 0.43 | 56.84± 0.14 | 48.57± 0.40 | 46.02± 0.90 | 41.21± 0.45 | 44.93± 0.61 | 45.67± 0.42 |
| 24 | 5.87±0.25 | 23.33± 0.56 | 39.54± 0.47 | 56.94± 0.18 | 48.67± 0.64 | 46.09± 0.86 | 41.28± 0.57 | 45.00± 0.51 | 45.80± 0.27 |

Table I-4: WVTR of neat PVA, PVA blends and PVA/ST/GL/HNT bionanocomposites at different HNT contents and different temperatures

| **Material Composition** | **WVTR (g/h·m$^2$)** | | | |
|---|---|---|---|---|
| | **25 ºC** | **35 ºC** | **45 ºC** | **55 ºC** |
| Neat PVA | 39.95± 3.90 | 41.94± 1.75 | 43.60± 2.37 | 45.97± 2.73 |
| PVA/GL | 42.78± 4.59 | 47.30± 0.52 | 58.42± 6.03 | 65.40± 6.01 |
| PVA/ST | 48.45± 2.78 | 55.36± 4.70 | 62.94± 5.35 | 69.76± 2.15 |
| PVA/ST/GL | 37.86± 4.15 | 46.28± 1.64 | 59.37± 1.47 | 62.89± 3.70 |
| PVA/ST/GL/0.25 wt% HNTs | 28.17± 1.09 | 38.49± 2.39 | 48.38± 2.36 | 55.69± 4.58 |
| PVA/ST/GL/0.5 wt% HNTs | 23.45± 3.08 | 29.30± 1.88 | 39.80± 2.09 | 44.09± 2.94 |
| PVA/ST/GL/1 wt% HNTs | 19.81± 0.64 | 23.64± 1.09 | 33.16± 4.15 | 39.04± 1.26 |
| PVA/ST/GL/3 wt% HNTs | 18.50± 1.60 | 21.84± 0.93 | 32.58± 1.24 | 38.26± 3.72 |
| PVA/ST/GL/5 wt% HNTs | 18.04± 0.73 | 20.96± 3.20 | 32.00± 2.06 | 36.11± 1.06 |

Table I-5: WVP of neat PVA, PVA blends and PVA/ST/GL/HNT bionanocomposites at different HNT contents and different temperatures

| **Material Composition** | **WVP (×10$^{-3}$ g·m/m$^2$·h·kPa)** | | | |
|---|---|---|---|---|
| | **25 ºC** | **35 ºC** | **45 ºC** | **55 ºC** |
| Neat PVA | 2.81± 0.17 | 2.85± 0.57 | 2.91± 0.34 | 2.95± 0.25 |
| PVA/GL | 3.28± 0.30 | 3.50± 0.29 | 4.30± 0.34 | 5.05± 0.14 |
| PVA/ST | 3.68± 0.23 | 3.99± 0.31 | 4.47± 0.11 | 5.25± 0.21 |
| PVA/ST/GL | 3.30± 0.27 | 3.35± 0.71 | 3.81± 0.58 | 4.49± 0.19 |
| PVA/ST/GL/0.25 wt% HNTs | 2.64± 0.19 | 2.76± 0.83 | 2.98± 0.26 | 3.17± 0.32 |
| PVA/ST/GL/0.5 wt% HNTs | 2.04± 0.49 | 2.25± 0.15 | 2.30± 0.36 | 2.67± 0.50 |
| PVA/ST/GL/1 wt% HNTs | 1.67± 0.22 | 1.80± 0.34 | 2.08± 0.30 | 2.27± 0.42 |
| PVA/ST/GL/3 wt% HNTs | 1.25± 0.38 | 1.38± 0.28 | 1.76± 0.29 | 2.05± 0.18 |
| PVA/ST/GL/5 wt% HNTs | 0.97± 0.20 | 1.29± 0.67 | 1.65± 0.14 | 1.97± 0.33 |

Table I-6: WVTR of neat PVA, PVA blends and PVA/ST/GL/HNT bionanocomposites at different HNT contents and different RH gradients

| **Material Composition** | **WVTR (g/h·m$^2$)** | | | |
|---|---|---|---|---|
| | **10% ΔRH** | **30% ΔRH** | **50% ΔRH** | **70% ΔRH** |
| Neat PVA | 7.82± 0.42 | 18.42± 0.85 | 39.95± 0.93 | 48.39± 0.87 |
| PVA/GL | 9.22± 0.51 | 24.30± 0.74 | 42.78± 0.79 | 59.39± 1.26 |
| PVA/ST | 12.52± 0.26 | 29.76± 0.29 | 48.45± 1.02 | 70.09± 3.17 |
| PVA/ST/GL | 10.17± 0.83 | 26.39± 0.60 | 37.86± 0.83 | 67.66± 0.98 |
| PVA/ST/GL/0.25 wt% HNTs | 8.67± 0.27 | 18.42± 0.28 | 28.17± 0.79 | 53.17± 0.52 |
| PVA/ST/GL/0.5 wt% HNTs | 7.05± 0.80 | 16.25± 0.24 | 23.45± 0.36 | 48.24± 0.73 |
| PVA/ST/GL/1 wt% HNTs | 6.33± 0.68 | 14.96± 0.31 | 19.81± 0.64 | 31.92± 0.49 |
| PVA/ST/GL/3 wt% HNTs | 5.96± 0.49 | 13.67± 0.47 | 18.50± 0.86 | 29.32± 0.90 |
| PVA/ST/GL/5 wt% HNTs | 5.70± 0.19 | 13.10± 0.17 | 18.04± 0.35 | 28.90± 0.27 |

Table I-7: WVP of neat PVA, PVA blends and PVA/ST/GL/HNT bionanocomposites at different HNT contents and different RH gradients

| **Material Composition** | **WVP ($\times 10^{-3}$ g·m/h·m$^2$·kPa)** | | | |
|---|---|---|---|---|
| | **10% ΔRH** | **30% ΔRH** | **50% ΔRH** | **70% ΔRH** |
| Neat PVA | 0.88± 0.14 | 1.98± 0.47 | 2.81± 0.70 | 3.15± 0.25 |
| PVA/GL | 1.36±0.11 | 2.29± 0.13 | 3.28± 0.38 | 3.67± 0.31 |
| PVA/ST | 1.98± 0.30 | 2.52± 0.45 | 3.68± 0.43 | 3.82± 0.27 |
| PVA/ST/GL | 1.67± 0.28 | 2.23± 0.72 | 3.30± 0.21 | 3.48± 0.60 |
| PVA/ST/GL/0.25 wt% HNTs | 1.13± 0.17 | 1.97± 0.19 | 2.64± 0.89 | 2.97± 0.32 |
| PVA/ST/GL/0.5 wt% HNTs | 0.80±0.20 | 1.64± 0.26 | 2.04± 0.49 | 2.20± 0.46 |
| PVA/ST/GL/1 wt% HNTs | 0.75± 0.46 | 1.26± 0.99 | 1.67± 0.27 | 1.85± 0.17 |
| PVA/ST/GL/3 wt% HNTs | 0.72± 0.34 | 0.97± 0.27 | 1.15± 0.18 | 1.39± 0.44 |
| PVA/ST/GL/5 wt% HNTs | 0.70± 0.52 | 0.81± 0.43 | 0.87± 0.17 | 1.21± 0.10 |

Table I-8: Gas permeability of neat PVA, PVA blends and PVA/ST/GL/HNT bionanocomposites at different HNT contents

| Material Composition | Gas permeability ($\times 10^{-8}$ m·m$^3$/m$^2$·min·kPa) | |
|---|---|---|
| | Oxygen | Air |
| Neat PVA | 1.83± 0.41 | 1.40± 0.17 |
| PVA/GL | 3.25± 0.35 | 2.48± 0.36 |
| PVA/ST | 3.50± 0.12 | 2.81± 0.08 |
| PVA/ST/GL | 3.14± 0.43 | 2.54± 0.12 |
| PVA/ST/GL/0.25 wt% HNTs | 2.61± 0.18 | 1.96± 0.05 |
| PVA/ST/GL/0.5 wt% HNTs | 2.07± 0.27 | 1.49± 0.28 |
| PVA/ST/GL/1 wt% HNTs | 1.48± 0.19 | 1.13± 0.16 |
| PVA/ST/GL/3 wt% HNTs | 0.99± 0.25 | 0.75± 0.26 |
| PVA/ST/GL/5 wt% HNTs | 0.79± 0.05 | 0.60± 0.15 |

Table I-9: Overall migration rates of neat PVA, PVA blends and PVA/ST/GL/HNT bionanocomposites at different HNT contents based on different food simulants

| Material composition | Overall migration rate (mg/kg) | | |
|---|---|---|---|
| | 10% Ethanol | 50% Ethanol | 3% Acidic acid |
| PVA/ST/GL | 97.45± 2.08 | 32.81± 0.45 | 0.87± 0.27 |
| PVA/ST/GL/0.25 wt% HNTs | 81.44± 3.72 | 26.27± 0.93 | 1.29± 0.53 |
| PVA/ST/GL/0.5 wt% HNTs | 82.71± 0.91 | 27.57± 1.37 | 2.63± 0.37 |
| PVA/ST/GL/1 wt% HNTs | 51.24± 1.61 | 28.02± 2.02 | 5.89± 0.46 |
| PVA/ST/GL/3 wt% HNTs | 52.76± 0.76 | 29.37± 0.83 | 6.88± 0.75 |
| PVA/ST/GL/5 wt% HNTs | 69.1± 3.64 | 36.86± 1.07 | 9.13± 0.39 |

Table I-10: $Al^{+}$ Migration rates of neat PVA, PVA blends and PVA/ST/GL/HNT bionanocomposites at different HNT content based on different food simulants

| **Material composition** | **Migration rate of $Al^{+}$ (mg/kg)** | | |
|---|---|---|---|
| | **10% Ethanol** | **50% Ethanol** | **3% Acidic acid** |
| PVA/ST/GL | 0 | 0 | 0 |
| PVA/ST/GL/0.25 wt% HNTs | 0.87± 0.21 | 0.99± 0.13 | 0.43± 0.35 |
| PVA/ST/GL/0.5 wt% HNTs | 1.33± 0.42 | 1.24± 0.72 | 0.82± 0.09 |
| PVA/ST/GL/1 wt% HNTs | 2.80±0.90 | 1.37±0.26 | 0.93± 0.27 |
| PVA/ST/GL/3 wt% HNTs | 4.19±0.17 | 2.90± 0.33 | 1.01± 0.29 |
| PVA/ST/GL/5 wt% HNTs | 7.54±0.94 | 4.77± 0.74 | 1.13± 0.51 |

Table I-11: $Si^{+}$ migration rates of neat PVA, PVA blends and PVA/ST/GL/HNT bionanocomposites at different HNT content based on different food simulants

| **Material composition** | **Migration rate of $Si^{+}$ (mg/kg)** | | |
|---|---|---|---|
| | **10% Ethanol** | **50% Ethanol** | **3% Acidic acid** |
| PVA/ST/GL | 0 | 0 | 0 |
| PVA/ST/GL/0.25 wt% HNTs | 1.45± 0.19 | 1.44± 0.25 | 0.52± 0.22 |
| PVA/ST/GL/0.5 wt% HNTs | 1.73± 0.37 | 1.67± 0.19 | 1.05± 0.14 |
| PVA/ST/GL/1 wt% HNTs | 3.11± 0.28 | 2.32± 0.26 | 1.75± 0.31 |
| PVA/ST/GL/3 wt% HNTs | 4.21± 0.50 | 2.38± 0.33 | 1.84± 0.11 |
| PVA/ST/GL/5 wt% HNTs | 7.61± 0.81 | 4.36± 0.19 | 2.03± 0.71 |

Table I-12: Relative weight loss of avocado in food packaging tests

| Time (day) | Relative weight loss rate of avocado (%) | | | |
|---|---|---|---|---|
| | **Control** | **Neat PVA** | **PVA/ST/GL** | **PVA/ST/GL/ 1 wt% HNTs** |
| 0 | 0 | 0 | 0 | 0 |
| 1 | 3.78± 0.40 | 1.83± 0.40 | 3.21± 0.21 | 2.60± 0.62 |
| 2 | 6.96± 0.63 | 4.21± 0.13 | 6.10± 1.2 | 4.86± 0.89 |
| 3 | 12.07± 1.17 | 8.43± 0.97 | 10.32± 0.76 | 6.28± 0.33 |
| 4 | 14.90± 0.59 | 10.63± 1.66 | 11.87± 1.50 | 8.670± 0.72 |
| 5 | 16.32± 0.93 | 12.80± 0.61 | 12.89± 0.58 | 9.82± 2.80 |
| 6 | 17.70±446 | 14.10± 1.98 | 14.51±892 | 10.75± 1.34 |
| 7 | 20.40± 2.65 | 16.25± 0.57 | 19.69± 0.90 | 13.08± 0.34 |
| 8 | 22.90± 0.35 | 18.55± 0.43 | 22.15± 2.03 | 15.33± 0.86 |
| 9 | 26.24± 0.48 | 21.98±63 | 24.37± 0.75 | 18.00± 0.46 |
| 10 | 30.50± 3.02 | 24.04± 0.87 | 27.04± 0.97 | 20.69± 1.30 |
| 11 | 32.13± 1.48 | 26.59± 0.81 | 30.65± 2.07 | 22.23± 1.35 |
| 12 | 34.70± 0.84 | 28.43± 0.98 | 33.03± 2.38 | 23.30± 0.67 |
| 13 | 40.86± 2.49 | 30.54± 1.79 | 35.15± 1.73 | 25.240± 0.83 |

Table I-13: Relative weight loss of peach in food packaging tests

| Time (day) | Relative weight loss rate of peach (%) | | | |
|---|---|---|---|---|
| | **Control** | **Neat PVA** | **PVA/ST/GL** | **PVA/ST/GL/1 wt% HNTs** |
| 0 | 0 | 0 | 0 | 0 |
| 1 | 3.54± 0.18 | 2.14± 0.54 | 1.73± 0.11 | 0.65± 0.73 |
| 2 | 5.71± 0.65 | 4.22± 0.46 | 4.05± 0.63 | 2.10± 0.48 |
| 3 | 8.15± 0.40 | 5.69± 0.71 | 5.03± 0.22 | 4.31± 0.54 |
| 4 | 10.17± 0.86 | 7.48± 0.79 | 7.20± 0.46 | 6.27± 0.14 |
| 5 | 11.48± 0.75 | 9.63± 0.34 | 9.42± 0.80 | 7.76± 0.17 |
| 6 | 13.75± 0.94 | 10.74± 0.51 | 11.97± 0.38 | 8.55± 0.66 |
| 7 | 15.07± 0.74 | 12.50± 0.79 | 13.54± 0.37 | 10.10± 0.90 |
| 8 | 17.33± 0.94 | 14.39± 0.30 | 16.65± 0.81 | 10.63± 0.65 |
| 9 | 19.58± 0.71 | 16.31± 0.61 | 17.83± 0.77 | 12.44± 0.38 |
| 10 | 21.85± 0.88 | 17.28± 0.96 | 20.18± 0.89 | 14.17± 0.35 |
| 11 | 24.28± 1.74 | 18.61± 0.77 | 21.54± 0.66 | 15.30± 0.651 |
| 12 | 25.41± 2.48 | 20.08± 1.34 | 24.41± 0.44 | 16.86± 0.51 |
| 13 | 27.35± 0.22 | 21.33± 0.43 | 25.93± 0.34 | 18.05± 0.78 |

# APPENDIX II: Authorship Contribution

**Paper:** Abdullah, Zainab Waheed, Yu Dong, Ian Jeffery Davies, and Salim Barbhuiya. 2017. "PVA, PVA Blends, and Their Nanocomposites for Biodegradable Packaging Application." *Polymer-Plastics Technology and Engineering* 56, no. 12: 1307-344.

**Author's affiliation:**

1- Zainab Waheed Abdullah, School of Civil and Mechanical Engineering, Faculty of Science and Engineering, Curtin University, Perth, Australia.

2- Yu Dong, School of Civil and Mechanical Engineering, Faculty of Science and Engineering, Curtin University, Perth, Australia.

3- Ian Jeffery Davies, School of Civil and Mechanical Engineering, Faculty of Science and Engineering, Curtin University, Perth, Australia.

4- Salim Barbhuiya, Institute for Resilient Infrastructure, University of Leeds. United Kingdom.

| | | Contribution | | | | |
|---|---|---|---|---|---|---|
| | | Conception | Paper drafting | Paper revising | Final approval | Signature |
| Authors | Zainab Waheed Abdullah | × | × | × | × | |
| | Yu Dong | × | | × | × | |
| | Ian Jeffery Davies | | | × | | |
| | Salim Barbhuiya | | | × | | |

**Paper:** Abdullah, Zainab Waheed, and Yu Dong. 2017. "Preparation and Characterisation of Polyvinyl Alcohol (PVA)/ Starch (ST)/ Halloysite Nanotube (HNT) Nanocomposite Films as Renewable Materials." *Journal of Materials Science* 53, no. 5: 3455-3469.

**Author's affiliation:**


1- Zainab Waheed Abdullah, School of Civil and Mechanical Engineering, Faculty of Science and Engineering, Curtin University, Perth, Australia.

2- Yu Dong, School of Civil and Mechanical Engineering, Faculty of Science and Engineering, Curtin University, Perth, Australia.


| | | Contribution | | | | |
|---|---|---|---|---|---|---|
| | | Conception | Paper drafting | Paper revising | Final approval | Signature |
| Authors | Zainab Waheed Abdullah | × | × | × | × | |
| | Yu Dong | × | | × | × | |

**Paper:** Abdullah, Zainab Waheed, and Yu Dong. 2018. "Recent Advances and Perspectives on Starch Nanocomposites for Packaging Applications." *Journal of Materials Science* 53, no. 22: 15319-5339.

**Author's affiliation:**

1- Zainab Waheed Abdullah, School of Civil and Mechanical Engineering, Faculty of Science and Engineering, Curtin University, Perth, Australia.

2- Yu Dong, School of Civil and Mechanical Engineering, Faculty of Science and Engineering, Curtin University, Perth, Australia.

| | | Contribution | | | | |
|---|---|---|---|---|---|---|
| | | Conception | Paper drafting | Paper revising | Final approval | Signature |
| Authors | Zainab Waheed Abdullah | × | × | × | × | |
| | Yu Dong | × | | × | × | |

**Paper:** Abdullah, Zainab Waheed, and Yu Dong. 2019. "Biodegradable and Water Resistant Polyvinyl Alcohol (PVA)/ Starch (ST)/Glycerol (GL)/ Halloysite Nanotube (HNT) Nanocomposite Films for Sustainable Food Packaging." *Frontiers in Materials* 6:58.

**Author's affiliation:**


1- Zainab Waheed Abdullah, School of Civil and Mechanical Engineering, Faculty of Science and Engineering, Curtin University, Perth, Australia.

2- Yu Dong, School of Civil and Mechanical Engineering, Faculty of Science and Engineering, Curtin University, Perth, Australia.


| | | Contribution | | | | |
|---|---|---|---|---|---|---|
| | | Conception | Paper drafting | Paper revising | Final approval | Signature |
| Authors | Zainab Waheed Abdullah | × | × | × | × | |
| | Yu Dong | × | | × | × | |

**Paper:** Abdullah, Zainab Waheed, Yu Dong, Ning Han, Shaomin Liu. 2019. "Water and Gas Barrier Properties of Polyvinyl Alcohol (PVA)/ Starch (ST)/ Glycerol (GL)/ Halloysite Nanotube (HNT) Bionanocomposite Films: Experimental Characterisation and Modelling Approach." *Composites Part B.* 174: 107033. doi.org/10.1016/j.compositesb.2019.107033.

**Author's affiliation:**

1- Zainab Waheed Abdullah, School of Civil and Mechanical Engineering, Faculty of Science and Engineering, Curtin University, Perth, Australia.

2- Yu Dong, School of Civil and Mechanical Engineering, Faculty of Science and Engineering, Curtin University, Perth, Australia.

3- Ning Han, Department of Chemical Engineering, Faculty of Science and Engineering, Curtin University, Australia.

4- Shaomin Liu, Department of Chemical Engineering, Faculty of Science and Engineering, Curtin University, Australia.

| | | Contribution | | | | |
|---|---|---|---|---|---|---|
| | | Conception | Paper drafting | Paper revising | Final approval | Signature |
| Authors | Zainab Waheed Abdullah | × | × | × | × | |
| | Yu Dong | × | | × | × | |
| | Ning Han | × | | | × | |
| | Shaomin Liu | × | | | × | |

**Paper:** Abdullah, Zainab Waheed, Y. Dong. 2020 “Sustainable food packaging materials using bionanocomposite films”, *JEC Composites Magazine*, 134:116-119

**Author’s affiliation:**


1- Zainab Waheed Abdullah, School of Civil and Mechanical Engineering, Faculty of Science and Engineering, Curtin University, Perth, Australia.

2- Yu Dong, School of Civil and Mechanical Engineering, Faculty of Science and Engineering, Curtin University, Perth, Australia.


| | | Contribution | | | | |
|---|---|---|---|---|---|---|
| | | Conception | Paper drafting | Paper revising | Final approval | Signature |
| Authors | Zainab Waheed Abdullah | × | × | × | × | |
| | Yu Dong | × | | × | × | |

**Book:** Abdullah, Zainab Waheed, Yu Dong, Polyvinyl Alcohol/ Halloysite Nanotube Bionanocomposites as Biodegradable Packaging Materials, 6 chapters, Springer Nature, Singapore, in press.

**Author's affiliation:**


1- Zainab Waheed Abdullah, School of Civil and Mechanical Engineering, Faculty of Science and Engineering, Curtin University, Perth, Australia.

2- Yu Dong, School of Civil and Mechanical Engineering, Faculty of Science and Engineering, Curtin University, Perth, Australia.


| | | Contribution | | | | |
|---|---|---|---|---|---|---|
| | | Conception | Paper drafting | Paper revising | Final approval | Signature |
| Authors | Zainab Waheed Abdullah | × | × | × | × | |
| | Yu Dong | × | | × | × | |

# APPENDIX III: Full Copyright Licence Permission

## ELSEVIER LICENSE
## TERMS AND CONDITIONS

Jun 21, 2019

---

This Agreement between Zainab Waheed Abdullah ("You") and Elsevier ("Elsevier") consists of your license details and the terms and conditions provided by Elsevier and Copyright Clearance Center.

| | |
|---|---|
| License Number | 4613530939666 |
| License date | Jun 21, 2019 |
| Licensed Content Publisher | Elsevier |
| Licensed Content Publication | Progress in Polymer Science |
| Licensed Content Title | Bio-nanocomposites for food packaging applications |
| Licensed Content Author | Jong-Whan Rhim, Hwan-Man Park, Chang-Sik Ha |
| Licensed Content Date | October–November 2013 |
| Licensed Content Volume | 38 |
| Licensed Content Issue | 10-11 |
| Licensed Content Pages | 24 |
| Start Page | 1629 |
| End Page | 1652 |
| Type of Use | reuse in a thesis/dissertation |
| Portion | figures/tables/illustrations |
| Number of figures/tables/illustrations | 2 |
| Format | both print and electronic |
| Are you the author of this Elsevier article? | No |
| Will you be translating? | No |

| | |
|---|---|
| Original figure numbers | Fig. 1. General properties required for food packaging materials. And Fig. 2. Classification of biopolymers. The abbreviations of materials mentioned here are listed in the list of abbreviations |
| Title of your thesis/dissertation | Polyvinyl Alcohol/ Starch/ Glycerol/ Halloysite Nanotube Bionanocomposites for Biodegradable Packaging Applications |
| Expected completion date | Dec 2019 |
| Estimated size (number of pages) | 250 |
| Requestor Location | Zainab Waheed Abdullah<br>1/49 Mosaic Street East Shelley. Perth<br><br>Perth, other WA6148<br>Australia<br>Attn: Zainab Waheed Abdullah |
| Publisher Tax ID | GB 494 6272 12 |
| Total | 0.00 USD |

# ELSEVIER LICENSE
# TERMS AND CONDITIONS

Jun 21, 2019

This Agreement between Zainab Waheed Abdullah ("You") and Elsevier ("Elsevier") consists of your license details and the terms and conditions provided by Elsevier and Copyright Clearance Center.

| | |
|---|---|
| License Number | 4613540372783 |
| License date | Jun 21, 2019 |
| Licensed Content Publisher | Elsevier |
| Licensed Content Publication | Carbohydrate Polymers |
| Licensed Content Title | Recent advances in starch, polyvinyl alcohol based polymer blends, nanocomposites and their biodegradability |
| Licensed Content Author | Xiaozhi Tang, Sajid Alavi |
| Licensed Content Date | Apr 22, 2011 |
| Licensed Content Volume | 85 |
| Licensed Content Issue | 1 |
| Licensed Content Pages | 10 |
| Start Page | 7 |
| End Page | 16 |
| Type of Use | reuse in a thesis/dissertation |
| Intended publisher of new work | other |
| Portion | figures/tables/illustrations |
| Number of figures/tables/illustrations | 2 |
| Format | both print and electronic |
| Are you the author of this Elsevier article? | No |
| Will you be translating? | No |
| Original figure numbers | Fig. 1. Effect of molecular weight and hydrolysis level on the physical properties of PVOH And Fig. 2. Possible hydrogen bond formation between starch and PVOH. |

| | |
|---|---|
| Title of your thesis/dissertation | Polyvinyl Alcohol/ Starch/ Glycerol/ Halloysite Nanotube Bionanocomposites for Biodegradable Packaging Applications |
| Expected completion date | Dec 2019 |
| Estimated size (number of pages) | 250 |
| Requestor Location | Zainab Waheed Abdullah<br>1/49 Mosaic Street East Shelley. Perth<br><br>Perth, other WA6148<br>Australia<br>Attn: Zainab Waheed Abdullah |
| Publisher Tax ID | GB 494 6272 12 |
| Total | 0.00 USD |

## ELSEVIER LICENSE
## TERMS AND CONDITIONS

Jun 21, 2019

---

This Agreement between Zainab Waheed Abdullah ("You") and Elsevier ("Elsevier") consists of your license details and the terms and conditions provided by Elsevier and Copyright Clearance Center.

| | |
|---|---|
| License Number | 4613550148322 |
| License date | Jun 21, 2019 |
| Licensed Content Publisher | Elsevier |
| Licensed Content Publication | Carbohydrate Polymers |
| Licensed Content Title | Chitosan films and blends for packaging material |
| Licensed Content Author | Lambertus A.M. van den Broek, Rutger J.I. Knoop, Frans H.J. Kappen, Carmen G. Boeriu |
| Licensed Content Date | Feb 13, 2015 |
| Licensed Content Volume | 116 |
| Licensed Content Issue | n/a |
| Licensed Content Pages | 6 |
| Start Page | 237 |

| | |
|---|---|
| End Page | 242 |
| Type of Use | reuse in a thesis/dissertation |
| Intended publisher of new work | other |
| Portion | figures/tables/illustrations |
| Number of figures/tables/illustrations | 1 |
| Format | both print and electronic |
| Are you the author of this Elsevier article? | No |
| Will you be translating? | No |
| Original figure numbers | Fig.1. Structure of chitin and chitosan |
| Title of your thesis/dissertation | Polyvinyl Alcohol/ Starch/ Glycerol/ Halloysite Nanotube Bionanocomposites for Biodegradable Packaging Applications |
| Expected completion date | Dec 2019 |
| Estimated size (number of pages) | 250 |
| Requestor Location | Zainab Waheed Abdullah<br>1/49 Mosaic Street East Shelley. Perth<br><br>Perth, other WA6148<br>Australia<br>Attn: Zainab Waheed Abdullah |
| Publisher Tax ID | GB 494 6272 12 |
| Total | 0.00 USD |

## ELSEVIER LICENSE
## TERMS AND CONDITIONS

Jun 21, 2019

---

This Agreement between Zainab Waheed Abdullah ("You") and Elsevier ("Elsevier") consists of your license details and the terms and conditions provided by Elsevier and Copyright Clearance Center.

| | |
|---|---|
| License Number | 4613550875884 |
| License date | Jun 21, 2019 |

| | |
|---|---|
| Licensed Content Publisher | Elsevier |
| Licensed Content Publication | Advances in Colloid and Interface Science |
| Licensed Content Title | Encapsulation of active ingredients in polysaccharide–protein complex coacervates |
| Licensed Content Author | Nirmala Devi, Mandip Sarmah, Bably Khatun, Tarun K. Maji |
| Licensed Content Date | Jan 1, 2017 |
| Licensed Content Volume | 239 |
| Licensed Content Issue | n/a |
| Licensed Content Pages | 10 |
| Start Page | 136 |
| End Page | 145 |
| Type of Use | reuse in a thesis/dissertation |
| Intended publisher of new work | other |
| Portion | figures/tables/illustrations |
| Number of figures/tables/illustrations | 1 |
| Format | both print and electronic |
| Are you the author of this Elsevier article? | No |
| Will you be translating? | No |
| Original figure numbers | Fig. 4. Structure of gelatin |
| Title of your thesis/dissertation | Polyvinyl Alcohol/ Starch/ Glycerol/ Halloysite Nanotube Bionanocomposites for Biodegradable Packaging Applications |
| Expected completion date | Dec 2019 |
| Estimated size (number of pages) | 250 |
| Requestor Location | Zainab Waheed Abdullah<br>1/49 Mosaic Street East Shelley. Perth<br><br>Perth, other WA6148<br>Australia<br>Attn: Zainab Waheed Abdullah |
| Publisher Tax ID | GB 494 6272 12 |

| | |
|---|---|
| Total | 0.00 USD |

## ELSEVIER LICENSE
## TERMS AND CONDITIONS

Jun 24, 2019

---

This Agreement between Zainab Waheed Abdullah ("You") and Elsevier ("Elsevier") consists of your license details and the terms and conditions provided by Elsevier and Copyright Clearance Center.

| | |
|---|---|
| License Number | 4615190323191 |
| License date | Jun 24, 2019 |
| Licensed Content Publisher | Elsevier |
| Licensed Content Publication | Journal of Food Engineering |
| Licensed Content Title | Physical and microstructural properties of biodegradable films based on pea starch and PVA |
| Licensed Content Author | Amalia I. Cano, Maite Cháfer, Amparo Chiralt, Chelo González-Martínez |
| Licensed Content Date | Dec 1, 2015 |
| Licensed Content Volume | 167 |
| Licensed Content Issue | n/a |
| Licensed Content Pages | 6 |
| Start Page | 59 |
| End Page | 64 |
| Type of Use | reuse in a thesis/dissertation |
| Intended publisher of new work | other |
| Portion | figures/tables/illustrations |
| Number of figures/tables/illustrations | 1 |
| Format | both print and electronic |
| Are you the author of this Elsevier article? | No |
| Will you be translating? | No |

| | |
|---|---|
| Original figure numbers | Fig. 1. SEM micrographs of surface (750) and cross section (1.500) of pea starch (PS), PVA and composite (PS:PVA) films |
| Title of your thesis/dissertation | Polyvinyl Alcohol/ Starch/ Glycerol/ Halloysite Nanotube Bionanocomposites for Biodegradable Packaging Applications |
| Expected completion date | Dec 2019 |
| Estimated size (number of pages) | 250 |
| Requestor Location | Zainab Waheed Abdullah<br>1/49 Mosaic Street East Shelley. Perth<br><br>Perth, other WA6148<br>Australia<br>Attn: Zainab Waheed Abdullah |
| Publisher Tax ID | GB 494 6272 12 |
| Total | 0.00 USD |

## SPRINGER NATURE LICENSE TERMS AND CONDITIONS

Jun 24, 2019

---

---

This Agreement between Zainab Waheed Abdullah ("You") and Springer Nature ("Springer Nature") consists of your license details and the terms and conditions provided by Springer Nature and Copyright Clearance Center.

| | |
|---|---|
| License Number | 4615200995881 |
| License date | Jun 24, 2019 |
| Licensed Content Publisher | Springer Nature |
| Licensed Content Publication | Springer eBook |
| Licensed Content Title | Multifunctionalized Carbon Nanotubes Polymer Composites: Properties and Applications |
| Licensed Content Author | Nurhidayatullaili Muhd Julkapli, Samira Bagheri, S. M. Sapuan |
| Licensed Content Date | Jan 1, 2015 |
| Type of Use | Thesis/Dissertation |

| | |
|---|---|
| Requestor type | academic/university or research institute |
| Format | print and electronic |
| Portion | figures/tables/illustrations |
| Number of figures/tables/illustrations | 3 |
| Will you be translating? | no |
| Circulation/distribution | <501 |
| Author of this Springer Nature content | no |
| Title | Polyvinyl Alcohol/ Starch/ Glycerol/ Halloysite Nanotube Bionanocomposites for Biodegradable Packaging Applications |
| Institution name | n/a |
| Expected presentation date | Dec 2019 |
| Portions | Fig. 1 Chemical structures of amylose (a) and amylopectin (b)<br>And<br>Fig. 1 Advantages and disadvantages of polymeric nanocomposites<br>Fig. 1 Schematics of a single cellulose chain repeat unit, |
| Requestor Location | Zainab Waheed Abdullah<br>1/49 Mosaic Street East Shelley. Perth<br><br>Perth, other WA6148<br>Australia<br>Attn: Zainab Waheed Abdullah |
| Total | 0.00 USD |

## JOHN WILEY AND SONS LICENSE TERMS AND CONDITIONS

Jun 24, 2019

---

This Agreement between Zainab Waheed Abdullah ("You") and John Wiley and Sons ("John Wiley and Sons") consists of your license details and the terms and conditions provided by John Wiley and Sons and Copyright Clearance Center.

| | |
|---|---|
| License Number | 4615220021552 |

| | |
|---|---|
| License date | Jun 24, 2019 |
| Licensed Content Publisher | John Wiley and Sons |
| Licensed Content Publication | Journal of Food Science |
| Licensed Content Title | Review: Nanocomposites in Food Packaging |
| Licensed Content Author | Amit Arora, G.W. Padua |
| Licensed Content Date | Jan 11, 2010 |
| Licensed Content Volume | 75 |
| Licensed Content Issue | 1 |
| Licensed Content Pages | 7 |
| Type of use | Dissertation/Thesis |
| Requestor type | University/Academic |
| Format | Print and electronic |
| Portion | Figure/table |
| Number of figures/tables | 1 |
| Original Wiley figure/table number(s) | Figure 2 -Polymer clay morphologies. |
| Will you be translating? | No |
| Title of your thesis / dissertation | Polyvinyl Alcohol/ Starch/ Glycerol/ Halloysite Nanotube Bionanocomposites for Biodegradable Packaging Applications |
| Expected completion date | Dec 2019 |
| Expected size (number of pages) | 250 |
| Requestor Location | Zainab Waheed Abdullah<br>1/49 Mosaic Street East Shelley. Perth<br><br>Perth, other WA6148<br>Australia<br>Attn: Zainab Waheed Abdullah |
| Publisher Tax ID | EU826007151 |
| Total | 0.00 USD |

# ELSEVIER LICENSE
# TERMS AND CONDITIONS

Jun 24, 2019

This Agreement between Zainab Waheed Abdullah ("You") and Elsevier ("Elsevier") consists of your license details and the terms and conditions provided by Elsevier and Copyright Clearance Center.

| | |
|---|---|
| License Number | 4615220290109 |
| License date | Jun 24, 2019 |
| Licensed Content Publisher | Elsevier |
| Licensed Content Publication | Applied Clay Science |
| Licensed Content Title | Applications and interfaces of halloysite nanocomposites |
| Licensed Content Author | Yi Zhang, Aidong Tang, Huaming Yang, Jing Ouyang |
| Licensed Content Date | Jan 1, 2016 |
| Licensed Content Volume | 119 |
| Licensed Content Issue | n/a |
| Licensed Content Pages | 10 |
| Start Page | 8 |
| End Page | 17 |
| Type of Use | reuse in a thesis/dissertation |
| Intended publisher of new work | other |
| Portion | figures/tables/illustrations |
| Number of figures/tables/illustrations | 1 |
| Format | both print and electronic |
| Are you the author of this Elsevier article? | No |
| Will you be translating? | No |
| Original figure numbers | Fig.1. b) Schematic diagrams of the crystalline structure of halloysite, and the structure of a halloysite nanotube. |

| | |
|---|---|
| Title of your thesis/dissertation | Polyvinyl Alcohol/ Starch/ Glycerol/ Halloysite Nanotube Bionanocomposites for Biodegradable Packaging Applications |
| Expected completion date | Dec 2019 |
| Estimated size (number of pages) | 250 |
| Requestor Location | Zainab Waheed Abdullah<br>1/49 Mosaic Street East Shelley. Perth<br><br>Perth, other WA6148<br>Australia<br>Attn: Zainab Waheed Abdullah |
| Publisher Tax ID | GB 494 6272 12 |
| Total | 0.00 USD |

## JOHN WILEY AND SONS LICENSE TERMS AND CONDITIONS

Jun 24, 2019

---

This Agreement between Zainab Waheed Abdullah ("You") and John Wiley and Sons ("John Wiley and Sons") consists of your license details and the terms and conditions provided by John Wiley and Sons and Copyright Clearance Center.

| | |
|---|---|
| License Number | 4615220518649 |
| License date | Jun 24, 2019 |
| Licensed Content Publisher | John Wiley and Sons |
| Licensed Content Publication | Advanced Materials |
| Licensed Content Title | Graphene and Graphene Oxide: Synthesis, Properties, and Applications |
| Licensed Content Author | Yanwu Zhu, Shanthi Murali, Weiwei Cai, et al |
| Licensed Content Date | Jun 29, 2010 |
| Licensed Content Volume | 22 |
| Licensed Content Issue | 35 |
| Licensed Content Pages | 19 |

| | |
|---|---|
| Type of use | Dissertation/Thesis |
| Requestor type | University/Academic |
| Format | Print and electronic |
| Portion | Figure/table |
| Number of figures/tables | 1 |
| Original Wiley figure/table number(s) | Figure 15. A proposed schematic of graphene oxide structure. |
| Will you be translating? | No |
| Title of your thesis / dissertation | Polyvinyl Alcohol/ Starch/ Glycerol/ Halloysite Nanotube Bionanocomposites for Biodegradable Packaging Applications |
| Expected completion date | Dec 2019 |
| Expected size (number of pages) | 250 |
| Requestor Location | Zainab Waheed Abdullah<br>1/49 Mosaic Street East Shelley. Perth<br><br>Perth, other WA6148<br>Australia<br>Attn: Zainab Waheed Abdullah |
| Publisher Tax ID | EU826007151 |
| Total | 0.00 USD |

## ELSEVIER LICENSE TERMS AND CONDITIONS

Jun 24, 2019

---

This Agreement between Zainab Waheed Abdullah ("You") and Elsevier ("Elsevier") consists of your license details and the terms and conditions provided by Elsevier and Copyright Clearance Center.

| | |
|---|---|
| License Number | 4615260493885 |
| License date | Jun 24, 2019 |
| Licensed Content Publisher | Elsevier |

| | |
|---|---|
| Licensed Content Publication | Journal of Membrane Science |
| Licensed Content Title | A review of the water barrier properties of polymer/clay and polymer/graphene nanocomposites |
| Licensed Content Author | B. Tan, N.L. Thomas |
| Licensed Content Date | Sep 15, 2016 |
| Licensed Content Volume | 514 |
| Licensed Content Issue | n/a |
| Licensed Content Pages | 18 |
| Start Page | 595 |
| End Page | 612 |
| Type of Use | reuse in a thesis/dissertation |
| Intended publisher of new work | other |
| Portion | figures/tables/illustrations |
| Number of figures/tables/illustrations | 1 |
| Format | both print and electronic |
| Are you the author of this Elsevier article? | No |
| Will you be translating? | No |
| Original figure numbers | Fig. 12. Schematic illustration of permeation via polymer/clay interfacial zones |
| Title of your thesis/dissertation | Polyvinyl Alcohol/ Starch/ Glycerol/ Halloysite Nanotube Bionanocomposites for Biodegradable Packaging Applications |
| Expected completion date | Dec 2019 |
| Estimated size (number of pages) | 250 |
| Requestor Location | Zainab Waheed Abdullah<br>1/49 Mosaic Street East Shelley. Perth<br><br>Perth, other WA6148<br>Australia<br>Attn: Zainab Waheed Abdullah |
| Publisher Tax ID | GB 494 6272 12 |
| Total | 0.00 USD |

# SPRINGER NATURE LICENSE TERMS AND CONDITIONS

Jun 24, 2019

This Agreement between Zainab Waheed Abdullah ("You") and Springer Nature ("Springer Nature") consists of your license details and the terms and conditions provided by Springer Nature and Copyright Clearance Center.

| | |
|---|---|
| License Number | 4615671003751 |
| License date | Jun 24, 2019 |
| Licensed Content Publisher | Springer Nature |
| Licensed Content Publication | Journal of Materials Science (full set) |
| Licensed Content Title | Preparation and characterisation of poly(vinyl) alcohol (PVA)/starch (ST)/halloysite nanotube (HNT) nanocomposite films as renewable materials |
| Licensed Content Author | Zainab Waheed Abdullah, Yu Dong |
| Licensed Content Date | Jan 1, 2017 |
| Licensed Content Volume | 53 |
| Licensed Content Issue | 5 |
| Type of Use | Thesis/Dissertation |
| Requestor type | academic/university or research institute |
| Format | print and electronic |
| Portion | figures/tables/illustrations |
| Number of figures/tables/illustrations | 10 |
| Will you be translating? | no |
| Circulation/distribution | 501 to 1000 |
| Author of this Springer Nature content | yes |
| Title | Polyvinyl Alcohol/ Starch/ Glycerol/ Halloysite Nanotube Bionanocomposites for Biodegradable Packaging Applications |
| Institution name | n/a |
| Expected presentation date | Dec 2019 |

| | |
|---|---|
| Portions | Figures: 2, 3, 4, 5, 6, 7 and 8<br>And<br>Tables: 2, 3 and 4 |
| Requestor Location | Zainab Waheed Abdullah<br>1/49 Mosaic Street East Shelley. Perth<br><br>Perth, other WA6148<br>Australia<br>Attn: Zainab Waheed Abdullah |
| Total | 0.00 USD |

## SPRINGER NATURE LICENSE TERMS AND CONDITIONS

Jun 26, 2019

---

This Agreement between Zainab Waheed Abdullah ("You") and Springer Nature ("Springer Nature") consists of your license details and the terms and conditions provided by Springer Nature and Copyright Clearance Center.

| | |
|---|---|
| License Number | 4616350410693 |
| License date | Jun 26, 2019 |
| Licensed Content Publisher | Springer Nature |
| Licensed Content Publication | Journal of Packaging Technology and Research |
| Licensed Content Title | Application of Biodegradable Polymers in Food Packaging Industry: A Comprehensive Review |
| Licensed Content Author | S. Mangaraj, Ajay Yadav, Lalit M. Bal et al |
| Licensed Content Date | Jan 1, 2018 |
| Licensed Content Volume | 3 |
| Licensed Content Issue | 1 |
| Type of Use | Thesis/Dissertation |
| Requestor type | academic/university or research institute |
| Format | print and electronic |
| Portion | figures/tables/illustrations |
| Number of figures/tables/illustrations | 1 |

| | |
|---|---|
| Will you be translating? | no |
| Circulation/distribution | 501 to 1000 |
| Author of this Springer Nature content | no |
| Title | Polyvinyl Alcohol/ Starch/ Glycerol/ Halloysite Nanotube Bionanocomposites for Biodegradable Packaging Applications |
| Institution name | n/a |
| Expected presentation date | Dec 2019 |
| Portions | Fig. 8 Biodegradation rate and EdK values of different biodegradable<br>biopolymers |
| Requestor Location | Zainab Waheed Abdullah<br>1/49 Mosaic Street East Shelley. Perth<br><br>Perth, other WA6148<br>Australia<br>Attn: Zainab Waheed Abdullah |
| Total | 0.00 USD |

| | |
|---|---|
| **Title:** | Water and gas barrier properties of poly(vinyl) alcohol (PVA)/starch (ST)/ glycerol (GL)/halloysite nanotube (HNT) bionanocomposite films: Experimental characterisation and modelling approach |
| **Author:** | Zainab Waheed Abdullah,Yu Dong,Ning Han,Shaomin Liu |
| **Publication:** | Composites Part B: Engineering |
| **Publisher:** | Elsevier |
| **Date:** | Available online 14 June 2019 |

Title: Modeling the Barrier Properties of Polymer-Layered Silicate Nanocomposites

Author: R. K. Bharadwaj

Publication: Macromolecules

Publisher: American Chemical Society

Date: Dec 1, 2001



**PERMISSION/LICENSE IS GRANTED FOR YOUR ORDER AT NO CHARGE**

This type of permission/license, instead of the standard Terms & Conditions, is sent to you because no fee is being charged for your order. Please note the following:

- Permission is granted for your request in both print and electronic formats, and translations.
- If figures and/or tables were requested, they may be adapted or used in part.
- Please print this page for your records and send a copy of it to your publisher/graduate school.
- Appropriate credit for the requested material should be given as follows: "Reprinted (adapted) with permission from (COMPLETE REFERENCE CITATION). Copyright (YEAR) American Chemical Society." Insert appropriate information in place of the capitalized words.
- One-time permission is granted only for the use specified in your request. No additional uses are granted (such as derivative works or other editions). For any other uses, please submit a new request.

If credit is given to another source for the material you requested, permission must be obtained from that source.


**Title:** Exploration of Epoxy Resins, Hardening Systems, and Epoxy/Carbon Nanotube Composite Designed for High Performance Materials: A Review

**Author:** Irum Rafique, , Ayesha Kausar, et al

**Publication:** Polymer-Plastics Technology and Engineering

**Publisher:** Taylor & Francis

**Date:** Feb 11, 2016

Rights managed by Taylor & Francis

Logged in as:
Zainab Abdullah
Account #:
3001094216
LOGOUT

## Thesis/Dissertation Reuse Request

Taylor & Francis is pleased to offer reuses of its content for a thesis or dissertation free of charge contingent on resubmission of permission request if work is published.

BACK CLOSE WINDOW



6/24/2019 Rightslink® by Copyright Clearance Center


**Title:** Effect of Additives on Properties of Polyvinyl Alcohol (PVA)/Tapioca Starch Biodegradable Films

**Author:** H. Ismail, , N. F. Zaaba

**Publication:** Polymer-Plastics Technology and Engineering

**Publisher:** Taylor & Francis

**Date:** Aug 1, 2011

Rights managed by Taylor & Francis

Logged in as:
Zainab Abdullah
Account #:
3001094216
LOGOUT

## Thesis/Dissertation Reuse Request

Taylor & Francis is pleased to offer reuses of its content for a thesis or dissertation free of charge contingent on resubmission of permission request if work is published.

BACK CLOSE WINDOW

Copyright © 2019 Copyright Clearance Center, Inc. All Rights Reserved. Privacy statement, Terms and Conditions.
Comments? We would like to hear from you. E-mail us at customercare@copyright.com


| | |
|---|---|
| **Title:** | Polymer Nanocomposites as a New Trend for Packaging Applications |
| **Author:** | Ahmed M. Youssef |
| **Publication:** | Polymer-Plastics Technology and Engineering |
| **Publisher:** | Taylor & Francis |
| **Date:** | May 28, 2013 |

Rights managed by Taylor & Francis

Logged in as:
Zainab Abdullah
Account #:
3001094216
LOGOUT

## Thesis/Dissertation Reuse Request

Taylor & Francis is pleased to offer reuses of its content for a thesis or dissertation free of charge contingent on resubmission of permission request if work is published.

BACK CLOSE WINDOW

Copyright Clearance Center

**Note:** Copyright.com supplies permissions but not the copyrighted content itself.

1 PAYMENT 2 REVIEW 3 CONFIRMATION

## Step 3: Order Confirmation

**Thank you for your order!** A confirmation for your order will be sent to your account email address. If you have questions about your order, you can call us 24 hrs/day, M-F at +1.855.239.3415 Toll Free, or write to us at info@copyright.com. This is not an invoice.

**Confirmation Number: 11826143**
**Order Date: 06/24/2019**

If you paid by credit card, your order will be finalized and your card will be charged within 24 hours. If you choose to be invoiced, you can change or cancel your order until the invoice is generated.

### Payment Information

Zainab Abdullah
z.abdullah1@student.curtin.edu.au
+61 (4)70226656
Payment Method: n/a

### Order Details

**RSC advances**

| | |
|---|---|
| **Order detail ID:** | 71929418 |
| **Order License Id:** | 4615230335071 |
| **ISSN:** | 2046-2069 |
| **Publication Type:** | e-Journal |
| **Volume:** | |
| **Issue:** | |
| **Start page:** | |
| **Publisher:** | RSC Publishing |

**Permission Status:** Granted
**Permission type:** Republish or display content
**Type of use:** Thesis/Dissertation

| | |
|---|---|
| **Requestor type** | Academic institution |
| **Format** | Print, Electronic |
| **Portion** | chart/graph/table/figure |
| **Number of charts/graphs/tables/figures** | 1 |
| **The requesting person/organization** | Zainab Abdullah |
| **Title or numeric reference of the portion(s)** | Fig. 6 Illustration of (a) in situ-polymerization, (b) melt intercalation, (c) solution intercalation |
| **Title of the article or chapter the portion is from** | Gas barrier properties of polymer/clay nanocomposites |
| **Editor of portion(s)** | N/A |
| **Author of portion(s)** | Yanbin Cui, S. Kumar, Balakantha Rao Kona and Daniel van Houcke |

| | |
|---|---|
| **Volume of serial or monograph** | N/A |
| **Page range of portion** | 63673 |
| **Publication date of portion** | 20th July 2015 |
| **Rights for** | Main product |
| **Duration of use** | Current edition and up to 5 years |
| **Creation of copies for the disabled** | no |
| **With minor editing privileges** | no |
| **For distribution to** | Worldwide |
| **In the following language(s)** | Original language of publication |
| **With incidental promotional use** | no |
| **Lifetime unit quantity of new product** | Up to 999 |
| **Title** | Polyvinyl Alcohol/ Starch/ Glycerol/ Halloysite Nanotube Bionanocomposites for Biodegradable Packaging Applications |
| **Institution name** | n/a |
| **Expected presentation date** | Dec 2019 |

**Note:** This item will be invoiced or charged separately through CCC's **RightsLink** service. More info **$ 0.00**

**Total order items: 1**

**This is not an invoice.**

**Order Total: 0.00 USD**

This page is available in the following languages:

# Creative Commons License Deed

## Attribution 4.0 International (CC BY 4.0)

This is a human-readable summary of (and not a substitute for) the license.

## You are free to:

**Share** — copy and redistribute the material in any medium or format

**Adapt** — remix, transform, and build upon the material

for any purpose, even commercially.

The licensor cannot revoke these freedoms as long as you follow the license terms.

## Under the following terms:

**Attribution** — You must give appropriate credit, provide a link to the license, and indicate if changes were made. You may do so in any reasonable manner, but not in any way that suggests the licensor endorses you or your use.

**No additional restrictions** — You may not apply legal terms or technological measures that legally restrict others from doing anything the license permits.